

Multi-Objective Optimisation of CCS using simulation, heat integration and cost estimation

Trent Harkin



**A thesis submitted in fulfilment of the degree of
Doctor of Philosophy**

**Department of Chemical Engineering,
Monash University
Australia**

January 2012

To my wife and family

Summary

Carbon capture and storage (CCS) using solvent based absorption has the potential to reduce the carbon intensity of power stations. The addition of CCS to power stations will increase the capital and operating expenditure of the power station and will reduce the net power produced from the power station. Therefore minimising both the capital cost and the energy penalty associated with CCS will be imperative to ensure that the cost of electricity remains competitive. A power station with solvent based CCS will have a range of new heat sources and sinks and utilising heat within the process will be important to minimise the increase in cost of electricity.

This thesis focuses on developing a multi-objective optimisation (MOO) framework comprising simulation, heat integration and cost estimation of a power station combined with a solvent based CCS plant. Simulation of the coal combustion and CCS equipment provides a rigorous model of the power station and solvent equipment and is therefore capable of modelling impacts of changes to design and operating parameters. The simulation is combined with a linear programming heat integration method to determine systematically and automatically the maximum amount of power that can be generated for a given set of design and operating parameters. Cost estimation is then used to determine the differential capital and operating cost to the power station with the addition of CCS. The MOO framework therefore allows optimisation of a range of operating and design variables to investigate trade-offs between capture rate and differential cost of electricity or any number of objectives.

Heat integration has shown to potentially lead to significant reductions in the energy penalty associated with the addition of CCS. When capturing 90 % of the CO₂ in the flue gas, energy penalties that can be as high as 38 % without heat integration, can be reduced to just 14 % with a fully optimised and heat integrated rate promoted potassium carbonate solvent process. However, the differential cost of electricity for the most heat integrated plant will be greater than for a system with moderate heat integration and the minimum differential cost of electricity for brown coal fired power stations in Australia will likely have an energy penalty of between 25 and 30 %. The differential cost of electricity for such a system would also be approximately 80 \$/(MW h) and the cost per tonne of CO₂ avoided would be approximately \$77. The heat exchanger minimum approach temperature and flue gas feed temperature are extremely important variables to minimise the cost of electricity, whilst to a lesser extent the solvent lean loading and temperature, the stripper pressure and stripper feed temperature are also important. As the solvent processes develop, and equipment that is fit for purpose is designed, the costs of adding CCS to a power station will reduce. The methodology developed and utilised in the thesis

will be helpful to compare different capture technologies and to ensure that they are integrated into the power station to reduce the energy penalty and the differential cost of electricity.

General Declaration
Monash University
Monash Research Graduate School

Declaration for thesis based or partially based on conjointly published or unpublished work

In accordance with Monash University Doctorate Regulation 17/ Doctor of Philosophy and Master of Philosophy (MPhil) regulations the following declarations are made:

I hereby declare that this thesis contains no material which has been accepted for the award of any other degree or diploma at any university or equivalent institution and that, to the best of my knowledge and belief, this thesis contains no material previously published or written by another person, except where due reference is made in the text of the thesis.

This thesis includes 3 original papers published in peer reviewed journals. The core theme of the thesis is “*Multi-Objective Optimisation of CCS using simulation, heat integration and cost estimation*”. The ideas, development and writing up of all the papers in the thesis were the principal responsibility of myself, the candidate, working within the Department of Chemical Engineering under the supervision of Associate Professor Andrew Hoadley.

The inclusion of co-authors reflects the fact that the work came from active collaboration between researchers and acknowledges input into team-based research.

In the case of 3, 5 and 8 my contribution to the work involved the following:

Thesis chapter	Publication title	Publication status	Nature and extent of candidate's contribution
3	Reducing the energy penalty of CO ₂ capture and compression using pinch analysis	Published: <i>Journal of Cleaner Production</i> 18 (2010) 857 – 866 doi: 10.1016/j.jclepro.2010.02.011	Initiation, key ideas, simulations, methodology, results interpretation, writing of paper.
5	Using multi-objective optimisation in the design of CO ₂ capture systems for retrofit to coal power systems	In Press: <i>Energy</i> 41 (1) (2012) 228 – 235 doi: 10.1016/j.energy.2011.06.031	Initiation, key ideas, simulations, methodology, results interpretation, writing of paper.
8	Optimisation of power stations with carbon-capture plants – the trade off between costs and net power	In Press: <i>Journal of Cleaner Production</i> doi: 10.1016/j.jclepro.2011.12.032	Initiation, key ideas, simulations, methodology, results interpretation, writing of paper.

I have not renumbered sections of submitted or published papers in order to generate a consistent presentation within the thesis.

Signed:

Date:

Under the Copyright Act 1968, this thesis must be used only under the normal conditions of scholarly fair dealing. In particular no results or conclusions should be extracted from it, nor should it be copied or closely paraphrased in whole or in part without the written consent of the author. Proper written acknowledgement should be made for any assistance obtained from this thesis.

I certify that I have made all reasonable efforts to secure copyright permissions for third-party content included in this thesis and have not knowingly added copyright content to my work without the owner's permission.

Acknowledgements

This thesis could not have completed without the direct or indirect support of several people whom I'd like to thank and acknowledge for their assistance; especially to my co-supervisors Andrew Hoadley (Monash University) and Barry Hooper (CO2CRC) whom without their influence this thesis would never have been started let alone completed.

I would like to thank Andrew for his inspiration, insight and ability to always suggest directions for the research. Without his direction, capacity to allow me to explore my own ideas and then understand how to achieve the desired outcome with the range of ideas we conceived, this thesis would never have been able to come together. I also need to thank Barry for his insight, optimism and trust during the years it has taken to complete this thesis. Without Barry's belief in the direction of the research and continual support, the research would not have had the same level of purpose. Both Andrew and Barry deserve my sincere thanks for the numerous times they were able to review work, within the very tight deadlines I often gave them, and for their constant understanding when "results should be available in a day or two".

I would also like to thank the Cooperative Research Centre for Greenhouse Gas Technologies (CO2CRC) for providing me with the opportunity and funding to do research in a field that has the best intentions to provide a means of minimising the impacts of human energy consumption on the environment whilst maintaining the standards of living that we are used to. It feels much better to be endeavouring to find solutions rather than ignoring the problems. By thanking the CO2CRC I am really thanking all the individuals within it. I would especially like to thank Abdul, Stacey and all the CO2CRC researchers from the Melbourne University solvents and membranes group, Monash university adsorbents group and the UNSW economics team. I hope I have been able to help you somewhere near as much as the help you all provided me.

I am very grateful to Prof. Rangaiah and his colleagues at the National University of Singapore for the kind use of their multi-objective optimisation software. Also, to Nipen Shah for his help with understanding how to interface the MOO software with process simulations.

Thank-you to the CO2CRC and Monash University for the opportunity to attend, and present, at numerous conferences; the benefits of these opportunities are immeasurable.

To my family; Anne, Gavan and Martine, thank-you for all your support and encouragement, which has not waived for the last 33 years. I have been very fortunate. And finally, to my wife Jo; you weren't meant to be my wife until after this thesis was complete, but I couldn't wait any longer! Thanks for your support from start to finish, without it I would not have been able to sanely or happily complete the thesis.

Contents

Summary	ii
Declaration	iv
Acknowledgements	vi
Table of Contents	vii
1. Chapter 1 – Introduction	1
1.1 Background	2
1.1.1 Climate Change	2
1.1.2 Carbon Capture and Storage	3
1.1.3 Process Design of CCS	6
1.2 Project Objectives	9
1.3 Research Objectives	9
1.4 Outline of Thesis	10
References	12
2. Review of the integration of solvent based PCC into coal fired power stations	13
2.1 Flue gas pretreatment	14
2.2 Solvent absorption of CO ₂	14
2.3 CCS Energy Penalty	17
2.4 Heat integration of power stations	20
2.5 Utility Targeting	22
2.6 Multi-Objective Optimisation	27
2.7 MOO and Heat Integration	30
2.8 Integration of Solvent Based Post-Combustion Capture into Coal-fired Power Stations	32
References	33
3. Reducing the energy penalty of CO₂ capture and compression using pinch analysis	40

3.1	Introduction	41
3.2	Declaration for Chapter 3	43
3.3	Publication – Journal of Cleaner Production 18 (2010) 857 – 866	44
	Introduction	44
	Background	44
	Solvent Absorption	45
	Energy Penalty	46
	Heat integration of power plants	47
	Methods for selection of optimal utilities	47
	Methodology	47
	Retrofit of CCS to brown coal power stations example	49
	Basis	49
	Results	50
	Discussion	50
	Integrated CCS and drying	50
	Effect of ΔT_{min}	52
	Conclusion	52
	Acknowledgement	52
	References	52
4.	Methodology for combining Multi-Objective Optimisation, Simulation and Heat Integration for Process Synthesis of CCS	54
4.1	Introduction	55
4.2	Methodology for the combination of MOO, simulation and automated heat integration	56
4.3	Superstructure method of Post Pinch Analysis Processing	64
4.4	Conclusion	68
	References	68

5.	Using multi-objective optimisation in the design of CO₂ capture systems for retrofit to coal power stations	70
5.1	Introduction	71
5.2	Declaration for Chapter 5	72
5.3	Publication	73
	Introduction	73
	Methodology	74
	Case 1a/b: Solvent loading and flowrate	75
	Case 2: Solvent Loading Flowrate and stripper pressure	75
	Case 3: Power station unit's net power output	75
	Case 4: Power station unit's net power output with heat integration	76
	Results	76
	Case 1a/b: Solvent Loading and Flowrate	76
	Case 2: Impact of stripper pressure	77
	Case 3: Impact of variables on the unit's net power output	77
	Case 4: Impact of variables on the power station net power with heat integration	77
	Discussion	78
	Impact of stripper pressure on optimal solutions	78
	Using CCS to control power station unit outputs	79
	Comparative studies	79
	Conclusion	80
	Acknowledgements	80
	References	80
6.	Using MOO and the superstructure method to determine the optimum stripper pressure for potassium carbonate based capture systems	81
6.1	Introduction	82

6.2	MOO Objectives and Decision Variables	82
6.3	Results and Discussion	83
6.3.1	Pareto fronts and decision variables	83
6.3.2	Impacts to the Process Heat Exchangers	91
6.3.3	Pinch Analysis Results	93
6.4	Conclusions	95
7.	Comparison of the extraction and superstructure method	96
7.1	Introduction	97
7.2	Case Study Background	97
7.3	Restricting the main steam flowrate	99
7.4	Superstructure versus the Extraction method	102
7.5	Conclusion	106
8.	Optimisation of power stations with carbon capture plants – the trade off's between costs and net power	107
8.1	Introduction	108
8.2	Declaration for Chapter 8	113
8.3	Publication	114
	Introduction	114
	Methodology	116
	Simulation and heat integration	117
	Cost estimation	117
	Capital Cost estimation	117
	Operating Costs	118
	Net present value	118
	Multi-objective optimisation	118
	Case study description and results	119

Discussion	120
Optimisation 1 – Maximise net power	120
Optimisation 2 – Minimise DCOE	121
Optimal ΔT_{min}	122
Optimal stripper pressure	122
Optimal flue gas temperature	122
Review of Technique	120
Conclusion	123
Acknowledgement	123
Appendix – Linear Model to Maximise the Power Generation	123
References	125
9. Conclusions and Recommended Further Investigations	126
 Appendices	
Appendix A Detailed description of heat integration program	138
Appendix B Capital Cost Estimation	180
Appendix C Operating Cost Estimation	202
Appendix D Heat Exchanger Area Estimation	208
Appendix E Redesigning the cold end of a lignite power station for CO ₂ capture	220
Appendix F A comparison of the process integration of Shockwave CO ₂ compression with conventional turbo machinery into PCC power station design	230
Appendix G Optimisation of pre-combustion capture for IGCC with a focus on the water balance	239

Chapter 1

Introduction to climate change and the role CO₂ capture and storage may play in mitigating climate change; and the potential improvements that can be made in the integration of CO₂ capture facilities.

1. Introduction

1.1 Background

1.1.1 Climate Change

The average surface temperature of the earth has warmed by about 0.74 °C since the start of the 20th century. It is very likely that the increase in global temperatures is caused by increased concentration of greenhouse gases caused by human activities. Without action to stabilise or reduce the level of greenhouse gases, it is likely that there will be adverse environmental, social and economic impacts.

With the aim of reducing the effects increasing concentrations of greenhouse gases (GHG's) in the atmosphere may have on our climate, Australia and many international governments are creating and implementing schemes to reduce anthropogenic carbon dioxide (CO₂) emissions. The intergovernmental panel on climate change's (IPCC) fourth assessment concluded that there is a very high confidence that the global net effect of human activities since 1750 has been one of warming, with a radiative forcing of +1.6 W/m² (IPCC (2007)). The contribution of GHG's has a combined radiative forcing of +2.3 W/m² leading to the IPCC to conclude that it is very likely that the increase in global average temperatures observed since the mid 20th century is due to the observed increase in anthropogenic GHG concentrations. The global atmospheric concentration of CO₂ increased from a pre-industrial value of 280 ppm to 390 ppm in early 2011. Therefore, reducing the amount of CO₂ released to the environment will be an important component in order to reduce the impacts of anthropogenic climate change.

Approximately 50 % of Australia's CO₂ equivalent emissions are from stationary sources and of those emissions 69 % are from fossil fuel fired power generation (refer to Figure 1-1)(DCC (2008)). In Victoria, power generation predominantly uses brown coal which emits high levels of CO₂ for each unit of electricity produced. Victoria has over 6000 MW of installed pulverized coal fired power stations and over 500 years of accessible brown coal for power generation (DPI (2008)).

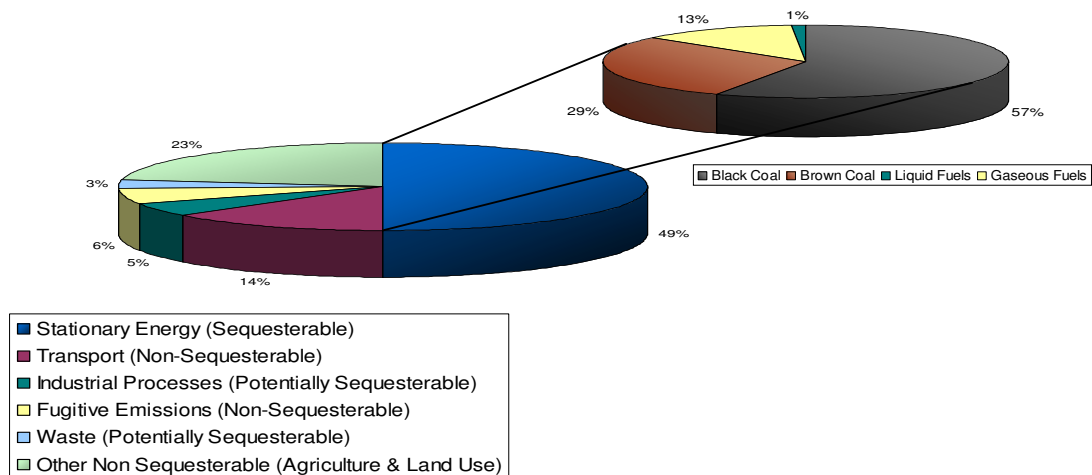


Figure 1-1: Australian anthropogenic CO₂ equivalent emissions (DCC (2008))

1.1.2 Carbon Capture & Storage

The least cost option to meet rising energy demands, at the same time as stabilising atmospheric CO₂ emissions, requires a portfolio of measures. These measures include a combination of improvements in energy efficiency, renewable energy generation (solar / wind / thermal / biomass / hydro), increased use of nuclear technology, fuel switching and CO₂ capture and storage (CCS). CCS requires equipment to separate and capture the CO₂ from the flue gas generated by power plants and large industrial plants, compressing the separated CO₂ into a supercritical fluid form and then storing it in geological structures (refer to Figure 1-2). It is possible to use CCS to reduce the emissions from any large scale stationary source of CO₂ and the most likely candidates include pulverised coal power plants, open and closed cycle natural gas power stations, upstream natural gas treatment plants and in the steel, cement and chemicals industries. The largest sources of stationary emissions are power stations, and hence this is the area where a significant amount of research is being focused. It is possible to design new power stations to include CCS or to retrofit existing power stations with CCS technology.

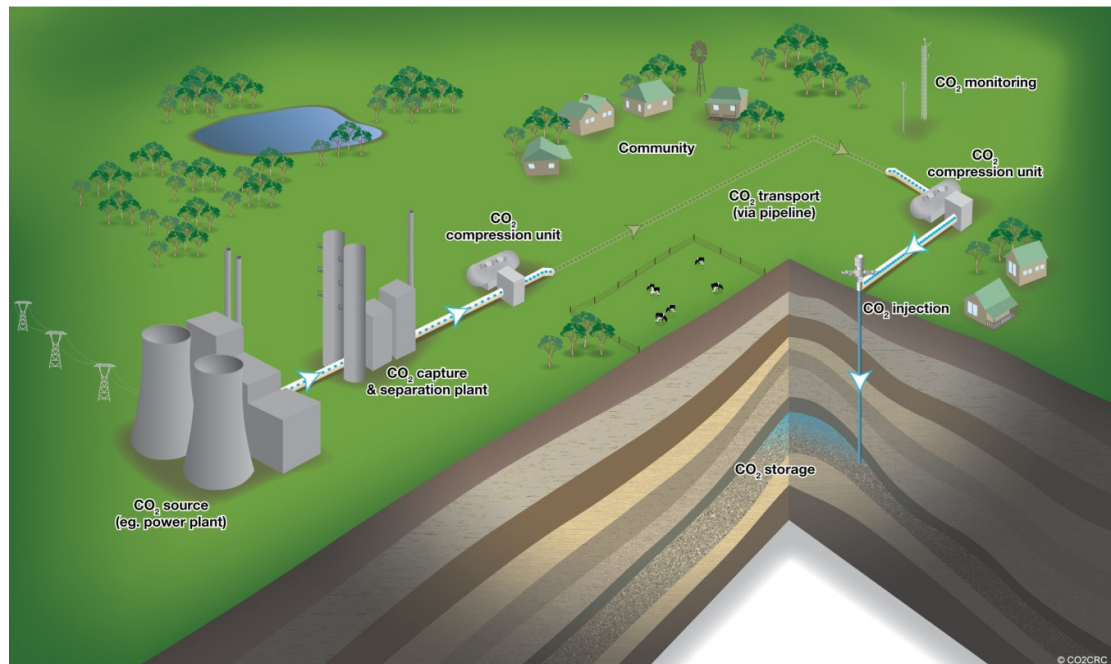


Figure 1-2: A simplified overview of the elements of a CO₂ capture and storage process for a power station (CO₂CRC).

The objective of CCS is to separate the CO₂ from its many sources of flue gases and purify it to a suitable level for transport and storage. The level of purification of CO₂ depends on the final destination of the CO₂. When used for industrial purposes such as food preparation or chemical production then the purity required is much higher than for geological storage. The majority of CCS projects will be geared towards geological storage as the current industrial usage of CO₂ is less than 1% of the anthropogenic emissions of CO₂ (IPCC (2005)).

Geological storage of CO₂ relies on compressing the CO₂ into a supercritical fluid which requires pressures of greater than the critical point of CO₂ which is 74 bar. The CO₂ is then transported and injected at least 800 m (IPCC (2005)) underground where it will remain, stored in permeable rock. The location of storage requires that the permeable rock is covered in an impermeable seal rock that forms a structural trapping mechanism to keep the CO₂ stored underground. The CO₂ will also be held in the porous rocks by a mechanism called residual trapping, where the CO₂ is trapped in discontinuous pockets in the pores of the rock where it will become immobile. Over time the trapped CO₂ will dissolve into salt water brines that are found in the porous rock increasing the density of the solution, which will then sink to the bottom of the rock formation helping to further trap the CO₂. Finally the CO₂ will undergo mineral trapping where the dissolved CO₂ will form carbonic acid and then react with minerals in the rock to form solid carbonate minerals.

The required purity of the CO₂ for geological storage is mainly an economic trade-off between the additional cost of purifying the CO₂ and the cost of transporting and storing dilute CO₂. For pure geological storage of CO₂ most studies use a CO₂ purity of greater than 95%. To minimise the amount of pore space required for storage, the CO₂ needs to be greater than 74 bar for pure CO₂ and will usually need to be compressed to between 100 bar and 150 bar to overcome pressure drops in transportation. The CO₂ in most cases will also need to be dehydrated to ensure that the hydrate formation and metal corrosion do not become issues. The level of H₂S in the CO₂ as well as other impurities like CH₄, O₂, CO and N₂ will also effect pipeline material selection.

CO₂ capture from power generation can be broken into three broad categories; post-combustion, pre-combustion and oxyfuel. Post-combustion capture (PCC) is the separation of the CO₂ from the other flue gases (mainly N₂) after the fuel has been combusted with air. Pre-combustion is the separation of CO₂ from synthesis gases (mainly H₂) in integrated gasification combine cycle (IGCC) power stations. Whilst oxyfuel is a process involving the combusting of the fuel with oxygen rather than air, which produces a flue gas stream highly concentrated with CO₂ that requires much less separation, as most of the nitrogen has already been separated from the oxygen upstream of the combustion.

Although there are many gasification units installed for chemical industries, there are currently few significant power stations using IGCC technology, whereas both post-combustion capture and oxyfuel are able to be retrofitted to the large installed base of pulverised coal, natural gas and oil fired power stations. Currently post-combustion capture appears to be a more mature technology compared to oxyfuel given that out of the 77 large scale integrated CCS projects identified by the Global CCS Institute (GCCSI) in 2010, 21 of those projects were for post-combustion compared to only four for oxyfuel (Global CCS Institute (2011)).

There are a number of technology options for separating the CO₂ from the other the other components of flue gases including chemical and physical solvent absorption, gas-solid based adsorption, membrane gas separation, low temperature separation and hybrid designs. CO₂ is currently separated from natural gas streams predominantly using chemical absorbents, although membranes and adsorption processes have started to gain acceptance. Separation of CO₂ from synthesis gas for ammonia and hydrogen production uses either adsorption or solvent based absorption. However, for post-combustion capture from power stations it is clear that solvent based technologies are closest to commercial deployment; as demonstrated by the existing commercial applications of CO₂ capture from flue gas, which all use amine based solvent absorption processes (Herzog (2000)).

Conventional solvent capture of CO₂ is a two step process involving an absorption step, where lean solvent is contacted with the flue gas stream to capture the CO₂. A second step occurs in a regeneration or stripping column where the solvent is either heated or the pressure is reduced to desorb the CO₂ from the solvent, generating a high purity stream of CO₂ and simultaneously regenerating the solvent which is returned to the absorption column.

The addition of CCS to a power station will increase the costs of the power station, as there will be additional capital costs for the construction of the CCS plant as well as significant increases in operating costs due to the additional energy expended to capture the CO₂ and compress it for transport and storage. For solvent capture the additional energy is required for regeneration of the solvent, solvent circulation, to provide motive energy to the flue gases to overcome the pressure drop in the absorber, for flue gas pre-treatment, additional cooling and for CO₂ compression. The additional energy reduces the efficiency of a power station, leading to either lower net power output from the power station or increases in the primary fuel to provide the additional heat and power required to perform the CCS.

Minimising the reduction in efficiency caused by CCS, or the energy penalty of CCS, will be important to minimise the costs associated with CCS. It is possible to reduce the energy penalty, and therefore the cost of CCS, by improving the efficiency of the carbon capture process, by improving the integration between the power station and the CCS plant and by optimising the design of the power station with CCS.

1.1.3 Process design of CCS

There is a range of solvents available, or that are undergoing Research and Development (R&D) for post-combustion capture of CO₂. The majority of these are amine based solvents, where MEA (monoethanolamine) is considered to be the benchmark solvent. The Fluor Econamine™ technology is one such MEA based solvent that has been used for post-combustion capture of CO₂ from various sources for use in food industry, enhanced oil recovery, chemical production and for development of CCS. A range of other amine based solvents are being demonstrated including; MHI's proprietary sterically hindered amine KS1, HTC Pureenergy's proprietary amine solvent, Siemens PostCap system using amino acid salts, IFP Energies nouvelles high concentration MEA solvent HiCapt+™ and the Alstom chilled ammonia process.

The solvent R&D is aimed to reduce the energy required for regeneration, increase the absorption kinetics to reduce the equipment size, produce solvents with low levels of degradation and that have low volatilities so the solvent is not emitted from the stacks of the absorber. However, one

consistent negative with amine systems is that they require low levels of Sulphur Oxides (SO_x) and Oxides of Nitrogen (NO_x) on the feed gas to avoid excessive solvent degradation. This is especially an issue for Australian power stations when considering that the majority of Australian power stations use low sulphur coals and are remotely located and thus do not have desulphurisation technologies. Therefore, in order to use amine solvents the power stations would also need to apply desulphurisation upstream of the CCS plant, which would add to the capital and operating costs of the project. The solvent process selection may also depend on other site specific fuel or environmental considerations. The chilled ammonia process appears to be an emerging solvent technology, however for the process to have low energy penalties the solvent will need to be chilled to low temperatures (<10 °C) and therefore in an Australian context the chilling will require significant amount of refrigeration which may lead to comparatively high energy penalties.

Potassium carbonates offer an alternative to amine based solvents, they are low cost solvents, have low volatilities, low rates of oxygen degradation and the incoming SO_x and NO_x can be absorbed and will form potentially useful potassium sulphates and nitrates avoiding the need for additional flue gas desulphurisation. However, the traditional 30 wt% potassium carbonate process has low kinetic rates and higher regeneration energy than MEA. Therefore, for post-combustion capture, the process requires modifications to improve the reaction kinetics and reduce the reaction energy to be competitive with the amine based solvents.

Almost all solvent systems are based around the same essential elements as represented by Figure 1-3; The flue gas feed gas fan increases the pressure of the flue gas to overcome the additional pressure drops in the feed cooler and absorber. The feed cooler reduces the temperature of the feed gas and as it will often be a direct contact cooler (DCC) it will also help to remove any fine particles upstream of the absorber. In the absorber, the lean solvent absorbs the CO₂ from the feed gas. Rich solvent loaded with CO₂ leaves the bottom of the absorber and is heated in the lean-rich heat exchanger. Solvent is then regenerated in the stripper by heating the solvent further using low pressure steam in the reboiler. Regenerated lean solvent from the bottom of the stripper is then cooled and returned to the top of the absorber. The CO₂ saturated with water leaves the top of the stripper, where most of the water will be condensed and recycled to the top of the stripper column. The cooled CO₂ is then compressed in a multi-stage compressor, further water will need to be removed in between each stage and often a separate dehydration process in between the stages may be required. There will be subtle differences between the typical solvent process and the process design offered by solvent vendors. Volatile amine solvents will require at minimum a water wash stage on the outlet of the absorber. A number of solvents may include a solvent reclamation process where a slipstream of the solvent

is sent to remove particles or components which build-up in the solvent. A range of alterations may help to reduce the regeneration energy including; absorber intercooling, staged stripper feeding, split flow arrangements, stripper overhead vapour recompression, rich solvent flashing, lean solvent vapour recompression and intermediate stripper recompression.

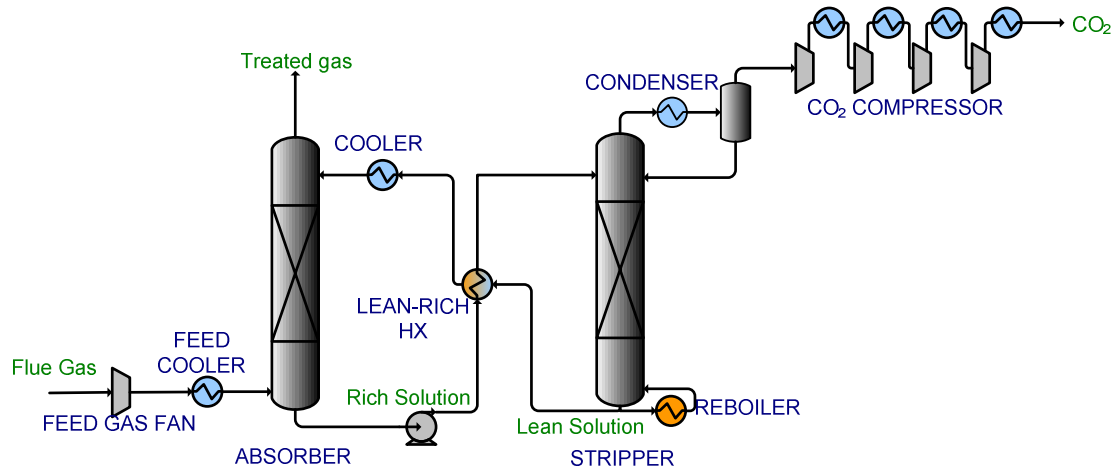


Figure 1-3: Typical solvent plant layout for Post-combustion capture.

Regardless of the design of the solvent plant there will be a requirement for solvent heating, which will generally require low pressure steam that is extracted from the steam turbine, thus reducing the power produced from the steam turbine. The amount of steam required for the solvent regeneration can be as much as 40 to 60 % of the total steam production (Klebes et al. (2010)). Therefore, it is anticipated that modifications will be required to the steam turbines to enable them to operate with reduced flowrates in the low pressure (LP) end of the turbines. Options to control the back end of the steam turbine include the addition of a new back pressure turbine, a LP throttle valve, a low pressure turbine with floating pressure or the use of a clutch in one of the flow paths of a two-flow path low pressure turbine.

The addition of post-combustion CCS to a pulverised coal power station will reduce the efficiency of the power station by between 24 and 40 % (Gibbins and Crane (2004) and IPCC (2005)), depending on the solvent process and the base power station fuel, location and design.

The addition of post-combustion CCS not only requires additional heating, but also requires additional cooling demands for the flue gas cooling, the lean solvent cooling, the stripper condenser and the CO₂ compressor intercoolers. It may be possible to re-use heat in these streams in the power station to reduce the energy penalty associated with CCS. Pinch analysis is a tool used in the chemical processing industry that enables the systematic evaluation of process-process heat exchange and therefore may be useful to identify and quantify potential energy savings.

1.2 Project Objectives

Given the large body of evidence to suggest that CO₂ emissions need to be reduced and the potential of new taxes or emissions trading schemes for CO₂ that may be implemented, it is clear that CCS may become an important mitigation option to avoid prematurely retiring the large base load of coal-fired electricity generation in Australia. When the scale of CCS projects is sufficiently large, the proportion of the overall cost of CCS due to storage reduces and up to 80 % of the costs can be attributed to the capture and compression of the CO₂. Therefore, it is paramount to reduce the cost of CCS, that the cost of CO₂ capture and compression is reduced. Ho et al. (2008) reported that the cost of CCS can be reduced by 25 % if the energy penalty of the CCS process can also be reduced by 25 %.

The project objective is to determine the potential for reductions in the cost of implementing CCS by improving the integration of the post-combustion solvent process with coal fired power stations, in particular in the Victorian and Australian market. The project scope includes the power station, the gas pre-treatment, solvent absorption and CO₂ compression, when cost estimations are made a nominal cost for storage is also included. The project has developed simulations of the typical Australian coal fired power stations, and typical solvent based PCC process. The simulations are used to analyse potential options for integration between the two systems to reduce the overall energy penalty. In this research, the basis for design is that the heat and power required for the CCS equipment will be drawn from the heat and power available within the power station and therefore the net power of the power station will be lowered with the addition of CCS

1.3 Research Objectives

The objectives of the project involve the application of heat integration methods to solvent-based post combustion capture from power station flue gas and the development of new optimisation methods for the design of these systems. This includes:

1. Using pinch analysis to identify the minimum energy penalty for a typical solvent system applied to a typical Australian coal fired power stations.
2. Using multi-objective optimisation to determine the impact of varying key operating parameters on the energy penalty.
3. The use of multi-objective optimisation combined with cost estimation to determine the important design and operating parameters of the addition of CCS to the power station.

4. Development of a computer algorithm to automate a method for determining targets for the minimum energy penalty.
5. Development of methods suitable for embedding in the optimisation process which estimate the operating and capital costs of the CCS plant.

1.4 Outline of Thesis

This thesis contains nine chapters, including the framing chapters of the introduction, background and the conclusion. Of the remaining six chapters, three are based on peer reviewed journal articles that have been accepted for publication. For those chapters based on journal articles (3, 5 and 8), the journal articles are included as whole articles, therefore the numbering of sections, tables, equations, figures and references in the article will be relevant only to that article.

Otherwise the numbering throughout the thesis is consistent between chapters. This thesis is constructed based on the guidelines of the Research Graduate School at Monash University for PhD Thesis by Publication (Monash Research Graduate School (2011)).

Chapter 2 provides the required background material on solvent based PCC, the energy penalty that is typical for these plants, generic methods of heat integration and utility targets and their application to power station design and multi-objective optimisation. This chapter shows the current methods of integration between the solvent plant and the power station and how heat integration and multi-objective optimisation might be able to be used in collaboration to achieve improvements in the overall design.

In Chapter 3, the integration of a generic solvent plant with two brown coal fired power stations is detailed. A numerical method to determine the optimal steam extraction rates from the steam turbine to satisfy the additional heat required for solvent regeneration is provided which enables the automatic calculation of the minimum energy penalty for the given process. The impact of a retrofit design, coal pre-drying and the minimum temperature driving force (ΔT_{\min}) of the heat exchange network is also analysed. As the analysis in this chapter is used for multiple power stations the impact of the power station design is also explained.

In Chapter 4, the generic structure that combines simulation, automated heat integration and multi-objective optimisation is provided. This chapter includes an explanation of a second method for automated heat integration for CCS projects by determining the optimum steam generation and extraction rates from the steam turbine. This method allows for more flexibility in the design of the steam cycle than the method described in Chapter 3.

In Chapter 5, multi-objective optimisation is used to show the importance of designing the CCS plant to be integrated with the power station. The minimum reboiler energy for a potassium carbonate solvent system is developed for a range of CO₂ capture rates, followed by determination of the minimum energy penalty with and without heat integration. The chapter shows the improvements in the energy penalty that can be gained by maximising the heat integration, that minimising the reboiler energy may not necessarily lead to the minimum energy penalty and that the optimum operating parameters may change depending on the objectives.

Chapter 6 provides an example of the automated heat integration method developed in Chapter 4. The example is for a potassium carbonate based capture plant integrated with a brown coal fired power station. The example is to maximise the CO₂ capture rate whilst maximising the net power from the power station by varying a number of the CO₂ capture plant variables, in particular trying to determine the optimum operating pressure of the solvent stripper.

Chapter 7 is used to compare the two automated heat integration methods developed in Chapters 3 and 4. The first “extraction” method is useful for retrofit’s but will not necessarily lead to the maximum amount of power that can be generated with the available heat. The second “superstructure” method allows for greater control of what parameters in the steam cycle are fixed and what can be altered, it will generally provide greater power than the extraction method, but may require greater modifications to an existing steam turbine to achieve those targets.

In Chapter 8 we introduce cost estimation to the multi-objective optimisation. The cost estimation enables the estimation of the differential cost of electricity (DCOE) due to the addition of the potassium carbonate based solvent system. Therefore, the optimum value of the operating variables of the CCS plant can be found to minimise the DCOE.

Chapter 9 presents the conclusions of the research and suggestions for future work.

There are seven appendices in the thesis which are used to provide detailed descriptions and equations that were used to develop the automated heat integration and cost estimation program or to show a range of case studies that have utilised the methodologies outlined in the thesis. Appendix A provides a skeleton of the steps used in the heat integration program.

Appendix B and C detail the cost functions used for capital and operating costs respectively.

Appendix D provides details of the methods used to estimate the area required for the heat exchanger network which is used to estimate costs. Appendix E is a paper written for the CCT2009 conference which shows how in certain circumstances the cold end of a power station can be redesigned to reduce the energy penalty associated with solvent based CO₂ capture, in particular the influence that the air-preheat temperature may have on the overall efficiency when CCS is

included. Appendix F is a paper published for GHGT-10 on the comparison between the process integration of shockwave CO₂ compression and conventional turbo machinery. Appendix G shows how the methodologies used in this thesis can also be applied to pre-combustion capture, the paper published for GHGT-10 describes the optimisation of pre-combustion capture for IGCC with a focus on the water balance.

References

- DCC (2008). National Greenhouse Gas Inventory. Department of Climate Change. Canberra.
- DPI (2008). Victoria's energy technology innovation strategy - your energy future lies in victoria. Department of Primary Industries. Victorian Government.
- Gibbins, J. R. and R. I. Crane (2004). "Scope for reductions in the cost of CO₂ capture using flue gas scrubbing with amine solvents." Proceedings of the Institution of Mechanical Engineers Part A - Journal of Power and Energy 218(A4): 231-239.
- Global CCS Institute (2011). The Global status of CCS: 2010. Canberra.
- Herzog, H. (2000). "The economics of CO₂ separation and capture." Technology Vol. 7 Supplement 1: 13-23.
- Ho, M., G. Allinson and D. Wiley (2008). Factors affecting the cost of capture for Australian lignite coal fired power plants Ninth International conference on greenhouse gas technologies (GHGT-9). Washington DC, USA, Elsevier.
- IPCC (2005). IPCC Special Report on Carbon Dioxide Capture and Storage. Prepared by Working Group III of the Intergovernmental Panel on Climate Change B. Metz, O. Davidson, H. C. de Coninck, M. Loos and L. A. Meyer.
- IPCC (2007). Climate Change 2007: Synthesis report.
- Klebes, J., S. Winter, M. Joormann and B. Stover (2010). "Steam Turbines and CO₂ sequestration." VGB PowerTech 12/2010: 74-79.
- Monash Research Graduate School. (2011). "Thesis by Published and Unpublished papers." Retrieved 1/6/2011, from <http://www.mrgs.monash.edu.au/research/examination/thesis-by-publication/index.html>.

Chapter 2

Review of the Integration of Solvent Based Post-Combustion Capture into Coal-fired Power Stations

2. Review of the Integration of Solvent Based Post-Combustion Capture into Coal-fired Power Stations

The concept of separating CO₂ from other gases is not new. Natural gas fields high in CO₂ have a proportion of the CO₂ removed to purify the natural gas. The CO₂ created in generating syngas is removed to supply a high purity hydrogen stream for ammonia production. CO₂ is even separated from flue gases for use in the food and beverage industry (Reddy et al. (2003)) and for the carbonation of brine (Herzog (2000)). So the operating principles of solvent based absorption of CO₂ is well known, however what has not been well known is how to best apply the CO₂ separation technologies to capture a significant proportion of the CO₂ in the flue gas of power stations. There is a high level of research currently underway in solvent based capture of CO₂ from power stations. Furthermore to optimise the process will require a wide understanding of all the components from the flue gas pre-treatment, the solvent process, the CO₂ compression and the steam cycle of the power station.

2.1 Flue Gas Pre-treatment

The solvent capture plant in a power station will be located downstream of any existing flue gas treatment; which may include desulphurisation and denitrification and will generally include dust removal in the form of electrostatic precipitation. The flue gas exiting the stack of an existing pulverised coal-fired power station will generally have temperatures above 100 °C and varying levels of impurities depending on the coal feedstock and the environmental regulations of the region. In Australia the coal feedstock has very low levels of sulphur, and as such the regulations do not require desulphurisation and therefore the levels of sulphur in the flue gas (100 ppm – 700 ppm) are greater than most developed regions of the world. In addition, the brown coal found in Victoria has a high moisture content and is inexpensive to mine, and as a consequence the flue gas being emitted has high temperatures (>180 °C) and high moisture content.

The flue gas pre-treatment required upstream of the solvent plant will depend on the pre-existing level of contaminants in the flue gas and the solvent system employed. However, as a minimum the flue gas will need to be cooled and have the pressure boosted upstream of the solvent absorber, as shown is Figure 1-3.

2.2 Solvent Absorption of CO₂

As described in Chapter 1, conventional solvent capture of CO₂ is a two step process involving an absorption step, where lean solvent is contacted with the flue gas stream to capture the CO₂, and

a second step that occurs in a stripping column where the solvent is either heated or the pressure is reduced to desorb the CO₂ from the solvent, generating a high purity stream of CO₂ and regenerating the solvent which is returned to the absorption column. Absorption is divided between two types of solvents: chemical and physical. In physical absorption, the absorption rate and solvent loading is a function of the solubility of the gaseous solute (CO₂) in the solvent, whereas with chemical absorption, there is a chemical reaction between the solute (CO₂) and the solvent. According to Kohl and Nielson (1997) chemical absorption is more suited than physical solvents to post-combustion capture where the partial pressure of CO₂ is very low; according to GPSA (2004) and UOP (2009), physical solvents will generally be used in pre-combustion capture where the partial pressure of CO₂ is greater than 345 kPa. The optimal absorption process will vary depending on the different feed gas conditions, required purity, contaminant levels, environmental restrictions and availability of utilities, as well as economic considerations.

There are many contaminants that can be part of the flue gas and therefore may end up being part of the final CO₂ stream. These include SO_x and NO_x, metals found in the coal – Hg, As, Se, Cd, Pb, Sb, Cr, Ni, V (IEA-GHG (2004)), Oxygen, Nitrogen, Chlorine, CO and Argon. The impact of these contaminants and whether they need to be removed upstream of the solvent process will largely depend on the choice of solvent. In some circumstances these impurities may follow the CO₂ through the solvent system in which case the level of contaminant that is tolerated in the product CO₂ will very much depend on the storage site requirements. In general, high levels of contaminants are tolerable in the CO₂ as indicated by an IEA-GRG (2004) report which considers separating out the SO₂ using a Cansolv® process and blending it back in with the CO₂. The main reason for avoiding contaminants in the CO₂ is when the CO₂ is used for geological storage the contaminants compete for pore space leading to a greater pore volume requirement per unit of CO₂.

A significant amount of research has and is being conducted on solvent absorption of CO₂. A thorough and detailed review of CO₂ capture from post combustion flue gases by solvent absorption/stripping has been covered by Davidson (2007), Davidson looks mainly at Monoethanolamine (MEA), which he considers the benchmark solvent by which the others are compared. The article reviews a number of factors including solvent degradation, process design and techno-economic aspects of CO₂ capture for post-combustion power stations.

The main contaminants in the flue gas streams that affect the solvent are oxides of sulphur (SO_x) and nitrogen (NO_x), oxygen, carbon monoxide and particulates. Leci (1996) discusses the process selection criteria for absorbents, in particular the impact of impurities. Rao and Rubin (2002), Davidson (2007) and Ho (2007) all discuss the required level of impurities for various solvents. The

recommended maximum economic level of SO_x and NO_x for most solvents is generally below 10ppm (Leci (1996)), however Dave et al (2001) suggest that the economical trade-off for an Australian black coal power station actually favours lower desulphurisation (DeSO_x) and denitrification (DeNO_x) than the recommended levels and allows for the loss of more solvent due to the higher levels of contaminants. Therefore, it is clear that there will be a trade-off between the capital and operating costs of pre-treatment and solvent replacement costs due to degradation. Alternatively it is possible with some solvents that the need for pre-treatment could be reduced significantly, Endo et al (2008) are looking at removing the need for DeSO_x and DeNO_x when using potassium carbonate based processes by separating the contaminants as K₂SO₄ and KNO₃ in a reclaimer. This has the benefit, particularly in Australia, of not needing to add DeSO_x and DeNO_x equipment and producing a stream of potassium sulphates and nitrates that may be useful by-product for sale as fertilisers.

The use of solvent absorption for large scale capture in power stations is being studied extensively. Rao and Rubin (2002), Romeo et al (2008), Gibbins and Crane (2004) and IEA GHG (2006) amongst others all describe power stations using MEA for CO₂ capture. The HiCaptTM process uses high strength MEA (40 wt%) combined with corrosion inhibitors to improve the standard MEA processes which use lower concentrations of MEA (Bouillon et al. (2011)). Gibbins and Crane (2004) and Mimura et al (1997) compare MEA to KS-1/2, a proprietary sterically hindered amine and found reductions in the solvent regeneration energy requirements with KS-1/2. The use of carbonates with and without promoters is being studied by the CO2CRC (Ghosh et al. (2008)) and Cullinane and Rochelle (2004) amongst others. The use of potassium carbonate promoted by piperazine by Oyeneke and Rochelle (2009) has also lead to study of concentrated piperazine as a stand-alone solvent by the same group at the University of Texas (Plaza et al. (2011)). There is also research into precipitating potassium carbonate processes which should reduce the energy requirements of the potassium carbonate process (CO2CRC Technologies Pty Ltd (2011), Svendsen et al. (2008), Schoon and Straelen (2011)). There are a number of proprietary solvents and solvent systems that are in various stages of development including; Chilled ammonia systems by Alstom (2006), Econoamine FG Plus by Fluor (Reddy et al. (2003)), PSR (Veawab et al. (2001)), AMP(methylaminopropanol)(Yeh and Pennline (2001)), CORAL (Feron and Jansen (2002)), a combination of AMP and piperazine in CESAR-1 (Knudsen et al. (2011)) , a proprietary amine system developed by HTC Pureenergy, an amino acid salt process called the PostCapTM process developed by Siemens (Schneider and Schramm (2011)), and GUSTAV 200 by BASF (Stoffregen (2011)). Due to the proprietary nature of many of the solvents the level of detail

provided for each solvent and solvent process varies considerably. Additionally, a significant amount of the solvent systems are only at the demonstration stage of development.

2.3 CCS Energy Penalty

The technology to capture CO₂ is available; however it may still be immature technology for implementation on flue gas at the scale of the equipment required. The main reason that CCS is slow to be implemented is the cost of constructing and operating the CCS plants with power stations. Without any regulations forcing power generators to reduce CO₂ emissions, or any financial incentives such as a price on carbon, either by a carbon tax or an emissions trading system, then there is no enticement for a commercial power generator to turn to CCS.

The cost of implementing CCS has been estimated, per tonne of CO₂ avoided, at between US\$29 and US\$51 for post combustion capture and US\$13 and US\$37 for precombustion capture (Gibbins and Crane (2004), IPCC (2005), Ho (2007)). Implementation of CCS will vary depending on the technology used, the location of the power station, the location and quality of the storage site and the design of the power station itself. Much of the cost of CCS is due to the amount of energy that is required to capture and transport the CO₂ from the flue gas, often referred to as the energy penalty of CCS. All the methods to capture CO₂ from the flue gases of power stations require significant amounts of energy to operate. Solvent absorption requires energy for solvent regeneration and solvent pumping, membrane systems and pressure/vacuum swing adsorption systems require energy to provide pressure differentials, temperature swing adsorption requires energy for regeneration and cryogenic separation requires energy for refrigeration. Further energy is required in all systems to compress the CO₂ into a supercritical fluid and transport it to the injection site. The efficiency of a power station can be reduced, by the addition of CCS, by approximately 24 to 40 % for PC plants, which equates to the higher heating value (HHV) efficiency of a typical brown coal power station reducing from 28 % down to between 17 % and 21 %. For IGCC plants the energy penalty is potentially lower, with estimates between 14 % to 24 % reductions due to the addition of CCS (Gibbins and Crane (2004), IPCC (2005)).

A number of definitions of energy penalty exist, but they all relate to the amount of energy or the reduction in efficiency from a power station due to the addition of CSS. Ho (2007) uses the definition provided by Equation [1], whilst the IPCC (2005) prefer the definition provided by Equation [2]. Equation [1] represents the reduction in efficiency of a power station, whilst equation [2] represents the increase in resource requirements to generate the same amount of power. A further definition of the energy penalty used by Oexmann et al. (2008) is provided in Equation [3] and it shows the reduction in power generated from the power station for each unit

of CO₂ captured. It can be useful for comparing the impact of the same capture technology on different types of power stations. Equations [1] and [3] are used throughout this work as they are good measures of the reduction in the energy output, which is usually more relevant for retrofitting power stations.

$$\text{Energy Penalty} = \Delta E = 1 - (\eta_{\text{CCS}} / \eta_{\text{ref}}) \quad [1]$$

$$\text{Energy Penalty}^* = \Delta E^* = (\eta_{\text{ref}} / \eta_{\text{CCS}}) - 1 \quad [2]$$

$$\text{Energy Penalty} = \Delta E = (P_{\text{ref}} - P_{\text{CCS}}) / \text{amount of CO}_2 \text{ captured} \quad [3]$$

The energy required for CCS plants can come from the power station itself or from an auxiliary power source, of course when an auxiliary power source is provided the CO₂ produced from the auxiliary power source must be taken into account. It is important to consider the loss of energy output from a power station or the additional amount of CO₂ produced to power the CCS equipment, which is why it is necessary to report the cost of CCS as the cost per tonne of CO₂ avoided and not the cost per tonne of CO₂ captured. Allinson et al (2007) provide a detailed argument to show why the cost of CO₂ avoided is much more important than the cost of CO₂ captured.

The energy penalty can be reduced in a number of ways, many of which are specific to the capture technology employed. For absorption, the solvent regeneration energy can be lowered by varying the solvent or the total reboiler energy can be lowered by improved process design of the solvent plant as detailed by Jassim and Rochelle (2006) and Davidson (2007). Simple changes to the absorber and stripper packing can improve the performance of a solvent (Svendsen et al. (2011)), however further examples of more elaborate improvements are provided by the Fluor Econamine Plus process, which uses a combination of improved solvent formulation coupled with an improved process layout to reduce the total energy consumption, up to 20% reductions have been achieved in pilot studies compared to original MEA plants (Reddy et al. (2003)). Le Moullec and Kanniche (2011) also simulated a number of variations in process flowsheets of solvent based CO₂ capture using MEA, including absorber intercooling, staged feed of stripper, split flow arrangements, stripper overhead recompression, stripper bottoms vapour recompression, stripper intermediate compression, rich solvent flashing and multi-column regeneration to reduce the energy penalty. Whilst the CESAR project (Knudsen et al. (2011)) actually installed absorber intercoolers and vapour recompression to determine the practical performance improvements in these process modifications. Plaza et al. (2011) have also looked at an inter-heated stripper column which reduces the thermal energy of regeneration by an estimated 10 %. However, often

in the analysis the re-use of heat available in the solvent process is not taken into consideration and therefore the energy penalty can also be improved by better integration of the technologies with the power stations.

Ho et al (2008) report that the cost of CCS can be reduced by 25 % if the energy penalty can be reduced by 25 %. Many authors have reported energy savings by better integration of the CCS plant with the power station. Aroonwilas and Veawab (2007) and Romeo et al (2008) state that the optimal location to extract power for a solvent system is from the LP turbine at the appropriate pressure to provide steam at lowest quality that satisfies the solvent system reboiler requirements. Mimura (1997) uses 14 % of the stripper condenser energy to heat the boiler feed water, Desederi (1999) and Romeo (2008) suggest utilizing some of the available heat from the CO₂ compressor intercoolers to heat the boiler feed water. Bozzutto (2001) uses an auxiliary turbine with steam from the IP/LP crossover to provide the steam at the required quality for the solvent reboiler, this method was considered by Zachary (2008) to provide the most efficient method of providing steam at the correct quality of steam compared to using throttling valves, floating pressure or clutch arrangements for dealing with steam extracted between the IP/LP turbines. An IEA GHG report (2006) utilizes a number of waste heat streams to increase the overall plant efficiency, they produce hot water for coal pre-drying in the flue gas line prior to the flue gas desulphurisation (FGD), the stripper condenser and the CO₂ compressor intercoolers and they also heat the boiler feedwater using the stripper condenser and CO₂ compressor intercoolers, completely removing the need for the existing boiler feedwater heaters. Pfaff et al (2009) integrates heat from the stripper condenser and the CO₂ compressor to heat the boiler feed water, which in turn is used to provide heat for the air-preheat. Pfaff et al. (2009) also look at providing less intercooling in the CO₂ compressors to provide additional heat for the boiler feed water, and in this case reducing the number of intercoolers from eight to two provided the best efficiency. Whilst in the paper they manage to reduce the energy penalty from 23 % to 21 %, there does not appear to be a systematic method to which the integration opportunities are tested. Jassim and Rochelle (2006) found that the optimised multiple pressure stripper required 3 % to 11 % less equivalent work than the equivalent simple solvent system. The solvent system for the multiple pressure stripping utilises waste heat from the compressors to reduce the reboiler requirement; however the study did not review whether this heat may also be better utilised within the power station itself to improve the overall efficiency at a reduced cost.

Alie et al (2001) review parameters in the MEA system of absorber height, lean solvent loading, stripper height and stripper temperature and look at the impact that these parameters have on the overall power output of a power station assuming that the reboiler energy is provided by

steam from the IP turbine. For each case the scenario that reduces the reboiler energy is also the same case that leads to the highest power output, except for the absorber height. As the absorber height is increased the blower energy increases and eventually becomes greater than the energy saved by reducing the reboiler heat.

Stankewitz et al (2009) used an ammonia Rankine cycle to generate more energy from the waste heat available in an MEA capture plant retrofitted to a power station. The energy penalty reduced from 28 % without the ammonia Rankine cycle to 22 % with it. However, the cooling water on the ammonia condenser is operated at 15 °C to 20 °C and therefore the same level of benefit would not be expected from warmer climates.

As can be seen, a number of different combinations have been suggested to utilise the waste heat to reduce the energy penalty associated with the addition of CCS to a power station. However, no study appears to use pinch analysis or MOO to systemically integrate the CCS plant with the power station or look at changes to the current design practices for power stations to include CCS.

2.4 Heat Integration of Power stations

Pinch analysis is the systematic analysis of the energy flow of a process, it is based on the first and second laws of thermodynamics in that energy must be conserved and that heat will flow in only one direction. Smith (2005) provides a detailed overview of the techniques of pinch analysis. However in summary, the temperature-enthalpy relationship of all the streams that require cooling in a process are aggregated and all the streams that require heating are aggregated into what are called the hot and cold composite curves (Refer to Figure 2-1). Heat exchange between the hot and cold composite curve can be maximised whilst there is a temperature difference between the two curves. For a given minimum temperature difference (ΔT_{\min}) the minimum hot and cold utility requirements can be determined. Determining the minimum energy requirements (MER) can be automated by the use of the Problem Table Algorithm (Linnhoff and Flower (1978)), which involves dividing the problem process into temperature intervals that have been shifted to increase the cold streams by $\frac{1}{2}\Delta T_{\min}$ and decrease the hot streams by the same amount, and then cascading surplus heat from the highest to lowest temperature to determine the minimum hot utility and concurrently the minimum cold utility. This cascade of heat is represented graphically using the grand composite curves (GCC) (Refer to Figure 2-2).

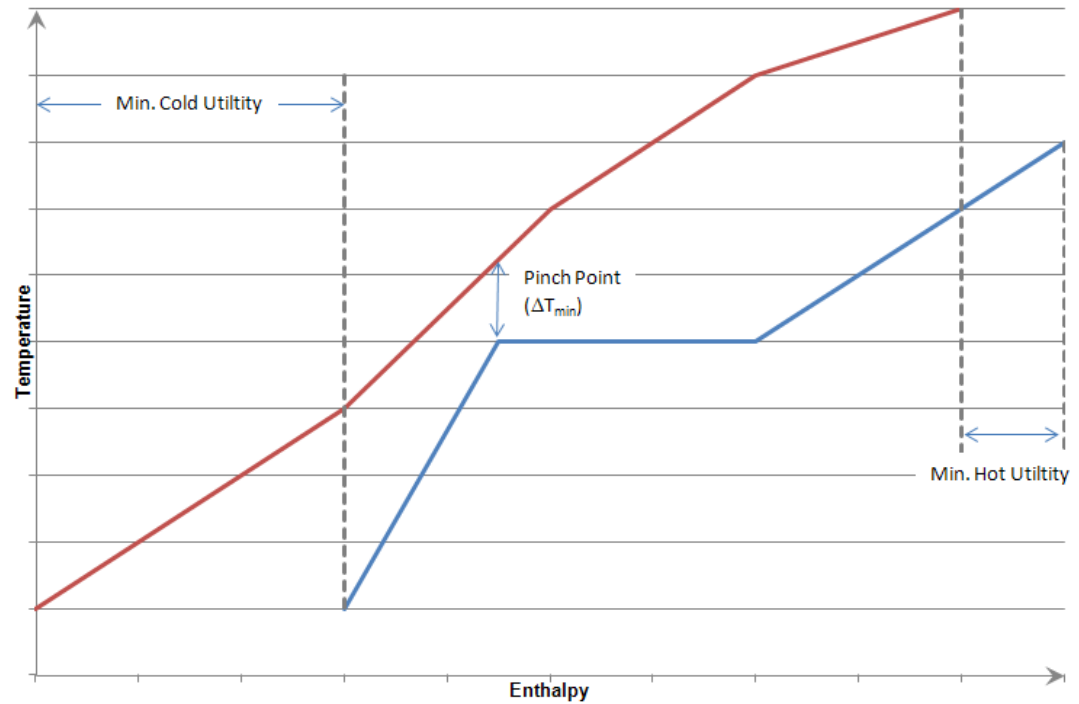


Figure 2-1: Example of the fundamentals of pinch analysis; the hot (—) and cold (—) composite curves.

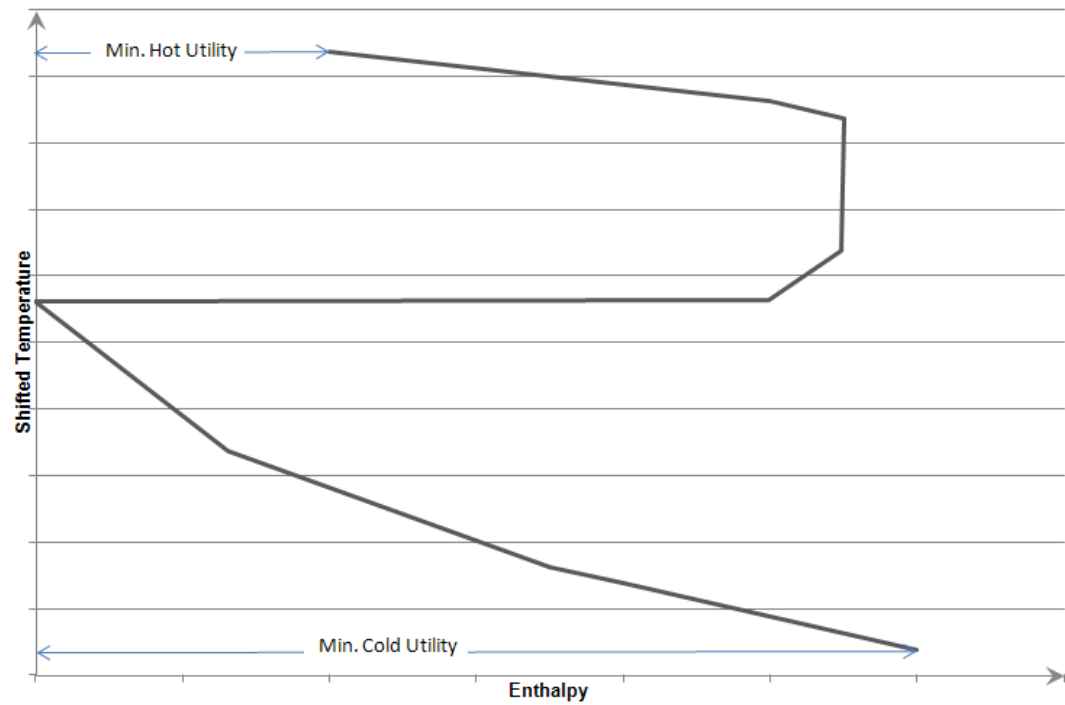


Figure 2-2: Example of the grand composite curve showing the minimum hot and cold utilities.

Although widely used in the processing industries, pinch analysis as a means of improving power station design has not been widely reported. A paper by Linnhoff and Alanis (1989) used pinch

analysis to show how it is possible to improve the efficiency of a power station. They used pinch analysis to reduce the fuel use by 2.8 % by determining the optimum amount of steam extracted from the turbines for a given number of boiler feedwater heaters and utilising topping and intermediate de-superheaters to achieve the required heat transfer. So although there has been little publicised about employing pinch analysis for use with power stations, this paper suggests, at least from an energy perspective, that it's use is well worth considering.

With the addition of CCS to a power station, there are additional hot streams; for a CCS plant using solvent absorption the flue gas is a hot stream as it will need to be cooled down for FGD and CO₂ capture, the lean solvent cooler, the stripper condenser and the CO₂ compressor intercoolers are also hot streams; there are also additional cold streams in the stripper reboiler and potentially the regeneration for the CO₂ dehydration process. Pinch analysis will enable the systematic review of the power station to ensure the plant with the new equipment and new heat sources and sinks are matched to maximise the efficiency of the process. With the addition of CCS equipment the power station now becomes more like a processing plant with both heat and power generation required. Therefore techniques reported by Linnhoff (1986) and Smith (2005) for furnace design and Smith (2005) for cogeneration of heat and power may be useful tools to redesign the power station with the new requirements of CCS included.

2.5 Utility Targeting

Various methods have been developed to determine the amount and in some cases the pressure of steam required to supply process heating demands. Some of those methods take into consideration the amount of cogeneration power that can be generated, however, only a few methods are suitable for optimising power stations.

Dhole and Linnhoff (1993) developed total site profiles from composite curves of all of the processes on a site by excluding the 'pockets' in the individual GCC's and combining the rest of the sources and sinks to form total site source sink profiles. Using the total site profiles steam targets can be found graphically including calculation of cogeneration power, however the method is based on steam as a constant temperature heat supply, does not include the boiler feedwater heating or ability to optimise the heat exchange between the process and the utility for steam generation (Refer to Figure 2-3).

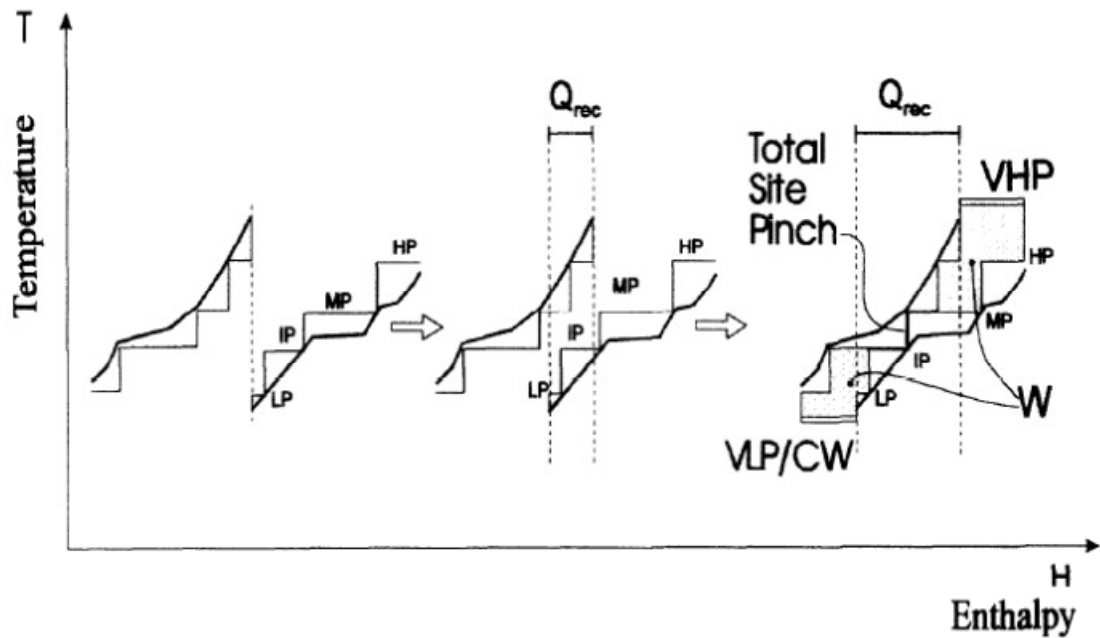


Figure 2-3: Total site composite curves and the total site pinch (Klemes et al. (1997)).

The total site profiles method has been extended by Mavromatis and Kokossis (1998a; 1998b) into the THM model which added steam turbine network optimisation of the cogeneration potential from total site profiles. The method decomposes complex turbines into a number of simple turbines, allows for variations in turbine efficiency at full and part load and optimises the range of options. The total site profiles and turbine network models are the basis of many methods (Klemes et al. (1997), Varbanov et al. (2004a; 2004b), Shang and Kokossis (2005), Gorsek et al. (2006), Bandyopadhyay et al. (2010)) for top level analysis and optimisation of utility systems. There are also many alternatives to the THM method just for shaftwork targeting which includes the T-H method by Raissi (1994), the bottom-up and top-down procedure (Kapil et al. (2010)) and the iterative bottom to top method (IBTM) (Ghannadzadeh et al. (2011)). However these methods are designed for process plants where the production of power is secondary to the production of another commodity. As such, these methods generally neglect the opportunity to integrate the power station with the process plant, and therefore do not rigorously include the sensible heat in the generation and usage of steam. Botros and Brisson II (2010) showed the importance of including the sensible heat components to maximise the power generation potential, but did not provide a method to determine the optimal design of a steam cycle to obtain that potential.

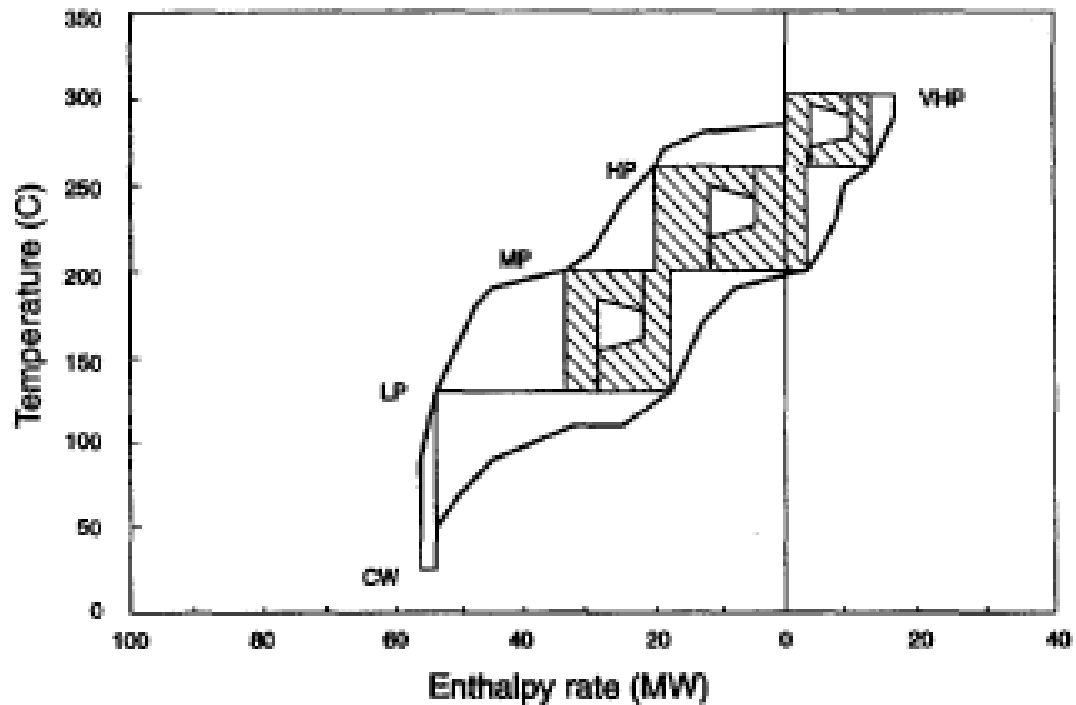


Figure 2-4: THM model used to estimate the potential for power production from steam turbines for total sites (Mavromatis and Kokossis (1998a))

Papoulias and Grossmann (1983) use a superstructure approach to optimising steam networks for process heating using mixed integer linear programming (MILP) to find an optimum. Their superstructure is made up of linearised representations of the processes, utility options and the cost functions. Although it will find an optimum solution to the given problem, it may not find the global optimum due to the linearisation of the problem and because there is also no interaction between the utility system and the process. Salama (2009) optimises the amount of each utility for multiple utilities using a geometrical approach to heat integration where the horizontal difference between the hot and cold composite curves are used to fit the utilities rather than the traditional problem table algorithm. The method finds the optimum amounts of utilities directly using a linear programming optimisation, but it is used to minimise the utility requirements rather than optimise the power generation.

Marechal and Kalitventzeff (1991) developed a mixed integer linear programming (MILP) algorithm to determine the minimum cost of energy requirements (MCER) rather than just the minimum energy requirements that are obtained by the problem table algorithm. They converted the problem table algorithm into a MILP formulation where the objective is to minimise the energy input of the utility by satisfying the constraints that are defined by cascading heat from the hottest to the coldest temperature, for every temperature interval defined by a process. Utilities, such as heater or steam cycle are then characterised by their intensive properties which define

the heat profile. The flowrates of each utility, the extensive property of the utilities, which provide the magnitude of the heat profile then become the variables in the MILP formulation. Each utility also has a linear cost function and the summation of the cost functions becomes the minimisation objective, rather than the minimisation of the utility energy consumption. They use a Rankine steam cycle as an example of a utility that can use the MILP approach and the impacts of the condensate preheating and the steam superheating and de-superheating can be taken into account in the MILP formulation.

Kalitventzeff (1993) used GCC's of an overall chemical complex and for individual processes within the complex to show how a steam network can be used to facilitate heat transfer between two processes. This helped to reduce the overall complex MER whilst maintaining a level of independence between the two processes. The same methodology is used by Marechal and Kalitventzeff (1996) with the development of the "integrated composite curves" (ICC), which show graphically the results of the MILP method. The ICC shows the GCC of the utilities separately from the rest of the process and allows the integration of the utilities with a process to be visualised (Refer to Figure 2-5).

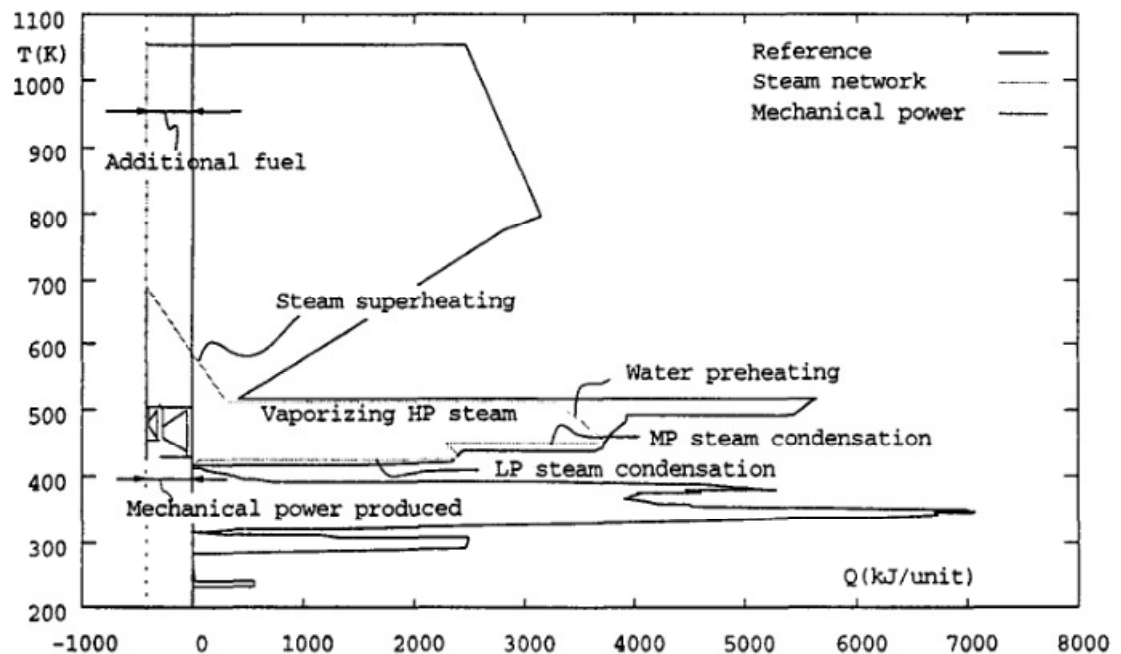


Figure 2-5: Integrated composite curves (Marechal and Kalitventzeff (1996))

As the steam network pressure must be fixed to use the MILP formulation, Marechal and Kalitventzeff (1997) developed an additional step in their optimisation routine to determine the optimal pressure levels of the steam networks prior to the use of the MILP formulation. The method, referred to as the integrated combined heat and power approach (ICHP) assumes that the mechanical power of the Rankine cycle is proportional to the area, which can be estimated by

rectangles on a temperature-enthalpy diagram. The height of the rectangle is fixed by the condensing / vaporisation temperatures of the steam, whilst the horizontal distance is determined by the available heat in a process. An algorithm was developed to automatically determine the best combination of rectangles to maximise the power produced by the Rankine cycles for a given process GCC. The steam cycles are then rigorously evaluated using the optimum pressures that were determined.

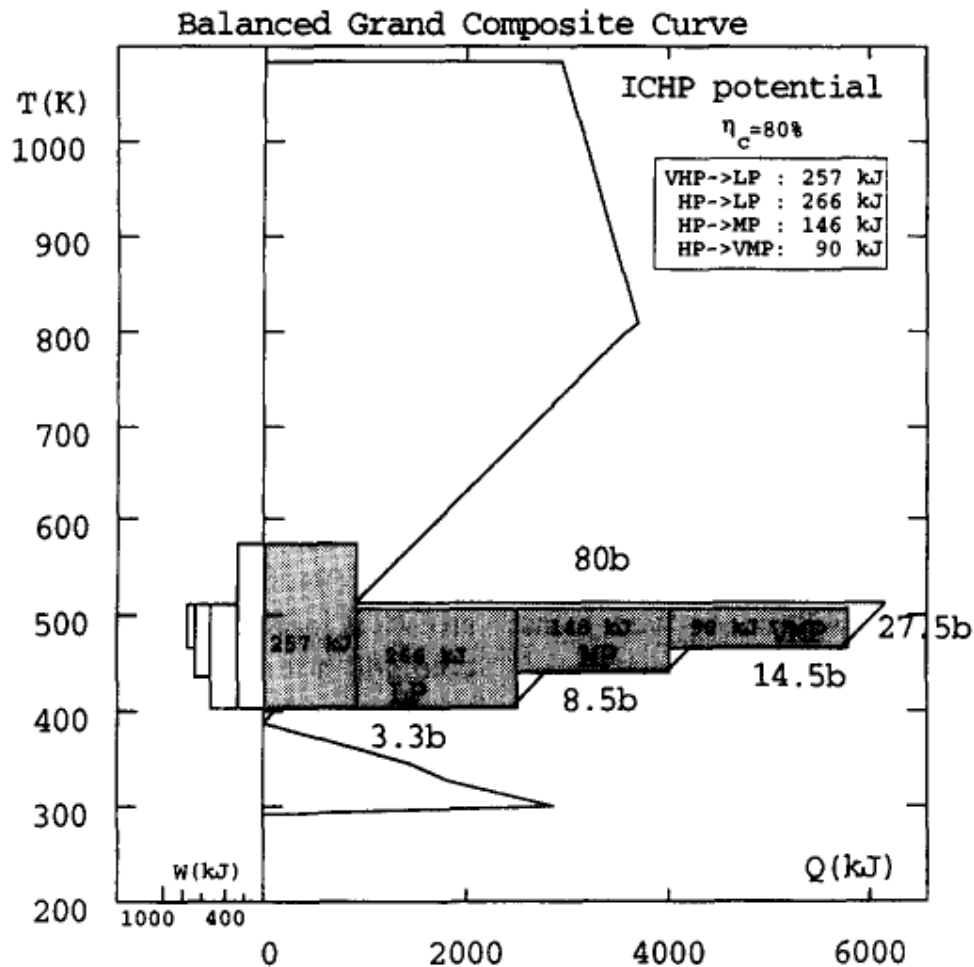


Figure 2-6: Graphical representation of the determination of the optimal pressure levels using the Integrated combined heat and power approach (ICHP) (Marechal and Kalitventzeff (1997)).

The MILP method uses linear models of the primary utilities, Marechal and Kalitventzeff (1998) provides details to many aspects of the linear models used for combustion processes, enriched air combustion, gas turbines and gas and diesel engines. The models also enable the MILP optimisation of specific parameters including air preheat and excess air.

A steam network superstructure was then developed by Marechal and Kalitventzeff (1999) to use with the ICHP method. The steam cycle utility superstructure includes multiple steam headers which are connected by multiple expansion turbines and isenthalpic let-down valves with direct

water injection for de-superheating the steam into the headers. Heat exchangers are included to utilise heat from the steam extracted from the steam headers or for steam generation to each of the steam headers. The network still uses a MILP formulation to minimise the cost of satisfying the minimum energy requirements by determining the optimum flowrates of the various streams in the network.

2.6 Multi-Objective Optimisation (MOO)

In process design there are often many objectives in the design and often those objectives are conflicting, where an improvement in one objective will lead to the deterioration in another. Early attempts to optimise such problems were performed by placing varying emphases / weightings on each of the objectives and optimising for the combined single objective. However, since 2000 over 80 articles have been written on using MOO in chemical engineering applications (Lee et al. (2008)). MOO enables a range of optimum solutions called Pareto-optimal solutions for conflicting objectives where each option is said to be non-dominated by other solutions, which means that the options although they may be better for one objective they will be worse for another objective. For example; if the multiple objectives were capital cost and efficiency obviously the motive would be to maximise the efficiency and minimise the capital cost, however normally it will be difficult to make changes that assist in both of these aims. Therefore, there will be a range of solutions from cheap but inefficient designs through to efficient but expensive designs, where each option is not necessarily better when considering both objectives as being equal important. This example is shown in Figure 2-7; the blue diamonds represent the Pareto-optimal solutions, whilst the red squares represent other solutions that are not Pareto-optimal solutions. The solutions represented by red squares are dominated by the Pareto-optimal solutions as for a given capital cost the efficiency is lower than those given by the Pareto-optimal solutions or the capital cost is higher for a given efficiency. The theory of MOO as applied to process design problems is detailed by Bhasker et al (2000) and Lee (2008).

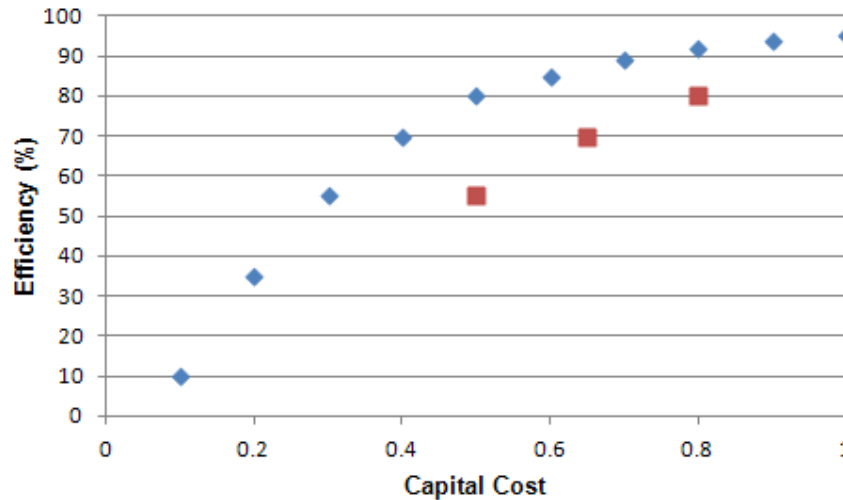


Figure 2-7: Example of a set of Pareto-optimal non-dominated solutions (◆) and three dominated solutions (■). The objective of the optimisation is to maximise the efficiency and minimise the capital cost.

There are a number of algorithms that have been applied for MOO problems and these are covered in detail by Deb (2001), Leyland (2002) and Konak et al. (2006). Deb (2001) suggests many advantages of using evolutionary algorithms (EA's) over optimisation techniques that use a single solution update in every iteration and that mainly use a deterministic transition rule, which he refers to as 'classical' optimisation techniques. The 'classical' optimisation techniques often have disadvantages when dealing with non-linear discontinuous problems with discrete solution regions such as those found in process design problems, those disadvantages include;

- Convergence to an optimal solution dependent on the initial chosen solution
- May converge to a sub-optimal solution
- Algorithms are not always efficient in handling problems with discrete search regions
- Algorithms cannot be used efficiently on parallel machines

A number of evolutionary algorithms have been designed to overcome the disadvantages reported for 'classical' optimisation techniques including; NSGAII (Nondominated sorting genetic algorithm) developed by Deb et al (2002), QMOO (Queuing multiple objective optimisation) used by Leyland (2002) and numerous others including VEGA (Vector evaluated genetic algorithm), MOGA (multi-objective genetic algorithm), NPGA (Niche Pareto genetic algorithm), SPEA (strength Pareto genetic algorithm) and DMOEA (Dynamic multi-objective evolutionary algorithm) which are detailed by Konak et al. (2006). Both NSGAII and QMOO have been used in optimisation of chemical engineering problems. NSGAII differs to QMOO in the way the algorithm develops the next set of population (children), in the preservation of elitism (preserving the best non-dominated species in the population) and preservation of diversity in the population. QMOO is

designed to cater for parallel computing and thus works extremely well with problems associated with energy systems where determining the objective functions can require significant computing time compared to the population generation and ranking steps. However the QMOO methods for asserting convergence pressure and even coverage do not work as well for problems with more than two objectives (Leyland (2002)). The NSGAI algorithm is shown (Deb et al. (2002)) to converge to a Pareto-optimal front comparable or better than a number of other EA's and is able to maintain a good spread of solutions across the Pareto-optimal front. The NSGAI source code is also freely available and an Excel version of the code has been produced by Sharma et al. (2011).

A number of authors have applied NSGAI code to process design problems; a hydrocracking unit was optimised by Bhutani et al (2006), a batch chemical process by Sarkar and Modak (2006) and a heat exchanger network was optimised by Agarwal and Gupta (2008). These involved optimising problems that were set up in programming languages (FORTRAN, C++, Visual Basic etc) and interfaced with the NSGAI code directly.

Bhutani et al. (2007) developed a multi-platform multi-language environment (MPMLE) using NSGAI coded in C++ for optimisation. HYSYS® provided the steady-state mass and energy flow model of a styrene plant and Visual Basic was used to interface between the simulation and the optimisation algorithm (Refer to Figure 2-8). The paper compared the optimisation of a styrene reactor created in HYSYS® to a model that was coded in FORTRAN and compared the results of the optimisation of the two using NSGAI. The computation time of the HYSYS® model was over 100 times longer than the model created in Fortran and therefore the overall optimisation using HYSYS® was considerably longer than Fortran, however he considered there to be other benefits for using the HYSYS® model compared to models developed in other languages. The benefits of using commercial process simulation packages like Aspen Plus® and HYSYS® is that they are commonly used in the process industries, have robust physical property packages, do not require as detailed programming skills and will usually be quicker to develop. Therefore, although the computational time to optimise problems using MPMLE will often be longer than specially designed models, the overall process will normally be shorter and will require less programming knowledge. The MPMLE developed by Bhutani et al. (2007) has also been used successfully by Shah et al. (2008) for the optimisation of refrigeration to liquefy natural gas.

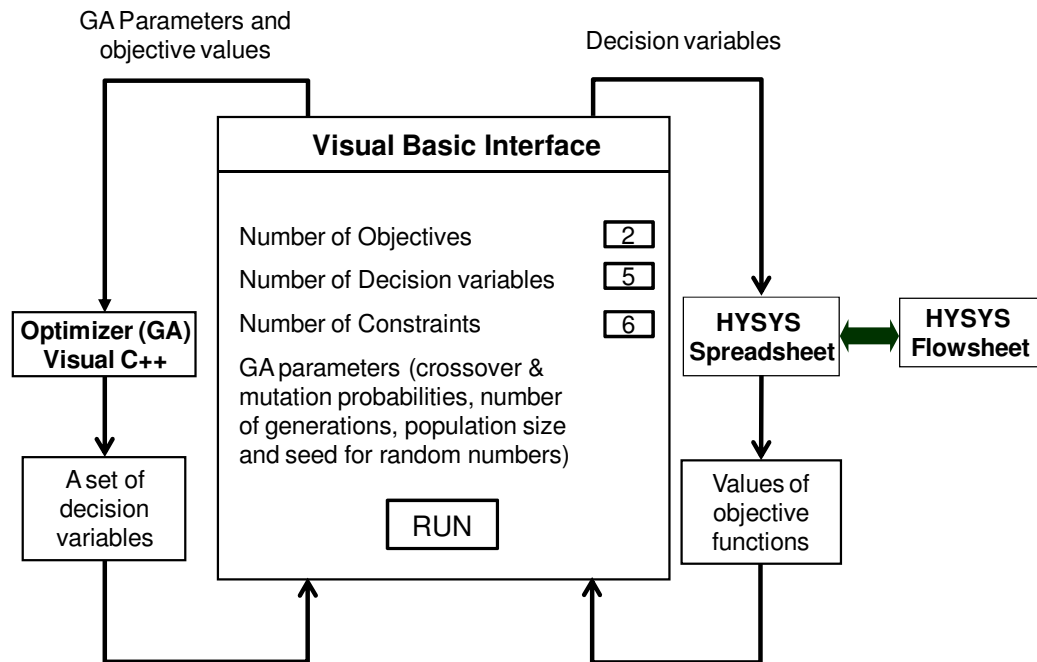


Figure 2-8: Graphical representation of the multi-platform multi-language environment (MPMLE) (Shah et al. (2008)).

Optimisation of power stations and cogeneration plants using genetic algorithms was performed by Pelster et al. (2001) who looked at a range of configurations for natural gas combined cycle (NGCC) power stations and determined the optimal configurations and operating variables for given economic conditions. The model was extended by Li et al. (2006) and Li et al. (2010) into a MOO framework. The first study compared the CO₂ emissions rate to the average cost of electricity (COE) and included an option of CO₂ capture using MEA. The study looked again at various NGCC configurations and their operating parameters, but also included the option of having CO₂ capture using MEA and enhanced gas recirculation. Whilst the second study neglected the option of CO₂ capture, but instead looked at the trade-off between CO₂ emission rates and specific investment costs for not only NGCC, but also stand alone gas turbines and engines. It shows that the COE for NGCC is highly dependent on the natural gas price and that in the European market it will generally be higher than the COE for coal, unless CO₂ pollution is internalised.

2.7 MOO and Heat Integration

Heat integration is useful for identifying the minimum energy requirements of a utility but is limited by needing to assume minimum approach temperatures; whereas MOO is able to provide a process to compare antagonising objectives but generally requires the process configurations to be identified or indeed a superstructure to be identified prior to the optimisation. Therefore,

combining heat integration and MOO allows the minimum energy requirements for a process to be calculated for a range of different assumptions, which means the minimum approach temperatures in the heat integration can vary and the heat exchanger network does not need to be defined at the process design stage of the optimisation. Although combining MOO and heat integration appears to be a very useful methodology the practise has been very limited to date, and only two studies have been found that have combined the two techniques.

Girardin et al. (2009) used the MILP method of heat integration developed by Marechal and Kalitventzeff (1991) and combined it with an evolutionary algorithm to determine the optimum steam cycle for an NGCC power station. They determined a Pareto front of the minimisation of the investment cost to the maximisation of the power output. Then using those solutions, they were able to estimate the levelised COE to determine the lowest COE. Under the economic conditions studied, they determined that three expansion levels in the steam resulted in the lowest COE.

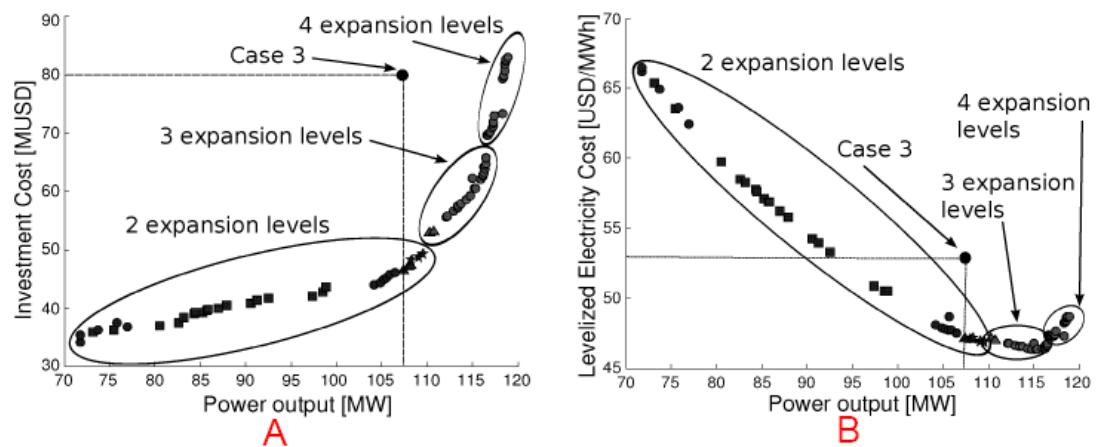


Figure 2-9: (A) NGCC Investment Cost versus power using 2, 3 or 4 steam levels. (B) The levelised COE versus power output for the optimisation solutions shown in A (Girardin et al. (2009)).

Even more recently Bernier et al. (2010) also used MOO for NGCC's, but included the option of CO₂ capture. The MEA capture plant was modelled in Aspen Plus® allowing the operating parameters of the capture plant to be varied during the optimisation. This paper therefore combined linear models of the NGCC plant, with simulations of the carbon capture equipment and the MILP optimisation of the steam cycle in a MOO optimisation framework. Rather than using the CO₂ emissions rate as one objective, the study used a life cycle assessment to determine the global warming potential of a process so that technology improvements that reduced methane could also be taken into account.

2.8 Integration of Solvent Based Post-Combustion Capture into Coal-fired Power Stations

As is noted in Section 2.3 the integration of CCS to power stations can be improved by ensuring that heat is utilised in the process in an efficient manner, however the attempts of most studies are not completed in a systematic method so it is difficult to determine with any confidence that the design is optimal. Heat integration using pinch analysis has proved itself to be a useful tool in minimising the utility requirements of chemical processes and cogeneration facilities. Even though pinch analysis has been used only sparingly for power stations, the benefits are possible and with the addition of the CCS equipment to a power station it starts to look more like a cogeneration plant where the benefits of pinch analysis are well established.

MOO is becoming an increasingly popular method for optimisation in the field of process design and its use on power stations to compare investment costs with efficiency is also well established. The benefits of combining MOO and heat integration have only been looked at very recently and on both occasions they were in the NGCC power generation sector. Combining heat integration and MOO requires an automated heat integration approach which can be completed using either the problem table algorithm or a linear programming approach as shown in Section 2.5.

Until the paper by Bernier et al. (2010) MOO and heat integration had not been applied to CCS for the power sector. Although there were certainly attempts to optimise the solvent CO₂ capture processes, in particular the reboiler energy or an equivalent electrical energy, these optimisation strategies invariably neglected to account for the potential for heat integration between the solvent process and the power station.

Given the objectives of this thesis, pinch analysis has not been widely used for CCS projects, and although MOO has been used for CCS projects, it has only been combined with heat integration by Bernier et al. (2010). There is certainly a gap in the use of heat integration for coal fired power stations with CCS projects, which has not been reported elsewhere. Where MOO and heat integration have been used together previously, it has been for greenfield NGCC power stations and there has not been any studies combining MOO and heat integration for a retrofit situation. The Bernier et al. (2010) paper used the steam network developed by Marechal and Kalitventzeff (1999) and therefore used saturated steam for heating purposes, utilising the benefits of the higher temperatures of superheated steam extracted from the turbines has not been explored. The previous studies have also only looked at the design of MEA solvent systems, whereas potassium carbonate systems allow a much wider range of operating variables and therefore a much greater potential for new flowsheet configurations and for optimisation in general.

References

- Agarwal, A. and S. K. Gupta (2008). "Multiobjective optimal design of heat exchanger networks using new adaptations of the elitist nondominated sorting genetic algorithm, NSGA-II." Industrial & Engineering Chemistry Research 47(10): 3489-3501.
- Alie, C. F. (2001). Simulation and optimization of a coal-fired power plant with integrated CO₂ capture using MEA scrubbing. Chemical Engineering. Masters of Applied Science in Chemical Engineering Thesis, University of Waterloo, Waterloo, Ontario.
- Allinson, G. and P. Neal (2007). Rules of thumb for adding the costs of capture and storage. CO2CRC Research Symposium 2007, Swan Valley, WA, Australia.
- Alstom. (2006). "ALSTOM to build pilot plant in the US to demonstrate its unique CO₂ capture process." Retrieved 3/2/2009, from www.power.alstom.com/pr_power_v2/2006/october/27531.EN.php?languageId=EN&dir=/pr_power_v2/2006/october/&idRubriqueCourante=32205.
- Aroonwilas, A. and A. Veawab (2007). "Integration of CO₂ capture unit using single- and blended- amines into supercritical coal-fired power plants: Implications for emission and energy management." International Journal of Greenhouse Gas Control 1(2): 143-150.
- Bandyopadhyay, S., J. Varghese and V. Bansal (2010). "Targeting for cogeneration potential through total site integration." Applied Thermal Engineering 30(1): 6-14.
- Bernier, E., F. Marechal and R. Samson (2010). "Multi-objective optimization of a natural gas-combined cycle with carbon dioxide capture in a life cycle perspective." Energy 35: 1121-1128.
- Bhasker, V., S. K. Gupta and A. K. Ray (2000). "Applications of multiobjective optimization in chemical engineering." Reviews in chemical engineering 16(1): 1-54.
- Bhutani, N., A. K. Ray and G. P. Rangaiah (2006). "Modeling, simulation, and multi-objective optimization of an industrial hydrocracking unit." Industrial & Engineering Chemistry Research 45(4): 1354-1372.
- Bhutani, N., A. Tarafder, G. P. Rangaiah and A. K. Ray (2007). "A Multi-platform, multi-language environment for process modelling, simulation and optimisation." International Journal of Computer Applications in Technology 30(3): 197-214.
- Botros, B. B. and J. G. Brisson II (2010). "Steam optimisation with increased flexibility in steam power island design." Chemical Engineering Transactions 21: 313 - 318.
- Bouillon, P. A., E. Lemaire, A. Mangiaracina and C. Tabasso (2011). First results of the 2.25t/h post-combustion CO₂ capture pilot plant of ENEL at the Brindisi coal power plant with MEA from 20 to 40 %wt. 1st post-combustion capture conference. Abu Dhabi, United Arab Emirates: Session 7.

- Bozzuto, C. R., N. Nsakala, G. N. Liljedahl, M. Palkes and J. L. Marion (2001). Engineering feasibility of CO₂ capture on an existing US coal-fired power plant. First National Conference on Carbon Sequestration. Washington.
- CO2CRC Technologies Pty Ltd (2011). A Process and Plant for Removing Acid Gases. Australia.
- Cullinane, J. T. and G. T. Rochelle (2004). "Carbon dioxide absorption with aqueous potassium carbonate promoted by piperazine." Chemical Engineering Science 59(17): 3619-3630.
- Dave, N. C., G. J. Duffy, J. H. Edwards and A. Lowe (2001). Economic evaluation of capture and sequestration of CO₂ from Australian black coal-fired power stations. Fifth International Conference on Greenhouse Gas Control Technologies (GHGT-5), Cairns, CSIRO Publishing.
- Davidson, R. M. (2007). Post combustion carbon capture from coal fired plants - solvent scrubbing. CCC/125. IEA Clean Coal Centre. Cheltenham, UK. CCC/125
- Deb, K. (2001). Multi-Objective Optimization using Evolutionary Algorithms, John Wiley & Sons, Ltd, Baffins Lane, West Sussex, England.
- Deb, K., A. Pratap, S. Agarwal and T. A. M. T. Meyarivan (2002). "A fast and elitist multiobjective genetic algorithm: NSGA-II." Evolutionary Computation, IEEE Transactions on 6(2): 182-197.
- Desideri, U. and A. Paolucci (1999). "Performance modelling of a carbon dioxide removal system for power plants." Energy Conversion and Management 40(18): 1899-1915.
- Dhole, V. R. and B. Linnhoff (1993). "Total site targets for fuel, cogeneration, emissions, and cooling." Computers and Chemical Engineering 17: S101-S109.
- Endo, K., S. Kentish and G. Stevens (2008). The fate of SO_x and NO_x in post-combustion carbon dioxide capture. CO2CRC Research Symposium, Queenstown, New Zealand.
- Feron, P. H. M. and A. E. Jansen (2002). "CO₂ separation with polyolefin membrane contactors and dedicated absorption liquids: performances and prospects." Separation and Purification Technology 27(3): 231-242.
- Ghannadzadeh, A., S. Perry and R. Smith (2011). A new shaftwork targeting model for total sites. 14th international conference on Process Integration, Modelling and Optimisation for Energy Saving and Pollution Reduction, Florence, Italy.
- Ghosh, U., S. Kentish and G. Stevens (2008). "Absorption of carbon dioxide into potassium carbonate promoted by boric acid." Energy Procedia 1(1): 1075-1081.
- Gibbins, J. R. and R. I. Crane (2004). "Scope for reductions in the cost of CO₂ capture using flue gas scrubbing with amine solvents." Proceedings of the Institution of Mechanical Engineers Part A - Journal of Power and Energy 218(A4): 231-239.
- Girardin, L., R. Bolliger and F. Marechal (2009). On the use of process integration techniques to generate optimal steam cycle configurations for the power plant industry. 12th international

- conference on Process Integration, Modelling and Optimisation for Energy Saving and Pollution Reduction (PRES'09), Rome, Italy.
- Gorsek, A., P. Glavic and M. Bogataj (2006). "Design of the optimal total site heat recovery system using SSSP approach." Chemical Engineering and Processing 45(5): 372-382.
- GPSA (2004). Engineering Data Book. Tulsa, Oklahoma.
- Herzog, H. (2000). "The economics of CO₂ separation and capture." Technology Vol. 7 Supplement 1: 13-23.
- Ho, M. (2007). Techno-economic modelling of CO₂ capture systems for Australian industrial sources. School of Chemical Sciences and Engineering. Doctor of Philosophy Thesis, UNSW.
- Ho, M., G. Allinson and D. Wiley (2008). Factors affecting the cost of capture for Australian lignite coal fired power plants Ninth International conference on greenhouse gas technologies (GHGT-9). Washington DC, USA, Elsevier.
- IEA-GHG (2004). Impact of Impurities in CO₂. IEA-GHG
- IEA-GHG (2006). CO₂ Capture in Low Rank Coal Power Plants. IEA Greenhouse Gas R&D Programme. Cheltenham, UK. 2006/1
- IPCC (2005). IPCC Special Report on Carbon Dioxide Capture and Storage. Prepared by Working Group III of the Intergovernmental Panel on Climate Change B. Metz, O. Davidson, H. C. de Coninck, M. Loos and L. A. Meyer
- Jassim, M. S. and G. T. Rochelle (2006). "Innovative absorber/stripper configurations for CO₂ capture by aqueous monoethanolamine." Industrial & Engineering Chemistry Research 45(8): 2465-2472.
- Kalitventzeff, B. (1993). Make use of the utility systems to obtain flexible heat exchanger network satisfying the minimum energy requirement. Energy Efficiency in process technology. P. A. Pilavachi, Elsevier applied science.
- Kapil, A., I. Bulatov, J. Kim and R. Smith (2010). "Exploitation of low-grade heat in site utility systems." Chemical Engineering Transactions 21: 367 - 372.
- Klimes, J., V. R. Dhole, K. Raissi, S. J. Perry and L. Puigjaner (1997). "Targeting and design methodology for reduction of fuel, power and CO₂ on total sites." Applied Thermal Engineering 17(8-10): 993-1003.
- Knudsen, J. N., J. Andersen and J. Jensen (2011). Results from test campaigns at the 1 t/h CO₂ PCC pilot plant in Esbjerg under the EU FP7 CESAR project. 1st Post-combustion capture conference, Abu Dhabi, United Arab Emirates.
- Kohl, A. L. and R. B. Nielson (1997). Gas Purification, Gul Publishing Co. Houston, TX, USA.

- Konak, A., D. W. Coit and A. E. Smith (2006). "Multi-objective optimization using genetic algorithms: A tutorial." Reliability Engineering and System Safety 91: 992 - 1007.
- Le Moullec, Y. and M. Kanniche (2011). Optimisation of MEA based post-combustion CO₂ capture process : flowsheeting and energetic integration. 1st Post Combustion Capture Conference. Abu Dhabi, United Arab Emirates: Session 2b.
- Leci, C. L. (1996). "Financial implications on power generation costs resulting from the parasitic effect of CO₂ capture using liquid scrubbing technology from power station flue gases." Energy Conversion and Management 37(6-8): 915-921.
- Lee, E. S. Q., A. Y. W. Ang and G. P. Rangaiah (2008). "Optimize your process plant for more than one objective." Chemical Engineering 115(9): 60-66.
- Leyland, G. B. (2002). Multi-objective optimisation applied to industrial energy problems Laboratory for industrial energy systems (LENI) Thesis, Lausanne.
- Li, H., F. Marechal, M. Burer and D. Favrat (2006). "Multi-objective optimization of an advanced combined cycle power plant including CO₂ separation options." Energy 31: 3117.
- Li, H. T., F. Marechal and D. Favrat (2010). "Power and cogeneration technology environmental performance typification in the context of CO(2) abatement part I: Power generation." Energy 35(8): 3143-3154.
- Linnhoff, B. (1986). The Process/Utility Interface. Second International Meeting on National Use of Energy. Liege, Belgium.
- Linnhoff, B. and F. J. Alanis (1989). "A systems approach based on pinch technology to commercial power station design." Analysis & Design of Energy Systems: Fundamentals & Mathematical Techniques 10(2) 31-43.
- Linnhoff, B. and J. R. Flower (1978). "Synthesis of heat-exchanger networks 1. Systematic generation of energy optimal networks." AIChE Journal 24(4): 633-642.
- Marechal, F. and B. Kalitventzeff (1991). Heat and mechanical power integration, a MILP approach for optimal integration of utility systems. 22nd Symposium of the working party on use of computers in chemical engineering, COPE'91., Barcelona, Spain, Elsevier.
- Marechal, F. and B. Kalitventzeff (1996). "Targeting the minimum cost of energy requirements: A new graphical technique for evaluating the integration of utility systems." Computers in Chemical Engineering 20(Supp.): S225 - S230.
- Marechal, F. and B. Kalitventzeff (1997). "Identification of the optimal pressure levels in steam networks using integrated combined heat and power method." Chemical Engineering Science 52(17): 2977-2989.

- Marechal, F. and B. Kalitventzeff (1998). "Process Integration : Selection of the optimal utility system." Computers in Chemical Engineering 22(Suppl.): S149 - S156.
- Marechal, F. and B. Kalitventzeff (1999). "Targeting the optimal integration of steam networks: Mathematical tools and methodology." Computers & Chemical Engineering 23: S133-S136.
- Mavromatis, S. P. and A. C. Kokossis (1998a). "Conceptual optimisation of utility networks for operational variations - I. Targets and level optimisation." Chemical Engineering Science 53(8): 1585-1608.
- Mavromatis, S. P. and A. C. Kokossis (1998b). "Conceptual optimisation of utility networks for operational variations - II. Network development and optimisation." Chemical Engineering Science 53(8): 1609-1630.
- Mimura, T., H. Simayoshi, T. Suda, M. Iijima and S. Mituoka (1997). "Development of energy saving technology for flue gas carbon dioxide recovery in power plant by chemical absorption method and steam system." Energy Conversion and Management 38(SUPPL. 1).
- Oexmann, J., C. Hensel and A. Kather (2008). "Post-combustion CO₂-capture from coal-fired power plants: Preliminary evaluation of an integrated chemical absorption process with piperazine-promoted potassium carbonate." International Journal of Greenhouse Gas Control 2: 539-552.
- Oyenekan, B. A. and G. T. Rochelle (2009). "Rate modeling of CO₂ stripping from potassium carbonate promoted by piperazine." International Journal of Greenhouse Gas Control 3(2): 121-132.
- Papoulias, S. A. and I. E. Grossmann (1983). "A structural optimization approach in process synthesis-I: Utility Systems." Computers & Chemical Engineering 7(6): 695-706.
- Pelster, S., D. Favrat and M. R. von Spakovsky (2001). "The Thermoeconomic and Environomic Modeling and Optimization of the Synthesis, Design, and Operation of Combined Cycles With Advanced Options." Journal of Engineering for Gas Turbines and Power 123(4).
- Pfaff, I., J. Oexmann and A. Kather (2009). Integration studies of post-combustion CO₂-capture process by wet chemical absorption into coal fired power plant. 4th International Conference on Clean Coal Technology : Carbon capture technologies II, Dresden, Germany.
- Plaza, J. M., D. H. Van Wagener, P. Fraile, E. Chen and G. T. Rochelle (2011). Modelling CO₂ capture using Concentrated PZ. 1st post-combustion capture conference. Abu Dhabi, United Arab Emirates: Session 5b.
- Raissi, K. (1994). Total Site Integration. PhD Thesis, UMIST, Manchester, UK.

- Rao, A. B. and E. S. Rubin (2002). "A technical, economic, and environmental assessment of amine-based CO₂ capture technology for power plant greenhouse gas control." Environmental Science & Technology 36(20): 4467-4475.
- Reddy, S., J. Scherffus, S. Freguia and C. Roberts (2003). Fluor's Econamine FG Plus Technology. Second National Conference on Carbon Sequestration. Alexandria, VA.
- Romeo, L. M., I. Bolea and J. M. Escosa (2008). "Integration of power plant and amine scrubbing to reduce CO₂ capture costs." Applied Thermal Engineering 28(8-9): 1039-1046.
- Salama, A. I. A. (2009). "Optimal assignment of multiple utilities in heat exchange networks." Applied Thermal Engineering 29(13): 2633-2642.
- Sarkar, D. and J. M. Modak (2006). "Optimal design of multiproduct batch chemical plant using NSGA-II." Asia-Pacific Journal of Chemical Engineering 1(1-2): 13-20.
- Schneider, R. and H. Schramm (2011). Environmentally friendly and economic carbon capture from power plant flue gases: The SIEMENS PostCap process. 1st Post Combustion Capture Conference. Abu Dhabi, United Arab Emirates: Session 3b.
- Schoon, L. and J. Straelen (2011). Development of a precipitating carbonate technology for post-combustion CO₂ capture. 6th Trondheim CCS conference. Trondheim, Norway: Session A5.
- Shah, N., A. F. A. Hoadley and G. P. Rangaiah (2008). Multi-objective optimisation of multi-stage gas phase refrigeration systems. Multi-objective optimisation: Techniques and Applications in Chemical Engineering. G. P. Rangaiah, World Scientific Publishing Company Pty Ltd, Singapore.
- Shang, Z. G. and A. Kokossis (2005). "A systematic approach to the synthesis and design of flexible site utility systems." Chemical Engineering Science 60(16): 4431-4451.
- Sharma, S., G. P. Rangaiah and K. S. Cheah (2011). "Multi-objective optimization using MS Excel with an application to design of a falling-film evaporator system." Food and Bioproducts Processing doi: 10.1016/j.fbp.2011.02.005.
- Smith, R. (2005). Chemical Process Design and Integration. West Sussex, England, John Wiley & Sons Ltd.
- Stankewitz, C., B. Epp and H. Fahlenkamp (2009). Integration of a CO₂ separation process in a coal fired power plant. Fourth International Conference on Clean Coal Technology : Carbon capture technologies I. Dresden, Germany.
- Stoffregen, T. (2011). New results from the PCC pilot plant Niederaussem. 1st Post Combustion Capture Conference. Abu Dhabi, United Arab Emirates: Session 7.
- Svendsen, H. F., F. A. Tobiesen, T. Mejdell and K. A. Hoff (2008). Method for capturing CO₂ from exhaust gas. World Intellectual Property Organization.

- Svendsen, H. F., A. Zakeri and A. Einbu (2011). Characterization of Packing Materials for CO₂ absorption. 1st Post Combustion Capture Conference, Abu Dhabi, United Arab Emirates.
- UOP (2009) "Selexol™ Process."
- Varbanov, P., S. Perry, Y. Makwana, X. X. Zhu and R. Smith (2004a). "Top-level analysis of site utility systems." Chemical Engineering Research & Design 82(A6): 784-795.
- Varbanov, P. S., S. Doyle and R. Smith (2004b). "Modelling and optimization of utility systems." Chemical Engineering Research & Design 82(A5): 561-578.
- Veawab, A., A. Aroonwilas, A. Chakma and P. Tontiwachwuthikal (2001). Solvent formulation for CO₂ separation from flue gas streams. First National Conference on Carbon Sequestration, Washington, DC.
- Yeh, J. T. and H. W. Pennline (2001). "Study of CO₂ absorption and desorption in a packed column." Energy Fuels 15(2): 274-278.
- Zachary, J. (2008). "Options for reducing a coal-fired power plant's carbon footprint: Part I." Power June 2008: 5.

Chapter 3

Reducing the energy penalty of CO₂ capture and compression using pinch analysis

Journal of Cleaner Production 18 (2010) 857 – 866

doi: 10.1016/j.jclepro.2010.02.011

3.1 Introduction

The first research objective of this thesis is to use pinch analysis to identify the minimum energy penalty for a typical solvent system applied to a typical Australian coal fired power station and it is this objective that is addressed in this chapter. However, in addressing this objective it is important to keep in mind that the final objective is to utilise pinch analysis with a multi-objective optimisation strategy, therefore it is important that the method used to develop the minimum energy penalty targets can be automated so that it can be used in conjunction with the optimisation framework.

The first paper, provided in Section 3.3, has two purposes.

The first purpose is to develop a method for applying pinch analysis to a power station retrofitted with CCS that can be automated for further use in an optimisation framework. The hot utility used in pinch analysis for power stations retrofitted with CCS is the steam extracted from the steam turbine. After the heat is extracted from the steam it becomes condensate which is returned to the boiler feed water heating circuit and becomes part of the cold streams. Therefore, as you change the amount of hot utility that is used, the cold composite curves will also change. Therefore, the standard problem table algorithm, as described in Chapter 2 Section 2.4, used for determining the minimum energy requirements is not able to be used in this circumstance and thus a new method has been developed and is detailed in the journal article.

The second purpose of the journal article is to determine the minimum energy penalty targets for typical brown coal fired power stations found in Australia, retrofitted with a state of the art solvent absorption process. In addition, the impacts of combining both CCS and coal pre-drying will be discussed to determine whether there is merit in looking at coal drying for Australian brown coal fired power stations if in the future CCS will need to be retrofitted to those same power stations. This objective is achieved by reviewing the impact of CCS and CCS plus coal pre-drying on two different brown coal fired power stations.

As the journal article found in Section 3.3 is the first article to utilise pinch analysis for the integration of CCS to pulverised coal power stations, a significant amount of the most relevant background material found in Chapter 2 is also provided in the article.

As well as the conclusions detailed in the article, the article manages to show that heat integration may help to reduce the energy penalty associated with the addition of CCS and provides a level of confidence that its inclusion in the optimisation framework will lead to further insight in how to design CCS plants for pulverised coal fired power stations.

The method described in this chapter is applied in Appendices E and F. In Appendix E it was found that the importance of the boiler air pre-heat is reduced with the addition of CCS. There is little benefit to the net power by increasing the air-preheat above the pinch point temperature, which is invariably located at the temperature of the solvent regeneration. The same paper also showed that, in the brown coal fired power station used in the analysis, that modifications to the cold end, the boiler feed water circuit upstream of the economiser and the flue gas downstream of the economiser, will achieve most of the reductions in the energy penalty that are suggested by the heat integration method given in this chapter. In Appendix F the impact of using a novel RAMGEN CO₂ compressor, based on supersonic compression, is compared to conventional in-line single shaft compressors. RAMGEN compressors have the potential for compression ratios of up to ten so that the CO₂ compression ratio of 100 can be performed in two stages rather than the conventional compressors that will require approximately eight stages for the same compression. Therefore, the RAMGEN compressors promise to have lower capital costs, similar power requirements and higher inter/after cooler temperatures. Moreover, the pinch analysis technique described in this chapter enabled the calculation of the improvement in the energy penalty that can be obtained by utilising the higher quality heat from the RAMGEN compressor inter/after coolers in the CO₂ capture and steam circuit.

3.2 Declaration for Chapter 3

Monash University

Declaration for Thesis Chapter 3

Declaration by candidate


In the case of Chapter 3, the nature and extent of my contribution to the work was the following:

Nature of contribution	Extent of contribution (%)
Initiation, key ideas, simulations, methodology, results interpretation, writing of paper.	80

The following co-authors contributed to the work. Co-authors who are students at Monash University must also indicate the extent of their contribution in percentage terms:

Name	Nature of contribution	Extent of contribution (%) for student co-authors only
Andrew Hoadley	Initiation, results interpretation, reviewing of paper.	
Barry Hooper	Initiation, results interpretation, reviewing of paper.	

Candidate's
Signature

	Date 14/12/2011
---	--------------------

Declaration by co-authors

The undersigned hereby certify that:

- (1) the above declaration correctly reflects the nature and extent of the candidate's contribution to this work, and the nature of the contribution of each of the co-authors.
- (2) they meet the criteria for authorship in that they have participated in the conception, execution, or interpretation, of at least that part of the publication in their field of expertise;
- (3) they take public responsibility for their part of the publication, except for the responsible author who accepts overall responsibility for the publication;
- (4) there are no other authors of the publication according to these criteria;
- (5) potential conflicts of interest have been disclosed to (a) granting bodies, (b) the editor or publisher of journals or other publications, and (c) the head of the responsible academic unit; and
- (6) the original data are stored at the following location(s) and will be held for at least five years from the date indicated below:

Location(s)

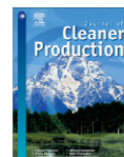
Cooperative Research Centre for Greenhouse gas Technologies, CO2CRC, Room 232, Level 2, Bldg 193, The University of Melbourne, Parkville VIC, 3010

[Please note that the location(s) must be institutional in nature, and should be indicated here as a department, centre or institute, with specific campus identification where relevant.]

Signature 1

	Date 21/12/11
	Date 14/12/11

Signature 2

Reducing the energy penalty of CO₂ capture and compression using pinch analysisTrent Harkin^{a,b,*}, Andrew Hoadley^b, Barry Hooper^a^a Cooperative Research Centre for Greenhouse Gas Technologies (CO₂CRC), the University of Melbourne, Melbourne, Vic 3010, Australia^b Department of Chemical Engineering, Monash University, Clayton, Vic 3800, Australia

ARTICLE INFO

Article history:

Received 14 August 2009

Received in revised form

4 February 2010

Accepted 5 February 2010

Available online 12 February 2010

Keywords:

Carbon capture

Heat integration

Power

Coal

ABSTRACT

Integration of CO₂ capture and storage (CCS) into coal-fired power stations is seen as a way of significantly reducing the carbon emissions from stationary sources. A large proportion of the estimated cost of CCS is because of the additional energy expended to capture the CO₂ and compress it for transport and storage, reducing the energy efficiency of the power plant. This study uses pinch analysis and heat integration to reduce the overall energy penalty and, therefore, the cost of implementing CCS for power plants where the additional heat and power for the CCS plant will be provided by the existing power plant. A combined pinch analysis and linear programming optimisation are applied to determine targets for the energy penalty of existing power plants. Two existing pulverised brown coal power plants with new CCS plants using solvent absorption are used as the basis for the study that show the energy penalty can be reduced by up to 50% by including effective heat integration. The energy penalty can be further reduced by pre-drying the coal.

© 2010 Elsevier Ltd. All rights reserved.

1. Introduction

Integration of Carbon Dioxide Capture and Storage (CCS) into coal fired power stations is seen as a way of significantly reducing the carbon emissions from stationary sources. Approximately 50% of Australia's CO₂ equivalent emissions are from stationary sources and of those nearly 70% are from fossil fuel fired power generation (Department of Climate Change, 2008). Therefore, if Australia is to make significant impacts in reducing the amount of CO₂ released to the atmosphere, reducing emissions from these power generators is critical. CCS involves the addition of equipment to separate and capture the CO₂ from the flue gas generated by the power plants, compressing the separated CO₂ into a supercritical fluid form and then storing it in geological structures. The CO₂ will generally be stored in permeable rock at least 800m underground where it will remain in the supercritical state, trapped by a combination of geological mechanisms.

A large proportion of the estimated cost of CCS is because of the additional energy expended to capture the CO₂ and compress it for transport and storage, which reduces the energy efficiency of the power plant. There are a number of CO₂ capture methods that can be used on power plant flue gases including chemical and physical

solvent absorption, gas–solid based adsorption, membrane gas separation, low temperature separation and hybrid designs. All of these methods require different amounts of heat and/or power in order to enable the CO₂ to be separated from the other flue gas components and then prepared for storage. The heat and/or power required for CCS can be obtained parasitically from the power plant, or from a purpose built utility. In the former case the addition of CCS will reduce the power output from the power plant, while the latter case will often generate CO₂ which may or may not be captured for storage.

The goal of this work is to determine, using heat integration analysis, the amount of electricity which may be exported from a power station, when a portion of the steam and electricity is used to run an amine-based solvent carbon capture plant. This paper considers a range of retrofit cases, with increasing levels of integration. Two different brown coal power stations are examined, both subcritical, but with different operating efficiencies prior to the retrofit of CCS. The results are considered in terms of the net power generation efficiency and carbon capture energy penalty and are of interest, because they shed new light on the energy penalty for the retrofit of carbon capture.

2. Background

Whilst there are no large scale CCS plants currently operating on flue gas, there are a number of plants that capture CO₂ for use in food production, urea production, carbonation of brines and enhanced oil recovery (Herzog, 2000). CO₂ is also currently separated from natural

* Corresponding author. Cooperative Research Centre for Greenhouse Gas Technologies (CO₂CRC), the University of Melbourne, Melbourne, Vic 3010, Australia. Tel.: +61 3 8344 5048; fax: +61 3 9347 7438.

E-mail address: t.harkin@unimelb.edu.au (T. Harkin).

Nomenclature			
Symbols		t	t^{th} Temperature interval in the combined list of temperatures in the GCC and the SCC (1 = hottest temperature (T_{top}), m = pinch point temperature)
h_i	Enthalpy of the steam at extraction point i , (kJ/kg)	T_{top}	The hottest temperature in the GCC or SCC
$h_{\text{isen-}i}$	Enthalpy of the steam at extraction point i assuming isentropic expansion from stage $i-1$, (kJ/kg)	Greek letters	
$H_{i,t}$	Enthalpy available in steam i between the steam at temperatures t and the turbine outlet. If t is greater than the steam supply temperature then it is the difference from the supply temperature down to the turbine outlet, (kJ/kg)	ΔE	Energy penalty (%)
M_i	Mass flowrate of the steam exiting the i^{th} section of the turbine, (kg/s)	ΔT_{min}	Minimum temperature driving force allowable in a heat exchanger ($^{\circ}\text{C}$)
P_i	Pressure of the steam exiting the i^{th} section of the turbine, (kPa)	η_{CCS}	Efficiency of a power plant with CCS and j (%)
Q_{xs}	The excess energy in the SCC above that required to meet the heat duty (kW)	η_{ref}	Efficiency of a power plant without CCS (%)
s_i	Entropy of the steam exiting the i^{th} section of the turbine, (kJ/kg K)	ω_j	Specific amount of power generated by the turbine from steam at the turbine section i to the outlet of the turbine (kJ/kg)
T_i	Temperature of the steam exiting the i^{th} section of the turbine, ($^{\circ}\text{C}$)	Abbreviations	
W	Turbine power that could be generated with the steam utilised from all extraction points, (kW)	CCS	Carbon capture and storage
W_{ij}	Work generated from the turbine between steam extraction points i and j , (kW)	DeSOx	Desulphurisation
Subscripts		DeNOx	Denitrification
i	i^{th} Section of the turbine (0 = steam supply, n = last steam extraction point, $n+1$ = steam outlet of turbine)	FGD	Flue gas desulphurisation
j	j^{th} Section of the turbine	GCC	Grand composite curve
m	The number of temperature intervals in the GCC and the SCC	HHV	Higher heating value
n	Total number of steam extraction points from the turbine not including the final section	HP	High pressure
		HPH	High pressure boiler feedwater heaters
		IP	Intermediate pressure
		LP	Low pressure (as in low pressure turbine)
		LPH	Low pressure boiler feedwater heaters
		MEA	Monoethanolamine
		MILP	Mixed integer linear programming
		MWe	Electrical energy (MW)
		NOx	Oxides of nitrogen
		SCC	Steam composite curve
		SOx	Oxides of sulphur

gas streams predominantly using chemical absorbents, although membranes and adsorption processes have started to gain acceptance as alternatives in certain applications (Pierantozzi, 2001). Separation of CO_2 from syngas for NH_3 and H_2 production also uses adsorption processes and solvent absorption. However, all operating commercial scale capture of CO_2 from flue gas in the power generation industry use amine-based solvent absorption processes (Herzog, 2000; GCCSI, 2009) and, therefore, these are considered the basis for the first generation of CCS plants that may be constructed.

2.1. Solvent absorption

Conventional solvent capture of CO_2 is a two-step process involving an absorption step, where lean solvent is contacted with the flue gas stream to capture the CO_2 ; a second step occurs in a stripping column where the solvent is either heated or the pressure is reduced to desorb the CO_2 from the solvent, generating a high purity stream of CO_2 and regenerating the solvent which is returned to the absorption column. Solvent systems can be roughly divided into chemical and physical solvents and the optimal absorption process will vary depending on the different flue gas conditions, the required purity, the contaminant levels, any environmental restrictions, and available utilities as well as economic considerations.

A significant amount of research has and is being conducted on solvent absorption of CO_2 . A thorough and detailed review of CO_2 capture from post-combustion flue gases by solvent absorption/ stripping has been covered by Davidson (2007). Davidson looked

mainly at Monoethanolamine (MEA), which he considers the benchmark solvent by which the others are compared. The article reviews a number of factors including solvent degradation, process design and techno-economic aspects of CO_2 capture for post-combustion power plants.

Solvent capture is affected by contaminants in the flue gas streams, oxides of sulphur (SOx) and nitrogen (NOx), oxygen, carbon monoxide and particulates. Leci (1996) discusses the process selection criteria for absorbents, in particular the impact of impurities. Rao and Rubin (2002), Davidson (2007) and Ho (2007) all discuss the required level of impurities required for solvents. However, Dave et al. (2001) suggest that the economic trade-off for an Australian black coal power plant actually favours lower desulphurisation (DeSOx) and denitrification (DeNOx) than the recommended levels, leading to greater loss of solvent because of the higher levels of contaminants. Endo et al. (2008) are looking at removing the need for DeSOx and DeNOx when using potassium carbonate based processes by separating the contaminants as K_2SO_4 and KNO_3 in a reclaimer.

The use of solvent absorption for large scale capture in power plants is being studied extensively. Rao and Rubin (2002), Romeo et al. (2008), Gibbins and Crane (2004) and IEA GHG (IEA-GHG, 2006) amongst others all describe power plants using MEA for CO_2 capture. Gibbins and Crane (2004) and Mimura et al. (1997) compared MEA to KS-1/2, a proprietary sterically hindered amine and found reductions in the solvent regeneration energy requirements with KS-1/2. The use of carbonates with and without

promoters is being studied by the CO2CRC (Ghosh et al., 2008) and Cullinane and Rochelle (2004) amongst others. Chilled ammonia systems are also being developed by Alstom (Alstom, 2006), whilst a number of proprietary solvents Econamine FG Plus (Reddy et al., 2003), PSR (Veawab et al., 2001), AMP (Yeh and Pennline, 2001), CORAL (Feron and Jansen, 2002) are also being developed.

2.2. Energy penalty

A typical solvent capture plant based on MEA with a single absorber, stripper and lean-rich heat exchanger (Refer to Fig. 1) requires significant amounts of heat at over 120 °C (3–4.5 GJ/tCO₂) to regenerate the solvent in the stripper reboiler as well as heat for the stripper feed which is usually provided by cooling of the lean solvent. The CCS plant also requires power to operate the CO₂ compressors and auxiliary equipment including the solvent pumps. The CCS plant will also reject heat from the stripper condenser and the compressor intercoolers. The addition of the CCS plant will invariably lead to a deficit of heat in the plant which has generally been proposed to be overcome by supplying heat by extracting steam from the LP turbine for the stripper reboiler. This reduces the electricity from the power plant and thus its net efficiency can be reduced by approximately 30–40% by the addition of CCS (IPCC, 2005).

The energy penalty has been defined in two slightly different ways; the reduction in the net electrical energy from a power plant caused by the addition of CCS, or the increase in the required fuel for a power plant to maintain its power output after addition of CCS. In this work, energy from the power cycle is being used for capture (which is a parasitic load), and, therefore, the net power from the plant will be reduced; thus the former interpretation is more relevant and is provided by equation (1). The energy penalty given by equation (1) is the percentage reduction of the efficiency of the power plant with CCS compared to the plant without CCS, which is also equal to the reduction in the net electrical power caused by CCS. The loss of electricity generated by a power plant or the additional amount of CO₂ produced to power the CCS plant is why the cost of CCS is reported as the cost per tonne of CO₂ avoided and not the cost per tonne of CO₂ captured. Allinson and Neal (2007) provided a detailed argument to show why the cost of CO₂ avoided is much more important than the cost of CO₂ captured. For the same amount of CO₂ captured, a reduction in energy penalty will lead to an increase in the amount of CO₂ avoided.

$$\text{Energy Penalty} = \Delta E = 1 - \left(\eta_{\text{CCS}} / \eta_{\text{ref}} \right) \quad (1)$$

The energy penalty can be reduced in a number of ways, many of which are specific to the capture technology employed. For absorption processes the solvent regeneration energy can be lowered by varying the solvent, or the total reboiler energy can be lowered by improved process design of the solvent plant (Davidson,

2007; Jassim and Rochelle, 2006). Examples of such improvements are provided by the Fluor Econamine Plus process, which uses a combination of improved solvent formulation coupled with an improved process design including split flow arrangements, absorber intercooling, integrated steam generation and stripping with flash steam to reduce the total energy consumption; up to 20% reductions have been achieved in pilot studies compared to original MEA plants (Reddy et al., 2003).

Many authors have investigated how to minimise the energy penalty associated with CCS, however, none appear to use pinch analysis. Aroonwilas and Veawab (2007) and Romeo et al. (2008) state that the optimal location to extract power for a solvent system is from the LP turbine at the appropriate pressure to provide steam at lowest quality that satisfies the solvent system reboiler requirements. Mimura et al. (1997) uses 14% of the stripper condenser energy to heat the boiler feedwater, Desideri and Paolucci (1999) and Romeo et al. (2008) suggest utilising some of the available heat from the CO₂ compressor intercoolers to heat the boiler feedwater. Bozzuto et al. (2001) uses an auxiliary turbine with steam from the IP/LP crossover to provide the steam at the required quality for the solvent reboiler; this method was considered by Zachary (2008) to provide the most efficient method of providing steam at the correct quality of steam compared to using throttling valves, floating pressure or clutch arrangements for dealing with steam extracted between the IP/LP turbines. An IEA GHG report (IEA-GHG, 2006) utilises a number of waste heat streams to increase the overall plant efficiency. They produce hot water for coal pre-drying in the flue gas line prior to the flue gas desulphurisation (FGD), the stripper condenser and the CO₂ compressor intercoolers and they also heat the boiler feedwater using the stripper condenser and CO₂ compressor intercoolers, completely removing the need for the existing boiler feedwater heaters. Pfaff et al. (2009) look at MEA plants and integrating heat from the stripper condenser and the CO₂ compressor to heat the boiler feedwater and in turn to provide heat for air preheat. They also look at providing less intercooling in the CO₂ compressor to provide additional heat for the boiler feedwater. Whilst Pfaff et al. managed to reduce the energy penalty from 23% to 21%, there does not appear to be a strict methodology to investigate integration opportunities. Jassim and Rochelle (2006) found that the optimised multiple pressure stripper required 3–11% less equivalent work than the equivalent simple solvent system. The solvent system for the multiple pressure stripping utilises waste heat from the compressors to reduce the reboiler requirement; however, the study did not review whether this heat is better utilised within the power plant itself to improve the overall efficiency.

Alie (2001) reviewed parameters in the MEA system of absorber height, lean solvent loading, stripper height and stripper temperature and looked at the impact these have on the overall power output of a plant assuming that the reboiler energy is provided by steam from the IP turbine. For each case the scenario that reduces the reboiler energy is also the same case that leads to the highest power output, except for the absorber height. As the absorber height is increased the blower energy increases and eventually becomes greater than the energy saved by reducing the reboiler heat.

Stankewitz et al. (2009) used an ammonia cycle to generate more energy from the waste heat available in an MEA plant retrofitted to a power plant. The energy penalty reduced from 28% without the ammonia cycle to 22% with it. However, the ammonia condenser was operated with cooling water at 15 °C and, therefore, the same level of benefit would not be expected from operation at warmer climates.

As can be seen a number of different combinations have been suggested to utilise the waste heat to reduce the energy penalty associated with the addition of CCS to a power plant. However, no study appears to use pinch analysis to systemically integrate the

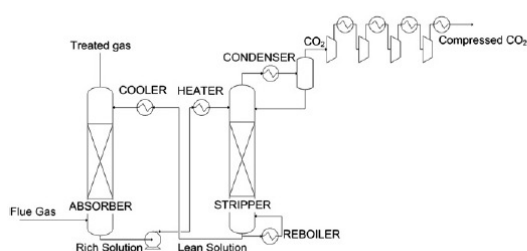


Fig. 1. Solvent capture plant.

CCS plant with the power plant. Pinch analysis has been used with success for the addition of CCS to pulp and paper mills (Hektor and Bernström, 2007; Mollersten et al., 2004).

2.3. Heat integration of power plants

Pinch analysis has been utilised in the process design of heat exchanger networks since it emerged as a tool in the late 1970s. Pinch analysis is the systematic analysis of the energy flow of a process. It is based on the first and second laws of thermodynamics in that energy must be conserved and that heat will flow in only one direction. Pinch analysis can be used as a targeting mechanism to calculate the minimum energy requirements of a given process. The targets are determined by ensuring that the flow of energy from the hot streams in a process (those streams that need to be cooled) to the cold streams (those streams that need to be heated) is maximised. The concept of composite curves was introduced by Hohman (1971), whereby all hot stream data are combined on a temperature–enthalpy diagram and all cold stream data are also combined on the same diagram. From these composite curves, minimum utility requirements, based on a specific minimum approach temperature between the hot and cold streams, can be determined. A methodology to produce heat exchanger networks that meet these targets was developed by Linnhoff and Flower (1978) and Umeda et al. (1978). Smith (2005) and Linnhoff et al. (1982) provide a thorough guide to the principles of pinch analysis.

With the addition of CCS to a power plant, there are additional hot and cold streams. For a CCS plant using solvent absorption, hot streams include the stripper condenser, the CO₂ compressor intercoolers and potentially the flue gas which may need to be cooled down further for CO₂ separation. There are also additional cold streams in the stripper reboiler and the regeneration for the CO₂ dehydration process. Pinch analysis will enable the systematic review of the power plant to ensure the plant with the new equipment and new heat sources and sinks are matched to maximise the efficiency of the process. With the addition of a CCS plant, the power plant now becomes more like a chemical plant with both heat and power generation required. Therefore, techniques reported by Smith (2005), Linnhoff (1986) and Hall and Linnhoff (1994) for furnace design and Smith (2005) for cogeneration of heat and power will provide useful tools to redesign the power plant with the new requirements of CCS included.

Although widely used in the processing industries, pinch analysis as a means of improving power plant design has not been widely reported. Linnhoff and Alanis (1989) used pinch analysis to show how it is possible to improve the efficiency of a power plant. They used pinch analysis to reduce the fuel use by 2.8% by determining the optimum amount of steam extracted from the turbines for a given number of boiler feedwater heaters and utilising topping and intermediate desuperheaters to achieve the required heat transfer.

2.4. Methods for selection of optimum utilities

Various methods have been developed to determine the amount and in some cases the pressure of steam required to supply process heating demands. Some of those methods take into consideration the amount of cogeneration power that can be generated, however, only a few methods are suitable for optimising power stations.

Dhole and Linnhoff (1993) developed total site profiles from the grand composite curves (GCC) of all of the processes on a site. The GCC represents, above the pinch the net heat required by the process at each temperature and below the pinch the net heat available by the process at each temperature. They excluded the ‘pockets’ in the individual grand composite curves and combined the rest of the sources and sinks to form total site source sink profiles. Using the

total site profiles steam targets can be found graphically including calculation of cogeneration power, however, the method is based on steam as a constant temperature heat supply, does not include the boiler feedwater heating or ability to optimise the heat exchange between the process and the utility for steam generation.

The total site profiles method has been extended by Mavromatis and Kokossis (1998a, 1998b) who added steam turbine network optimisation of the cogeneration potential from total site profiles. The method decomposes complex turbines into a number of simple turbines, allows for variations in turbine efficiency at full and part load and optimises the range of options. The total site profiles and turbine network models are the basis of many methods (Klemes et al., 1997; Varbanov et al., 2004a, 2004b; Bandyopadhyay et al., 2010; Gorsek et al., 2006; Shang and Kokossis, 2005) for top level analysis and optimisation of utility systems. All of these methods are designed for optimisation of utility systems including cogeneration of heat and power rather than trying to minimise the energy penalty associated with retrofitting a single power station with additional heat sources and sinks.

Papoulias and Grossmann (1983) used a superstructure approach to optimise steam networks for process heating using mixed integer linear programming (MILP) to find an optimum. The superstructure is made up of linearised representations of the processes, utility options and the cost functions. Although it will find an optimum solution to the given problem, it may not find the global optimum due to the linearisation of the problem and because there is also no interaction between the utility system and the process.

Salama (2009) optimises the amount of each utility for multiple utilities using a geometrical approach to heat integration where the horizontal difference between the hot and cold composite curves are used to fit the utilities rather than the traditional problem table algorithm. The method finds optimum amounts of utilities directly using a linear programming optimisation but it is used to minimise the utility requirements rather than optimise the power generation.

Marechal and Kalitventzeff (1999) developed a method which is based around a steam network superstructure. Unlike the other methods the structure allows for use of the steam superheat, latent heat and subcooling. The structure also allows for either process heating and/or steam heating of the boiler feedwaters. The method can easily be applied to power stations and to compare different forms of generators. The method is very useful for greenfield processes where the utility is designed to satisfy the process requirements.

3. Methodology

Pinch analysis can be used to determine the composite curves and grand composite curves for the power plant combined with the CCS plant. In general there will be a deficit of heat due to the addition of the CO₂ capture plant. This heat can be provided by extracting steam from the turbine, for this work we are considering retrofit applications, where we will assume that the steam levels available to use as additional heat for the CCS plant, are fixed at the existing turbine extraction points. Fig. 2 provides a representative diagram of a brown coal power plant combined with CCS. As can be seen from the diagram, steam extracted from the turbine is currently used in the LP and HP feedwater heaters and the deaerator, which is typical of most power plants.

For retrofit applications, such as we are looking at in this work, it would be advantageous to supply the deficit of heat for the CO₂ separation from the existing extraction points of the turbine to minimise the alterations. As shown in Fig. 2 the steam, once condensed, is returned to the steam cycle in a number of different ways; by direct injection as per the deaerator, by the return of hot condensate like the steam from HPH 1&2, and via drain pumps like

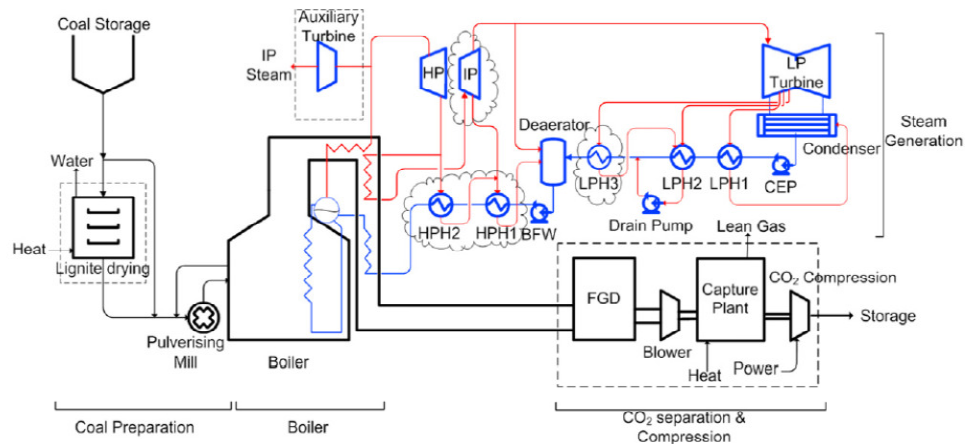


Fig. 2. Steam turbine model. The dotted lines represent the new equipment that may be added for CCS. Equipment that is in Plant B but not in Plant A has been clouded.

LPH 2&3, and by injection of the condensate back into the condenser like LPH 1. Because the steam being used as a source of heat, rejoins the feedwater section of the steam circuit the 'hot utility' then joins in with other 'cold streams'. So when trying to optimise the use of extraction steam as a source of heat for both the existing feedwater heater requirements and the new CCS requirements, the fact that the hot utility rejoins the steam circuit and thus becomes part of the cold streams and cold composite curves, means the traditional pinch design methods cannot be easily applied due to a number of issues:

1. The cold composite curves will change depending on where the steam is returned to the steam cycle. The cold composite curves upstream of the returned steam/condensate will have a smaller flowrate and therefore greater gradient compared to the curves downstream of the injected steam/condensate.
2. The target temperature of the hot utility changes depending on how the steam is used. Injected steam has a different target compared to steam used in heat exchangers. Therefore, the amount of energy that is extracted from the steam changes depending on where it is reinjected back into the process.
3. The hot utility/extracted steam may cross the process pinch point as it is cooled thereby adding utility heat below the pinch point and possibly moving the temperature of the pinch point. As the pinch point moves the amount of hot utility increases, which means the amount of steam extracted increases which can lead to further increases in the pinch temperature, and, therefore, targeting the amount of steam to be extracted requires an iterative solution.

The above issues makes the problem of trying to determine the minimum amount of steam to be extracted difficult as the cold composite curve and, therefore, the heating requirements change as the amount of steam extracted from the turbines change. Also, the return location of the steam needs to be identified before targeting is complete. To enable consistency, and to allow targets to be obtained prior to the matches being identified the following method is proposed:

1. The cold composite curves are held constant and are based on a water flowrate equal to the amount of steam generated.

2. All extraction steam is cooled down to the condenser temperature and returned to the steam cycle at the surface condenser.

This procedure enables the targeting process to proceed with consistent cold composite curves and hot utility target temperatures. This is proposed to reduce the number of variables to just the steam extraction rates, therefore, making it straightforward to compare the energy penalty of different processes without having to determine the final design, and by not assuming a return location of the steam/condensate, undue restrictions are not placed on the design. However, the extraction steam will invariably cross the process pinch, possibly move the process pinch and will have multiple solutions that achieve the required heating load. There will be many solutions with different amounts of the steam at various levels that satisfy the heating demand.

To overcome these issues Linnhoff and Alanis (1989) created a number of simultaneous equations to determine the amount of steam to be extracted by creating a pinch at every steam level; however, this method assumes that pinch points are all located at the condensing temperature of the steam, which may not always be the case. There is also a general rule in pinch analysis that you should maximise the use of the lowest quality utility first before using higher quality utilities. However, when including the steam superheat in the steam curves there are opportunities to use lower rates of higher pressure steam to overcome pinch points which actually increase the available power generation.

Therefore, to determine the amount of steam that should be extracted from the turbine the following method was derived.

Given that the objective is to maximise the power generated/minimise the amount of power 'lost' by the extraction steam. The amount of steam extracted at each level becomes an optimisation problem with n number of variables, where n is the number of steam levels not including the last, normally condensing, stage (as represented by Fig. 3). The last stage is not considered as this stage is set by the lowest cold sink, which is usually cooling water and should not provide any useful heat.

The amount of power lost by extracting steam, between each level i , can be calculated using equation (2), which is the difference in enthalpy for an isentropic expansion of the steam to the next level multiplied by the isentropic efficiency of the turbine.

$$W_{i,i+1} = M_i \cdot \eta_{i,i+1} \cdot (h_i - h_{isen}(P_{i+1}, S_i)) \quad (2)$$

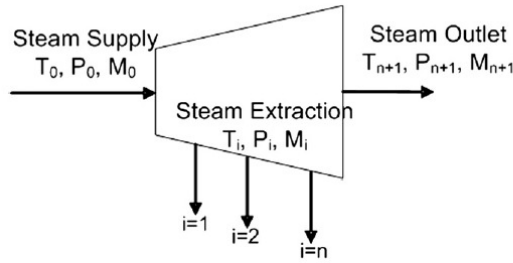


Fig. 3. Steam turbine model.

And, therefore, the total power lost for the steam extraction at each level can be calculated by summing up the energy lost in each stage of the turbine downstream where the steam was extracted (Equation (3)).

$$W_{i,n+1} = M_i \sum_{j=i}^n \eta_{i,j+1} (h_i - h_{isen}(P_{i+1}, S_i)) = M_i \omega_i \quad (3)$$

And the total power lost from all of the steam extraction points is the summation of the power lost by the steam extracted at each extraction point (Equation (4)).

$$W = \sum_{i=1}^n M_i \sum_{j=i}^n \eta_{i,j+1} (h_i - h_{isen}(P_{i+1}, S_i)) = \sum_{i=1}^n M_i \omega_i \quad (4)$$

There are also two constraints: the first that the extraction steam provides sufficient energy to overcome the deficit of heat required by the process and that this energy is provided at temperatures greater than that required by the process. This can be shown by plotting the steam composite curve (SCC), the composite curve of all the extraction steam, on the same graph as the GCC. These two constraints are met when the deficit of heat shown by the GCC is supplied by the SCC and the SCC lies to the left of the GCC for all temperatures above the pinch point (Refer to Fig. 7).

When each steam extraction level temperature and pressure is fixed, as they have been in this retrofit case, the amount of energy lost from the turbine and the amount of energy available in the steam are both linear and, therefore, the problem can be solved by linear programming to minimise the amount of power lost from the turbine (Eq. (5)) subject to a series of inequality equations which are provided by the two aforementioned constraints. The only variables in this problem are the mass flowrates of steam extracted at each steam level.

Obj. Function :

$$\text{Minimise} = \sum_{i=1}^n M_i \omega_i = W \quad (5)$$

Subject to:

$$\sum_{i=1}^n M_i H_{i,Ttop} \geq GCC_{Ttop} \quad (6)$$

$$\forall t = 2, 3, \dots, m \quad \sum_{i=1}^n M_i H_{i,t} \leq GCC_t + Q_{xs} \quad (7)$$

Where :

$$Q_{xs} = \sum_{i=1}^n M_i H_{i,Ttop} - GCC_{Ttop} \quad (8)$$

The first constraint (Eq. (6)) is to ensure that the amount of energy provided by the SCC is greater than the deficit of heat required by the process as indicated by the GCC. The second constraint (Eq. (7)) is a series of constraints that ensures that at every temperature from the highest GCC temperature to the pinch point the SCC lies to the left of the GCC, that is, there is sufficient energy in the steam for the process requirements. The term Q_{xs} (Eqs. (7) and (8)) is required so that the SCC starts at the same relative enthalpy as the deficit of heat represented by the GCC and allows for the situation where the optimal amount of steam extracted may be higher than the deficit of heat.

The problem can be arranged as a matrix with n columns and $m+1$ rows. The first row of the matrix is made up of the coefficients for the specific amount of power lost for each steam level (ω_i). The number of rows for the inequality constraints are defined from the number of temperature intervals (m) in the GCC and SCC. The coefficients for the subsequent rows of the matrix are made up of the amount of energy ($H_{i,t}$) in the extraction steam from each temperature interval down to the GCC pinch point. The variable matrix is the quantity of steam extracted at each steam level (M_n). The solution matrix includes the right hand sides of equations (5)–(7).

Matrix form:

$$\begin{bmatrix} \omega_1 & \omega_2 & \dots & \omega_n \\ H_{1,Ttop} & H_{2,Ttop} & \dots & H_{n,Ttop} \\ H_{1,2} & H_{2,2} & \dots & H_{n,2} \\ \vdots & \vdots & \ddots & \vdots \\ H_{1,m} & H_{2,m} & \dots & H_{n,m} \end{bmatrix} \begin{bmatrix} M_1 \\ M_2 \\ \vdots \\ M_n \end{bmatrix} \begin{bmatrix} = \\ \geq \\ \leq \\ \vdots \\ \leq \end{bmatrix} \begin{bmatrix} W \\ GCC_{Ttop} \\ GCC_2 + Q_{xs} \\ \vdots \\ GCC_m + Q_{xs} \end{bmatrix}$$

This can then be solved using the simplex algorithm method of linear programming which is included in many mathematical software packages.

4. Retrofit of CCS to brown coal power stations example

4.1. Basis

This methodology will be applied to two existing brown coal power stations with new solvent-based CCS plants and with the option of adding lignite pre-drying. It is well known that pre-drying lignite increases the efficiency of conventional brown coal fired power plants (Allardice et al., 2004), however, the impact of adding both CCS and pre-drying from an overall heat integration perspective has not to the authors' knowledge been studied previously.

Six cases have been reviewed,

1. Base case – this is the existing plant with no flue gas desulphurisation (FGD) or carbon capture plant.
2. CCS – this case includes CCS and FGD with no heat integration.
3. Integrated CCS – includes CCS and FGD with maximum heat integration.
4. Retrofit – includes CCS and FGD but only allowing modifications downstream of the economiser on the flue gas and up to the deaerator on the boiler feedwater.
5. CCS & drying – coal dewatering and CCS with maximum heat integration.
6. CCS/drying/increased steam – utilises the additional heat content in the pre-dried coal to produce additional steam which is utilised in an auxiliary turbine for additional heat and power.

For each case the amount of raw coal fed to the plant is held constant and the amount and quality of steam produced from the boiler is held constant for all but Case 6. The same coal with approximately 60% moisture is used for both power plants.

Power Station A is a 200-MWe (nominal) subcritical pulverised brown coal fired power plant that operates with a HP and LP turbine and no steam reheat. Steam is currently extracted from the exhaust of the high pressure turbine for deaeration and is also extracted from two points on the LP turbine for heating the boiler feedwater upstream of the deaerator. A boiler feedwater economiser and air preheater cool the flue gases down before exiting the stack at 260 °C.

Power Station B is a 500-MWe (nominal) subcritical pulverised brown coal fired power station that operates with HP, IP and LP turbines with reheat between the HP and IP turbine. There are 3 LP heaters and 2 HP heaters all supplied with steam extracted from the turbines. The flue gas from this plant exits at around 190 °C.

A model of the base power plants have been developed in Aspen Plus® including the coal drying in the pulverizing mill, coal combustion, flue gas heat recovery and simulation of the steam cycle. For this study as the flue gas has greater than 200 ppmv of SO_x and less than 10 ppm of NO₂ it is assumed that FGD will be required but there will be no additional equipment for NO_x removal. The solvent capture plant and CO₂ compression were also modelled in Aspen Plus® based on an MEA plant, however, the heating/cooling curves of the MEA system heat exchangers predicted by the model were prorated for a reboiler duty from 4.4 GJ/tCO₂ to 3 GJ/tCO₂, to provide results comparable to the leading solvent technologies that report reboiler duties of 2.7–3.3 GJ/tCO₂ (IPCC, 2005).

The CO₂ is compressed to 100 bar using a 4-stage compressor with intercooling and water removal between the second and third stages of compression. Where lignite pre-drying has been considered, the drying is assumed to occur at atmospheric conditions (100 °C) and the coal is dried to 45 wt.% moisture, which is the anticipated minimum that can be handled by the existing boiler plants without major modifications.

All power requirements for the CCS equipment, flue gas blower, solvent pumps and CO₂ compressors will be driven by electrical motors.

4.2. Results

Table 1 includes the main parameters of the power plant for the 6 different cases for both Plants A and B. The table includes the base power plant (Case 1) parameters and the impact of adding on CCS without heat integration Case 2. Cases 3–6 utilise the linear programming method to determine the optimum steam extraction rates to minimise the amount of power lost from the turbine caused by the addition of CCS. This enables the calculation of the power plant net electrical output, efficiency, CO₂ emissions and the energy penalty associated with the additions of CCS. Plant A has 3 steam extraction points; HP exhaust (177 °C), LP Bleed 1 (120 °C) and LP 2 (84 °C), whilst Plant B has 6 steam extraction points; HP exhaust (351 °C), IP Bleed 1 & 2 (429 °C/318 °C) and LP Bleed 1, 2 & 3 (247 °C, 179 °C, 79 °C).

4.3. Discussion

The energy penalty for both Plants A and B can be reduced by ensuring proper heat integration is applied as can be seen by the reduction in energy penalty for Case 3 compared to Case 2 (Refer to Fig. 4). Further reductions in the energy penalty may be possible with the addition of drying as can be seen by Cases 5 and 6 (Fig. 4). The energy penalty for Plant B is always less than that for Plant A for the same case, which is due to Plant B's steam cycle being more efficient. The amount of CO₂ required to be captured and compressed per MW of power produced in Plant B will be less than Plant A, and, therefore, the capture plant will have lower heat and power requirements and, therefore, energy penalty.

The hot composite curve, the upper curve in Fig. 5(a) and (b) shows the amount of heat that is available in the process, which is mainly in the flue gas; the extraction steam is represented by the horizontal portion of the hot composite. The cold composite curve, the lower curve in Fig 5(a) and (b) represents the streams that require heating, which is predominantly the steam generation and air preheat. For the base cases (Case 1) which show the existing plants, the hot and cold curves are balanced which means the process heating demands are met by the flue gas and extraction steam.

The base cases are threshold problems with neutral ΔT_{\min} of 30 °C and 55 °C, respectively. The neutral ΔT_{\min} (Farhad et al., 2008) is the ΔT_{\min} for which the power plant could be redesigned with a new heat exchanger network to achieve the same efficiency. The temperature driving forces of the existing plant range from less than 3 °C in the surface heaters to greater than 400 °C in the firebox of the boiler.

In Case 2, where CCS is added without heat integration, the heat for the solvent regeneration is supplied from the next available turbine extraction points, ~180 °C for both plants. Approximately 48% and 41% of the steam generated by the boilers is required to meet this demand for Plants A and B, respectively. The largest users of heat and power for the power plants are the requirement for heat in the stripper reboiler and power for the CO₂ compressor. The heat for the stripper reboiler is represented by the large horizontal heat load on the cold composite curves at a temperature of 120 °C shown in Fig. 5. The heat load for the reboiler, 226 MW and 416 MW for Plants A and B, respectively, are much greater than the heat deficit of 125 MW and 233 MW for the power plant with CCS for a ΔT_{\min} of 3 °C and with the existing amount of steam extraction. This shows that there is some heat still available in the power plant which can reduce the amount of steam extraction required.

Where the CCS plants are added with complete heat integration (Case 3) using a ΔT_{\min} of 3 °C (Fig. 6), the energy penalty is reduced from 39% to 23.5% and 28% to 14% for Plants A and B, respectively. The reduction in energy penalty in Plant A is due to the 50% reduction in the required HP steam extraction for the stripper reboiler. Whereas, in Plant B the savings are mainly due to a reduction in the HP steam requirement which is currently used for the HP feedwater heaters, the amount of steam extracted at the level required for the stripper reboiler (LP Bleed 2) is only reduced by 3%.

This suggests that Plant A may have an easier task of retrofitting the power plant with CCS measures to reduce the energy penalty. This can be seen in Case 4 where only the flue gas downstream of the existing economiser and the boiler feedwater up to the deaerator are considered for possible heat exchanger modifications. For Plant A the energy penalty does not change between this case and the fully integrated system (Case 3). By contrast with Plant B the energy penalty of the reduced exchanger modification case is 19% compared to the fully integrated energy penalty of 14%, which implies that changes will need to be made to the HP feedwater heater section and possibly require further heat exchange area in the reheat section if the current reheater tubes do not allow for an increase in flowrate that will accompany a reduction in the HP steam extraction.

The amount of heat provided by the extraction can be more closely viewed using the grand composite curves with the steam composite curves overlayed. The results for Case 3 for Plants A and B are shown in Fig. 7. These also show how the linear programming method works by ensuring that the steam composite curves must lie to the left of the grand composite curves down to the pinch point to ensure there is sufficient heat in the steam to meet the heating requirements.

4.3.1. Integrated CCS and drying (Cases 5 and 6)

The addition of pre-drying reduces the energy penalty of Plants A and B by 2% and 3%, respectively, when compared to the integrated CCS case without pre-drying. With coal pre-drying included,

Table 1
Power plant performance.

Case		Plant A						Plant B					
		1	2	3	4	5	6	1	2	3	4	5	6
Moisture content (to mill)	wt.%	61	61	61	61	45	45	61	61	61	61	45	45
Steam production	kg/s	208	208	208	208	208	248	433	433	433	433	433	491
Steam extraction rates – optimised using the linear programming method													
HP exhaust	kg/s	11	112	54	54	42	53	46	46	2.0	46	2.0	39
IP bleed 1	kg/s	–	–	–	–	–	–	20	20	21	20	4	23
IP bleed 2	kg/s	–	–	–	–	–	–	15	15	4	15	0	3
LP bleed 1	kg/s	11	11	0.2	0.2	7	7	14	14	3	0	0	2
LP bleed 2	kg/s	9	9	0	0	0	0	26	207	201	134	213	144
LP bleed 3	kg/s	–	–	–	–	–	–	15	15	0	0	0	0
Power plant output – based on the steam extraction rates given													
Electricity produced	MW	220	172	205	205	208	203	520	441	509	484	524	481
Plant auxiliary power	MW	14	22	22	22	22	23	30	44	44	44	44	44
CO ₂ compression power	MW	–	25	24	24	25	2 ^a	–	45	45	45	45	2 ^a
Net electrical power	MW	206	125	158	158	161	178	490	352	420	435	435	436
Net cycle HHV efficiency	%	23	14	18	18	18	20	28	20	24	25	25	25
Reduction in Eff.	%Pts	–	9	5	5	5	3	–	8	4	5	3	3
Energy penalty	%	–	39	23.5	23.5	22	14	–	28	14	19	11	11
CO ₂ emissions	t/MWh	1.46	0.24	0.19	0.19	0.15	0.14	1.15	0.16	0.13	0.14	0.13	0.13

^a The compression power in this case is offset by the addition of an auxiliary turbine.

the air preheat is removed entirely to reduce the maximum combustion temperature, however, in this case the theoretical flue gas temperature still increases by around 100 °C. This increase may limit the level of pre-drying that is able to be achieved due to constraints of the existing boilers.

From the results of Case 5 & 6 it appears that the value of pre-heating the air in a power plant may be reduced when CCS is added. Air-preheating on a conventional power plant increases the efficiency by reducing the stack losses, however, as the flue gas exhaust temperature will need to be lowered for current solvent CO₂ capture technologies, the stack losses are lowered and the flue gas energy may be better utilised for other duties.

For Case 6, it is assumed additional steam is produced and is utilised in a new auxiliary turbine. For Plant A there is sufficient heat in the boiler flue gas to provide at least 20% additional steam, which can be used to provide enough energy in the auxiliary turbine to offset the CO₂ compression power and provide steam at the desired level for the solvent stripper. However, for Plant B the generation of extra steam requires more extraction steam from the HP and IP turbines, which reduces the amount of power that they produce.

The energy penalty for Case 6 reduces for Plant A from 22% to 14%, however, for Plant B the energy penalty remains at 11%.

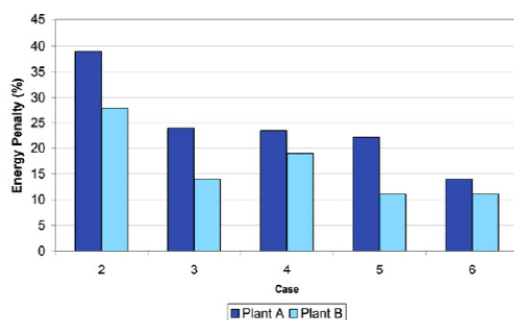


Fig. 4. Energy penalty of Plants A and B.

Therefore, the addition of a new turbine and potentially boiler modifications makes sense for Plant A, but not for Plant B. The generation of additional steam helps to increase the efficiency of the power plant in a similar manner to the feedwater heaters, by increasing the average temperature of heat addition. Therefore, this is valuable for Plant A. However, for Plant B this is offset by the use of an auxiliary turbine that does not include reheat, therefore, the power generated by this turbine is less than that generated in the main turbine and the benefit is negated.

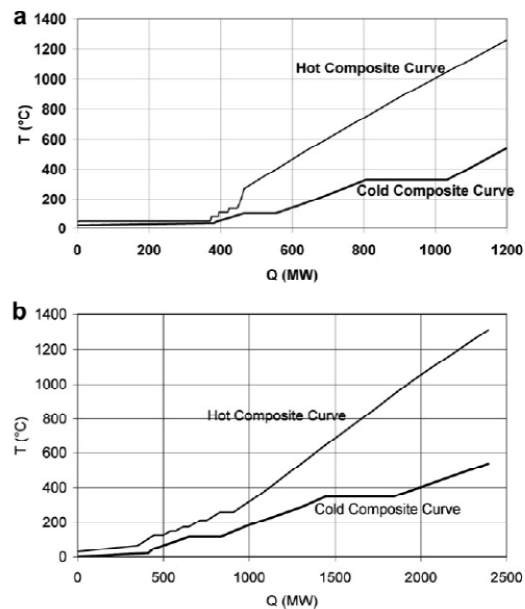


Fig. 5. (a) Base plant composite curves – Plant A. (b) Base plant composite curves – Plant B.

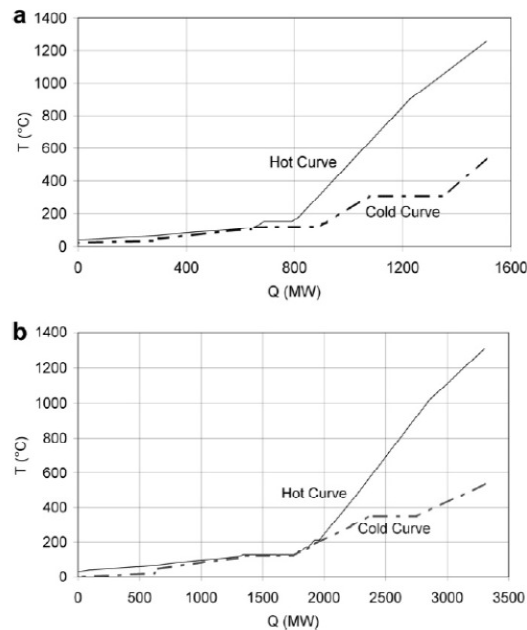


Fig. 6. (a) Case 3 composite curves – Plant A. (b) Case 3 composite curves – Plant B.

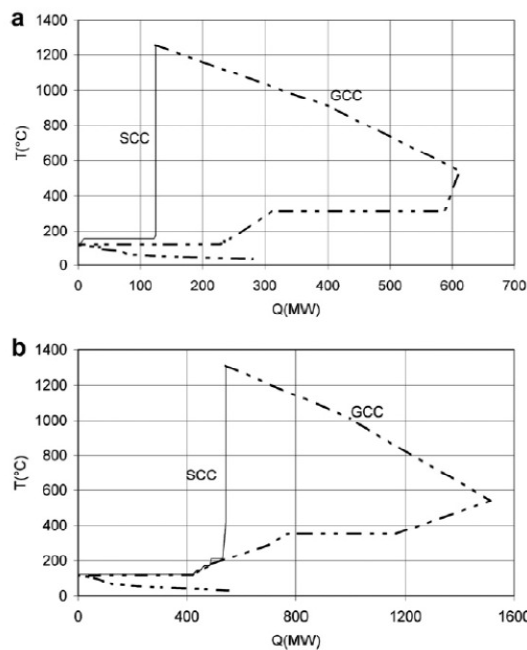


Fig. 7. (a) Case 3 grand composite curves with steam curves overlaid – Plant A. (b) Case 3 grand composite curves with steam curves overlaid – Plant B.

Table 2
Effect of ΔT_{\min} on the extraction steam flow(kg/s) and gross electricity production of Plant A.

ΔT_{\min}	HP (177 °C)	LP 1 (110 °C)	LP 2 (84 °C)	Gross power (MW)
3	54	0	0	205
10	57.7	4	0	201
20	76.7	12.5	0	190

The additional modifications, including the changes to the heat exchanger network, the pre-drier and the existing and new turbines required to lower the energy penalty will increase the cost of the retrofit. The economic optimum will likely be at an energy penalty that is higher than the minimum. The energy penalty may also be higher than the minimum to ensure that the plant integration does not affect the operability of the power plant, especially when turndown effects are taken into consideration.

4.3.2. Effect of ΔT_{\min}

The effect of altering the ΔT_{\min} on the amount of extraction steam required and the amount of gross electricity that is produced is shown in Table 2. For this study an optimistic ΔT_{\min} of 3 °C is used for all cases. In reality the economic ΔT_{\min} for each type of process will be different and variable minimum temperature driving forces for different processes should be used in future work. However, it can be seen that even with a global ΔT_{\min} of 20 °C the amount of power produced for Plant A is still better than that for the unintegrated case (Case 2) (172 MW).

5. Conclusion

The energy penalty associated with CCS can be reduced by redesigning the power stations' heat exchanger network and good use of the available waste heat, some existing design rules for power plants may no longer be the most efficient and economic and new rules will need to be determined for both retrofit and greenfield power plants. A combined pinch point and linear programming optimisation method has been suggested to develop targets for the energy penalty of individual power plants. The targets show some sensitivity to ΔT_{\min} and further economic optimisation is required to determine the final penalty. However, the results indicate that with heat integration and coal pre-drying, a CCS retrofit may not incur the large energy penalties quoted in the literature.

Acknowledgements

This work is prepared as part of the Latrobe Valley PCC project with support of the Victorian Government ETIS Brown Coal R&D program; International Power and the Cooperative Research Centre for Greenhouse Gas Technologies (CO2CRC), which is funded through the Australian Government's Cooperative Research Centre Program, other Federal and State Government programs, CO2CRC participants and wider industry.

References

- Alie, C.F., 2001. Simulation and optimization of a coal-fired power plant with integrated CO₂ capture using MEA scrubbing. PhD thesis. Chemical Engineering, University of Waterloo.
- Allardice, D.J., Chaffee, A.L., Jackson, W.R., Marshall, M., Chun-Zhu, L., 2004. Water in brown coal and its removal. In: Chun-Zhu, L. (Ed.), *Advances in the science of Victorian brown coal*. Elsevier Science, Amsterdam, pp. 85–133.
- Allinson, G., Neal P., 2007. Rules of thumb for adding the costs of capture and storage. In: CO2CRC Research Symposium, 2007, Swan Valley, WA, Australia.
- Alstom, 2006. Alstom to build pilot plant in the US to demonstrate its unique CO₂ capture process. Available at: <www.poweralstom.com/pr_power_v2/2006/october/27531.EN.php?languageId=EN&dir=/pr_power_v2/2006/october/8idRubriqueCourante=32205> [accessed 03.02.09].

- Aroonwilas, A., Veawab, A., 2007. Integration of CO₂ capture unit using single- and blended-amines into supercritical coal-fired power plants: implications for emission and energy management. *Int. J. Greenhouse Gas Control* 1 (2), 143–150.
- Bandhyopadhyay, S., Varghese, J., Bansal, V., 2010. Targeting for cogeneration potential through total site integration. *Appl. Therm. Eng.* 30 (1), 6–14.
- Bozzuto, C.R., Nsakala, N., Lilijedahl, G.N., Palkes, M., Marion, J.L., 2001. Engineering feasibility of CO₂ capture on an existing US coal-fired power plant. In: First National Conference on Carbon Sequestration, Washington.
- Cullinane, J.T., Rochelle, G.T., 2004. Carbon dioxide absorption with aqueous potassium carbonate promoted by piperazine. *Chem. Eng. Sci.* 59 (17), 3619–3630.
- Dave, N.C., Duffy, G.J., Edwards, J.H., Lowe, A., 2001. Economic evaluation of capture and sequestration of CO₂ from Australian black coal-fired power stations. In: Fifth International Conference on Greenhouse Gas Control Technologies (GHGT-5). CSIRO Publishing, Cairns.
- Davidson, R.M., 2007. Post-combustion carbon capture from coal fired plants – solvent scrubbing, in CCC/125. IEA Clean Coal Centre.
- Department of Climate Change, 2008. National greenhouse gas inventory. Commonwealth of Australia, Canberra.
- Desideri, U., Paolucci, A., 1999. Performance modelling of a carbon dioxide removal system for power plants. *Energ. Convers. Manage.* 40 (18), 1899–1915.
- Dhole, V.R., Linnhoff, B., 1993. Total site targets for fuel, cogeneration, emissions, and cooling. *Comput. Chem. Eng.* 17, S101–S109.
- Endo, K., Kentish, S., Stevens, G., 2008. The fate of SO_x and NO_x in post-combustion carbon dioxide capture. In: CO₂CRC Research Symposium, Queenstown, New Zealand.
- Farhad, S., Saffar-Avval, M., Younessi-Sinaki, M., 2008. Efficient design of feedwater heaters network in steam power plants using pinch technology and exergy analysis. *Int. J. Energy Res.* 32 (1), 1–11.
- Feron, P.H.M., Jansen, A.E., 2002. CO₂ separation with polyolefin membrane contactors and dedicated absorption liquids: performances and prospects. *Sep. Purif. Technol.* 27 (3), 231–242.
- GCCSI, 2009. Strategic analysis of the global status of carbon capture and storage – report 1: status of carbon capture and storage projects globally. Global CCS Institute.
- Ghosh, U., Kentish, S., Stevens, G., 2008. Absorption of carbon dioxide into potassium carbonate promoted by boric acid. In: Ninth International Conference on Greenhouse Gas Control Technologies (GHGT-9). Elsevier, Washington DC, USA.
- Gibbins, J.R., Crane, R.L., 2004. Scope for reductions in the cost of CO₂ capture using flue gas scrubbing with amine solvents. *Proc. Inst. Mech. Eng. Part A J. Power Energy* 218 (A4), 231–239.
- Gorsek, A., Glavic, P., Bogataj, M., 2006. Design of the optimal total site heat recovery system using SSSP approach. *Chem. Eng. Process.* 45 (5), 372–382.
- Hall, S.G., Linnhoff, B., 1994. Targeting for furnace systems using pinch analysis. *Ind. Eng. Chem. Res.* 33 (12), 3187–3195.
- Hektor, E., Berntsson, T., 2007. Future CO₂ removal from pulp mills – process integration consequences. *Energ. Convers. Manage.* 48 (11), 3025–3033.
- Herzog, H., 2000. The economics of CO₂ separation and capture. *Technology* 7 (Suppl. 1), 13–23.
- Ho, M., 2007. Techno-economic modelling of CO₂ capture systems for Australian industrial sources. PhD thesis. School of Chemical Sciences and Engineering, UNSW.
- Hohman, E.C., 1971. Optimum networks of heat exchange. PhD thesis. University of Southern California.
- IEA GHG, 2006. CO₂ Capture in low rank coal power plants. In: IEA greenhouse gas R&D programme. Report number: 2006/1.
- IPCC, 2005. IPCC special report on carbon dioxide capture and storage. Prepared by Working Group III of the Intergovernmental Panel on Climate Change [Metz, B., Davidson, O., de Coninck, H.C., Loos, M., and Meyer, L.A. (Eds.)]. p. 442.
- Jassim, M.S., Rochelle, G.T., 2006. Innovative absorber/stripper configurations for CO₂ capture by aqueous monoethanolamine. *Ind. Eng. Chem. Res.* 45 (8), 2465–2472.
- Klemes, J., Dhole, V.R., Raissi, K., Perry, S.J., Puigjaner, L., 1997. Targeting and design methodology for reduction of fuel, power and CO₂ on total sites. *Appl. Therm. Eng.* 17 (8–10), 993–1003.
- Pierantozzi, R., 2001. Carbon Dioxide. In: Kirk-Othmer encyclopedia of chemical technology. Wiley InterScience, pp. 803–822.
- Leci, C.L., 1996. Financial implications on power generation costs resulting from the parasitic effect of CO₂ capture using liquid scrubbing technology from power station flue gases. *Energ. Convers. Manage.* 37 (6–8), 915–921.
- Linnhoff, B., Alanis, F.J., 1989. A systems approach based on pinch technology to commercial power station design. In: Analysis and design of energy systems: fundamentals and mathematical techniques, 10(2), pp. 31–43.
- Linnhoff, B., Flower, J.R., 1978. Synthesis of heat-exchanger networks 1. Systematic generation of energy optimal networks. *AIChE J.* 24 (4), 633–642.
- Linnhoff, B., Townsend, D.W., Boland, D., Hewitt, G.F., Thomas, B.E.A., Guy, A.R., et al., 1982. A user guide on process integration for the efficient use of energy. IChemE, UK.
- Linnhoff, B., 1986. The process/utility interface. In: Second International Meeting on National Use of Energy, Liege, Belgium.
- Marechal, F., Kalitventzeff, B., 1999. Targeting the optimal integration of steam networks: mathematical tools and methodology. *Comput. Chem. Eng.* 23, S133–S136.
- Mavromatis, S.P., Kokossis, A.C., 1998a. Conceptual optimisation of utility networks for operational variations – I. Targets and level optimisation. *Chem. Eng. Sci.* 53 (8), 1585–1608.
- Mavromatis, S.P., Kokossis, A.C., 1998b. Conceptual optimisation of utility networks for operational variations – II. Network development and optimisation. *Chem. Eng. Sci.* 53 (8), 1609–1630.
- Mimura, T., Simayoshi, H., Suda, T., Iijima, M., Mituoka, S., 1997. Development of energy saving technology for flue gas carbon dioxide recovery in power plant by chemical absorption method and steam system. *Energ. Convers. Manage.* 38 (Suppl. 1).
- Mollersten, K., Gao, L., Yan, J.Y., Obersteiner, M., 2004. Efficient energy systems with CO₂ capture and storage from renewable biomass in pulp and paper mills. *Renew. Energ.* 29 (9), 1583–1598.
- Papoulias, S.A., Grossmann, I.E., 1983. A structural optimization approach in process synthesis-I: utility systems. *Comput. Chem. Eng.* 7 (6), 695–706.
- Pfaff, I., Oexmann, J., Kather, A., 2009. Integration studies of post-combustion CO₂-capture process by wet chemical absorption into coal fired power plant. In: 4th International Conference on Clean Coal Technology: Carbon Capture Technologies II, Dresden, Germany.
- Rao, A.B., Rubin, E.S., 2002. A technical, economic, and environmental assessment of amine-based CO₂ capture technology for power plant greenhouse gas control. *Environ. Sci. Technol.* 36 (20), 4467–4475.
- Reddy, S., Scherffus, J., Freguia, S., Roberts, C., 2003. Fluor's Econamine FG Plus Technology. In: Second National Conference on Carbon Sequestration, Alexandria, VA.
- Romeo, L.M., Bolea, I., Escosa, J.M., 2008. Integration of power plant and amine scrubbing to reduce CO₂ capture costs. *Appl. Therm. Eng.* 28 (8–9), 1039–1046.
- Salama, A.I.A., 2009. Optimal assignment of multiple utilities in heat exchange networks. *Appl. Therm. Eng.* 29 (13), 2633–2642.
- Shang, Z.G., Kokossis, A., 2005. A systematic approach to the synthesis and design of flexible site utility systems. *Chem. Eng. Sci.* 60 (16), 4431–4451.
- Smith, R., 2005. Chemical process design and integration. John Wiley & Sons Ltd., West Sussex, England.
- Stankewitz, C., Epp, B., Fahlenkamp, H., 2009. Integration of a CO₂ separation process in a coal fired power plant. In: Fourth International Conference on Clean Coal Technology: Carbon capture technologies I, Dresden, Germany.
- Umeda, T., Itoh, J., Shiroko, K., 1978. Heat-exchange system synthesis. *Chem. Eng. Prog.* 74 (7), 70–76.
- Varbanov, P., Perry, S., Makwana, Y., Zhu, X.X., Smith, R., 2004a. Top-level analysis of site utility systems. *Chem. Eng. Res. Des.* 82 (A6), 784–795.
- Varbanov, P.S., Doyle, S., Smith, R., 2004b. Modelling and optimization of utility systems. *Chem. Eng. Res. Des.* 82 (A5), 561–578.
- Veawab, A., Aroonwilas, A., Chakma, A., Tontiwachwuthikol, P., 2001. Solvent formulation for CO₂ separation from flue gas streams. In: First National Conference on Carbon Sequestration, Washington, DC.
- Yeh, J.T., Pennline, H.W., 2001. Study of CO₂ absorption and desorption in a packed column. *Energ. Fuel* 15 (2), 274–278.
- Zachary, J., June 2008. Options for reducing a coal-fired power plant's carbon footprint: part I. *Power* 2008, 5.

Chapter 4

**Methodology for combining Multi-Objective Optimisation,
Simulation and Heat Integration for Process Synthesis of CCS**

4. Methodology for combining Multi-Objective Optimisation, Simulation and Heat Integration for Process Synthesis of CCS

4.1 Introduction

The second objective of this thesis is to combine multi-objective optimisation (MOO) with energy targeting using heat integration to determine the impact of varying key operating parameters on the energy penalty associated with adding CCS to a power station. This chapter provides the methodology for how the energy targeting, simulation and multi-objective optimisation are united.

Process synthesis of a new or retrofit process traditionally involves a hierarchy commencing with reactor conditions, separation and recycle systems and then energy minimisation. Though clearly, the amount of energy consumed in a process, will have a large bearing on the financial conditions of the process. The development of pinch analysis has been an important advancement as it enables the estimation of the energy requirements of a process before the heat exchanger network is designed.

A traditional optimisation of a process would use a search procedure to determine the best design and the solution would be a single point for the parameter being optimised. Alternatively, MOO can be used to determine a range of solutions for two or more objectives. MOO uses evolutionary or stochastic search procedures that are robust techniques suitable for non-continuous and non-linear objective functions and constraints. Furthermore, MOO provides greater knowledge of the entire solution space and the variables that are important to optimise the multiple objectives.

Optimisation of a process may involve structural or parametric optimisation. When the process involves new equipment or major retrofits then structural optimisation will be important. Structural optimisation requires either a range of distinct structural options, or the use of a superstructure of the process that includes all the potential structural options. However, structural optimisation with rigorous process simulation can be difficult as the simulation needs to be robust for all the many and varied solution options.

In Chapter 3 it was shown that heat integration using pinch analysis can lead to a reduction in the energy penalty associated with the addition of CCS to a power station. For power stations with CCS the majority of the structural optimisation that is possible revolves around heat exchanger networks. Therefore, the combination of both heat integration and multi-objective optimisation is able to blend the benefits of energy targeting with parametric optimisation of the power station and the capture technology. This methodology is explained in Section 4.2.

In Chapter 3, a method was provided for automating the pinch analysis of retrofitting power stations with CCS. The method is useful for a process that requires additional heat, where the additional heat will be supplied by extracting steam from an existing steam turbine. The method assumes that the quantities of steam that are extracted are small, so that the efficiency of the turbine is not greatly affected by the increase in extraction steam, or that the changes in the steam extraction rates are accompanied by modifications to the turbine to maintain the turbine efficiency. This method uses a set of linear equations to determine the amount of steam that needs to be extracted from each extraction point of the steam turbine to satisfy the deficit of heat in the process whilst minimising the amount of power lost in the steam turbine by the extraction steam. This method, however useful, is limited by a number of factors; the extraction steam must be downstream of any steam reheaters and the method does not allow for steam generation and induction into the steam turbine at any steam level other than the main steam pressure.

Generating steam at lower steam levels can help offset the losses caused by the steam extraction.

A variation on the method provided in Chapter 3 is presented in Section 4.3 of this chapter. The new method is able to be used for more complex steam cycle designs and to recover more heat from the process for power generation. The new method is a superior method for new power stations, as the steam cycle can be specifically designed to extract as much power as possible from the available heat, the new method may also prove to be valid and valuable for retrofits as well. A more detailed analysis of the differences between the two methods is provided in Chapter 7.

4.2 Methodology for the combination of MOO, simulation and automated heat integration

Energy targeting using simulation, heat integration and multi-objective optimisation (MOO) requires two phases; the problem definition stage and the optimisation stage. The algorithm which details each step of both the problem definition and optimisation stages is shown in Figure 4-1. Each step, 1 to 12, is then explained in further detail in Sections 4.2.1 to 4.2.12. The methodology is not restricted to the optimisation of power stations with CCS. Therefore the methodology is explained both in general terms and as it is employed in this thesis. A detailed explanation of the programming code developed to apply this methodology is provided in Appendix A.

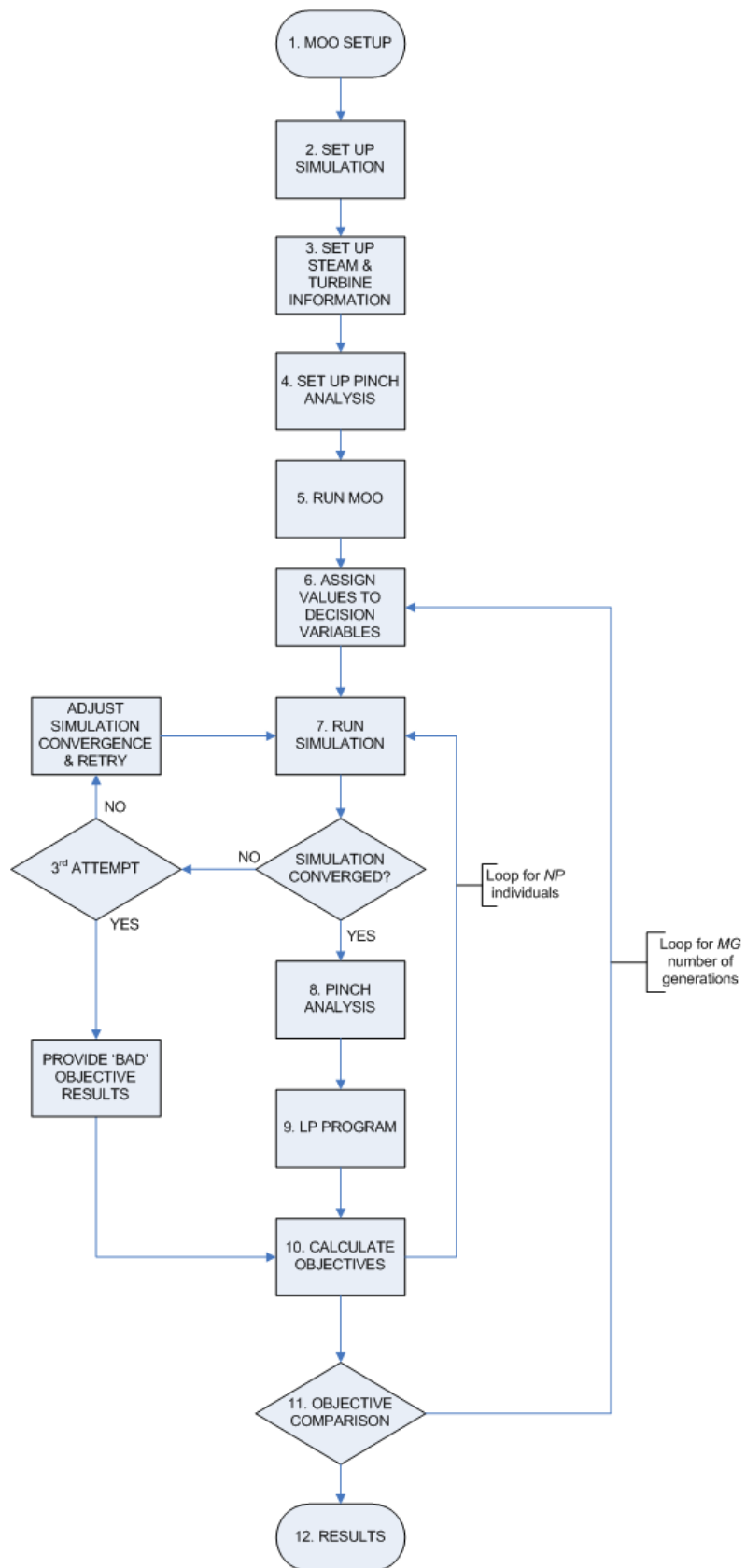


Figure 4-1: Algorithm for combined multi-objective optimisation, simulation and heat integration

4.2.1 MOO Setup – Problem Definition

The first step of the process is to select the objective/objectives, the decision variables, constraints and the MOO parameters for the particular study. In this work we have used the elitist Non-dominated Sorting Genetic Algorithm (NSGAI) (Deb et al. (2002)) for the optimisation algorithm. It is applied in this thesis using an Excel® interface written in Visual Basic® (VBA), where the NSGAI algorithm is coded directly into VBA (Sharma et al. (2011)). Previously Bhutani et al. (2007) interfaced a C++ version of the NSGAI code with VBA to enable the optimiser to interface with a simulation package. Whilst the VBA version created by Sharma et al. (2011) is slower than the C++ version, the use of VBA has the benefit of using Excel and the associated functions directly and the optimisation computation times is insignificant when compared to the simulation computation time. Other MOO programs and other programming languages could equally be used.

As described by Deb et al. (2002), the NSGAI code works by creating a population of NP individuals and each individual has its own values for each of the decision variables. In the first iteration these values will be randomly generated, however for subsequent iterations these values are based on methods that model natural selection to try to find the global optimal solutions. A subset of the NP top ranking individuals is stored as the parent population. The results of every new generation, the offspring, is compared to the parent population and the NP top ranked individuals from the combined list of parents and offspring is now stored as the new parent population used to generate the subsequent generations.

New generations of individuals are created by combining two of the parents. The new individuals can also have random changes, called mutations, made to the values of the variables to enable the individuals to have variations in the values of the decision variables to the parents. This process is continued for MG number of generations.

The MOO algorithm requires NSGAI specific parameters to be defined; which include the population size (NP), the number of generations (MG), the random seed, the selection type, crossover type, crossover probability, mutation type and mutation probability. There are also problem specific parameters that need to be defined; the number of objectives and whether those objectives are to be maximised or minimised. For each decision variable the range (minimum and maximum) of values needs to be provided along with the accuracy of the binary data (the number of bits) for each decision variable; which sets values that the individual may take for each decision variable. For example, a decision variable with a range of 0(minimum) to 1.5(maximum) and a bit size (b) of 2 will have intervals of 0.5 (calculated by Equation [1]) and

therefore that decision variable could take the form of any of the following variables 0, 0.5, 1 or 1.5. Obviously for real variables the bit size should be large to ensure the representation as a continuous variable.

$$\text{Interval Size} = (\text{Max}-\text{Min}) / (2^b-1) \quad [1]$$

Inequality constraints can also be included in the problem definition. The constraints may be one of the objectives or may be a separate variable altogether. Mathematically a MOO problem with two objectives can be described as;

$$\text{Minimise or Maximise } f_1(x) \quad [2]$$

$$\text{Minimise or Maximise } f_2(x) \quad [3]$$

$$\text{Subject to } x^l \leq x \leq x^u \quad (\text{bounds on decision variables}) \quad [4]$$

$$g(x) \leq 0 \quad (\text{inequality constraints}) \quad [5]$$

4.2.2 Set up Simulation

The process is simulated directly in simulation software that can have input and output parameters controlled by VBA such as Aspen Plus®, HYSYS® or PRO/II™. The simulations need to be designed so that the decision variables are process input specifications so that changes in the decision variables will make the appropriate changes in the simulation. Any results required from the simulation to calculate the objectives and constraints also need to be determined and made so that they can be exported from the simulation package. In Aspen Plus® it is straightforward to use a 'Calculator Block' to receive all the decision variables from the optimisation program and then these variables can be exported to their appropriate location in the simulation. Likewise the results from the simulation could be exported to another 'Calculator Block' for easy transfer back to the optimisation program. In HYSYS® the same method can be used with the use of a 'Spreadsheet' function as detailed by Bhutani et al. (2007).

4.2.3 Set up problem specific analysis (Steam Cycle & Turbine Information)

In this step the information for the utilities for the heat pinch analysis is defined in Excel. For example details of the temperature-enthalpy relationship and cost of various heating and cooling utilities can be provided or the detailed information for a steam cycle can be added to Excel. For the optimisation of power stations with CCS, the steam turbine information is input into Excel, including the pressure and temperature of the main steam, the pressure of all other steam mains, the outlet temperature of any reheat sections and the condensing temperature or pressure (Appendix A, Section 3.3). This step is used to define both the quality of the steam available for

process heating and the amount of electricity that the steam can produce. It is also possible to include the pressure/temperature levels of the steam headers as decision variables in the MOO.

4.2.4 Set up Heat Pinch Analysis

The simulation streams that should be included in the heat pinch analysis need to be selected. In this application a VBA program is used, which provides all the available process streams in the defined simulation and then requires the user to select from that list the processes that represent the hot/cold streams required for pinch analysis (Appendix A, Section 3.4).

For the optimisation of power stations with solvent based CO₂ capture this will generally include the flue gas, the air-preheat, the lean and rich solvent heat exchangers, the solvent reboiler, the stripper condenser and the CO₂ compressor intercoolers. Of course, if the user decides that any of the existing heat exchangers should not be impacted, these can be left out of the analysis.

4.2.5 Run MOO

At this stage of the process the MOO program can be run (Appendix A, Section 4.1). The MOO program will run steps 7 to 10 for each individual in each generation, therefore NP times, before progressing to step 11. Steps 6 to 11 are then run MG times before the results are provided in Step 12. Therefore the program loops through a total of $NP \times MG$ times.

4.2.6 Assign Values to Decision Variable

The MOO program will assign values to each decision variable for each individual in the generation in question. In the first iteration the values for each decision variable will be selected using a random number generator to attain a value that is within the range provided for each variable. In subsequent iterations the values of the decision variables will be generated using the rules established in the NSGAI algorithm which involves 'selecting' two of the parents, combining the decision variables of the two parents to form the decision variables of the offspring using 'crossover' rules and then allowing 'mutation' rules to potentially alter the values of decision variables.

4.2.7 Run Simulation

For each individual, the decision variables that have been selected by the MOO program are exported using VBA to the process simulation program (AspenPlus®/HYSYS/PRO/II etc.)(Appendix A, Section 4.3). The VBA program will also be used to start the process simulator and wait until the simulation has converged using the values of the decision variables for the given individual. The work by Bhutani et al. (2007) explains in detail the method for running HYSYS from VBA for MOO.

During this step it is also possible to check that the process simulator has converged and if the simulation has converged then the program can proceed. If the simulation has not converged or has converged with errors, it is possible and advisable to make adjustments to the simulation to help it converge at this stage. For example, when using Aspen Plus® as the process simulator, if the simulation has not converged then it can be reinitialised, before trying to get the simulation to converge a second time. Also it may be useful to first converge the simulation with a set of decision variables that are known to enable the simulation to converge and then re-trying the individual's decision variables, as the simulation packages often need a good initialising point to enable them to converge.

Retrying to get a converged simulation from the given decision variables is more important when using complex simulations especially those with complex distillation columns. It is also important when setting up the simulations to check them for their robustness and to set iteration limits on recycle streams or distillation columns that provide sufficient time to enable the simulation to converge, but will not waste time on simulations that will not converge.

If it is not possible to converge the simulation, the VBA program should apply bad values to the objectives and return to the start of step 7 for the next individual to be tested. Bad values will be very large values for minimisation objectives or very small values for maximisation objectives and this in turn penalises the input parameters that led to the non convergence.

4.2.8 Pinch Analysis

Once the process simulation is complete and converged, the stream temperature-enthalpy (T-H) data for the selected streams are extracted from the process simulator. The T-H data for each stream is then simplified using a VBA based algorithm. The simplification of the T-H data aims to reduce the number of points that define the T-H curve for the stream by linearising sections of the curve that remain linear within an acceptable margin (Refer to Figure 4-2)(see Appendix A, Section 4.4.2 for details of linearising algorithm). Applying the conservative methodology outlined by Smith (2005) whereby the linearisation of hot streams will always be to colder temperatures than those extracted from the simulation and the opposite for the cold streams. The stream data is then compiled into composite curves and grand composite curves using a VBA program (Appendix A, Section 4.4.3) to automate the established Problem Table Algorithm (Linnhoff and Flower (1978)).

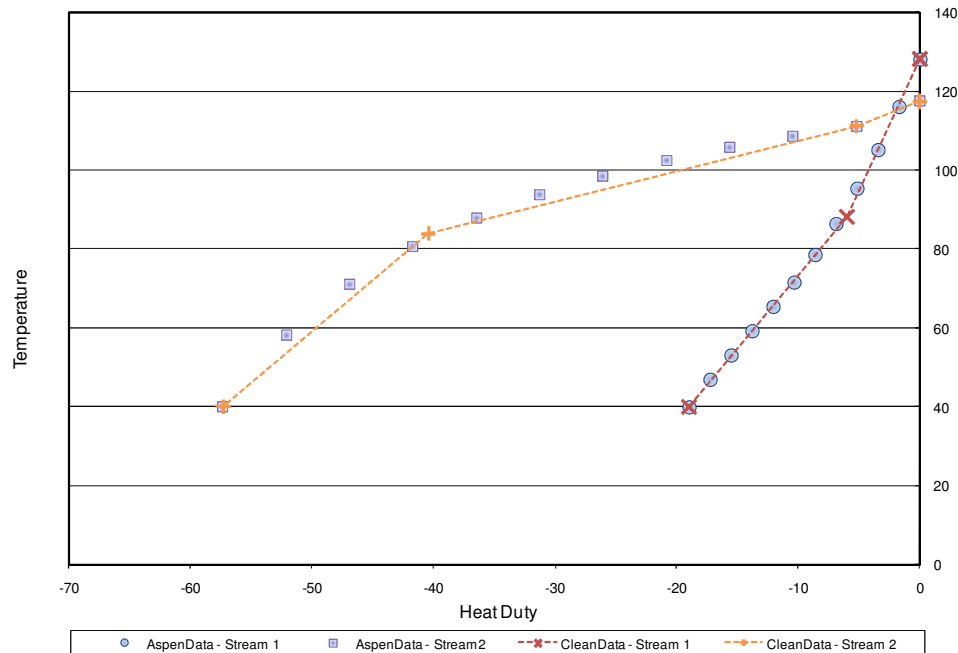


Figure 4-2: Example of the simplification of the T-H data by linearising the heat curve data extracted from Aspen.

The composite curves (CC) and grand composite curves (GCC) provide the details on the amount of heat that needs to be supplied and/or removed from the process and at what temperature the heat is supplied or available. The GCC is used as the basis for the post pinch analysis processing described in Section 4.2.9.

4.2.9 Post Pinch Analysis Processing (Automated Linear Programming)

The GCC is used to optimise the quantities of each utility required for the simulated system. The optimisation will depend on the problem specific definition, but where utilities are needed to satisfy the process requirements they will be optimised to determine the least cost/highest profit mix of utilities, whilst for utility providers it will be based on maximising the production of the desired utility. For the optimisation of power stations with CCS, an automated linear programming technique is used. The automated linear programming is an Excel / VBA based algorithm that calculates the maximum amount of power that can be generated for a given grand composite curve with a given turbine (Appendix A, Section 4.5).

As discussed in the introduction an automatic linear programming pinch analysis technique was developed in Chapter 3 and a second method will be detailed in Section 4.3 of this chapter. The first method which is referred to as the 'extraction' method can be used when steam is extracted from an existing steam turbine to provide heat for a process that requires additional heat. It can be used when a process modification is made to a power station that leads to a deficit of heat,

such as created by the addition of a solvent CO₂ capture plant. The second method, referred to as the 'superstructure' method, is more flexible and can be used for new or existing steam turbines. It is used to predict the maximum amount of power that can be generated in the steam turbine given the excess heat that is available in a process as detailed by the GCC. The aim of both methods however, is to predict, for a given process combined with a given turbine, what the maximum amount of power that can be generated in that process. Therefore, for each individual option that is simulated it is possible to calculate the maximum amount of power that can be generated from the process with the given values of each decision variable in that individual.

4.2.10 Calculate Objectives

The objectives of the particular study are calculated or imported from the simulation, the heat integration and/or the post pinch analysis processing (automated linear programming pinch analysis). This step will often include the estimation of capital and/or operating expenses or other objectives, such as the emissions intensity of the process, that arise from results calculated in previous steps. Whatever the objectives are of the particular study, they need to be exported back to MOO program for each individual in the population.

4.2.11 Objective Comparison

The MOO program stores the objective values for each individual and after the objective values for the entire generation are calculated, the results for that generation are combined with the results from the parent population to form a set of options made up of the $2 \times NP$ individuals. The NP individuals that have the best results with relation to the objectives, the Pareto optimal solutions, will remain in the solution set. The best results are determined by ranking the $2 \times NP$ individuals based on the number of other solutions which dominate them, and then further sorted based on their level of 'crowding comparison'. So the NP individuals that firstly, have the least number of other individuals that dominated them, and then secondly, that are least crowded by other solutions in the objective space, are those that become the parent solutions for the subsequent generation. The new NP parent solutions will form a Pareto-optimal front, with results that are distributed as much as possible in the solution space.

The NP individuals in the new parent set are then used to create the offspring as described in Step 6, and then steps 6 to 11 are repeated MG times.

4.2.12 Results

After MG number of generations the final NP best individuals is the final population set. The population provides a set of solutions that are the Pareto optimal solutions for the $MG \times NP$ individuals that were tested in running the program. The population set can be used to extract

significant amounts of information. Not only will the Pareto optimal front provide insight as to the rate of trade-off between the objectives, the solution set also enable the designer to examine what decision variables are likely to provide the best results with regard to the objectives. It can be used to show what values of the decision variables are preferable for certain regions of the optimisation space and to some extent the level of impact of each of the decision variables. If the results after *MG* generations do not provide conclusive results and the resultant parent set is still changing considerably in the later generations, then it is possible to run the MOO program for further generations using the solution set from the first optimisation as the initial population in the new run.

4.3 Superstructure method of Post Pinch Analysis Processing

As mentioned in Section 4.2.9 two methods have been developed to predict the maximum amount of power that can be generated from a GCC for power stations fitted with CCS. As discussed, the extraction method presented in Chapter 3 can be used to automatically determine the steam extraction rates to overcome the deficit of heat that occurs due to the addition of CCS to a power station. However, the method only concentrates on the extraction steam requirements and does not allow the optimisation of the steam generation rates and therefore a new method, called the 'superstructure' method has been developed and is now explained.

For the 'extraction' method, detailed in Chapter 3, the optimisation of the extraction steam rates can be arranged as a set of linear equations provided the extraction steam pressures are fixed, and therefore can be solved rapidly using linear algorithms. A similar approach is applied to the 'superstructure' method to develop a set of linear equations that can be used for more complex steam cycle designs and to recover more heat from the process for power generation. Like the 'extraction' method, the 'superstructure' method assumes that the efficiency of the steam turbines do not change with the amount of steam that is generated or extracted from the turbine.

The method requires defining a steam cycle to optimise with the power station and CCS process GCC. The steam cycle could be that of an existing steam cycle for a retrofit or a completely alternative cycle for a new power station. For the sake of explaining the method a steam turbine model, with three steam mains and a single stage of reheat is provided in Figure 4-3 for reference. For this method to work, obviously there needs to be net heat available in the process, and this targeting method determines the optimal steam generation and extraction rates for the given turbine to maximise the power generated from the available heat. The first task in determining the energy targets of the process is to provide the details of the steam cycle; including the main steam pressure and temperature (P_1 and T_1), the reheat temperature for any reheat stages (T_{R2}),

the pressure of all the steam headers including the last condensing stage (P_2 to P_n), any pressure drops in the heat exchangers and the efficiency of each stage of the turbine.

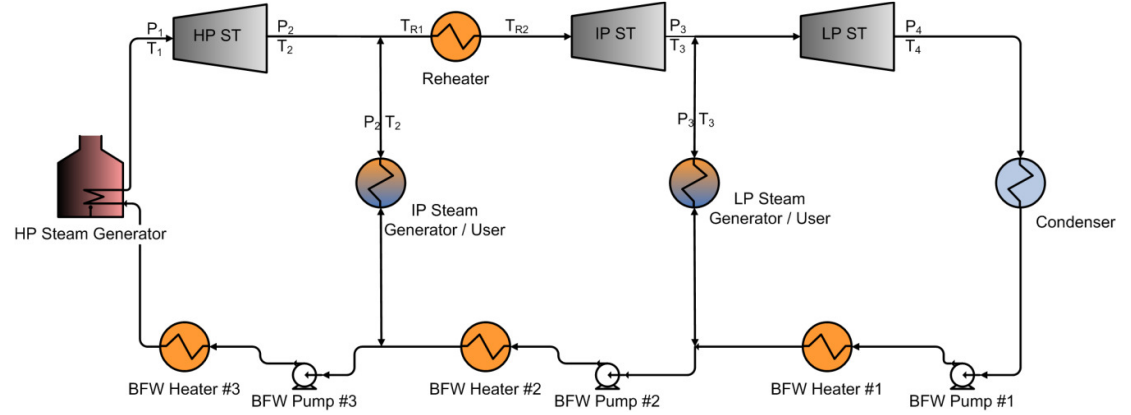


Figure 4-3: Steam turbine with three pressure levels and a single stage of reheat

Once the details of the steam cycle are determined or assumed, the power generated by steam through each stage of the steam turbine can be calculated by multiplying the flowrate of steam for the given stage of the turbine by the specific amount of work that the steam will generate, as represented by Equation [6].

$$W_{i,i+1} = F_i \cdot \eta_{i,i+1} (H_i - H_{iseni}(P_{i+1}, S_i)) \quad [6]$$

Therefore the total amount of power that is generated by steam at level i is calculated by the summation of the power produced through each steam turbine from level i to the condensing stage (stage n) as per equation [7].

$$W_{i,n} = F_i \sum_{i=i}^{i=n-1} \eta_{i,i+1} (H_i - H_{iseni}(P_{i+1}, S_i)) = F_i \omega_i \quad [7]$$

If steam is extracted/used at any stage that steam will no longer produce power and therefore the contribution of that steam needs to be subtracted from the total power calculation, which is accounted for, by subtracting the flowrate of steam extracted (f_i) as per equation [8].

$$W = \sum_{i=1}^{i=n-1} (F_i - f_i) \cdot \sum_{i=i}^{i=n-1} \eta_{i,i+1} (H_i - H_{iseni}(P_{i+1}, S_i)) = \sum_{i=1}^{i=n-1} (F_i - f_i) \cdot \omega_i \quad [8]$$

Equation [8] calculates the amount of power that will be generated for a given rate of steam generated and extracted at each steam level. Therefore this is the value that we are trying to maximise using linear programming. As can be seen from the equations [6] to [8], provided that the steam pressure levels are pre-defined then equation [8] is linear.

The next stage of determining the steam turbine energy targets is to add the thermodynamic constraint to the linear programming problem. The thermodynamic constraint is that steam can only be generated where there is a net surplus of heat in the process. This can be evaluated by

generating steam composite curves (SCC) which must be less than or equal to the energy in the GCC at every temperature.

The SCC is generated by determining the amount of energy (ΔH_i) required to generate the F_i kilograms of steam and the amount of energy (Δh_i) that can be used by the f_i kilograms of steam extracted from the steam turbine. Firstly a list of all the temperatures that make up the GCC is generated (referred to as t_0 to t_{max}). Then for each steam level the energy difference between the steam in the steam header, and the steam/condensate at each temperature on the list, is calculated (Refer to equation [9] and [10]). When the steam header occurs upstream of a reheater, the energy required by the reheater is included in the energy of the steam. For steam generation, the enthalpy is calculated at a temperature $\frac{1}{2} \Delta T_{min}$ above the actual temperature of the steam. The GCC temperatures already take into account a decrease of the hot streams by $\frac{1}{2} \Delta T_{min}$, so when the two are combined, a total of ΔT_{min} is taken into account. Likewise the enthalpy of the steam that is extracted from the turbine and used for heating is calculated at a temperature $\frac{1}{2} \Delta T_{min}$ greater than the actual temperature.

$$\Delta H_{i,t} = H_i - H_{i,t} \quad [9]$$

If i includes reheat and $t > T_{R1}$ then: $\Delta H_{i,t} = H_i - H_{i,t} + H_{i,R2} - H_{i,t}$

$$\Delta h_{i,t} = h_i - h_{i,t} \quad [10]$$

If i includes reheat and $t > T_{R1}$ then: $\Delta h_{i,t} = h_i - h_{i,t} + h_{i,R2} - h_{i,t}$

The SCC is therefore the list of net heat required by the steam cycle at every temperature and is created by the summation of energy for the generation and extraction of each steam level at every temperature as defined by Equation [11].

$$\forall t = t_0 \text{ to } t_{max}: \quad \sum_{i=1}^{i=n} (F_i \Delta H_{i,t} - f_i \Delta h_{i,t}) \leq H_{GCC,t} \quad [11]$$

One further constraint is added that the steam extracted from the turbine must clearly be no larger than the net steam generated in the stages upstream, ie. the steam must have been generated before it is able to be used (Refer to equation [12]). Determining the turbine energy targets is therefore a constrained linear programming problem as defined by equations [8], [11] and [12].

$$\text{Maximise} \quad W = \sum_{i=1}^{i=n-1} (F_i - f_i) \cdot \omega_i \quad [8]$$

$$\text{Subject to} \quad \forall t = t_0 \text{ to } t_{max}: \quad \sum_{i=1}^{i=n} (F_i \Delta H_{i,t} - f_i \Delta h_{i,t}) \leq H_{GCC,t} \quad [11]$$

$$\forall i = 1 \text{ to } n: \quad \sum_{i=1}^{i=n} (F_i - f_i) \geq 0 \quad [12]$$

It helps to understand the linear optimisation problem by representing the constraints as two matrices of conditional constraints, as follows;

$$\begin{bmatrix} \Delta H_{1,t_0} & \Delta H_{2,t_0} & \cdots & \Delta H_{n,t_0} & -\Delta h_{1,t_0} & \cdots & -\Delta h_{n,t_0} \\ \Delta H_{1,t_1} & \Delta H_{2,t_1} & \cdots & \Delta H_{n,t_1} & -\Delta h_{1,t_1} & \cdots & -\Delta h_{n,t_1} \\ \vdots & \vdots & \ddots & \vdots & \vdots & \ddots & \vdots \\ \Delta H_{1,t_{max}} & \Delta H_{2,t_{max}} & \cdots & \Delta H_{n,t_{max}} & -\Delta h_{1,t_{max}} & \cdots & -\Delta h_{n,t_{max}} \end{bmatrix} \begin{bmatrix} F_1 \\ F_2 \\ \vdots \\ F_n \\ f_1 \\ \vdots \\ f_n \end{bmatrix} \leq \begin{bmatrix} H_{GCC,t_0} \\ H_{GCC,t_1} \\ \vdots \\ H_{GCC,t_{max}} \end{bmatrix} \quad [11]$$

$$\begin{bmatrix} 1 & 0 & \cdots & 0 & -1 & \cdots & 0 \\ 1 & 1 & \cdots & 0 & -1 & \cdots & 0 \\ \vdots & \vdots & \ddots & \vdots & \vdots & \ddots & \vdots \\ 1 & 1 & \cdots & 1 & -1 & \cdots & -1 \end{bmatrix} \begin{bmatrix} F_1 \\ F_2 \\ \vdots \\ F_n \\ f_1 \\ \vdots \\ f_n \end{bmatrix} \leq \begin{bmatrix} 0 \\ 0 \\ \vdots \\ 0 \end{bmatrix} \quad [12]$$

The maximum steam turbine energy targets can then be solved using linear programming, producing the maximum amount of energy for a given turbine from the given GCC. An example of the SCC plotted with the GCC is shown in Figure 4.3. The method described can also be used with other equality constraints to enable the method to be used for retrofit applications, for example the main steam flowrate (F_1) may be set to be equal to the existing main steam flowrate and the linear programming problem will still be able to be solved using linear programming algorithms.

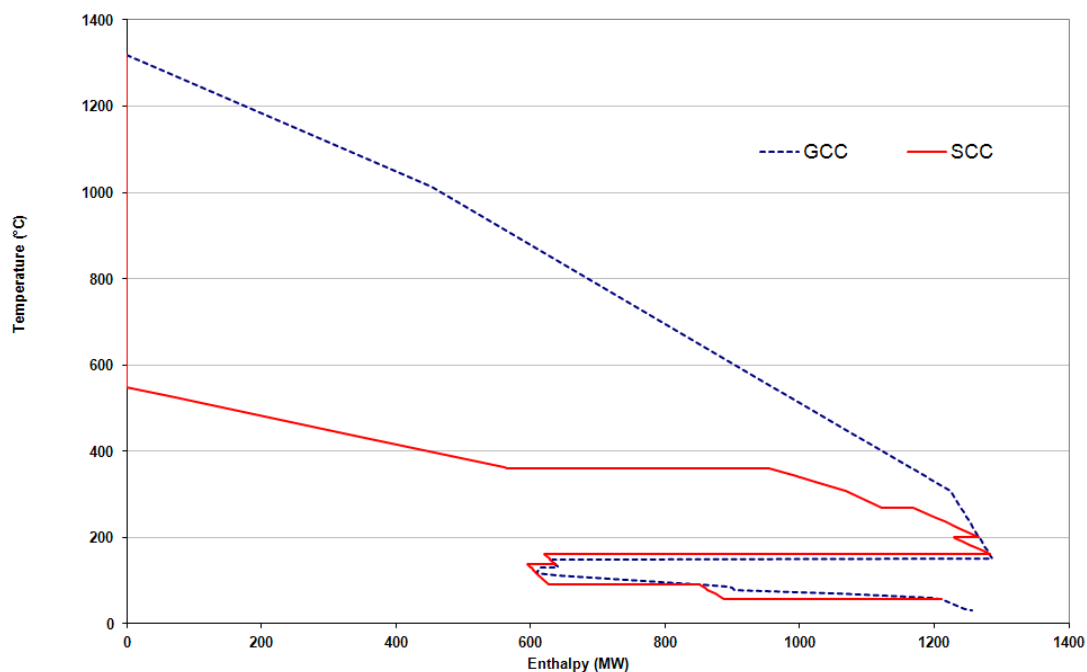


Figure 4-4: Example of the SCC developed for the GCC using 'superstructure' method of linear programming pinch analysis.

4.4 Conclusion

This chapter provided a methodology for the combination of MOO with simulation and automated heat integration. This combination is not only applicable to the application of power stations with CCS but has a wide range of other energy intensive industries. Two methods have now been presented for the automated pinch analysis, the 'extraction' method in Chapter 3 and the 'superstructure' method in this chapter. The two methods are compared in Chapter 7. The detailed explanation of the code required to implement the combined MOO, simulation and heat integration approach is provided in Appendix A.

References

- Bhutani, N., A. Tarafder, G. P. Rangaiah and A. K. Ray (2007). "A Multi-platform, multi-language environment for process modelling, simulation and optimisation." *International Journal of Computer Applications in Technology* 30(3): 197-214.
- Deb, K., A. Pratap, S. Agarwal and T. A. M. T. Meyarivan (2002). "A fast and elitist multiobjective genetic algorithm: NSGA-II." *Evolutionary Computation, IEEE Transactions on* 6(2): 182-197.
- Linnhoff, B. and J. R. Flower (1978). "Synthesis of heat-exchanger networks 1. Systematic generation of energy optimal networks." *AIChE Journal* 24(4): 633-642.

- Sharma, S., G. P. Rangaiah and K. S. Cheah (2011). "Multi-objective optimization using MS Excel with an application to design of a falling-film evaporator system." Food and Bioprocess Processing doi: 10.1016/j.fbp.2011.02.005.
- Smith, R. (2005). Chemical Process Design and Integration. West Sussex, England, John Wiley & Sons Ltd.

Chapter 5

Using multi-objective optimisation in the design of CO₂ capture systems for retrofit to coal power stations.

Energy 41 (1) (2012) 228 – 235 (In Press)

doi: 10.1016/j.energy.2011.06.031

5.1 Introduction

This chapter is based on an article published in Energy which shows how improvements can be obtained in the performance of a power station fitted with CCS by the use of heat integration and multi-objective optimisation. The article also shows how optimisation of the CO₂ capture process without taking CO₂ compression and the power station into account can result in different designs and operating conditions when compared to a design that considers the process holistically.

This paper uses the optimisation framework explained in Chapter 4 that combines heat integration with multi-objective optimisation, but goes into more detail into how the optimisation can lead to improvements in design and what level of improvement may exist in maximising the heat integration between the power station and the CCS equipment.

As the case study in this chapter is based on the retrofit of CCS equipment to an existing power station which uses a simple steam cycle with no reheat, the paper uses the linear programming method developed in Chapter 3 rather than the method developed in Chapter 4.

The paper also only uses three decision variables; the solvent loading and flowrate and the stripper pressure, and therefore when compared to results provided in Chapters 6, and 8 will not necessarily be the optimum design. However, this chapter is able to illustrate most clearly the value of using MOO and the importance of heat integration. The paper is also used to determine what range of values the most important operating variables should take.

This paper compares the results found from the research in this thesis for potassium carbonate solvent based CCS with results of other papers that also use potassium carbonate. The comparison shows the importance of not only the solvent plant design, but also the power station design and its operating environment on the energy penalty incurred by adding CCS.

5.2 Declaration for Chapter 5

Monash University

Declaration for Thesis Chapter 5

Declaration by candidate

In the case of Chapter 5, the nature and extent of my contribution to the work was the following:

Nature of contribution	Extent of contribution (%)
Initiation, key ideas, simulations, methodology, results interpretation, writing of paper.	80

The following co-authors contributed to the work. Co-authors who are students at Monash University must also indicate the extent of their contribution in percentage terms:

Name	Nature of contribution	Extent of contribution (%) for student co-authors only
Andrew Hoadley	Initiation, results interpretation, reviewing of paper.	
Barry Hooper	Initiation, results interpretation, reviewing of paper.	

Candidate's
Signature



Date
18/12/11

Declaration by co-authors

The undersigned hereby certify that:

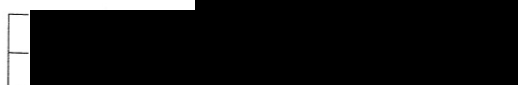
- (1) the above declaration correctly reflects the nature and extent of the candidate's contribution to this work, and the nature of the contribution of each of the co-authors.
- (2) they meet the criteria for authorship in that they have participated in the conception, execution, or interpretation, of at least that part of the publication in their field of expertise;
- (3) they take public responsibility for their part of the publication, except for the responsible author who accepts overall responsibility for the publication;
- (4) there are no other authors of the publication according to these criteria;
- (5) potential conflicts of interest have been disclosed to (a) granting bodies, (b) the editor or publisher of journals or other publications, and (c) the head of the responsible academic unit; and
- (6) the original data are stored at the following location(s) and will be held for at least five years from the date indicated below:

Location(s)

Cooperative Research Centre for Greenhouse gas Technologies, CO2CRC,
Room 232, Level 2, Bldg 193, The University of Melbourne, Parkville VIC, 3010

[Please note that the location(s) must be institutional in nature, and should be indicated here as a department, centre or institute, with specific campus identification where relevant.]

Signature 1



Date
21/12/11

Signature 2



14/12/11



Using multi-objective optimisation in the design of CO₂ capture systems for retrofit to coal power stations

Trent Harkin^{a,b,*}, Andrew Hoadley^b, Barry Hooper^a

^a Cooperative Research Centre for Greenhouse Gas Technologies (CO2CRC), The University of Melbourne, Vic., 3010, Australia

^b Department of Chemical Engineering, Monash University, Clayton Vic., 3168, Australia

ARTICLE INFO

Article history:

Received 1 October 2010

Received in revised form

28 May 2011

Accepted 11 June 2011

Available online xxx

Keywords:

Multi-objective optimisation

Carbon capture

Carbonate

ABSTRACT

An Aspen Plus® simulation of an existing power station with a potassium carbonate based carbon capture (CCS) plant including CO₂ compression is combined with an Excel based genetic algorithm to optimise the net power output of the power station and amount of CO₂ captured for a range of solvent flowrates, lean loading and stripper pressures. The net power output was compared for a CCS plant that is added to the power station without any heat integration to a system where heat integration is maximised by the use of pinch analysis and linear optimisation to calculate the amount of steam required to be extracted from the turbine to meet the additional heating requirements of the CCS plant. The multi-objective optimisation of the process identified that lean solvent loading and stripper pressure will have a large impact on the net power output and amount of CO₂ captured. The curves developed in the multi-objective optimisation can provide not only the ability to determine the CO₂ capture rate to maximise the profit at a given time due to fluctuating electricity prices, but will also provide the optimum solvent flowrate and lean loading to achieve that maximum capture rate for a given net power. The paper shows that the design of the optimum carbon capture plant will depend not only on the specific capture process but also on the conditions of the power station and the importance in optimising the whole process at the same time. The minimum energy penalty for the potassium carbonate system combined with the reference power station modeled in this paper is 1.02 MJ_e/kgCO₂ with a reboiler regeneration energy of 5.3 MJ_{th}/kgCO₂. In this example optimisation and heat integration was able to reduce the energy penalty by 0.4 MJ_e/kgCO₂.

Crown Copyright © 2011 Published by Elsevier Ltd. All rights reserved.

1. Introduction

Existing coal fired power stations represent an estimated 60% of anthropogenic carbon emissions. CO₂ capture and storage (CCS) from these power stations is one of the key technologies required to stabilise atmospheric CO₂ concentrations, however the addition of CCS to existing power plants could lead to a reduction in efficiency of 10–15% points [1]. The reduction in net power produced from a power station can be referred to as the energy penalty. The energy penalty can be defined in many ways and in this paper is defined as the loss in electricity per mass (MJ_e/kg) of CO₂ captured and compressed to the transport pressure of 100 bar.

For existing pulverised coal fired power stations CO₂ capture can be retrofitted to the power station by converting to oxyfuel combustion or adding post-combustion separation technologies. For post-combustion capture the CO₂ can be separated using a variety of technologies including solvent absorption, adsorption or membrane based processes. Solvent-based separation is deemed to be the most advanced of the separation technologies with scale-up issues, solvent degradation, capital and operating costs being the largest obstacles for implementation. A significant amount of research is being conducted into developing solvent-based processes. The solvents are generally amine based, but alternatives such as potassium carbonate based processes are also being developed.

Potassium carbonate has been used to separate acid gases including CO₂ in the gas industries for over 40 years and is being considered as an alternative to amine based solvents [2,3] for application in CCS projects. The potassium carbonate processes has a number of advantages when compared to amine based processes; lower volatility, lower raw material costs, lower rates of degradation, oxygen tolerance and the ability to absorb the incoming SO_x

Abbreviations: CCS, carbon capture and storage; MOO, multi-objective optimisation.

* Corresponding author. Cooperative Research Centre for Greenhouse Gas Technologies (CO2CRC), The University of Melbourne, Vic., 3010, Australia. Tel.: +61 3 8344 504; fax: +61 3 9347 7438.

E-mail address: t.harkin@unimelb.edu.au (T. Harkin).

0360-5442/\$ – see front matter Crown Copyright © 2011 Published by Elsevier Ltd. All rights reserved.

doi:10.1016/j.energy.2011.06.031

Please cite this article in press as: Harkin T, et al., Using multi-objective optimisation in the design of CO₂ capture systems for retrofit to coal power stations, Energy (2011), doi:10.1016/j.energy.2011.06.031

and NO_x compounds to form potentially useful potassium sulphates/nitrates avoiding the need for upstream flue gas treatment. This is especially relevant in locations, such as Australia, that use low sulphur coals and therefore do not currently have any flue gas desulphurisation installed. However a disadvantage of the traditional 30 wt% potassium carbonate solution is the higher energy of regeneration and lower reaction kinetics when compared to the leading amine solvents. Therefore, it is important to make sure that the potassium carbonate process is optimised to minimise the energy requirements of the process.

The potassium carbonate process has a much wider operating range when compared to amines as they are not constrained by the temperature limits imposed by thermal degradation of the amines. With less stringent temperature limits the potassium carbonate system has a number of variables that can be adjusted over a wide range of conditions; these variables will often have antagonising impacts on the objectives for the system. For example, to minimise the additional power consumed by the addition of CCS, the solvent regeneration may be operated under vacuum, which, for potassium carbonate solvents, leads to reductions in the energy consumption in the reboiler. The temperature required for reboiling decreases, allowing lower quality steam to be used for solvent regeneration, however low pressure leads to increased CO₂ compression requirements. There will also be impacts on the capital costs due to the increase in equipment sizes due to operation at low pressure.

Notwithstanding the regenerator pressure, there are a number of other solvent plant variables that may be adjusted including the solvent flowrate, lean solvent CO₂ loading, rich solvent loading, flue gas temperature, column heights, absorber pressure and solution temperatures throughout the system. These variables will have different impacts on the operation of the solvent plant and with the addition of the solvent plant to the power station, they will also impact the operation of the power station itself. Each CCS project may have many objectives; including maximising the net power output of the power station, minimising the CO₂ emissions, minimising the capital and/or operating costs, maximising profit and maximising the operability, reliability and flexibility of the power station.

Reducing the amount of thermal energy required to regenerate the solvent is often used as the prime objective when trying to optimise the solvent process and is usually quoted for amine processes as operation between 3 and 5 MJ/kgCO₂ [4,5]. As noted by Jassim and Rochelle [6] the primary objective for analysing modifications to a solvent plant should be the minimisation of the reboiler energy. However, this was in relation to monoethanolamine (MEA) systems where the reboiler energy is improved by increasing the stripper pressure and the stripper pressure is limited by thermal degradation of the solvent, so the stripper pressure is usually fixed at between 200 and 250 kPa. For potassium carbonate solvents where the stripper pressure has opposing effects on the energy required for solvent regeneration and compression, it is not obvious that minimising the reboiler energy requirements will lead to the most optimum process. Therefore it is important when analysing the impact of the addition of CCS, with any solvent system, but especially for potassium carbonate, that the whole system is included in the optimisation process. Pfaff et al [7], noted the importance of boundary conditions on the energy penalty of a system with the type of coal, power station, ambient conditions and level of CO₂ compression and integration all having an impact on the energy penalty of a system. In their paper they also looked at a range of options for integrating the heat available in an MEA based solvent system into the power station water-steam-cycle to reduce the energy penalty, however they did not consider making adjustments to the solvent system variables in order to reduce the energy penalty even further.

This paper is used to determine the impact of changing a number of key variables for a power station retrofitted with a potassium carbonate based CCS system and the importance of optimising those variables with a whole system in mind. The paper describes a method that includes simulation, heat integration and multi-objective optimisation. The optimisation in this paper is restricted to analysing the impacts on the net power produced from the power station, however the same method can be used to analyse the impact of changing the key variables on the capital and operating costs as well. In this paper three variables will be analysed for a potassium carbonate system; the solvent lean loading, the solvent flowrate and the stripper pressure. The solvent lean loading and flowrate impact the amount of CO₂ absorbed, and when combined with the regenerator pressure, have a large influence on the amount of energy required for solvent regeneration. The impact of adjusting these variables on the amount of CO₂ captured and the stripper reboiler energy will be reviewed and then compared to the impact on the net power output of a power station with and without maximum heat recovery. In this way the importance of optimising the process as an integrated process will be shown.

Varying the solvent lean loading and flowrate alters the amount of CO₂ absorbed, however it also demonstrates the impact of changing the CO₂ capture rate on the energy penalty caused by the addition of CCS. This information will be important when considering what level of CO₂ capture should be implemented at any time to maximise the power station profits, when subjected to a carbon price on emissions.

2. Methodology

This paper aims to optimise the integration of a potassium carbonate solvent system with a brown coal fired power station unit. The example power station unit is a subcritical unit with a nominal capacity of 200 MWe (refer to Fig. 1). It uses 312 t/h of lignite and due to the high moisture content operates with an efficiency of 23% higher heating value (HHV), resulting in a CO₂ emission intensity of 1.46 t/MWh without CCS. The solvent plant (refer to Fig. 2) is added on to the outlet of the existing power station unit to capture the CO₂, which is then compressed to 10 MPa for transport and storage.

A range of configurations for the power station unit and solvent plant was modelled using Aspen Plus®. Cases 1 and 2 are to determine the solvent loading and flowrate and stripper pressure for minimising the reboiler energy. Cases 3 and 4 determine whether the optimised variables are different when considering the power station unit's net power rather than just the reboiler energy requirements. Further details on the four cases are provided in Sections 2.1–2.4 below.

The optimisation process adopted in this paper uses a combination of simulation, automated heat integration and multi-objective optimisation (MOO). Given the large number of potential objectives and antagonising impacts created by a number of the variables that can be adjusted in the CCS plant, the use of MOO should prove to be a useful tool for better process design of power stations with CCS. In MOO the multiple objectives are treated with equal weighting and a range of solutions, called the 'Pareto-optimal' solutions are found which are all non-dominated solutions – i.e. there are no other solutions that were found that are better in relation to all the objectives. MOO provides a number of solutions and therefore options, from which the designer can then make the final selection. It may also provide insight into what impact the variables have on the optimised solution, for example if a variable is always at one limit then by increasing this limit the overall solution may be improved. A number of algorithms are

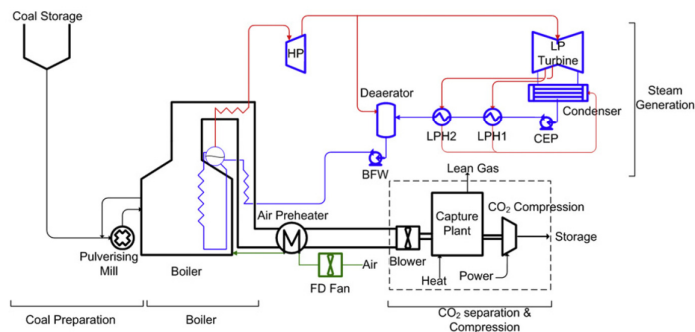


Fig. 1. Power station model. Dotted lines represent the new equipment required for the addition of CCS.

available for MOO each with their own advantages and disadvantages; details on different algorithms used to optimise engineering problems can be found in Rangaiah [8].

In Case 4 of this paper, automated heat integration is performed using pinch analysis. Pinch analysis [9,10] can be used to provide targets as to the minimum additional amount of energy required for a process by maximising the use of waste heat in the process. Significant amounts of heat are required for solvent regeneration, which generally comes from extracting steam from the steam turbine of the power station and possibly from excess thermal heat in the flue gas. The use of pinch analysis enables the automatic calculation of the minimum amount of steam required to be extracted from the turbine and will therefore maximise the power output from the power station.

The MOO algorithm used for this analysis is an Excel based genetic algorithm based on NSGA-II [11] code developed by Sharama et al [12]. In this algorithm the input variables are binary and so the range and number of bits for each variable must be selected for each case. The MOO program is used to determine a population set of decision variables within the range of variables, each set of variables are then input into the Aspen Plus® model of the power station unit with CCS. Once, the process is simulated, results from the simulation are used to evaluate the various objectives for each case which are exported back to the MOO program. The MOO program then uses these results to determine a new population set of decision variables and continues optimising these for a given number of generations (refer to Fig. 3). This approach is based on work by Bhutani et al [13], which uses NSGA-II code written in C++ interfaced with HYSYS using Visual Basic.

2.1. Case 1a/b: solvent loading and flowrate

The aim of this case is to determine what the minimum reboiler energy requirements are for a given amount of CO₂ captured; therefore the objectives for this case are to maximise the amount of CO₂ captured and minimise the reboiler energy. For this case the flue gas from the power station unit, downstream of the electrostatic precipitator, is cooled to 40 °C before it is added to the solvent plant, the lean solvent enters the absorber at 65 °C and the stripper pressure is fixed at 150 kPa. The column heights are also fixed at 20 m and 15 m for the absorber and stripper respectively, and are modelled using the Aspen Plus® Rate Based RadFrac column. The range for each of the variables for this case and the others are shown in Table 1.

2.2. Case 2: solvent loading, flowrate and stripper pressure

This case is an extension of the first cases however it includes a third variable; the stripper pressure to show the importance of this variable on minimising the regenerator reboiler energy. The rest of the power station unit and solvent plant are kept constant as in the first case. The variable ranges have also been increased; which are shown in Table 1.

2.3. Case 3: power station unit's net power output

The third case uses the same three variables and the same ranges as Case 2, but rather than minimise the reboiler energy, the optimisation objectives are to maximise the power station unit's

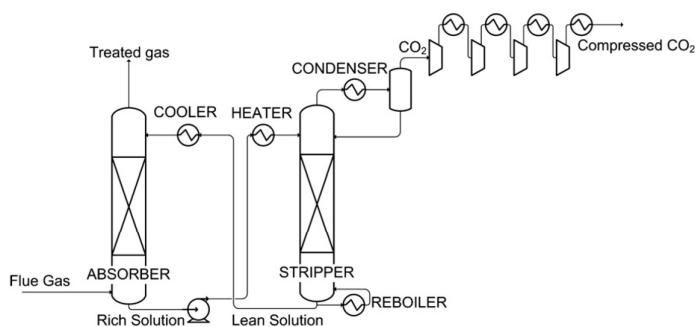


Fig. 2. Model of the solvent plant.

Please cite this article in press as: Harkin T, et al., Using multi-objective optimisation in the design of CO₂ capture systems for retrofit to coal power stations, Energy (2011), doi:10.1016/j.energy.2011.06.031

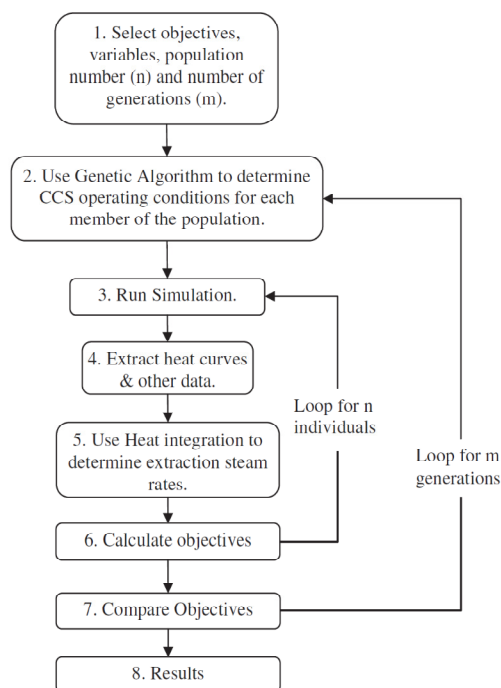


Fig. 3. Structure of the MOO using simulation and heat integration.

net power output whilst maximising the CO₂ captured. The unit's net power is reduced by the addition of the CCS plant; flue gas pressure is increased by the use of a fan, the solvent is circulated by pumps and the CO₂ compressors all require power. Heat for the solvent reboiler is supplied from steam extracted from the steam turbine which also leads to a reduction in the power produced by the power station unit. In this case, the steam extraction is from an existing bleed point on the exhaust of the high-pressure turbine (560 kPa/177 °C) and the amount of steam that needs to be extracted from the turbine is calculated based on the reboiler energy demands. For this paper it is assumed that the turbine efficiency is not affected by the reduction in steam flow from the

turbine. The net power produced from the power station unit is therefore calculated by the amount of power produced by the turbine minus the existing power loads and the new power loads caused by the addition of CCS.

2.4. Case 4: power station unit's net power output with heat integration

The last case reviews the importance of heat integration to maximise the power station net penalty and shows how the optimum value of the same three key operating variables (solvent flowrate, loading and stripper pressure) are impacted by heat integration. When CCS is added to the power station unit there are a number of waste heat sources that are also added; the CO₂ compressors, the stripper condenser and flue gas which should be cooled down prior to the solvent plant. These waste heat sources may be able to be utilised elsewhere in the power station and the CCS plant to reduce the amount of steam that needs to be extracted from the turbine and increase the power produced from the turbine.

For this case, after the simulation has solved in Aspen Plus® the stream data for all the hot and cold streams are automatically extracted from the simulation and processed using the pinch analysis problem table algorithm. This calculates the deficit of heat in the given process. The amount of steam extracted from the turbine to maximise the net power is then calculated using a linear programming method detailed in [14]. The optimisation objectives for this case are therefore the same as Case 3, to maximise the power station net output whilst maximising the amount of CO₂ captured.

3. Results

3.1. Case 1a/b: solvent loading and flowrate

The optimised results for these two cases show the minimum reboiler energy for a given capture rate given all variables are held constant except the solvent lean loading and flowrate. In this example, two different ranges have been used for the two decision variables; a tight range with solvent lean loading of 0.21–0.23 molCO₂/molK₂CO₃(s) and 2200–2300 kg/s of lean solvent and a wider range with lean loading of 0.15–0.36 molCO₂/molK₂CO₃(s) and 2000–3260 kg/s, the Pareto-optimal solutions for these cases are shown together in Fig. 4.

When the tighter range (Case 1a) was used, as expected the range of CO₂ captured is low, capturing between 85 and 89% of the

Table 1
Variable range and objectives.

Case	Solvent flowrate (kg/s)	Lean loading (molCO ₂ /molK ₂ CO ₃)	Stripper pressure (kPaa)	Objective 1	Objective 2
1a	2200–2300	0.21–0.23	150	Maximise CO ₂ capture (% CO ₂)	Minimise reboiler energy (MJ/kg)
1b	2000–3260	0.15–0.36	150	Maximise CO ₂ capture (% CO ₂)	Minimise reboiler energy (MJ/kg)
2	1000–4150	0.1–0.4	30–330	Maximise CO ₂ capture (% CO ₂)	Minimise reboiler energy (MJ/kg)
3	1000–4150	0.1–0.4	30–330	Maximise CO ₂ capture (% CO ₂)	Maximise power station net power (MW)
4	1000–4150	0.1–0.4	30–330	Maximise CO ₂ capture (% CO ₂)	Maximise power station net power (MW)

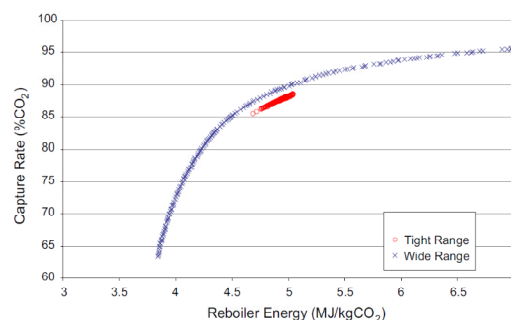


Fig. 4. Pareto-optimal solutions for Case 1a – Tight range and Case 1b – Wide range.

Please cite this article in press as: Harkin T, et al., Using multi-objective optimisation in the design of CO₂ capture systems for retrofit to coal power stations, Energy (2011), doi:10.1016/j.energy.2011.06.031

CO₂, whereas with the wider allowable range of flowrate and lean loading (Case 1b) the range of CO₂ captured is increased to between 63 and 96%. In addition, for a given reboiler energy the results using the tight range capture less CO₂ than when compared to wider range of flowrates and solvent loading. All of the tight range results were dominated by the solutions from the wider range, which means that to minimise the reboiler energy, it is important for further studies not to limit the range of loadings and flowrates.

There is a near-linear relationship between the reboiler energy for the Pareto-optimised solutions and the lean solvent loading (refer to Fig. 5) for both Cases 1a and 1b over the middle range of lean solvent loadings (0.19–0.26 molCO₂/molK₂CO₃(s)). However for the wider range, the optimal solutions for high solvent loadings tend to result in a minimum reboiler energy of around 3.8 MJ/kg CO₂. At the other end of the scale, to obtain solvent loadings below about 0.18 molCO₂/molK₂CO₃(s), the reboiler energy required to obtain the desired lean loading increases rapidly and is greater than 6 MJ/kg CO₂.

An explanation for the solutions from the wider range case being superior to the tighter case is that the solvent flowrate for the tighter case is limited by the chosen range of solvent flowrates. This is shown by the Pareto-optimal solutions for the tighter case which are all close to the upper bounds of 2300 kg/s as shown in Fig. 6. Therefore, to optimise the system for both the amount of CO₂ captured and reboiler energy, flowrates higher than 2300 kg/s are required for solvent loadings between 0.21 and 0.22 molCO₂/molK₂CO₃(s).

3.2. Case 2: impact of stripper pressure

Where the previous examples all maintained a constant stripper pressure of 150 kPaa, the following cases look at the impact of varying the pressure on the reboiler energy. As discussed in the introduction, a lower pressure is thought to reduce the reboiler energy for a carbonate system. This is confirmed in Fig. 7 where the variable pressure solutions result in a lower reboiler duty for a given CO₂ capture rate compared to the fixed pressure solutions and in Fig. 8 where all the optimised solutions for the variable pressure case are close to 30 kPaa; the lowest possible pressure allowed in the range.

The optimal solutions again have solvent loading as nearly linear with the reboiler energy with a minimum of approximately 1 MJ_{th}/kgCO₂ for a solvent loading of 0.4 molCO₂/molK₂CO₃(s) and a maximum of over 6 MJ_{th}/kgCO₂ for solvent loadings of 0.15 molCO₂/molK₂CO₃(s).

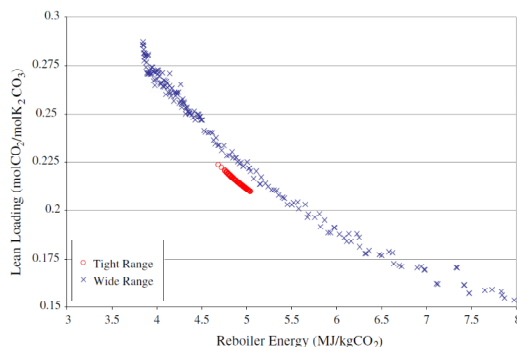


Fig. 5. Impact of the lean solvent loading on the reboiler energy.

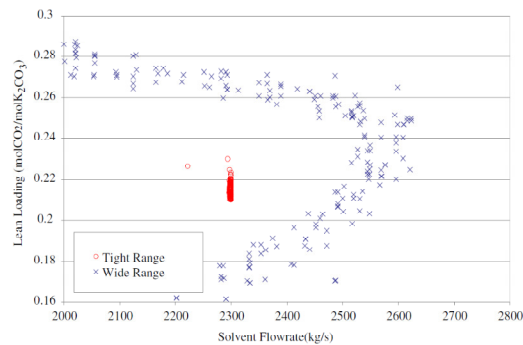


Fig. 6. Correlation between solvent lean loading and flowrate.

3.3. Case 3: impact of variables on the power station unit's net power

This case looks at maximising the power station unit's net power output rather than the reboiler energy by varying the solvent loading, flowrate and stripper pressure. The Case 3 results are provided in Fig. 9 which shows, as you would expect, that as the rate of CO₂ captured increases, the net power produced from the unit decreases.

For Case 3, the stripper pressure (when the overall net power from the power station unit is considered) do not all tend to 30 kPaa. The pressure is around 30 kPaa at lower capture rates, but tends to higher pressures from 75 to 90% capture (Refer to Fig. 10 and Fig. 11). The optimised solutions for the solvent loadings for Cases 2 and 3 are very similar for the CO₂ capture rate.

3.4. Case 4: impact of variables on the power station net power with heat integration

The final case looks at the impact of the three variables on the overall net power of the power station when heat recovery is maximised and the Pareto-optimal solutions for this case are shown in Fig. 9. These solutions are all dominant over the solutions determined in Case 3, which does not consider heat integration of the CCS plant with the power station. The power station unit's net power output from the heat integrated case is between 20 and 30 MW higher than the net power produced when heat integration is not included. The maximum capture rate of CO₂ is also greater for

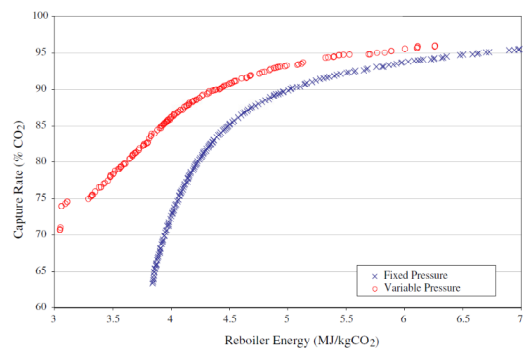


Fig. 7. Impact of stripper pressure on the Pareto-optimal solutions of the reboiler energy and capture rate.

Please cite this article in press as: Harkin T, et al., Using multi-objective optimisation in the design of CO₂ capture systems for retrofit to coal power stations, Energy (2011), doi:10.1016/j.energy.2011.06.031

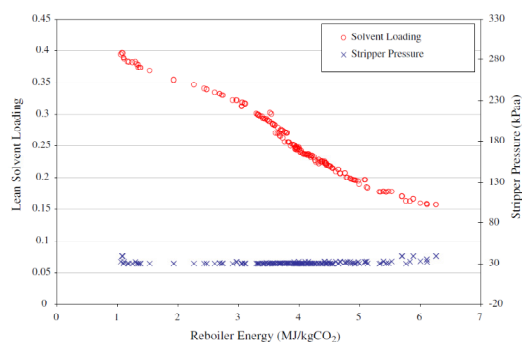


Fig. 8. Solvent loading and stripper pressure for the optimised points shown with the stripper reboiler energy.

Case 4 compared to Case 3 (refer to Fig. 9). Case 3 is limited to 90% capture of CO₂ as the steam demand for any further capture exceeds the amount of steam available from the turbine of the power station unit.

The optimised points for Case 4 show that low stripper pressures are not necessarily preferred when the overall power plant is taken into consideration. As shown in Fig. 11, the stripper pressure tends to be between 170 and 250 kPaa.

It is also interesting to note that the optimal solvent lean loading for the heat integrated case is quite different to the others at capture rates lower than 80% as shown in Fig. 12. Cases 2 and 3 appear to have a reasonably uniform relationship between the capture rate of CO₂ and the lean solvent loading. In contrast with Case 4 where the optimum lean loading of the solvent is 0.26 molCO₂/molK₂CO₃, for capture rates between 40 and 80%. Above 80% capture rates the optimum lean solvent loading are very similar for all three cases.

4. Discussion

4.1. Impact of stripper pressure on the optimal solutions

There is a definite trend in the CCS industry to focus on trying to minimise the reboiler energy of the solvent plant, which is important to help to reduce the amount of energy that the CCS plant will take from the power station unit. However, it is not the

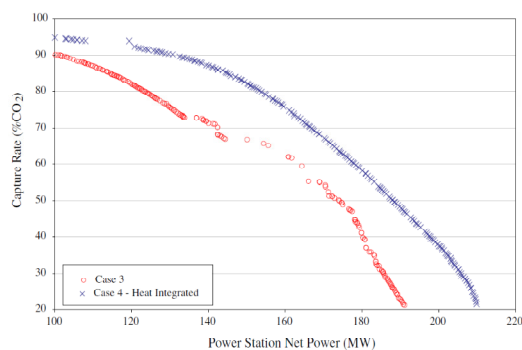


Fig. 9. Optimal solutions for Case 3 without heat integration and Case 4 with heat integration.

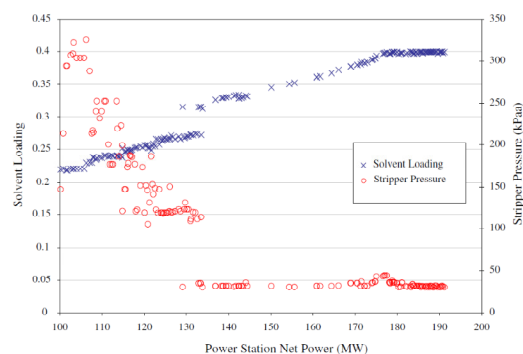


Fig. 10. Solvent loading and stripper pressure for the Pareto-optimal solutions for Case 3.

entire picture. To ensure the impact the CCS plant has on the power station is minimised, the solvent plant must be optimised with the power station in mind.

In order to reduce the reboiler energy for a potassium carbonate based CCS plant, the stripper pressure should be as low as possible. However when the impact on the power station is considered the optimal pressure depends largely on the amount of CO₂ captured, it is around 30 kPaa for capture rates lower than 70%, increases up to around 300 kPaa at 90% and then decreases back to around 30% at even higher capture rates, whereas the optimum pressure for the solvent plant with heat integration with the power station is between 170 and 250 kPaa. The reason for this change is that the higher pressure reduces the power requirement of the CO₂ compressor giving a higher net output.

In order to compare Cases 2, 3 and 4 consider a capture rate of 90%. Interestingly for all of these cases the Pareto-optimal solution had lean solvent loadings of 0.22 molCO₂/molK₂CO₃ and solvent flowrate of 2600 kg/s. Therefore, the only difference between each of these cases is the stripper pressure and the objective. Table 2 shows the reboiler energy requirements, the CO₂ compressor power, the power produced from the turbine taking into account the steam that needs to be extracted and thus the net power generated by the power station for a range of stripper pressures for the optimal solvent loading and flowrate for 90% capture of CO₂. They are shown for a power station without any heat recovery between the power station and the CCS equipment and also for maximum heat integration between the power station and CCS equipment.

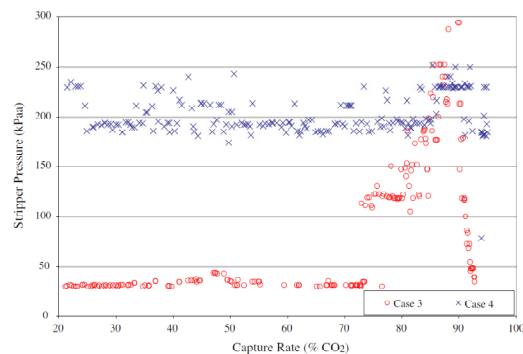


Fig. 11. Stripper pressure for the optimised points of Case 3 and 4.

Please cite this article in press as: Harkin T, et al., Using multi-objective optimisation in the design of CO₂ capture systems for retrofit to coal power stations, Energy (2011), doi:10.1016/j.energy.2011.06.031

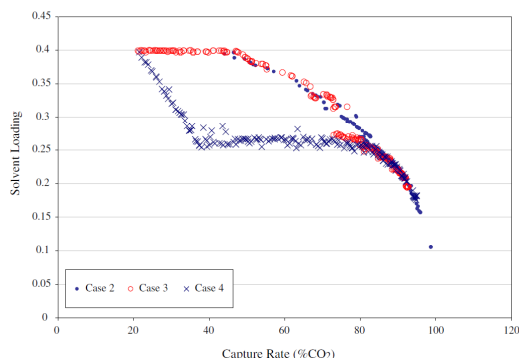


Fig. 12. Solvent loading for optimised solutions for Cases 2, 3 and 4.

If the objective is to minimise the solvent plant reboiler energy (Case 2), then from the results shown in Table 2 it can be seen that this would be achieved by having the lowest stripper pressure.

When the compressor power is taken into consideration for Case 3, the optimum solution is at a stripper pressure of approximately 90 kPaa, as there is a 10 MW advantage in the compressor power requirement and only a 7 MW penalty in the power generated in the turbine. What can also be noted is that as the pressure is increased from 90 kPaa to 250 kPaa the net power output is very similar. There is a 7 MW of reduction in the compressor power, but also 7 MW less of power generated from the turbine. The similarity in these results explains why at capture rates greater than 75% there is no clear optimal stripper pressure for Case 3 as the optimal solutions include stripper pressures between 50 kPaa and 250 kPaa (refer to Figs. 10 and 11).

When including maximum heat recovery between the power station unit and the CCS equipment the trade-off between compressor power requirements and power generated by the turbine favours pressures of 170–250 kPaa (refer to Table 2). The solutions do not improve above 250 kPaa as the reboiler temperature increases to a point where higher pressure steam is required to satisfy the reboiler duty.

4.2. Using CCS to control power station unit outputs

It is possible to design the CCS plant with a range of solvent flowrates and lean solvent loadings, therefore the capture rates can be adjusted. As can be seen in Fig. 9 as the capture rate is increased the power station unit net power production decreases. Therefore, during peak hours when the demand and therefore price of electricity increases, the capture rate of CO₂ could be reduced to increase

the net power generated by the power station unit and therefore maximise the power stations profits. Likewise the power station unit could increase the capture rate of CO₂ when electricity prices are lower, to reduce the emissions intensity of the power station.

As the changes in capture rate would change the amount of steam that needs to be extracted from the turbine, the control of the turbine over a range of steam extraction rates would be important. The CO₂ compressor turndowns may also limit the range of CO₂ capture rates, however the operating range of the compressors are likely to be improved by having multiple compressors in parallel which is likely to be the situation on any large scale CCS project.

4.3. Comparative studies

Due to the low kinetic rates of carbon dioxide absorption into potassium carbonate at the low partial pressures found in the flue gas of pulverised coal fired power stations, the solvent is usually combined with a promoter to increase the kinetic rates. Oyeneken and Rochelle [15] have reported optimum operating points for potassium carbonate promoted with piperazine, Oexmann et al. [16] have reported similar and also include un-promoted potassium carbonate results in the same work.

Whilst the optimum regenerator pressure for Case 4 from this paper is around 170–250 kPaa the results from both Oexmann et al (30 kPaa) and Oyeneken and Rochelle (160 kPaa) are both lower, although the Oyeneken and Rochelle optimum was for promoted potassium carbonate and Oexmann et al. also found that with high concentrations of piperazine, higher pressures are more favourable than for pure potassium carbonate solutions.

The reboiler energy requirements for Oexmann et al. were 3.16 MJ/kgCO₂ at a regenerator pressure of 30 kPaa, which is significantly lower than the 4.45 and 5.30 MJ/kgCO₂ values generated by the model used in this paper for the same pressure and a pressure of 250 kPaa respectively. Variation between the two models can be explained by differences in the feed conditions, the absorber and regenerator models and the thermodynamic model used. Notwithstanding, the energy penalty for Case 4 (1.02 MJ/kgCO₂) is similar to Oexmann et al. (1.03 MJ/kgCO₂) and the fact that they are so close even though the reboiler duties are so different can be explained by the differences in the energy penalty for compression, the benefit of heat integration and the boundary conditions of the steam cycle.

The energy penalty for compressors and auxiliaries in this paper for a regenerator operating at 30 kPaa and 250 kPaa are 0.52 and 0.30 MJ/kgCO₂, which is lower in comparison to Oexmann et al. at 30 kPaa which has an energy penalty of 0.66 MJ/kgCO₂. Another large difference is due to the steam cycle conditions, including the steam extraction temperature and the steam turbine condensing temperature. Reductions in the turbine exhaust temperature lead to increases in the amount of power 'lost' by extracting steam from the turbine and as the extraction steam temperature increases the amount of power lost from the turbine also increases.

As an indicator, to remove the impact of different thermal energy requirements of the solvents, the ratio of the power produced from a unit of steam to the thermal energy that steam can supply, referred to here as the 'steam penalty', can be used. For Oexmann et al the steam penalty is 0.12 MJ_e/MJ_{th}, whereas in this paper the value is greater at 0.21 MJ_e/MJ_{th}. If the steam extraction temperatures used in this paper were not restricted to using the extraction temperatures of the existing turbine and were allowed to vary to the value used in Oexmann et al., the steam penalty can be reduced by 0.13 MJ_e/MJ_{th}. Nevertheless the Oexmann et al. steam penalty would also be reduced by 0.04 MJ_e/MJ_{th} if the condensing

Table 2
Comparison of solutions for 90% capture rate of CO₂.

Stripper pressure (kPaa)	Reboiler energy (MJ/kgCO ₂)	CO ₂ comp. power (MW)	Turbine power (MW)	Net power output (MW)
No heat integration				
30	4.45	37	149	96
90	4.90	27	142	99
250	5.30	20	135	99
Including heat integration				
30	4.45	37	169	116
90	4.90	27	167	123
250	5.30	20	165	129

Please cite this article in press as: Harkin T, et al., Using multi-objective optimisation in the design of CO₂ capture systems for retrofit to coal power stations, Energy (2011), doi:10.1016/j.energy.2011.06.031

Table 3

Comparison of the results from this paper to those from Oexmann et al [16], and Oyeneken and Rochelle [15].

		New results	Oexmann et al.	Oyeneken and Rochelle
Turbine condensing temperature	°C	52	31	40
Energy penalty	MJ _e /kgCO ₂	1.02	1.03	0.86
Reboiler duty	MJ _{th} /kgCO ₂	5.30	3.16	3.11
Extraction steam temperature	°C	162	86	121
Regenerator pressure	kPaa	250	30	160
Impact on energy penalty:				
Condensing temperature	MJ _e /kgCO ₂	–	+ 0.14	+ 0.07
Heat integration	MJ _e /kgCO ₂	–	+ 0.40	+ 0.40
Compressor and auxiliary power	MJ _e /kgCO ₂	–	+ 0.36	+ 0.08
Reboiler duty and steam penalty	MJ _e /kgCO ₂	–	– 0.89	– 0.71

temperature used in that paper of 31 °C were increased to the 52 °C used in this paper. The steam penalty for Oyeneken and Rochelle is also lower than this paper at 0.15 MJ_e/MJ_{th}, due to the lower steam turbine efficiency and lower extraction steam temperature and combined with the low energy of regeneration results in an overall low energy penalty of 0.86 MJ_e/kgCO₂.

The energy penalty for the process developed in this paper, when no heat integration is taken into account is 1.42 MJ_e/kgCO₂, which is much greater than the Oexmann et al. result due to the high steam penalty and the high reboiler energy used in this paper. However, it highlights the importance of the heat integration as it is able to lower the energy penalty by 0.40 MJ_e/kgCO₂. A comparison of the differences between this paper and the results from Oexmann et al. and Oyeneken and Rochelle is provided in Table 3 with a breakdown of what causes the differences in energy penalty.

What is important to note in this comparison is that the feed conditions, environment conditions, equipment design and the solvent characteristics will have a large impact on the resultant energy penalty and therefore due to differences in each plant the optimum operating point may also vary. It must also be noted that the method of design will also have an impact. Where this paper used extraction steam at temperatures set by the existing equipment, Oexmann et al. and Oyeneken and Rochelle optimised with steam temperature levels set 10 °C above the reboiler temperature. Therefore, if the optimisation carried out in this process was repeated with a variable steam pressure, the optimum regenerator pressure may be different again. This shows the importance in optimising the process as a whole and ensuring that the boundary and the design conditions of the particular power station are considered in the design of the solvent plant.

5. Conclusion

To minimise the reduction in power output from a power station unit with the addition of CCS, the design of a solvent-based CCS plant should be conducted with the understanding of how the power station will interact with the CCS equipment. In the case of potassium carbonate based solvent plants, the stripper pressure will be an important variable. Stripper pressures in the range of 170 kPaa–250 kPaa were found to be the optimal solutions for the power station provided in this paper. The optimal pressure may change depending on the power station, the available temperatures of the extraction steam and the design methodology employed. However, the minimum energy penalty for the example used in this paper was 1.02 MJ_e/kgCO₂ with a reboiler regeneration energy of 5.3 MW_{th}/kgCO₂, with further improvements in the design of the

solvent and/or solvent plant, the reboiler energy demand may decrease and when combined with heat integration the potential for reductions in the energy penalty is possible. The importance of heat integration was highlighted with a reduction in the energy penalty of 0.40 MJ_e/kgCO₂ in the example provided in this paper with the addition of heat integration.

MOO of the power station and the CCS equipment can highlight the impact the CCS equipment will have on the net power generation of a power plant and can be used to design better integrated systems. MOO also enables curves of the power station power output versus amount of CO₂ captured to be generated, this information can be used by the power station operators to determine the optimum operating parameters to maximise profit by varying the capture rates in response to fluctuations in the electricity price.

Acknowledgements

Work is prepared as part of the Latrobe Valley PCC project with support of the Victorian Government ETIS Brown Coal R&D program; International Power and the Cooperative Research Centre for Greenhouse Gas Technologies (CO2CRC), which is funded through the Australian Government's Cooperative Research Centre Program, other federal and state government programs, CO2CRC participants and wider industry.

References

- [1] IPCC. Prepared by working group III of the intergovernmental panel on climate change. In: Metz B, Davidson O, de Coninck HC, Loos M, Meyer LA, editors. IPCC special report on carbon dioxide capture and storage; 2005.
- [2] Ghosh U, Kentish S, Stevens G. Absorption of carbon dioxide into potassium carbonate promoted by boric acid. In: Ninth international conference on Greenhouse Gas Control Technologies (GHGT-9). Washington DC, USA: Elsevier; 2008.
- [3] Cullinane JT, Rochelle GT. Carbon dioxide absorption with aqueous potassium carbonate promoted by piperazine. Chemical Engineering Science 2004; 59(17):3619–30.
- [4] Page SC, Williamson AG, Mason IG. Carbon capture and storage: fundamental thermodynamics and current technology. Energy Policy 2009;37(9):3314–24.
- [5] Pellegrini G, Strube R, Manfrida G. Comparative study of chemical absorbents in postcombustion CO₂ capture. Energy 2010;35:851–7.
- [6] Jassim MS, Rochelle GT. Innovative absorber/stripper configurations for CO₂ capture by aqueous monoethanolamine. Industrial & Engineering Chemistry Research 2006;45(8):2465–72.
- [7] Pfaff I, Oexmann J, Kather A. Integration studies of post-combustion CO₂-capture process by wet chemical absorption into coal fired power plant. Conference integration studies of post-combustion CO₂-capture process by wet chemical absorption into coal fired power plant. Dresden, Germany.
- [8] Rangaiah GP. Multi-objective optimization: techniques and applications in chemical engineering. Singapore: World Scientific; 2009.
- [9] Linnhoff B, Townsend DW, Boland D, Hewitt GF, Thomas BEA, Guy AR, et al. A user guide on process integration for the efficient use of energy. UK: IChemE; 1982.
- [10] Smith K. Chemical process design and integration. West Sussex, England: John Wiley & Sons Ltd; 2005.
- [11] Deb K, Pratap A, Agarwal S, Meyarivan T. A fast and elitist multiobjective genetic algorithm: NSGA-II. evolutionary computation. IEEE Transactions 2002;6(2):182–97.
- [12] Sharma S, Rangaiah GP, Cheah KS. Multi-objective optimization using a MS Excel with an application to design of a falling-film evaporator system. Food and Bioprocess Processing 2011. doi: 10.1016/j.fbp.2011.02.005.
- [13] Bhutani N, Tarafder A, Rangaiah GP, Ray AK. A multi-platform, multi-language environment for process modelling, simulation and optimisation. International Journal of Computer Applications in Technology 2007;30(3): 197–214.
- [14] Harkin T, Hoadley A, Hooper B. Reducing the energy penalty of CO₂ capture and compression using pinch analysis. Journal of Cleaner Production 2010; 18(9):857–66.
- [15] Oyeneken BA, Rochelle GT. Rate modeling of CO₂ stripping from potassium carbonate promoted by piperazine. International Journal of Greenhouse Gas Control 2009;3(2):121–32.
- [16] Oexmann J, Hensel C, Kather A. Post-combustion CO₂-capture from coal-fired power plants: preliminary evaluation of an integrated chemical absorption process with piperazine-promoted potassium carbonate. International Journal of Greenhouse Gas Control 2008;2:539–52.

Please cite this article in press as: Harkin T, et al., Using multi-objective optimisation in the design of CO₂ capture systems for retrofit to coal power stations, Energy (2011), doi:10.1016/j.energy.2011.06.031

Chapter 6

Using MOO and the superstructure method to determine the optimum stripper pressure for potassium carbonate based capture systems

6. Using MOO and the superstructure method to determine the optimum stripper pressure for potassium carbonate based capture systems

6.1 Introduction

In Chapter 5 the importance of studying the power station and the CCS equipment as a whole was recognised. Simulation, heat integration and MOO were used on a potassium carbonate CO₂ capture system retrofitted to a brown coal fired power station to reduce the energy penalty. However, the optimisation for simplicity sake included only 3 optimisation variables; the solvent lean loading and flowrate and the stripper pressure. In this chapter the number of variables that are involved in the optimisation process is increased. Additionally, in Chapter 5 the stripper pressure that maximised the net power from the power station when heat integration was taken into account was identified as the stripper pressure that provided a reboiler temperature equal to the extraction steam temperature plus the given ΔT_{\min} . The optimal stripper pressure was more a factor of the steam turbine extraction temperature and pressure than anything else. Therefore, another aspect that will be evaluated in this chapter is the impact of varying the extraction steam pressure to match the process GCC or more specifically, the stripper reboiler temperature. The extraction steam pressure will be adjusted to have a condensing temperature that is equal to the minimum allowable approach temperature above the stripper reboiler. The intention is to determine what the optimum stripper pressure is to maximise the power stations net power.

The case study provided in Chapter 5 was performed on a brown coal fired power station with a subcritical steam cycle with no reheat. To ensure this case study is more relevant to the majority of the brown coal fired power stations in Victoria, the power station used in this chapter is also subcritical but with a single stage of reheat. This chapter is also the first to utilise the superstructure method of linear programming pinch analysis that was detailed in Chapter 4.

6.2 MOO Objectives and Decision Variables

As the amount of CO₂ captured by the CCS process will impact the net power of the power station, this case study maximises both the net power and the amount of CO₂ captured. In this case study the decision variables (Refer to Table 6-1) contains a list of solvent plant parameters which are adjusted to determine the optimum operating values to maximise the power from the power station.

The steam cycle for the process is a subcritical steam cycle (164 bar, 538 °C) with a single reheat stage (41 bar, 538 °C). There are two and four steam extraction points on the IP turbine and LP

turbine, respectively. The turbine efficiencies are based on the isentropic efficiencies of the existing base power station ranging from 85 to 90 %. The base power station without CO₂ capture has a nominal 500 MWe net power production, producing 156 kg/s of CO₂. The potassium carbonate based CO₂ capture plant is modelled in Aspen Plus® using rate based distillation for both the absorber and stripper. The grand composite curve and linear programming was conducted with a ΔT_{\min} of 6 °C, the extraction pressure of the steam extracted for the solvent regeneration was manipulated to have a condensing temperature of 6 °C above the reboiler temperature. This is in contrast to the methods used in Chapter 5 where the extraction pressure was considered to be a constant value, which impacted the optimum stripper pressures, as the pressure converged to provide a reboiler temperature ΔT_{\min} less than the condensing temperature of the constant steam turbine extraction pressures.

Table 6-1: Decision variables for the optimisation of the solvent capture plant

Decision Variables	Units	Lower Limit	Upper Limit
Solvent Lean Loading	mol HCO ₃ ⁻ /mol K ⁺	0.11	0.416
Solvent Temperature	°C	40	71.5
Solvent Flowrate	kg/s	800	5910
Absorber Feed Gas Temperature	°C	40	71.5
Absorber Packing Height	m	10	47.5
Stripper Packing Height	m	10	47.5
Stripper Pressure	bar	0.5	8.165
Stripper Feed Temperature	°C	70	133.5
Constraints			
CO ₂ capture rate	%	< 95	

6.3 Results and Discussion

6.3.1 Pareto fronts and decision variables

Figure 6-1 to Figure 6-8 show results of the MOO which simultaneously maximises CO₂ capture rate and net power from the power station. The non-dominated solutions are presented in Figure 6-1. Due to the energy requirements of the CO₂ capture process, the higher the CO₂ capture rate the lower the net power produced from the power station. The results indicate that there is

sufficient heat in the process to maintain the power stations 500 MW output whilst capturing and compressing up to 40 % of the CO₂, provided that existing and new heat exchangers are designed for an approach temperature of 6 °C. In comparison the energy penalty at capture rates of 90 % is approximately 14 %. Figure 6-2 shows for capture rates between 50 and 90 % of the net power after the 14th, 28th, and 42nd generation of the MOO study. By the 14th and 28th generation, the net power is within 10 MW and 2 MW respectively of the net power provided by the 42nd generation. This indicates that as the number of generations approaches 42, the incremental improvement is reducing, and that any further improvement in the objective beyond 42 generations is likely to be small.

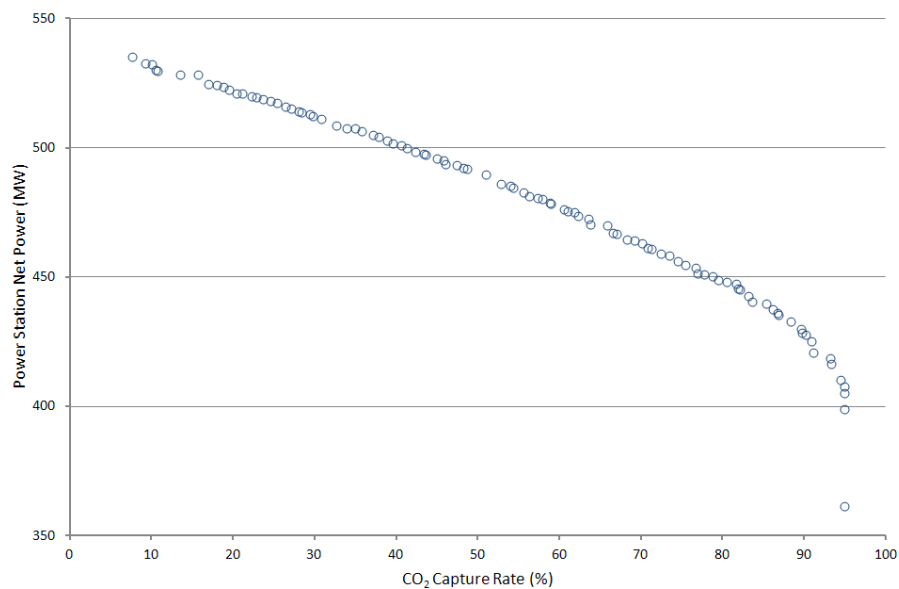


Figure 6-1: Pareto front for the MOO results to maximise the CO₂ capture rate and the power station net power.

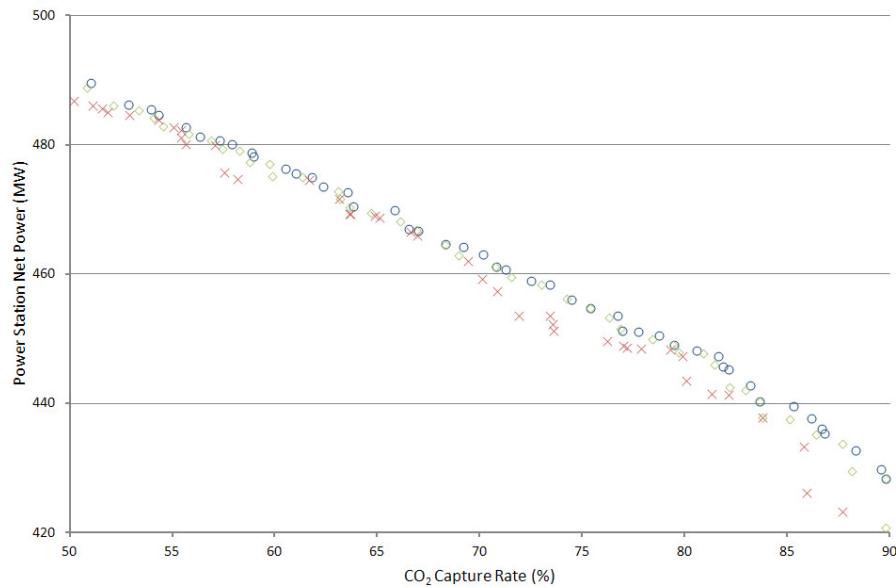


Figure 6-2: Pareto front between 50% and 90% capture after the 14th generation (X), 28th generation (◇) and the 42nd generation (O).

The Pareto-optimal solutions can also be used to determine the importance of the decision variables and the optimum value of those variables. The values of some of the decision variables are shown in Figure 6-3 to Figure 6-8 for the Pareto-optimal solutions after 14 and 42 generations. In Figure 6-3 the plots of flue gas temperature show a strong tendency towards the low end of the range, even after only 14 generations. This is likely to be as a result of the lower water content in flue gas with lower gas temperatures. The lower water content provides two advantages; it increases the CO₂ concentration and reduces the amount of water absorbed by the solvent which will subsequently need to be removed from the solvent to maintain solvent concentration and will

therefore require additional heat in the stripper reboiler to boil off the extra water.

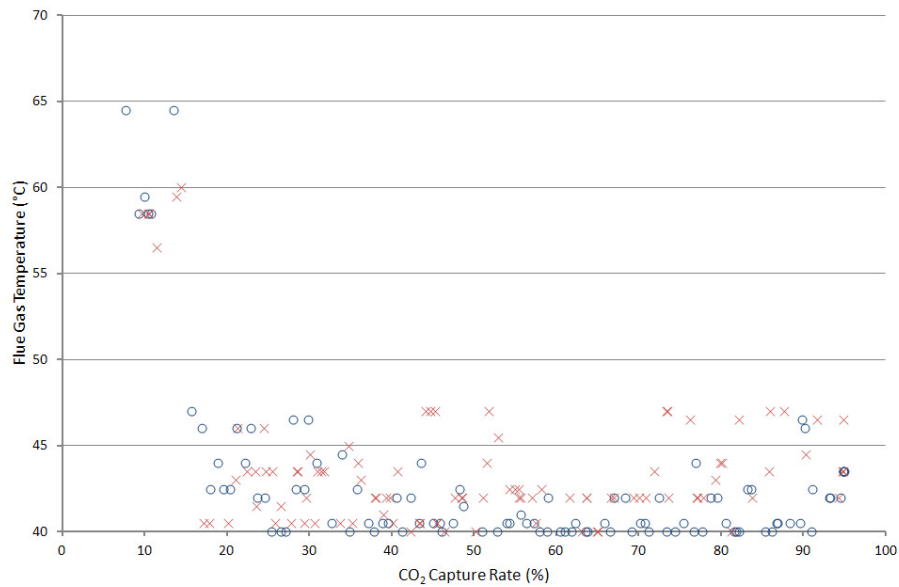


Figure 6-3: Flue gas temperature for the Pareto-optimal solutions after the 14th (×) and 42nd generations (○).

The results for the solvent temperature (Figure 6-4) on the other hand are less defined even after 42 generations; this is likely to be a result of the antagonising behaviour of the solvent temperature where lower temperatures help absorption by lowering the CO₂ vapour pressure in equilibrium with the solvent and higher solvent temperatures improve the absorption kinetics. Therefore, even after 42 generations there is no clear optimum solvent temperature, which indicates that the solvent temperature, within the range supplied, does not have a major impact on the net power. That is not to say that the solvent temperature is not important for other reasons. The solvent temperature will have a large impact on the amount water that is absorbed from or desorbed into the CO₂ lean flue gas. If the temperature difference between the solvent temperature and the flue gas temperature is high, then the solvent will lose water which will require significant quantities of make-up water. Conversely if the temperature difference is small, then water in the flue gas will be absorbed into the solvent which will increase the reboiler duty to maintain the solvent strength. As the optimal flue gas temperatures are all on the lower side (<45°C), having excess water absorbed into the solvent is unlikely to be an issue unless the solvent temperature is also < 45 °C, hence the solvent temperature in almost all cases is above 45 °C. However above that the solvent temperature has minimal impact on the net power, but to avoid losing significant quantities of water in the lean flue gas the optimum temperature would be limited to a few degrees hotter than the flue gas temperature.

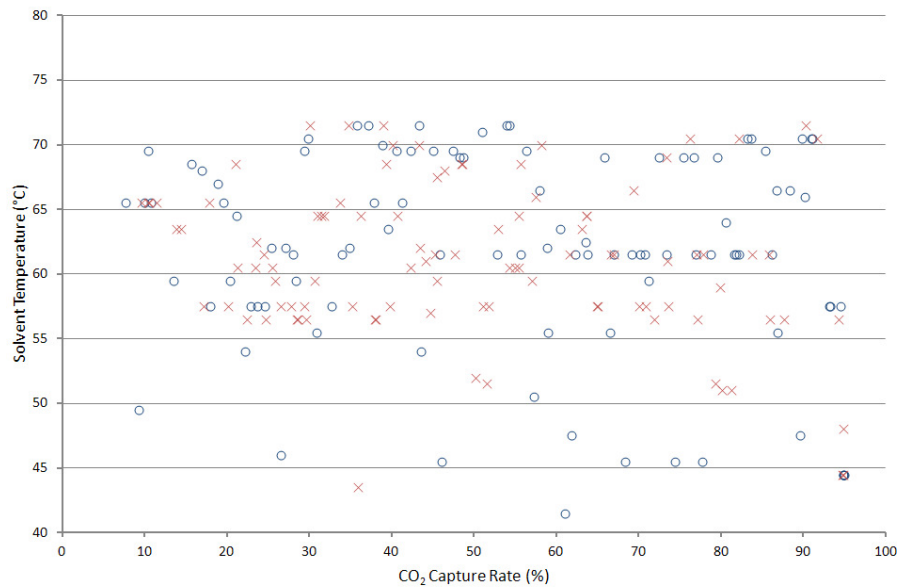


Figure 6-4: Solvent temperature for the Pareto-optimal solutions after the 14th (×) and 42nd generations (○).

The solvent lean loading has a strong influence on the net power of the power station as revealed by the similarity between the results after 14 generations and 42 generations (Figure 6-5). The optimum lean loading, for capture rates between 30 % and 80 %, is approximately $0.22 \pm 0.4 \text{ mol HCO}_3^- / \text{mol K}^+$. At lower capture rates, higher lean loadings appear to be preferable. However in the 80% to 90% capture range (the normal design range for large scale capture plants), the optimum lean loading for all results fall in the 0.15 to 0.20 $\text{mol HCO}_3^- / \text{mol K}^+$. Lower lean loadings means the capacity of the solvent to absorb CO_2 increases which reduces the quantity of the solvent required for absorption and increases the driving forces at the top of the absorber. Additionally, because the solvent flowrate is reduced, the specific heat required to heat the solvent is reduced and the motive power to pump the solvent from the absorber to the stripper is reduced. However, this is offset against the increased reboiler duty required to achieve the lower lean loadings. Therefore, being able to determine the optimum lean loading is an important element the MOO is able to achieve.

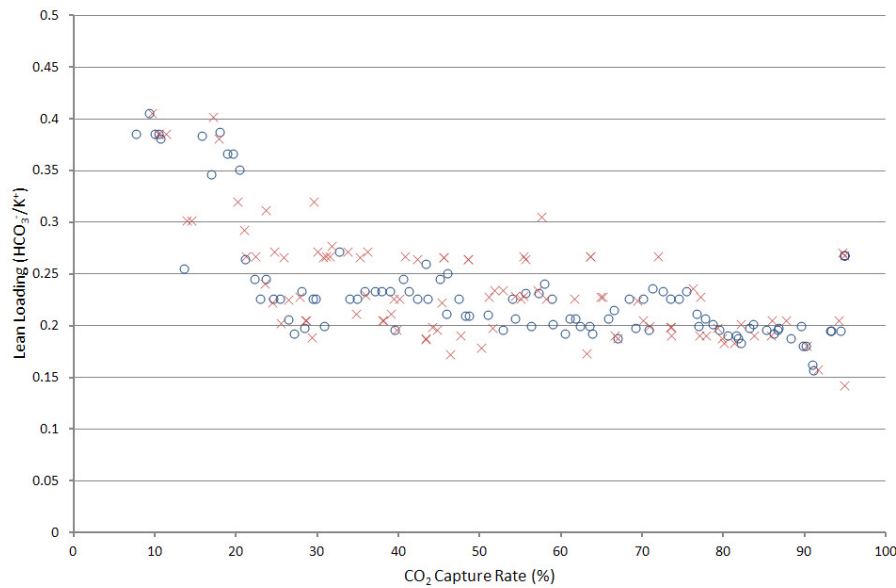


Figure 6-5: Solvent lean loading for the Pareto-optimal solutions after the 14th (X) and 42nd generations (O).

The stripper pressure (Figure 6-6), which was thought to have a significant influence on the net power turns out to have less of an impact than many other variables. After 14 generations there is a spread of pressures, after 42 generations the pressure is tending towards 4 bar for capture rates between 15 and 80 % and 5 bar to 7 bar for capture rates greater than 80 %. However, as the correlation between the stripper pressure and net power is not strong, other factors including capital cost and other economic factors may determine the optimal stripper pressures. The stripper pressure has antagonising impacts on the net power, but it appears that the trade-off between the reboiler duty and the CO₂ compressor power means that the pressure is not the most important parameter to optimise in order to maximise the net power. In this case study where the steam turbine extraction pressure is able to vary according to the reboiler temperature, the stripper pressure is not an important parameter. Whereas, when the steam turbine pressures were fixed, the stripper pressure was a strong decision variable and the value of the stripper pressure was important to maximise the net power of the power station. Therefore, it appears, that for CCS projects that are retrofits to existing power stations, it is likely that to maximise the power produced by the steam turbine, the stripper pressure should be matched to the available steam pressures. However, when there is freedom in the steam turbine pressure, the optimal stripper pressure can be selected for other, either operational or economic, considerations.

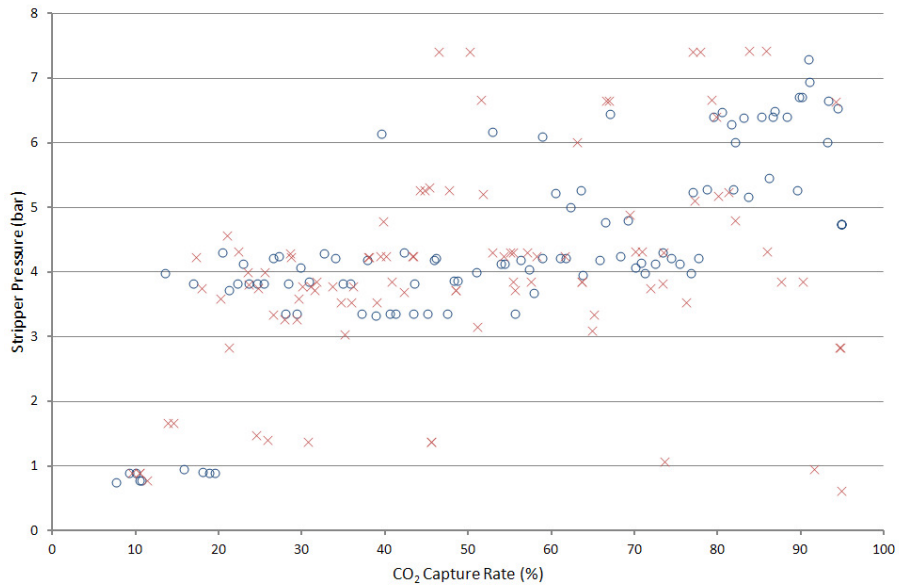


Figure 6-6: Stripper pressure for the Pareto-optimal solutions after the 14th (X) and 42nd generations (O).

The optimum solvent flowrate (Figure 6-7) has a strong correlation with the capture rate and apart from at the extreme capture rates the correlation is almost constant per tonne of CO₂ captured. The solvent flowrate is also influenced largely by the lean loadings. In a solvent with relatively fast kinetics, if the lean loading is constant then the solvent flowrate the only other major handle to adjust the CO₂ capture rate. As there is little change in the lean loadings between capture rates greater than 30 %, it is not surprising that the solvent flowrate provides a strong correlation with the capture rate. This further reiterates (as proposed in Chapter 5) the potential to use the solvent flowrate to provide the flexibility to alter the CO₂ capture rate and therefore the power stations net power.

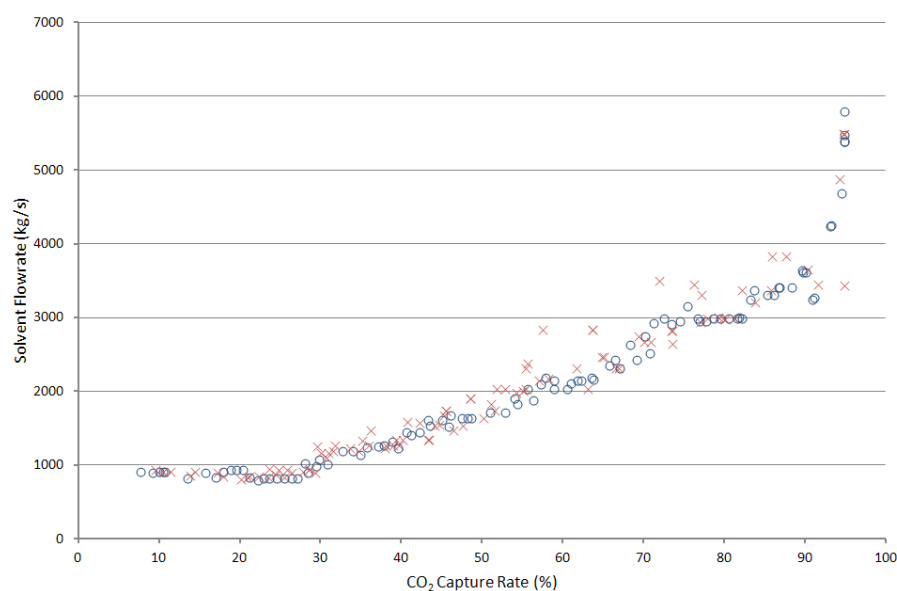


Figure 6-7: Solvent Flowrate for the Pareto-optimal solutions after the 14th (×) and 42nd generations (○).

The results for the stripper feed temperature (Figure 6-8) are all at the upper end of the range with most of the results above 120 °C. This result is not unexpected as the feed temperature would be approaching the solvent bubble point at the stripper pressures that predominated. It is not surprising that the optimum temperature is close to the bubble point given that the lean and rich solvents have a similar heat capacity and the rich solvent will leave the bottom of the stripper at the bubble point and therefore the hot lean solvent can be used to heat up the cold rich solvent. This approach is suggested by most solvent vendors which utilise a lean-rich heat exchanger for this purpose.

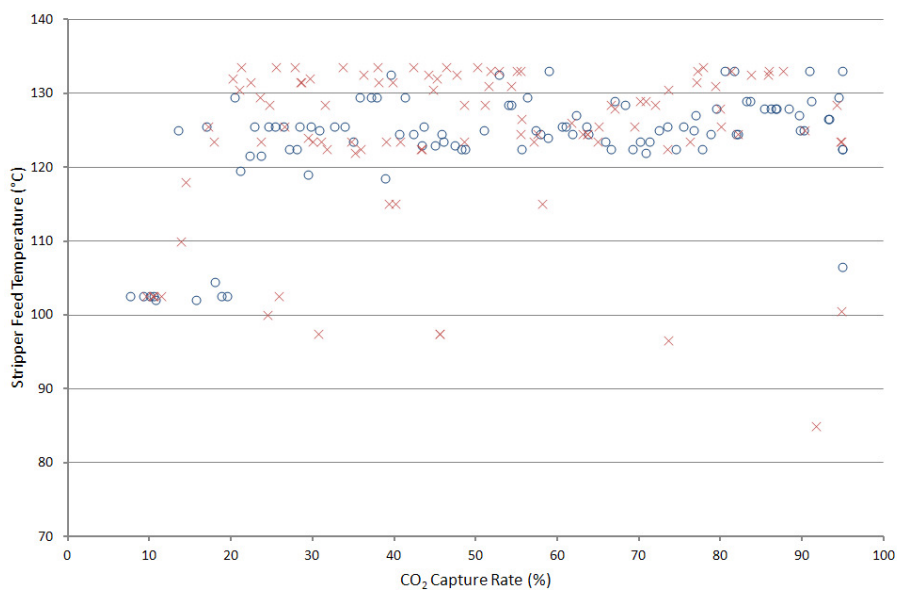


Figure 6-8: Stripper Feed Temperature for the Pareto-optimal solutions after the 14th (×) and 42nd generations (○).

6.3.2 Impacts to the Process Heat Exchangers

It is also interesting to not only review the results of the decision variables, but also the impact on various heat exchanger duties as a result of the optimisation. Select results are shown in Figure 6-9 to Figure 6-12. The lean and rich heat exchanger duties (Figure 6-9) show similar changes as a function of capture rate as they are both mainly impacted by the solvent flowrate. However, at low capture rates the rich heat exchanger duty is greater than the lean solvent duty, whereas as the capture rates increases the lean solvent cooling duty becomes larger than the rich heat exchanger heating duty. Assuming that a lean-rich heat exchanger is the preferred arrangement for heat exchange of the lean and rich solvent streams, then the results presented in Figure 6-9 mean that the optimum at low capture rates requires a trim rich solvent heater whilst at higher capture rates a trim cooler is required for the lean solvent. Lean solvent coolers downstream of the lean-rich heat exchangers are common in solvent capture processes and the results from this work confirm that they will indeed often be the optimum arrangement.

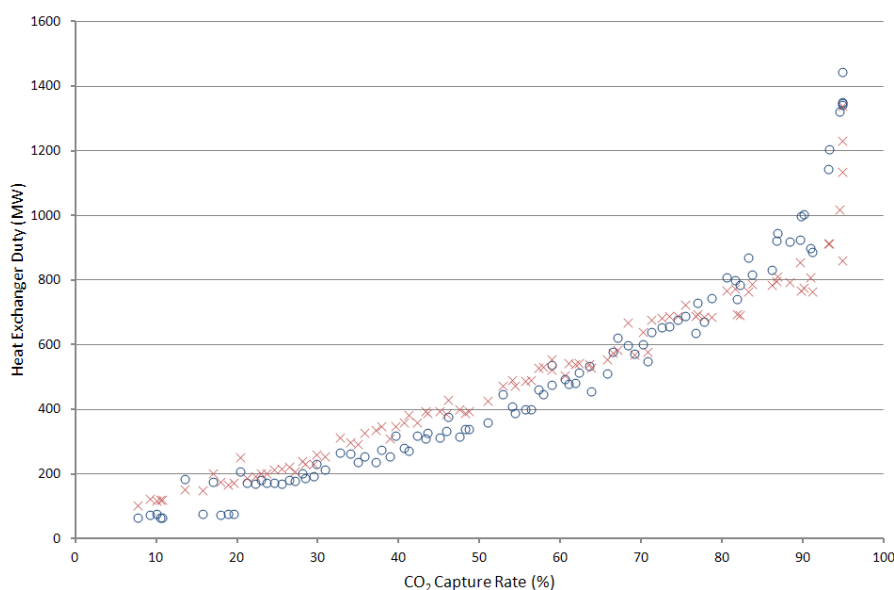


Figure 6-9: Lean Solvent Cooler (○) and Rich Solvent Heater (×) duties for the Pareto-optimal solutions.

Interestingly the reboiler heat duty shows a clear trend (Figure 6-10) with respect to the capture rate, which is irrespective of the fact that the stripper pressure is not consistent. On the other hand the stripper condenser heat duty (Figure 6-11) is a lot less consistent; it is also impacted by the stripper pressure and several other factors. The condenser duty increases as the CO₂ capture rate increases due to the increase in the CO₂ and accompanying water exiting the stripper. As the stripper pressure increases the condensation will occur at a higher temperature, however from the optimised results, it appears that the actual amount of heat extracted from the condenser decreases as the pressure increases. Therefore, assuming that the heat in the condenser can be

utilised back into the steam cycle, the impact of pressure again has conflicting impacts. As the pressure increases the heat duty decreases. However, the quality of the heat duty also increases, because of the increase in temperature. These conflicts continue to explain why the stripper pressure does not actually have as large an influence on the energy of a process as first expected.

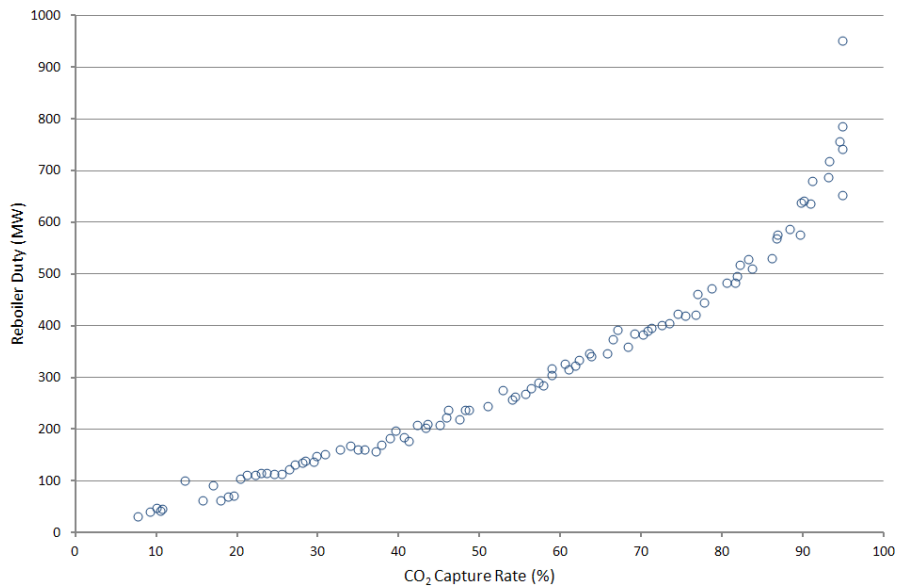


Figure 6-10: Stripper duty for the Pareto-optimal solutions

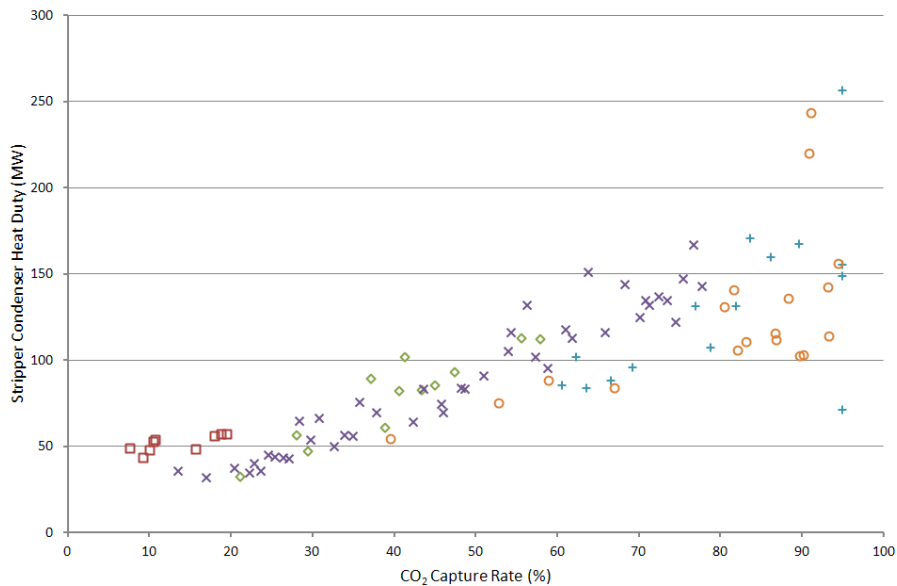


Figure 6-11: Stripper condenser heat duty for the Pareto-optimal solutions for stripper pressures <1 bar (\square), 3-3.7 bar (\diamond), 3.8-4.3 bar (\times), 4.7-5.4 bar ($+$), >6 bar (\circ).

The reboiler duty per unit of CO₂ captured varies from just above 2 GJ/t to above 5 GJ/t. At capture rates less than 50 %, the reboiler energy is mainly around the 3 GJ/t mark and that gradually increases as the CO₂ capture rate increases. The increase will be due to the decrease in

the lean loading at higher capture rates, combined with an increase in the solvent flowrate to absorb the increasing amount of CO₂. There is close to a 25 % difference between the results at 80 % capture and 90 % capture. This highlights the importance, when reviewing claims of the energy intensity of different solvent vendors, to understand the basis of those claims to make an even comparison.

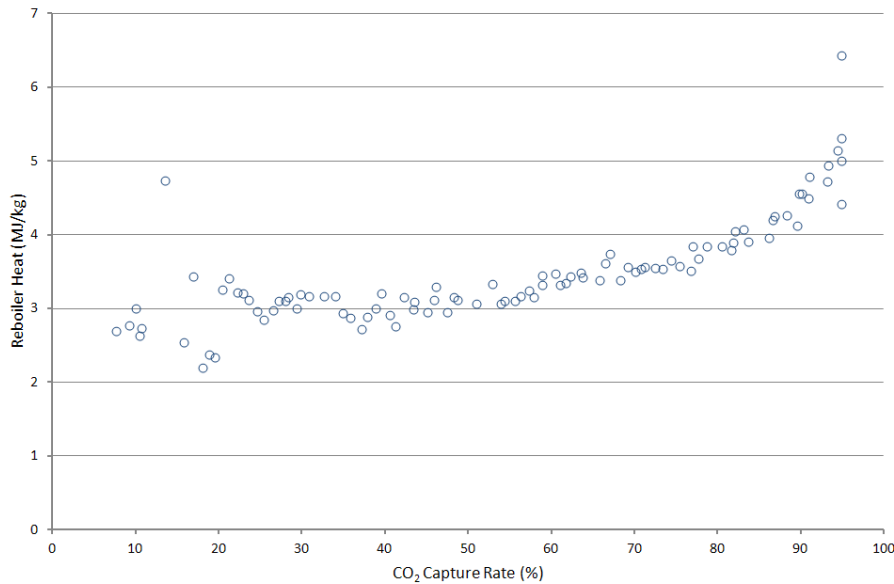


Figure 6-12: Stripper reboiler heat duty per unit of CO₂ captured for the Pareto-optimal solutions.

6.3.3 Pinch Analysis Results

The GCC combined with the SCC of the optimal solutions for a capture rate of 50 % and 85 % are provided in Figure 6-13 and Figure 6-14 respectively. The GCC for both capture rates are the same above the temperature of the stripper reboiler, which is represented by the horizontal section on the GCC at 150 °C for 50 % capture and 170 °C for 85 % capture. Obviously, the reboiler for the 85 % capture case has a higher duty which requires more steam to be extracted from the turbine. This is shown by the large horizontal section of the SCC at 170 °C. It is also possible to see on the GCC the increase in optimal stripper pressure from 4 bar in the 50 % case to 6.4 bar in the 85 % case, which increases both the reboiler temperature and the required extraction pressure and therefore the extraction steam temperature as shown by the SCC. There are also a number of utility pinch points that are created in these two cases by the linear programming optimisation of the steam rates, as represented by the points where the SCC touches the GCC.

The steam cycle has seven steam levels. The actual rates of generation or usage of those steam levels can be seen on the SCC as the horizontal portions on the curve, and the size is a representation of the quantity of steam generated / used at each level. When capturing 50 % of

the CO₂, only five of those steam levels have more than 20 kg/s of steam generated /used. In comparison, six steam levels have more than 20 kg/s of steam generated /used for the 85 % capture rate. As the number of steam levels used for generation / extraction increases the complexity and cost of the heat exchanger network also increases, but the exergy loss between the GCC and the SCC will be reduced. The MOO could be used to determine the impact of reducing the number of steam levels on the net power by creating Pareto fronts where the number of steam levels are constrained or when a minimum extraction steam rate is set.

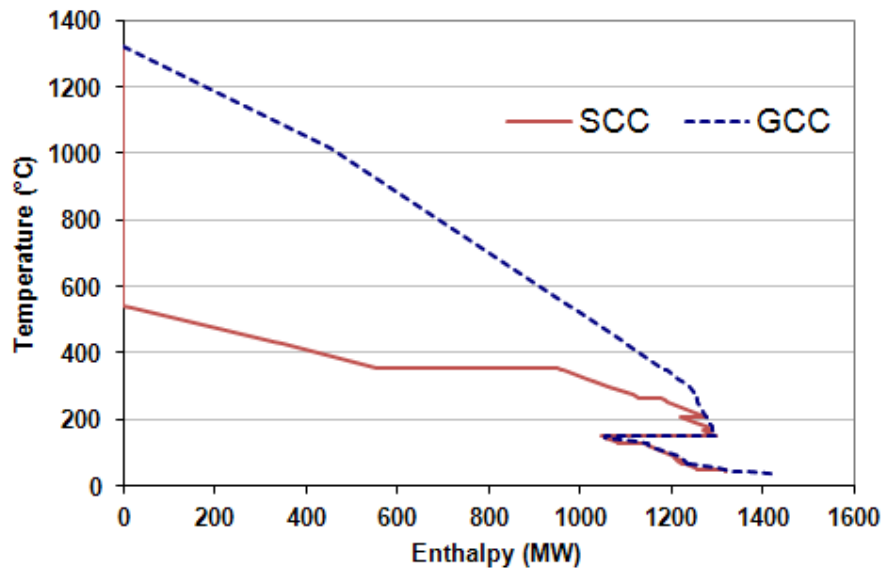


Figure 6-13: GCC and SCC for the Pareto-optimal solution with 50 % capture rate of CO₂.

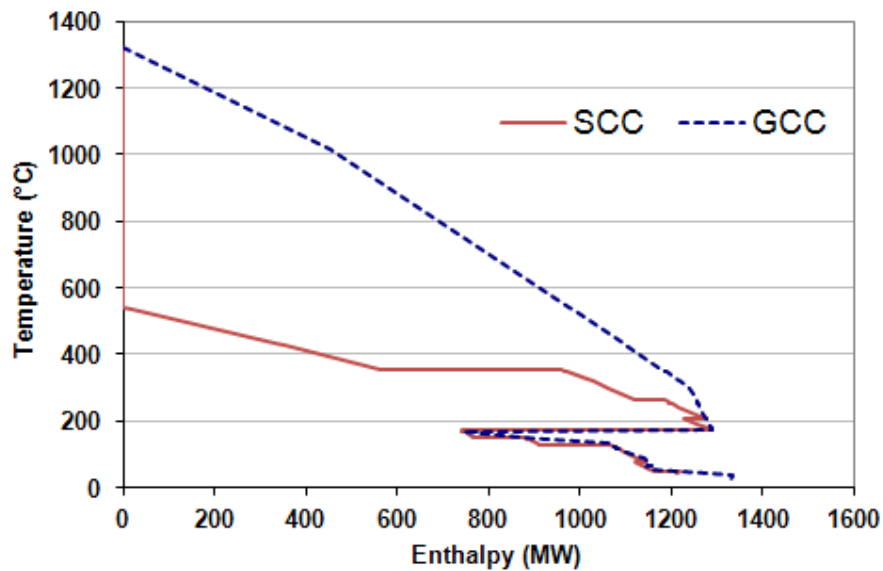


Figure 6-14: GCC and SCC for the Pareto-optimal solution with 85 % capture rate of CO₂.

6.4 Conclusions

The superstructure method is very useful method to optimise the power station with CCS for steam cycles that include a level of reheat. The energy penalty for the addition of potassium carbonate based CO₂ capture systems can be as low as 14 % when capturing 90 % of the CO₂ with a ΔT_{\min} of 6 °C. The MOO combined with simulation and the superstructure method of automated heat integration enables the determination of the optimum operating parameters of the solvent plant. It also can be used to determine what variables have the greatest influence on the net power by the speed of the convergence of the variables to the value which provides the optimum result.

The actual stripper pressure is actually not as important as ensuring the stripper pressure is set to produce a reboiler temperature that is able to be serviced by the available steam. The flue gas temperature should be less than 45 °C to maximise the net power, whilst the solvent temperature should be set for the water balance rather than for its impact on the net power. The optimum lean loading is between 0.15 and 0.20 mol HCO₃⁻/mol K⁺ for capture rates of 80 % to 90 %. The solvent flowrate is the main variable to control the capture rate, and can be used to adjust the capture rate to exploit fluctuations in electricity market prices. The number of steam levels will impact the net power of the power station, the capital costs of the project and the operational complexity. Optimising the number of steam mains will be important aspect of the design phase.

Chapter 7

Comparison of the extraction and the superstructure method

7. Comparison of the extraction and the superstructure method.

7.1 Introduction

In Chapters 3 and 5 a method that determined the required quantity of extraction steam to cover the deficit of heat created by the addition of CCS to the power station at the minimum loss of power from the steam turbine was developed and utilised. This method will be referred to as the '*extraction*' method as it optimises the extraction steam from the steam turbine. Chapter 4 on the other hand introduced a second method based on the same principles, but it determines for a given steam cycle what the optimum steam generation and extraction rates are to maximise the power generation from the steam turbine. As this method is based on a given steam cycle superstructure, this method is referred to as the '*superstructure*' method and was used in the example provided in Chapter 6.

In previous chapters the extraction method has been considered for retrofit applications whilst the superstructure method has been considered for greenfield power stations. The limitations of the extraction method in terms of only optimising the steam extraction rates downstream of a reheater have already been discussed in Chapter 4. The superstructure method can also be restricted so that any limitations that may exist on an existing steam turbine may be included in the problem definition and the optimum result can still be obtained with the constraint added. The work in Chapter 6 and Chapter 8 use the superstructure method, however in both cases the main HP steam rate is restricted to the value of the main steam rate of the base power station.

This chapter will be used to illustrate the improvements that can be achieved by using the superstructure method instead of the extraction method and the potential for large reductions in the energy penalty when the main steam rate does not have an upper limit.

7.2 Case Study Background

The case study used for the illustration is based on the case study provided in Chapter 5 and Chapter 6. It is a pulverised brown coal fired power station with a subcritical steam cycle with a single stage of reheat (refer to Figure 7-1), whilst the CCS plant is based on a potassium carbonate solvent. The decision variables for the optimisation included the lean solvent loading, flowrate and temperature, the flue gas temperature, the stripper feed temperature, the absorber and stripper height and the stripper pressure.

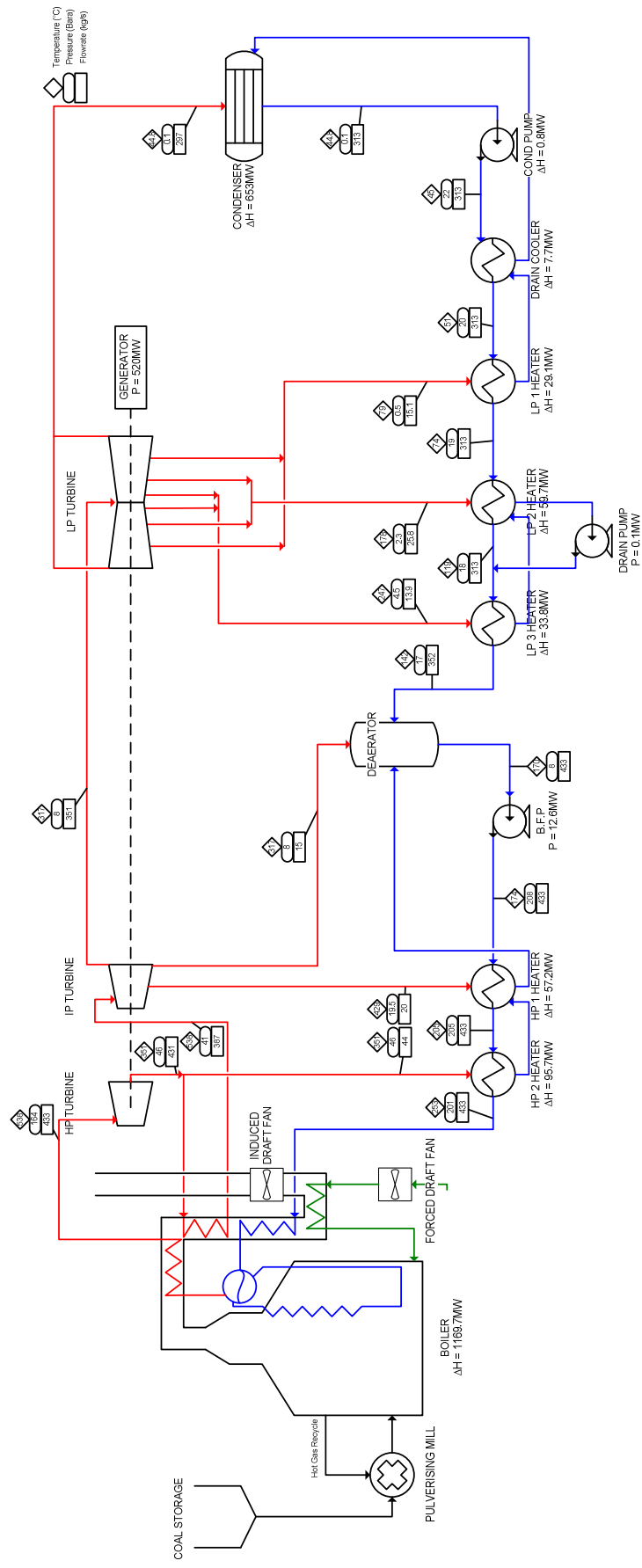


Figure 7-1: Base power station without CCS

7.3 Restricting the main steam flowrate

The MOO performed in Chapter 6 was to maximise both the net power and the CO₂ capture rate using the superstructure method with the main steam rate constrained to 433 kg/s as per the base power station without CCS. The MOO results obtained in Chapter 6 are reconstructed in Figure 7-2; additionally, the results without any limitations on the main steam rate are also provided for comparison. It is clear from these results that limiting the amount of main HP steam that is generated also limits the amount of power that is generated, for a given coal rate and CO₂ capture rate. Without a limitation on the main steam flow the net power is between 10 MW and 15 MW greater than with the main steam rate limited.

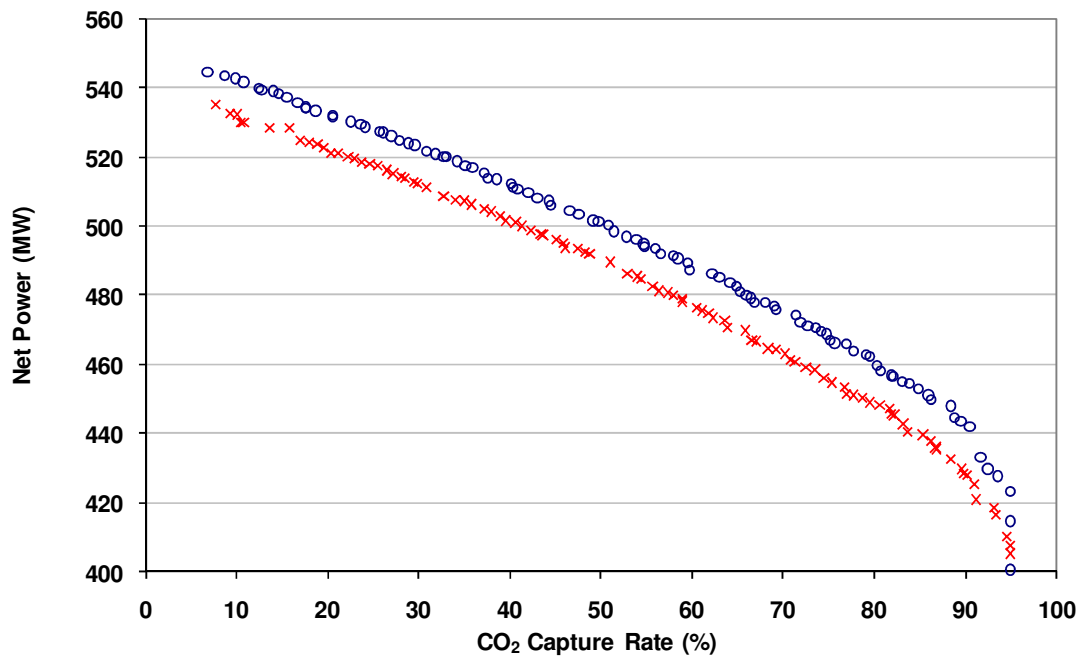


Figure 7-2: Optimised solutions to maximise both the CO₂ capture rate and the net power using the superstructure method with no restrictions (○) and with the main steam flowrate restricted to the flowrate of the base power station (×).

The reason behind the difference can be better understood by taking one of the optimised results and reviewing the GCC and SCC for both cases. Using the values of the decision variables for the optimised solution for a CO₂ capture rate of 85 % with the main steam flowrate limited and determining both the GCC and the SCC for the plant under these conditions, using the superstructure method with and without the main steam flowrate (refer to Figure 7-3). As all the decision variables are the same, the GCC between the two cases are identical, however the SCC's are different for the two cases.

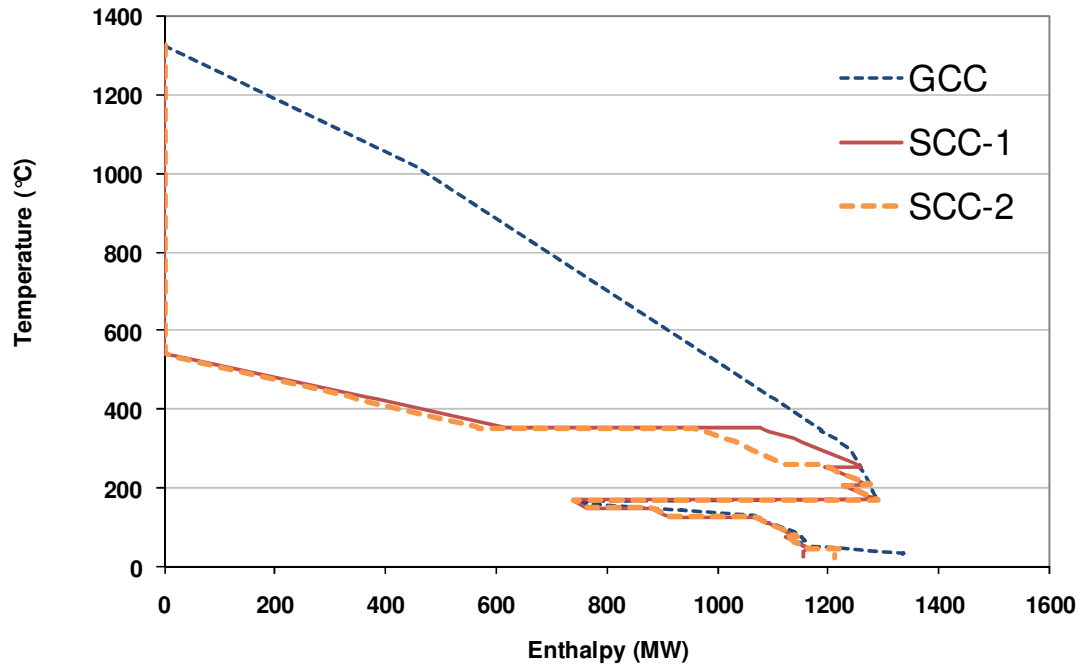


Figure 7-3: GCC(--) and SCC of the superstructure method using no restrictions (—)(SCC-1) and with the main steam rate restricted to the flowrate of the base power station (- -)(SCC-2).

The steam generation and extraction rates for the two cases are provided in Table 7-1. It can be noted from the SCC's and the steam generation and extraction rates, the difference between the two cases is in the high pressure turbine. When the HP steam rate is limited to 433 kg/s, to utilise all of the available heat, the optimum steam rates generate a further 39 kg/s of steam at the intermediate pressure steam level. As can be seen in Figure 7-3 when the main steam flowrate is not limited, the actual amount of HP steam that can be generated is higher at 503 kg/s. However to generate the additional HP steam requires steam to be extracted from the outlet of the high pressure turbine to provide some of the boiler feed water heating. The gross power generated by steam turbine for the case where the main steam flowrate is limited to 433 kg/s is 511 MW whereas the unlimited case produced 524 MW. The difference in the power generated between the cases is visible in the SCC's as the additional area under the SCC for the unrestricted case compared to the case that was limited.

Table 7-1: Steam generation (+ve) and extraction rates (-ve) for the optimised solutions with the main steam flowrate limited to 433 kg/s and then unlimited main steam flowrate.

Steam Level	Limited Main Steam Flowrate (kg/s)	Unlimited Main steam Flowrate (kg/s)
High Pressure	433	503
Intermediate pressure	39	-37
Intermediate Pressure – 2	-26	-26
Low Pressure	-271	-271
Low Pressure – 2	54	54
Low Pressure – 3	71	71
Low Pressure – 4	-10	-10
Condensate	-290	-283

The power produced by each section of the turbine for; the base case, the case with CCS and a main steam flow rate limited to 433 kg/s and the case with CCS but without any limitations on the main steam flowrate are provided in Table 7-2. The gross turbine power for the unrestricted case is actually greater than for the base case without CCS. However, the distribution of the power has shifted. The base case produces 43 % of its power from the low pressure turbine, however with the large amount of LP steam required for the solvent regeneration the amount of power that can be generated in this section of the turbine reduces. The optimised solution for the unrestricted case with CCS produces only 34 % of its power from the LP turbine. The amount of power produced in the high and intermediate pressure turbines needs to increase to maximise the amount of power produced from the turbines.

Table 7-2: Power produced by the steam turbine for the base case without CCS, with CCS and with the HP steam rate set to 433 kg/s and with CCS and with no limitations on the HP steam rate.

Steam Turbine Section	Base Case	CCS & no Heat Integration	CCS (443kg /s) (MW)	CCS (503 kg/s) (MW)
High Pressure	135	135	135	157
Intermediate pressure – 1	83	83	102	100
Intermediate Pressure – 2	79	79	92	90
Low Pressure – 1	47	16	25	24
Low Pressure – 2	43	15	29	28
Low Pressure – 3	73	28	70	68
Low Pressure – 4	60	23	58	57
Total	520	379	511	524

7.4 Superstructure versus the Extraction Method

In Section 7.3 the impact of restricting the main steam flow rate was shown to reduce the maximum gross power that can be produced by the steam cycle. In the same manner, the extraction method is actually restricting the steam generation to the same rates as per an existing steam cycle and only changing the extraction steam rates downstream of any reheaters. The same example as used in section 7.3 is also used to determine the impact of using the extraction method. The SCC and GCC are provided in Figure 7-4 and the gross power for the steam turbine is 433 MW. Clearly the extraction method will generally not provide the maximum amount of power that could be generated from the heat available in the power station with the addition of CCS. Figure 7-4 shows that additional high pressure steam could be generated by utilising the large temperature difference in the pocket of the GCC that is located after where the SCC ends (enthalpy between 1136 MW and 1300MW). Also there is considerable low grade heat that can be used to generate additional low pressure steam to help increase the power produced from the turbine. This is represented by the large temperature difference between the GCC and the SCC for temperatures less than 164 °C.

Using the extraction method the main HP steam generation and the IP steam extraction rates are constrained to the base power station rates of 433 kg/s and 45.8 kg/s respectively. To provide the deficit of heat due to the addition of CCS the extraction method determined that a further 194 kg/s of steam needs to be extracted from the IP-LP crossover. Therefore, using the extraction method will not necessarily require any changes to be made to the HP and IP turbines but will still have approximately 50 % of the steam removed from the LP turbine. Therefore, modifications to the LP turbine will be required.

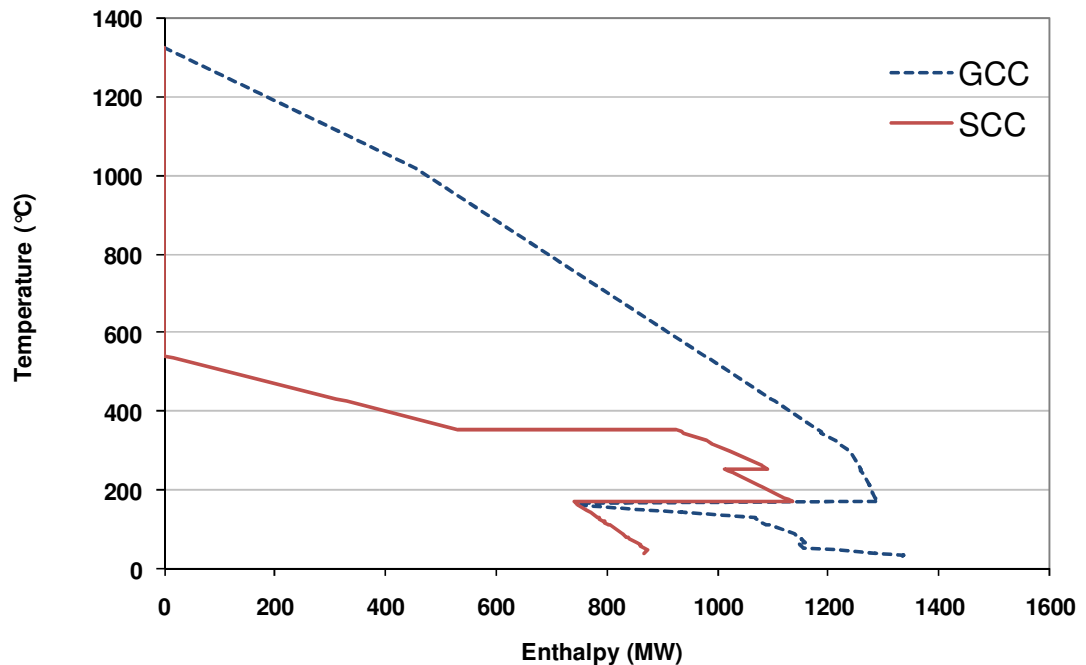


Figure 7-4: SCC (—) and GCC (--) for the power station with 85 % capture using the extraction method.

In contrast to the extraction method, the superstructure method allows changes to be made to the steam flowrates throughout the steam turbine, and therefore changes may be need to be made to the entire steam turbine equipment. Additionally, due to the changes in the steam rates the heat distribution in the boiler will vary. Using the example provided in this chapter the heat distribution in the existing boiler (refer to Figure 7-5) is compared to the heat distribution that is suggested by the superstructure method (refer to Figure 7-6). Due to the larger heat load for the additional steam generation using the results from the superstructure method, the temperature driving forces between the flue gas and the steam circuit is reduced. This is especially noticeable in the reheat section of the boiler. Additionally, the flue gas alone cannot supply the required heat for the steam circuit assuming that the economiser feed temperature remains constant (258 °C). There is a temperature crossover between the cold end of the economiser and the flue gas (Figure 7-6). The explanation for the crossover can be seen when the superheat energy for the steam extracted from the turbines is included in the analysis. This heat can be used to pre-heat the boiler feed water to increase the feed temperature to the economiser, making the heat transfer feasible (refer to Figure 7-7). However, it becomes clear that the temperature difference between the economiser and the air-preheat and the flue gas reduces compared to the base case.

When the temperature driving forces between the flue gas and the steam circuit and air-preheat are reduced, the required area for heat transfer increases. Therefore, the opportunity for the existing power station to produce the maximum power suggested by the superstructure method,

without making wholesale changes to the boiler, will be limited by the actual heat transfer area of the existing boiler. Therefore, the potential for large reductions in the energy penalty by optimising the steam cycle will vary between power stations and will be largely impacted by any design margins that may have been designed into the original boilers. Understanding the potential maximum steam rate of the existing boiler and steam turbine will enable an upper limit to be placed on the main steam rate and/or reheat steam rate in the superstructure problem definition, which will enable the superstructure method to provide results that are more likely to be able to be implemented with limited changes to the boiler. The final physical design will also not only be impacted by the amount of area, but also the location of the heat exchanger area and the temperature profile throughout the boiler. There is a need to ensure that the heat transfer can occur where it is supposed to in the boiler and this would require more sophisticated computational fluid mechanics modelling in order to validate the changes to the boiler heat transfer.

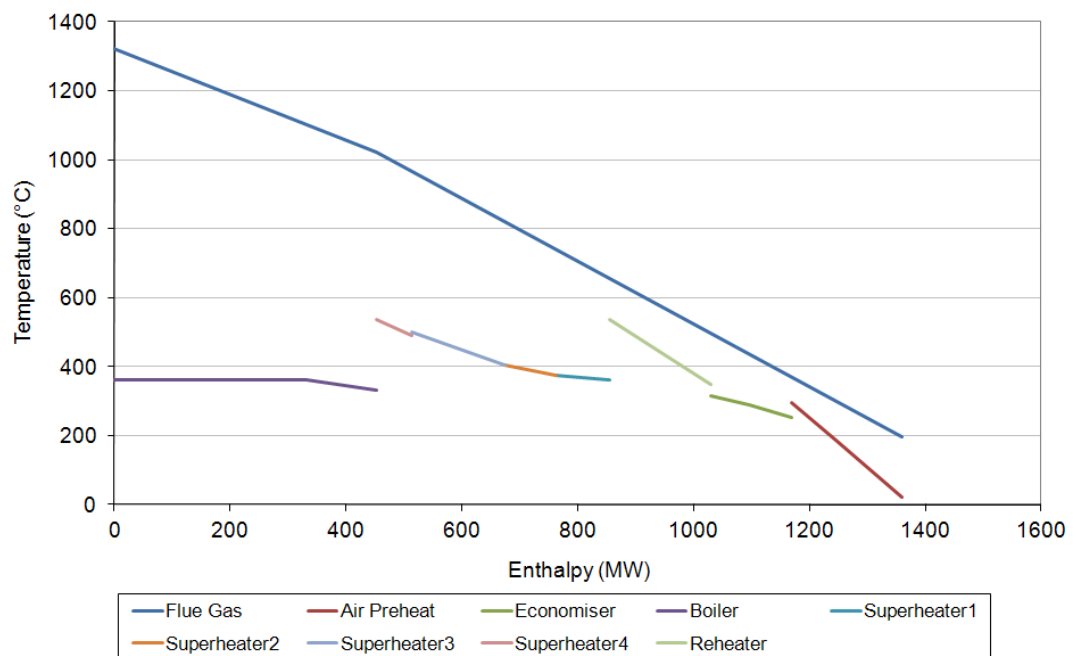


Figure 7-5: Temperature profiles in the boiler of the existing coal fired power station

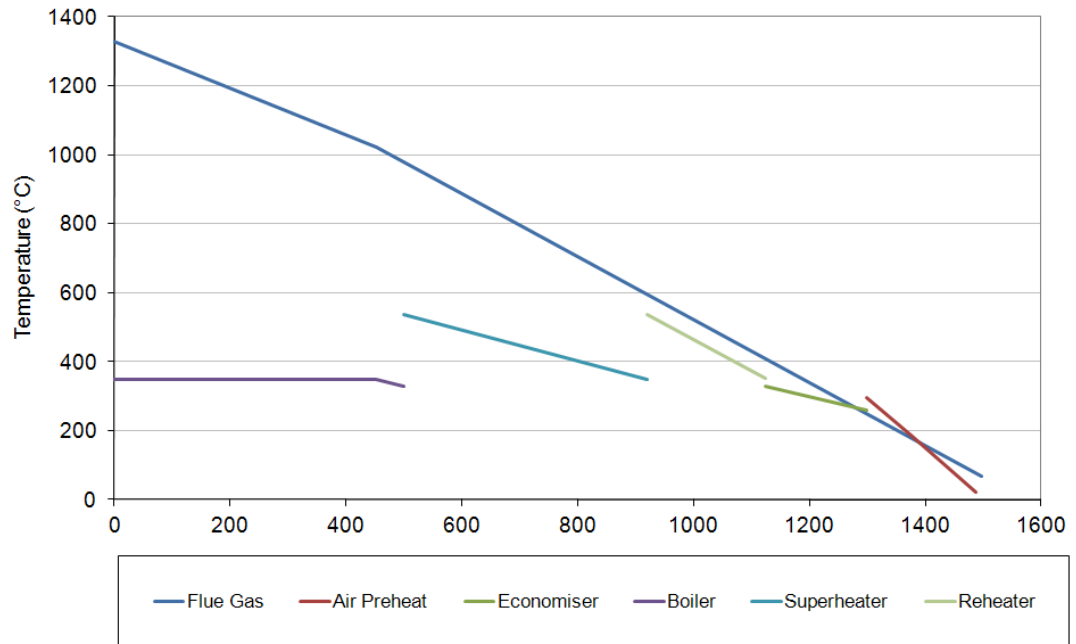


Figure 7-6: Temperature profiles in the boiler of the coal fired power station with steam rates optimised using the superstructure method

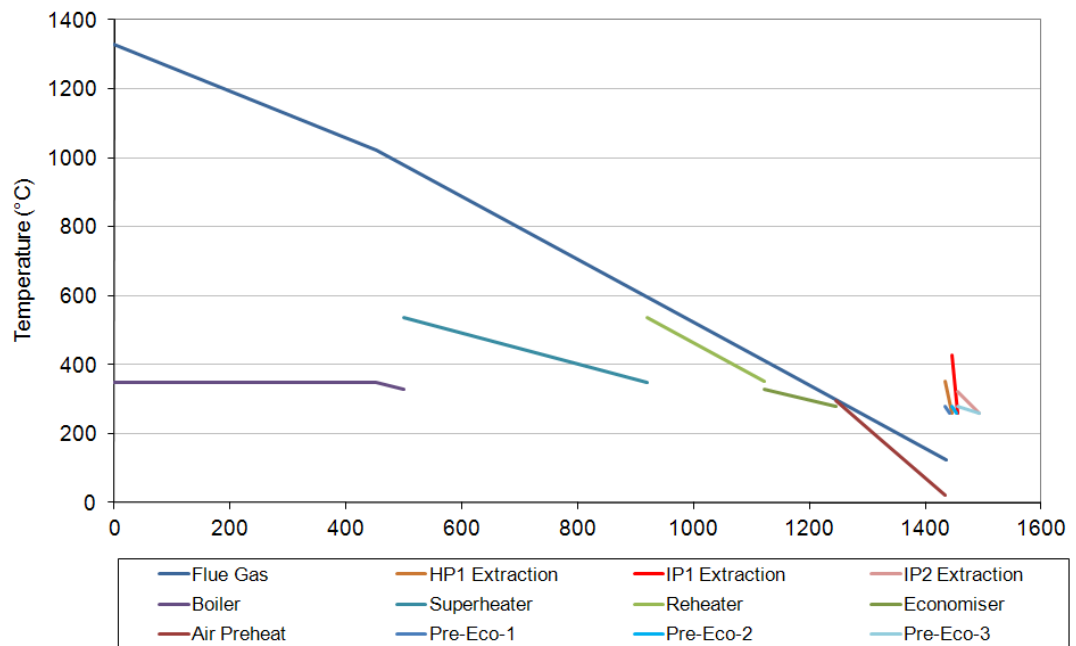


Figure 7-7: Temperature profiles in the boiler of the coal fired power station with steam rates optimised using the superstructure method including the increased feed water temperature to the boiler using the extraction steam superheat.

7.5 Conclusion

The extraction method is a subset of the superstructure method where a number of restrictions are placed on the superstructure. The superstructure method without restrictions will provide the maximum power generated by the power station for the given steam cycle. On the other hand, the extraction method or superstructure method with restrictions will not necessarily provide the maximum power from the power station, but could be useful when it is envisaged that a retrofit of the existing steam turbine will occur. Therefore, the limits of the existing steam turbine can be included in the problem definition and then the maximum power generated for the given steam cycle with limitations can be determined.

To maximise the amount of power generated from a power station with solvent based CCS, it will generally be necessary to increase the power produced in the front end of the steam turbines (the HP and IP turbines) as the amount of power generated in the lower end will be reduced. Methods to combat the reduction in steam flow in the LP section of the turbine have been reviewed by other authors (refer to Chapter 2 Section 2.3), however methods to handle efficiently an increase in the HP and IP steam generation in the turbines should also be investigated as well as whether additional heat exchanger area would be required to generate the additional steam.

Using the superstructure method will help to identify what potential additional net power the power station may produce by utilising existing design margins, modifying or replacing the existing turbine. Understanding the limitations of the existing turbine and boiler will be crucial to determining the maximum net power that can be produced by the power station retrofitted with CCS.

Chapter 8

Optimisation of power stations with carbon-capture plants – the trade off between costs and net power

Journal of Cleaner Production: In Press

doi: [10.1016/j.jclepro.2011.12.032](https://doi.org/10.1016/j.jclepro.2011.12.032)

8.1 Introduction

This chapter is based on an article submitted to the Journal of Cleaner Production for a special issue from selected papers given at PRES'11 (14th international conference on Process Integration, Modelling and Optimisation for Energy Saving and Pollution Reduction). The paper is used to show how MOO using simulation and heat integration can be improved with the addition of cost estimation to help to optimise the CCS process; the third and final objective of this thesis.

The paper also includes details of the process required to link the MOO with the simulation, heat integration and cost estimation using the superstructure method of automated heat integration. The paper therefore duplicates some of the content provided in Chapter 4 for setting up the superstructure method, but is added in this paper to provide an outline of the architecture developed in this thesis to a wide audience.

The paper, provided in section 8.3, uses the same case study as used in Chapters 5 and 6. However, with the addition of the cost estimation the objectives for the optimisation study in this chapter are different to those in Chapters 5 and 6. The work in this chapter uses the superstructure method of linear programming to determine the maximum amount of power that can be generated by the steam cycle for the given potassium carbonate based solvent absorption process. However, the main steam flowrate has been restricted to the main steam flowrate of the base power station (433 kg/s). Therefore, there is a potential for lower energy penalties than those suggested by this paper, based on the findings presented in Chapter 7, if the main steam flowrate was not restricted.

The paper provides details as to how the capital and operating costs are estimated, however due to brevity, important details have been omitted. Cost estimation of the CCS equipment is difficult. Much of the equipment has not been supplied for CCS purposes at the scale required for capturing CO₂ from the flue gas of power stations. Without equipment that is purpose built for CCS at scale, the costs must be determined from analogous equipment and there are many possible correlations that could have been chosen for the cost estimation. Appendices B and C provide details of a number of correlations for capital and operating costs, respectively. The correlations that are actually used in the optimisation in this chapter are given in the paper in section 8.3.

Only one set of cost estimation correlations have been used in the optimisation results presented in this chapter, however it is acknowledged that the equipment capital costs could vary as shown by the range of cost functions provided in Appendix B. Therefore two additional optimisations were performed with capital equipment costs 20 % greater and less than the estimated costs as

per the cost functions and results are provided in Figure 8-1 to 8-4. It is clear that the capital cost functions of the equipment will have a major impact on both the cost of electricity and the cost of CO₂ capture. The DCOE (Figure 8-1) decreases by approximately 8 \$/MWh (12%) with a 20 % decrease in the capital costs and increases by 6 \$/MWh (10%) with a 20 % increase in the capital costs at a capture rate of 80 %. Therefore it is clear that ensuring equipment is designed fit for purpose to minimise the capital costs will be important. The impact of capital costs on the cost of CCS is shown by the results provided in Figure 8-2, where the cost of CCS per tonne of CO₂ at a capture rate of 80 % increases or decreases by around 9 \$/t (12%) if the capital costs are 20 % greater than or less than the estimated costs. When capital costs are reduced by 20 %, the cost of capture has less variation at the higher capture rates (approx. >60 %), compared to the cases with higher capital cost functions which require increasing capture rates to minimise the cost of CCS.

The energy penalty for the optimal solutions also changes depending on the capital costs (Figure 8-3). Although there is significant scatter in the energy penalty of the optimal cases, there is a definite trend, as indicated by the linear trend lines plotted in Figure 8-3, that the energy penalty reduces as the capital costs of the equipment is reduced, especially at higher capture rates. This is due to the lower capital costs leading to higher amounts of heat exchanger area being incorporated. In fact, the total cost for heat exchangers actually increases as the capital cost functions reduce (Figure 8-4), because the additional cost for the heat exchangers is less than the value for the additional power that can be produced from the power station.

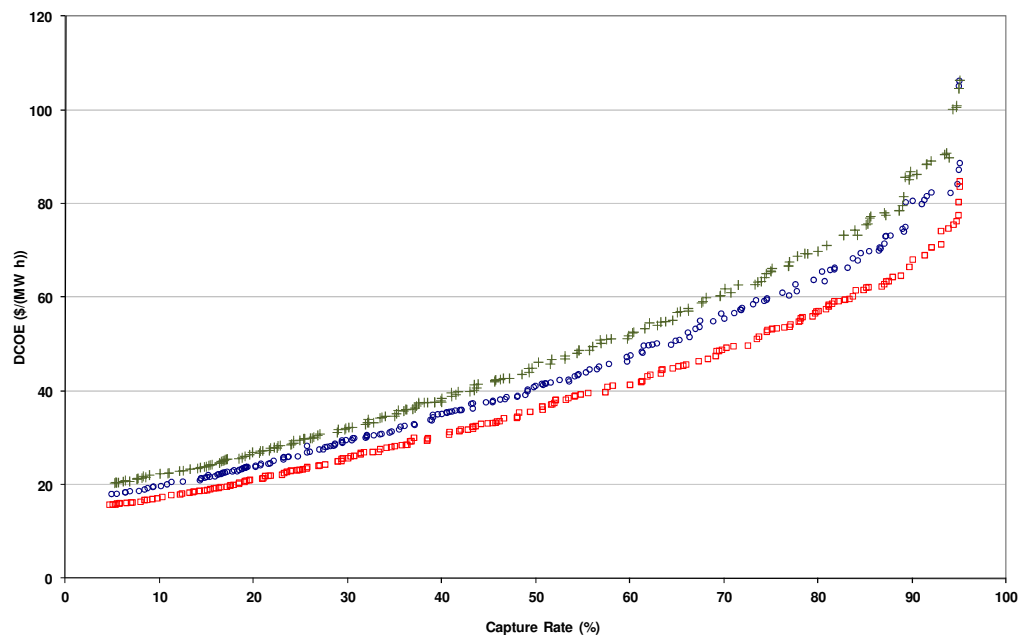


Figure 8-1: Pareto optimal solutions for the minimisation of DCOE and maximisation of capture rate (○) with capital costs 20 % greater (+) and less (□) than the estimated cost functions.

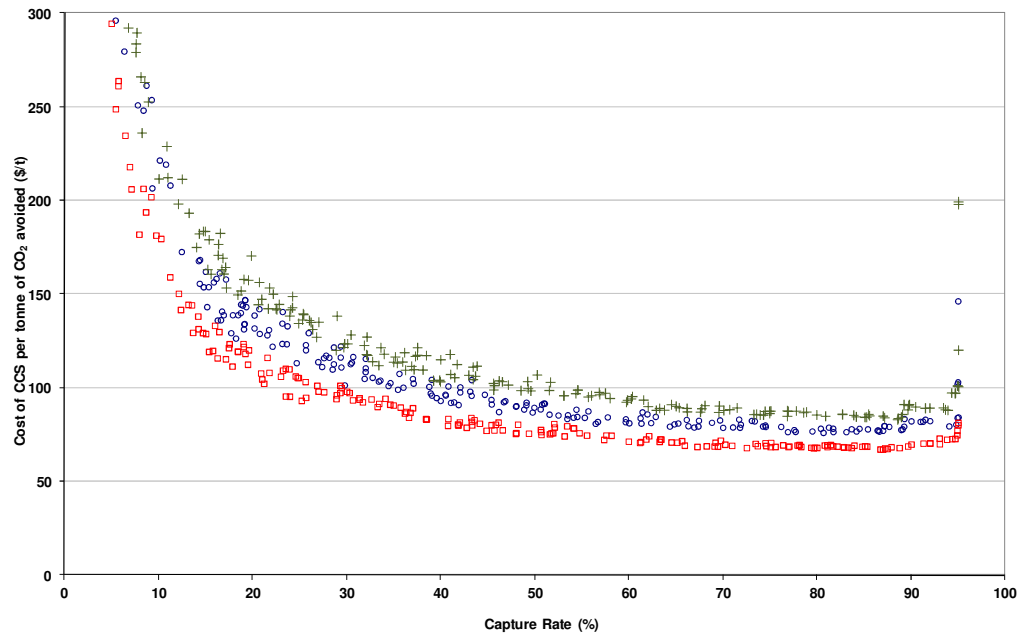


Figure 8-2: The cost of CCS for the Pareto optimal solutions (○) with capital costs 20 % greater (+) and less (□) than the estimated cost functions.

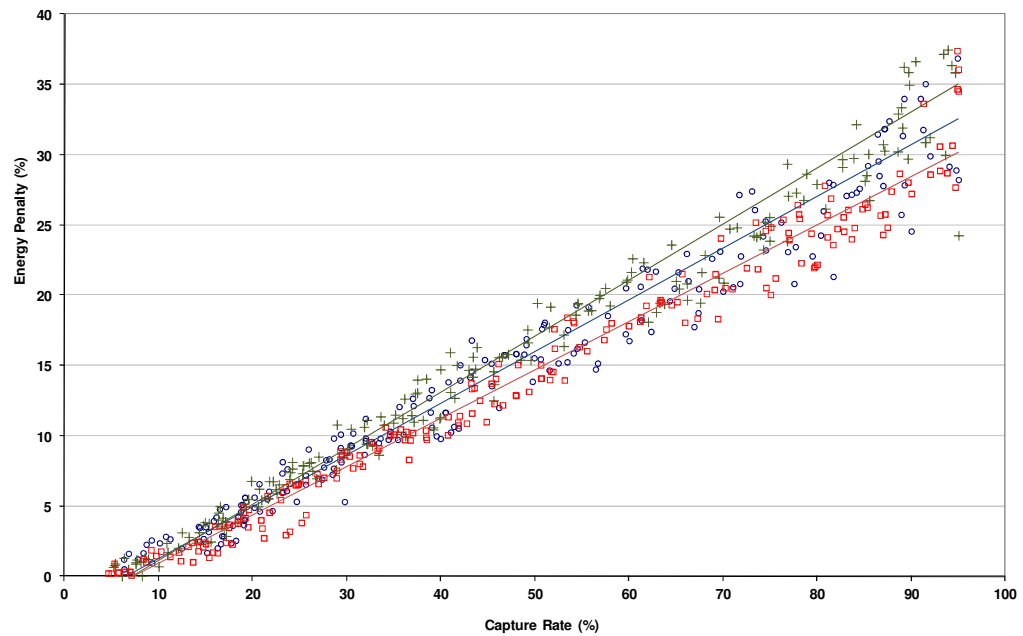


Figure 8-3: Energy penalty for the Pareto optimal solutions (○) with capital costs 20 % greater (+) and less (□) than the estimated cost functions. Solid lines represent linear trend lines for the given data sets.

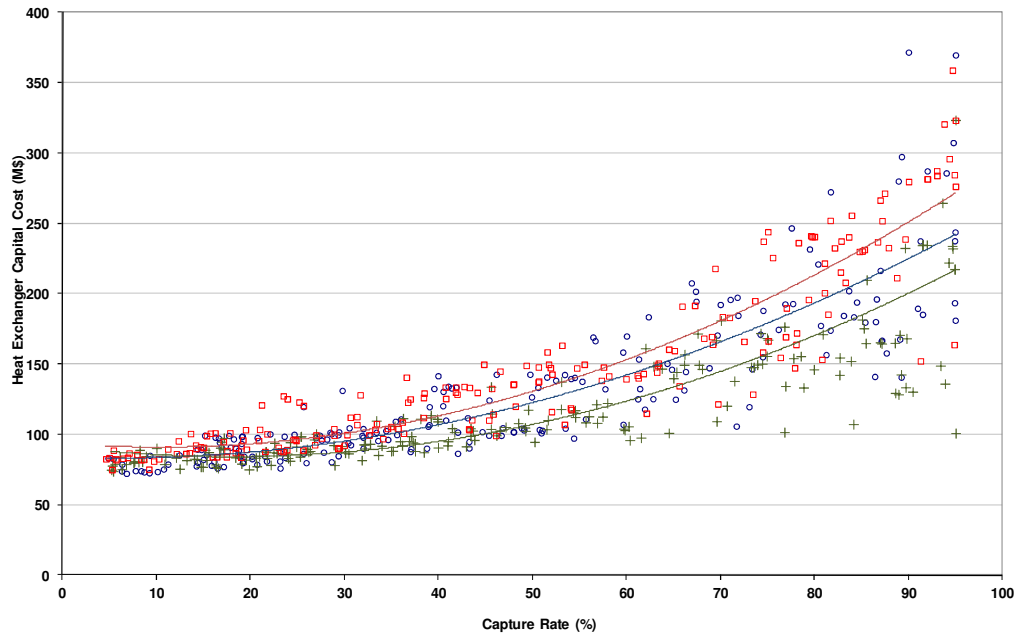


Figure 8-4: Heat exchanger purchased capital costs for the Pareto optimal solutions (\circ) with capital costs 20 % greater (+) and less (\square) than the estimated cost functions. Solid lines represent quadratic trend lines for the given data sets.

In general MOO provides more insightful results when the objectives are antagonistic. In this chapter the optimisation process compares the two primary objectives of maximising the net power or minimising the differential cost of electricity (DCOE) whilst simultaneously maximising the amount of CO₂ captured (as the second objective). The first and second objectives are antagonistic as increasing CO₂ capture will reduce the net power and increase the cost of electricity.

Numerous other optimisation objectives may be used to optimise the CCS process costs. Some alternative objectives that were also tested did not provide particularly useful results. For example, minimising the cost of CO₂ capture whilst maximising the CO₂ capture rate gave a very narrow range of results (Pareto curve) as the cost of capture generally reduces as the amount of CO₂ captured is increased. MOO using the objectives of minimising the capital costs whilst maximising the net power from the power station would be a useful optimisation process, however it requires the selection of a defined CO₂ capture rate which constrains the combination of variables in the CO₂ capture plant that will be able to achieve the desired capture rate. Therefore, this optimisation could be used as a secondary optimisation step once a number of the variables have been fixed by the kind of targeting optimisation that is performed in this chapter.

From a commercial stand-point, minimising the DCOE, as per the second optimisation problem presented in the paper, would appear to be more important than maximising the net power as per the first optimisation problem presented in the paper. The paper shows that very different results are obtained depending on the objective used in the optimisation. The minimum energy penalty may be as low as 14 % for a CO₂ capture rate of 90 %, but the economic energy penalty will be between 25 % and 30 %. Nonetheless, by performing two very different optimisations it enables the designer to compare the values of the decision variables when trying to maximise the net power compared to minimise the DCOE. This allows many insights to be gained.

One of the insights identified in the example provided in the paper, is that the flue gas temperature to maximise the net power is much lower than the flue gas temperature to minimise the DCOE. On interrogation of the results it is clear that lower flue gas temperatures lead to lower solvent regeneration energy requirements and therefore a lower energy penalty. However, the reason that the low flue gas temperatures were not selected when optimising to minimise the DCOE, is due to the large heat exchanger area required for flue gas condensation which leads to increased costs as the flue gas temperature decreases. Therefore, utilising a direct contact cooler rather than an indirect heat exchanger for the condensation duty could reduce the cooling costs and therefore lead to lower flue gas temperatures and higher net power at a lower DCOE.

The combination of MOO, simulation, automated heat integration and cost estimation is shown in the paper to provide greater understanding of the impact of many of the variables involved in the design and integration of CCS to power stations.

8.2 Declaration for Chapter 8

Monash University

Declaration for Thesis Chapter 8

Declaration by candidate

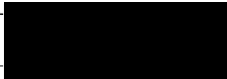
In the case of Chapter 8, the nature and extent of my contribution to the work was the following:

Nature of contribution	Extent of contribution (%)
Initiation, key ideas, simulations, methodology, results interpretation, writing of paper.	80

The following co-authors contributed to the work. Co-authors who are students at Monash University must also indicate the extent of their contribution in percentage terms:

Name	Nature of contribution	Extent of contribution (%) for student co-authors only
Andrew Hoadley	Initiation, results interpretation, reviewing of paper.	
Barry Hooper	Initiation, results interpretation, reviewing of paper.	

Candidate's
Signature

	Date 14/12/2011
---	--------------------

Declaration by co-authors

The undersigned hereby certify that:

- (1) the above declaration correctly reflects the nature and extent of the candidate's contribution to this work, and the nature of the contribution of each of the co-authors.
- (2) they meet the criteria for authorship in that they have participated in the conception, execution, or interpretation, of at least that part of the publication in their field of expertise;
- (3) they take public responsibility for their part of the publication, except for the responsible author who accepts overall responsibility for the publication;
- (4) there are no other authors of the publication according to these criteria;
- (5) potential conflicts of interest have been disclosed to (a) granting bodies, (b) the editor or publisher of journals or other publications, and (c) the head of the responsible academic unit; and
- (6) the original data are stored at the following location(s) and will be held for at least five years from the date indicated below:

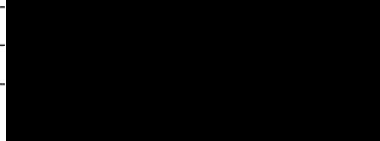
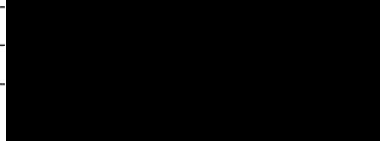
Location(s)

Cooperative Research Centre for Greenhouse gas Technologies, CO2CRC,
Room 232, Level 2, Bldg 193, The University of Melbourne, Parkville VIC, 3010

[Please note that the location(s) must be institutional in nature, and should be indicated here as a department, centre or institute, with specific campus identification where relevant.]

Signature 1

Signature 2

	Date 21/12/11
	14/12/11



Contents lists available at SciVerse ScienceDirect

Journal of Cleaner Production

journal homepage: www.elsevier.com/locate/jclepro

Optimisation of power stations with carbon capture plants – the trade-off between costs and net power

Trent Harkin^{a,b,*}, Andrew Hoadley^{a,b}, Barry Hooper^a

^a Cooperative Research Centre for Greenhouse Gas Technologies (CO2CRC), The University of Melbourne, Vic. 3010, Australia
^b Department of Chemical Engineering, Monash University, Clayton, Vic. 3800, Australia

ARTICLE INFO

Article history:

Received 12 August 2011
 Received in revised form
 26 December 2011
 Accepted 26 December 2011
 Available online xxx

Keywords:

CCS
 Potassium carbonate
 Heat integration
 Power
 Cost estimation
 Optimisation

ABSTRACT

The addition of carbon capture and storage to a power station will impact the net power generated and increase the cost of electricity produced from the power stations. A method is presented to help design the carbon capture and compression process retrofitted to the power station. It combines simulation, automated heat integration and multi-objective optimisation. The methodology is applied to a coal fired power station combined with potassium carbonate based solvent absorption. To capture 90% of the CO₂ emissions the energy penalty, the ratio of the change in efficiency of the power station due to the addition of carbon capture and storage relative to the efficiency of the original power station, can be reduced from 38% to 14% using this method. However to minimise the cost of electricity, more modest reductions in energy penalty of 25%–30% are recommended.

© 2012 Published by Elsevier Ltd.

1. Introduction

Carbon Dioxide (CO₂) separation using solvent based absorption is considered to be the leading technology for the immediate implementation of post-combustion CO₂ capture (PCC) from power stations. However, it reduces the efficiency of the power station due to the impact of the additional heat and power required to separate, capture and compress the CO₂. There is also a significant capital and operating cost associated with the new carbon capture and storage (CCS) equipment, which will increase the power stations cost of electricity (COE). When designing a CCS plant for a particular power station, there are many objectives that need to be considered; the capital cost of the new infrastructure, the operating costs, net power generated, the operability of the power station and the environmental impact of the CCS plant. When determining the optimal design of the power station with CCS, there will often be conflict between these objectives and selection of the final design will require trade-offs to be made between the various objectives.

Although CO₂ absorption is widely used in the gas processing industries for separation of CO₂ from natural gas and synthesis gas, separating the CO₂ from flue gases of power stations has specific challenges that need addressing; The low partial pressure of CO₂ limits the driving forces for absorption, the oxygen, and the oxides of sulphur (SO_x) and nitrogen (NO_x) in the flue gas can react and degrade the solvents and the scale of the equipment required for significant reductions in CO₂ emissions is orders of magnitude larger than what has been demonstrated. Therefore significant amount of research is being conducted into improving the CO₂ absorption technology by using improved solvent formulation, process flow-sheet modifications and better integration with the power station.

Monoethanolamine (MEA) with a mass fraction of 30% is widely considered as the benchmark solvent for PCC (Davidson, 2007), however other solvents are being investigated to replace it, with the aim to reduce the regeneration energy requirements, the rate of solvent degradation, corrosion and cost of the system. These include; higher strength (40%) MEA with corrosion inhibitors in the HiCaptTM process (Bouillon et al., 2011), an advanced proprietary amine used in the Econoamine FG Plus system developed by Fluor (Reddy et al., 2003), a proprietary sterically hindered amine KS-1 (Mimura et al., 1997), a chilled ammonia process being developed by Alstom (Zachary, 2008), an amino acid salt process called the PostCapTM process by Siemens (Schneider and Schramm, 2011), Gustav 200 by BASF (Stoffregen, 2011), concentrated piperazine

* Corresponding author. Cooperative Research Centre for Greenhouse Gas Technologies (CO2CRC), The University of Melbourne, Vic. 3010, Australia. Tel.: +61 3 8344 5048; fax: +61 3 9347 7438.
 E-mail address: t.harkin@unimelb.edu.au (T. Harkin).

Nomenclature			
A	Heat exchanger area m^2	$\Delta h_{i,t}$	Enthalpy available in the steam in steam level i when steam temperature is reduced from the maximum to temperature t kJ/kg
C_{rb}	Currency conversion factor	$\Delta H_{i,t}$	Enthalpy required of steam in steam level i to produce steam from temperature t to the maximum steam temperature kJ/kg
F_i	Flowrate of steam generated in steam level i kg/s	Δp	Pressure change/pump differential pressure kPa
$H_{GCC,t}$	Enthalpy of the GCC at temperature t kW	ΔT_{\min}	Minimum temperature driving force K
$h_{i,t}$	Enthalpy of steam in steam level i at temperature t (temperature adjusted by $-\frac{1}{2}\Delta T_{\min}$) kJ/kg	$\eta_{i,j}$	Isentropic efficiency of the steam turbine between stages i and j
H_i	Enthalpy of the steam in steam level i kJ/kg	Φ	Pump capacity factor ($Q_P \times \Delta p$) ($\text{m}^3 \text{kPa/s}$)
$H_{i,t}$	Enthalpy of steam in steam level i at temperature t (temperature adjusted by $+\frac{1}{2}\Delta T_{\min}$) kJ/kg	ψ	Vessel mass kg
$H_{isen,i}$	Enthalpy of steam isentropically expanded from steam level i to the next steam level kJ/kg	ω_i	Power coefficient - the amount of work generated by a unit of steam through all the steam turbines from steam level i to condensate stream kJ/kg
i	Steam level	Abbreviations	
n	Total number of steam levels	CCS	Carbon Capture and Storage
N	Number of heat exchangers	COE	Cost of electricity
p	Vessel pressure bar	DCC	Direct contact cooler
P_c	CO_2 compressor power kW	DCOE	Differential cost of electricity
P_i	Steam pressure of steam level i kPa	GCC	Grand composite curve
P_{ST}	Steam turbine power kW	HX	Heat Exchanger
$q_{j,k}$	Enthalpy of stream j in enthalpy interval k W	MEA	Monoethanolamine
Q_{FD}	Forced draft fan flowrate m^3/s	MOO	Multi-objective optimisation
Q_P	Pump flowrate m^3/s	NPV	Net Present Value
s_i	Entropy of steam at steam level i $\text{kJ}/(\text{kg K})$	NOx	Oxides of nitrogen
$T_{1,2,3,4}$	Steam temperature $^\circ\text{C}$	PCC	Post-combustion capture
T_{R2}	Reheat steam temperature $^\circ\text{C}$	SCC	Steam composite curve
$W_{i,j}$	Amount of work generated by steam through the turbine from level i to j kW	SOx	Oxides of sulphur
W	Total power generated by the steam turbine kW		
Y_{rb}	Conversion factor for the year		
δ_j	Film heat transfer coefficient of stream j $\text{W}/(\text{m}^2 \text{K})$		

(Plaza et al., 2011), potassium carbonates promoted by boric acid by the CO2CRC (Ghosh et al., 2008) and piperazine at the University of Texas (Oyeneke and Rochelle, 2009) and precipitating potassium carbonate systems by the CO2CRC, Shell and NTNU (CO2CRC Technologies Pty Ltd, 2011; Schoon and Straelen, 2011; Svendsen et al., 2008).

Along with the new solvents being researched and developed, research is also conducted into the process flowsheet of the absorption process. The standard absorption process involves lean solvent contacting with the flue gas in the absorber, the solvent absorbs the CO_2 and the rich solvent is then sent to the stripper where heat is added to liberate the CO_2 and regenerate the solvent which is re-cycled to the absorber (Refer to Fig. 1). Numerous modifications can be made to the standard design including using absorber inter-cooling, split flow arrangements, vapour recompression and multi-column regeneration. A summary of many of these modifications can be found in a paper by Cousins et al. (2011b) and these modifications are analysed for MEA by Jassim and Rochelle (2006), Le Moullec and Kanniche (2011) and Cousins et al. (2011a). In the later paper the process modifications are compared by the impact on the reboiler energy, which means that the impact on the electrical load by the modifications are not taken into account, whereas the former two papers have tried to convert the reboiler duty into an equivalent electrical duty using a Carnot efficiency to account for the steam that is extracted from the turbine to provide heat in the reboiler. This enables a fairer comparison between the flowsheet modifications. However, as Cousins et al. (2011a) point out the results may vary depending on the type of solvent that is used in the analysis and equally the power station analysis will impact the preferred flowsheet. Karimi et al. (2011) also look at the various flowsheet modifications for

MEA and use a Carnot efficiency to estimate the lowest energy intensive flowsheet, but also estimate the costs for each option to enable a comparison between the energy savings and the costs required to achieve those savings.

However, whilst improvements in the solvent and the solvent absorption flowsheet are important how they are integrated with the power station is equally important. Using heat in the CCS process back into the steam cycle can help to reduce the energy penalty of the addition of CCS. Mimura et al. (1997) use 14% of the heat in the stripper condenser to heat the boiler feed water and Desideri and Paolucci (1999) and Romeo et al. (2008) suggest utilising heat from the CO_2 compressor intercoolers to also provide heat to the boiler feed water. An IEA-GHG (2006) report goes further by utilising a number of waste heat streams to increase the overall power station efficiency, they produce hot water for coal pre-drying in the flue gas cooler prior to the flue gas desulphurisation, the stripper condenser and the CO_2 compressor intercoolers, they also heat the boiler feed water using the stripper condenser and CO_2 compressor intercoolers completely removing the need for the existing steam heated feed water heaters. Pfaff et al. (2010) also use the heat in the stripper condenser and CO_2 compressor for boiler feed water heating, but also use hot water as a heat carrier for some of the air-preheat. They also review the ideal level of inter-cooling in the CO_2 compressors to trade-off between the additional compression power of installing less coolers and the improved quality of heat that is then available in the intercoolers for use in the steam cycle.

The importance of re-using the heat from the CO_2 capture plant into the power station steam cycle is demonstrated by those papers provided in the previous paragraph and therefore developing methods to systematically determine the best opportunities for heat integration are important. Previous methods to systematically

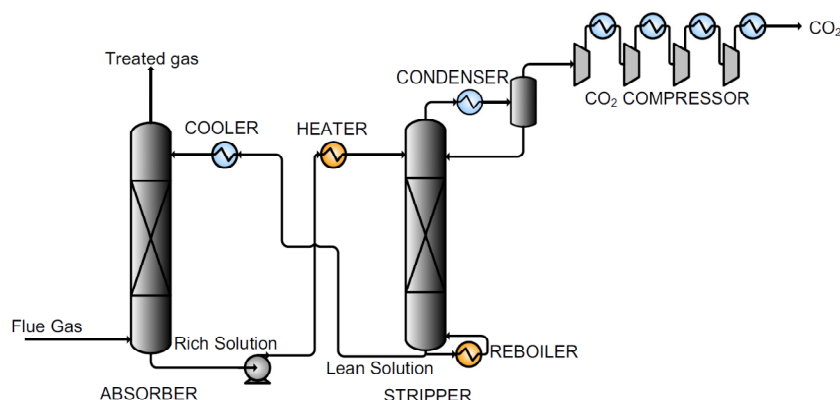


Fig. 1. Process diagram of the solvent based post-combustion CO₂ capture plant.

analyse the heat integration aspects of power stations include that by Linnhoff and Alanis (1989) who used pinch analysis in the design of power stations; steam extraction rates were calculated assuming a pinch occurs at each steam condensing temperature. Unfortunately, this is not always the case for power stations with CCS and this will not necessarily provide the greatest amount of power from the power station. Ataei and Yoo (2010) showed this by using combined pinch and exergy analysis to optimise the steam extraction rates to increase the power station efficiency compared to using pinch analysis alone. The total site analysis method presented by Dhole and Linnhoff (1993) and Klemes et al. (1997) are also used for steam cycle design, but they are geared mainly for cogeneration and do not take into account the sensible heating in the production and use of steam which is a significant proportion of the heat in a power station. Kapil et al. (2010) and Botros and Brisson II (2010) included the sensible heat required for the steam production. They calculated the mass flowrates through the steam cycle using a bottom-up or iterative procedure. The methodology used in this paper and described in the following sections includes the sensible heat in both the generation and use of steam and uses linear programming to automatically calculate the mass flowrates that maximise the power from the steam turbine. This method follows on from an earlier Journal of Cleaner Production article by Harkin et al. (2010) that used the pinch analysis fundamentals to determine systematically the possible benefits that the heat integration may have in reducing the energy penalty due to the addition of CCS. That paper determined the optimum steam extraction rates from the steam turbine to minimise the energy penalty of the addition of CCS to an existing power station using a linear programming algorithm. By using pinch analysis incorporating both the details of the power station and the CCS equipment the heat from the CCS plant can be incorporated back into the steam cycle. Khalilpour and Abbas (2011) have also used pinch analysis for PCC and also concluded that the energy penalty can be reduced using pinch analysis. However, they restricted their analysis to the cold end of the power station as "it is obvious that hot boiler streams should be paired with combustion gases". Whilst this may be true, it is possible that the boiler feed water temperature can be increased with the additional heat available in the capture and compression process and therefore the importance of varying the steam flowrates throughout the steam cycle, not just the steam extraction rates, can be important. The linear programming algorithm described in Harkin et al. (2010) has been modified to enable

the optimisation of the steam rates throughout the steam cycle, as explained in more detail in section 2.1 and the Appendix.

Due to the multiple, often conflicting, objectives that will exist when designing a power station with CCS the optimum setting of a specific operating variable or design scheme may not be certain until a full analysis of the system is completed. For example: the solvent stripper pressure will have impacts on the amount of heat required for solvent regeneration, the temperature of the heat required, the CO₂ compressor power and the related capital costs. Changing the stripper pressure will have conflicting impacts that will be desirable for some objectives and negative for others and therefore the optimum pressure is not immediately apparent. Multi-objective-optimisation (MOO) enables the optimisation of two or more objectives that may not be directly related and is often best utilised when the objectives are antagonistic. For example, when designing a power station, design changes that increase the efficiency will often also increase the capital cost of the power station, therefore MOO will determine a range of non-dominated options from small improvements in efficiency with minimal capital cost increases to large improvements in efficiency with large increases in capital costs.

Between 2000 and 2008 over 80 articles were written on MOO for use in chemical engineering applications (Lee et al., 2008), an overview of MOO and how it is applied to chemical engineering systems is provided by Rangaiah (2009). More recently MOO was used by Harkin et al. (2011) to illustrate the value of using MOO for the optimisation of power stations with CCS by illustrating the importance of both heat integration and optimising the power stations and the CCS operating parameters as a whole system. The following work extends on the basic optimisation of the energy penalty by including the optimisation of more operating variables and including the cost estimation of the proposed equipment. Bernier et al. (2010) utilised a similar approach with mixed integer linear programming algorithm to optimise the steam cycle combined with MOO for the optimisation of Natural Gas Combined Cycles with CCS. They optimise the CCS plant and steam cycle to minimise the global warming potential of the power station using a life cycle analysis whilst trying to minimise the power station COE.

2. Methodology

The methodology used in this paper for the design of power stations with CCS involves a combination of simulation, automated

heat integration using linear programming, cost estimation and MOO, the calculation sequence is depicted in Fig. 2. Bhutani et al. (2007) combined commercial simulation packages with a MOO program, whilst Harkin et al. (2011) shows how the addition of automated heat integration can benefit the optimisation of carbon capture technologies added to power stations. This paper adds the step of cost estimation in the overall optimisation scheme. This has been incorporated into the proprietary software/methodologies that have been developed to optimise the performance of fossil fuel industries on the addition of CCS equipment. Heat integration has the benefit of not needing to design the heat exchanger network prior to completing the design, but is disadvantaged by requiring the specification of the minimum approach temperature between the streams in a process to be defined to determine the minimum energy targets. When MOO is combined with heat integration, the minimum approach temperature can be varied, amongst a range of other operating variables, and therefore the trade-off between the energy savings of small approach temperatures and the additional capital costs can be taken into account alongside the other process modifications being investigated. This approach allows the optimisation of many parameters at once so that design changes can be reviewed for a given solvent and power station by comparing all the results on an optimised basis.

2.1. Simulation and heat integration

The power station (represented by the simplified diagram in Fig. 3) and the CCS plant (represented in Fig. 1) are modelled using Aspen Plus[®]. The simulation is used to develop heat curves of the process streams for the given design and operating variables that are specified in the simulation; the heat exchangers are modelled as simple heaters and coolers because at this stage of the design, the form of the heat exchanger network is not assumed, instead the targets for the best heat integration arrangement will be shown by the subsequent heat integration step. The temperature-enthalpy relationship (heat curves) of the streams that provide or require heat are automatically extracted into an Excel[®] based heat integration program. The heat integration program is a proprietary program that has been developed to import/extract data using Microsoft's Visual Basic via ActiveX automation from Aspen Plus[®]. Data is extracted from the heat curve results of selected heat exchangers or the reboiler and condensers associated with Radfrac columns. The program uses the heat curves of all the hot and cold streams in the power station (excluding the steam cycle) and the CCS equipment to generate grand composite curves (GCC) of the process using the problem table algorithm (Linnhoff and Flower, 1978). The GCC of a power station, excluding the steam cycle, represents the amount of heat that is available for use in the steam cycle at any given temperature, and therefore it is possible to design an optimum steam cycle for any given GCC.

The details of the structure and conditions of the steam cycle are added to the Excel[®] program; this could be a new steam cycle or an existing steam cycle in the case of a CCS retrofit. The heat integration program then determines for the steam cycle provided, the maximum amount of power that can be generated from the power station GCC, by constructing a steam composite curve (SCC) under

the GCC (refer to Fig. 4). The SCC is the equivalent of the GCC for the steam cycle, including the heat required to generate the steam and the heat available from steam extracted from the turbine. For a given steam cycle with defined steam pressures, both the amount of heat required for the steam generation/use and the amount of power generated by the steam turbine are linear. Therefore, the rates of steam generated/used at each level to maximise the net power produced from the steam turbine can be determined using a simplex algorithm. The method is described in more detail in Harkin et al. (2010), however in that paper the linear algorithm is to optimise the extraction steam rates, in this paper the linear programming equations allow the steam cycle, both generation and extraction rates to be optimised. The details of the linear model are provided in the Appendix.

2.2. Cost estimation

2.2.1. Capital cost estimation

Estimations of the capital and operating costs of the CCS infrastructure can be conducted once the heat integration step has been completed; the costs include all new equipment required for the addition of CCS and include costs for turbine modifications and the heat exchanger network that will be required to provide the maximum amount of power from the power station.

The capital costs of the equipment are based on the results obtained from the simulation and heat integration program. The cost functions used for the main equipment are provided in Table 1, where some of the functions are based on curves fitted from data found in the references. The cost for the steam turbine is based on the full replacement costs; in reality there may be significant savings due to being able to re-use significant parts of the turbine or at least the turbine auxiliaries. The compressor knock-out drums, and stripper separator are assumed to be constructed from 304 stainless and the cost is based on vessel mass and pressure. The vessels are sized using the K-factor method from Gas Processors Suppliers Association (1998). The absorber and stripper are also sized based on the metal mass of the vessels. The heights of these columns are based on one and a half times the packing height and the diameter is calculated in the simulation based on the specific packing specified in the simulation. These columns have a maximum size of 12.8 m in diameter; therefore multiple columns will be used when diameters greater than 12.8 m are required. The thicknesses of all vessels are calculated based on guidelines of AS1210 (Standards Australia Limited, 2010). The cost estimation for the pumps, fans and compressors are based on the flowrates, power and capacity factors, the details of which can be extracted from the Aspen Plus[®] simulation.

The heat exchanger network costs are estimated based on the estimated area of the required network as per the method described by Smith (2005). The area is estimated using the balanced composite curves, which are the hot and cold composite curves of the process and utilities, the utilities in this example being the steam cycle and cooling water. The balanced composite curves are divided into vertical enthalpy intervals and the contribution of the heat duty divided by the film coefficients ($q_{i,k}/\delta_i$) of each hot and cold stream are multiplied by the logarithmic mean temperature

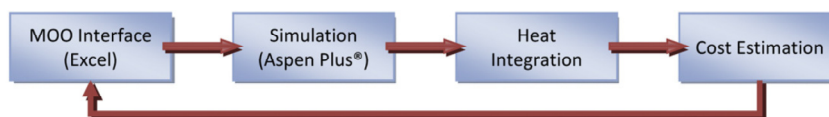


Fig. 2. Optimisation approach for power stations with CCS.

Please cite this article in press as: Harkin, T., et al., Optimisation of power stations with carbon capture plants – the trade-off between costs and net power, Journal of Cleaner Production (2012), doi:10.1016/j.jclepro.2011.12.032

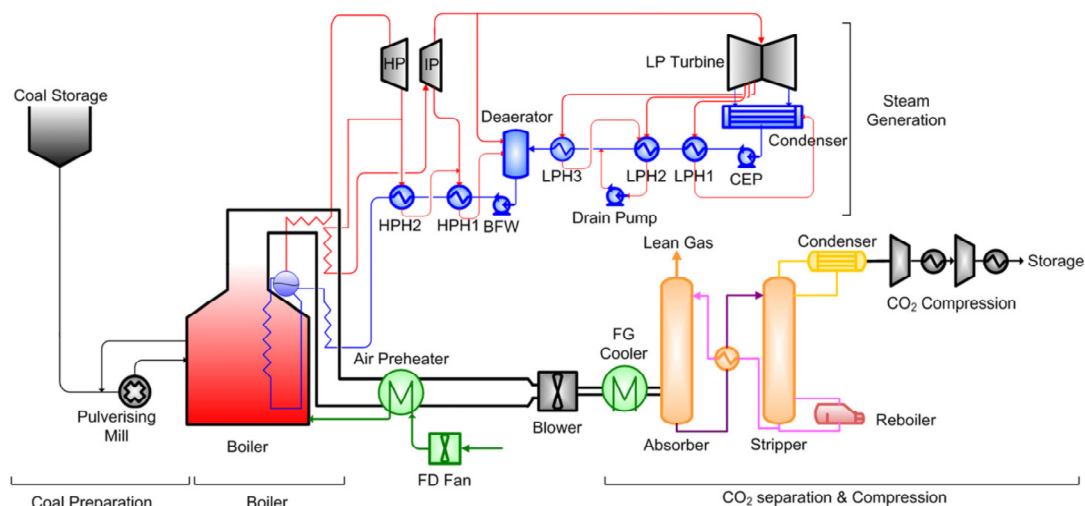


Fig. 3. Process diagram of a typical Victorian coal fired power station.

duty of the enthalpy interval to determine the area of that enthalpy interval. The summation of the area intervals provides an estimate of the total area required. In the case of retrofits, the contribution of the existing area is subtracted from the total area using the same methodology to determine the new area required. The number of heat exchangers that are required (N) is estimated as equal to the number of process streams that are involved in the heat integration.

The purchased costs of the process equipment are used to estimate the total capital costs using the CO2CRC costing factors as described by Allinson et al. (2006). In this example, the total capital costs using the CO2CRC costing factors are 180% of the purchased costs.

2.2.2. Operating costs

The operating costs are also based on the CO2CRC costing methodology described by Allinson et al. (2006). The fixed costs including insurance and maintenance costs are taken as 6% of the total capital costs. The fixed labour costs are determined on the

basis of two operating personnel and one maintenance person on shift using a five shift roster. The supervision costs increase the labour costs by 20% and the administration and general overheads by a further 30% at a nominal individual cost of \$82 000 per year based on the salaries provided by IEA-GHG (2006). Variable costs for the plant include costs for cooling water, process make-up water, and chemical replacement costs. The capital cost for new cooling towers is including by assuming an annual capital charge for the cooling water.

The CO₂ storage costs are included as an operating cost at 5.8 dollars per tonne of CO₂ stored. The storage cost is taken from Hooper et al. (2005) which is based on the assumption of large scale aggregated transport and storage. The reduction of power from the power station is included as an operating cost at the rate of the difference in the nominal power station output without CCS and with CCS assuming a current wholesale price of electricity of 40 \$/(MW h) as per Dreher et al. (2011).

2.2.3. Net present value

The capital and operating costs are used to determine the net present value of the project assuming two years of construction, an operating life of 25 years and a year of decommissioning that costs 25% of the total capital costs of the project. A discount rate of 7% is assumed for the life of the project. The differential cost of electricity (DCOE) is calculated as the present value of the total costs divided by the present value of the electricity production ($DCOE = NPV_{TotalCosts} / NPV_{NetElectricity}$) as per Allinson et al. (2006).

2.3. Multi-objective optimisation

The results are analysed using a MOO program to determine the optimal solutions. The NSGAII (Deb et al., 2002) genetic algorithm is used for the MOO, utilising an Excel based version of the algorithm developed by Sharma et al. (2011). As explained in the introduction, MOO allows the trade-off to be analysed between two or more competing objectives. The genetic algorithms commonly used in MOO require defining a population number and a number of generations. The population number sets the number of individual

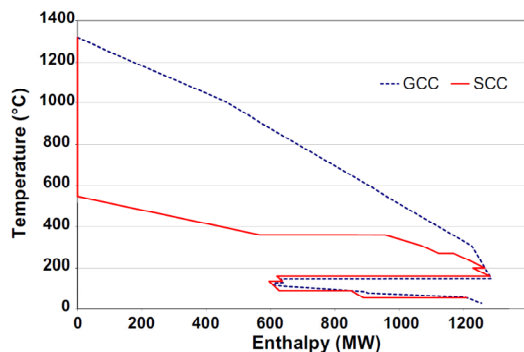


Fig. 4. Output of the heat integration program to determine the steam cycle shown by the SCC, to maximise the net power for the given GCC of the power station with CCS.

Please cite this article in press as: Harkin, T., et al., Optimisation of power stations with carbon capture plants – the trade-off between costs and net power, Journal of Cleaner Production (2012), doi:10.1016/j.jclepro.2011.12.032

Table 1
CCS equipment purchase cost functions.

Equipment	Currency (C_b)	Year (Y_b)	Capital cost function (\$A(2008))	Reference
Forced draft fan	0.55	396	$\left(\frac{1}{C_b}\right) \left(\frac{575}{Y_b}\right) (341Q_{FD} + 1696)$	Peters et al. (2003)
Solvent and boiler feed water pumps	0.55	396	$\Phi < 200 : \left(\frac{1}{C_b}\right) \left(\frac{575}{Y_b}\right) \times 10^{[2.5+3.26\log(\Phi)-2.37\log(\Phi)^2+0.62\log(\Phi)^3]}$ $\Phi > 200 : \left(\frac{1}{C_b}\right) \left(\frac{575}{Y_b}\right) \times 265280 \times (Q_p/0.372)$	Peters et al. (2003) Furukawa and Bartoo (1997)
CO ₂ Compressor	0.55	396	$\left(\frac{1}{C_b}\right) \left(\frac{575}{Y_b}\right) \times 873 \times p_c^{0.9438}$	Peters et al. (2003)
Steam turbine	0.55	396	$\left(\frac{1}{C_b}\right) \left(\frac{575}{Y_b}\right) \times 10^{[1.93778+1.45483\log(P_{ST})-0.08838(P_{ST})^2]}$	Girardin et al. (2009)
Compressor knock-out drums, stripper separator, absorber and stripper.	0.55	396	$\left(\frac{1}{C_b}\right) \left(\frac{575}{Y_b}\right) \times 73 \times (0.091p^{0.849} + 0.83) \times \psi^{0.66}$	Peters et al. (2003)
Heat exchangers	0.76	500	$\left(\frac{1}{C_b}\right) \left(\frac{575}{Y_b}\right) \times 7038 \times N(A/N)^{0.7948}$	Girardin et al. (2009)

cases that are studied for each generation. For the first generation, the values of all the operating variables that are specified to be optimised are randomly selected from a given range of values. The objectives are then analysed for each individual and at the conclusion of each generation the individuals are ranked according to how they compare to the other individuals with respect to all of the objectives. The ranking is first based on the individuals Pareto dominance followed by the crowding distance assignment, for more details refer to Sharma et al. (2011). The values of the operating variables for subsequent individuals are generated by combining the values of two of the best individuals from previous generations. The best results from all the generations are referred to as the Pareto optimal front, where the solutions given in this front are non-dominated by any other individuals with respect to all of the objectives. An example of the Pareto front can be seen for the case study provided in the following sections in Fig. 5.

3. Case study description and results

The methodology described in Section 2 is applied to a brown coal fired power station, typical of those found in Victoria, Australia. Victorian brown coal has high moisture content of 60% mass fraction, however it is easily mined and therefore due to the low cost of coal production, the power stations have been designed with low capital costs and low efficiencies to minimise the COE. The low

sulphur coal found in this region also means that the power stations do not require desulphurisation equipment.

The CO₂CRC has been investigating the use of potassium carbonate for CO₂ capture from power stations as it has many potential advantages over more commonly used amine based solvents; including low volatility, lower cost, lower rates of degradation and the ability to absorb the incoming SO_x and NO_x compounds and form potentially useful potassium sulphates and nitrates avoiding the need for additional equipment for removal of the SO_x and NO_x. However, with the traditional 30% mass fraction potassium carbonate process when used in low CO₂ partial pressure as with post-combustion capture, the drawbacks include low kinetic rates of reaction without the use of promoters and the process will generally require more regeneration energy than amine based solvents. Precipitating potassium carbonate solvent systems promise to overcome both the kinetic and energy drawbacks of the potassium carbonate system for post-combustion capture. However as the simulation models for the precipitating system are under development this case study looks at the traditional 30% mass fraction potassium carbonate solvent with rate promotion.

This case study considers a nominal 500 MW electrical power station prior to the addition of the CCS equipment. The captured CO₂ will be compressed to 100 bar for transport. The simulation includes the coal combustion, flue gas cooling, air-preheat and CO₂ compression all modelled using the Peng-Robinson equation of state with Boston-Mathias modifications using a lignite coal with a heat of combustion of 26249 kJ kg⁻¹ dry coal. The potassium carbonate system is modelled using the electrolyte NRTL model and the absorber and stripper are modelled using rate-based Radfrac columns. The absorption model is based on the model produced by Aspen Technology Inc. (2008) with the electrolyte pair parameters adjusted as per Endo et al. (2011). The rate limiting reaction of carbon dioxide and hydroxide to form bicarbonate is also considered to be an equilibrium reaction rather than a kinetic reaction to account for the addition of the rate promotion in the system. The absorber and stripper are modelled with 20 stages of 38 mm IMTP packing. The steam cycle in this optimisation problem is set with a main steam flowrate equal to the existing main steam rate to minimise the changes to the existing power station. When the potassium carbonate based CCS equipment capturing 90% of the CO₂ is retrofitted to the power station, without consideration of heat integration or optimisation, the net power from the power station is reduced to 310 MW electrical, a 38% reduction in net power.

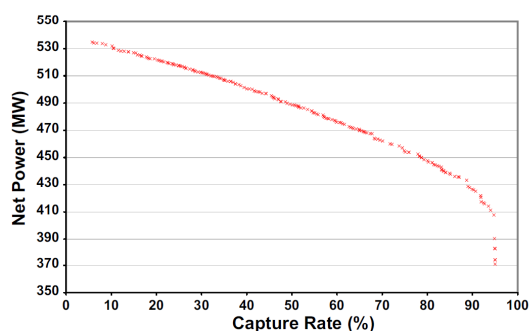


Fig. 5. Pareto optimal solutions for the net power generation versus CO₂ capture rate (Opt. 1).

Please cite this article in press as: Harkin, T., et al., Optimisation of power stations with carbon capture plants – the trade-off between costs and net power, Journal of Cleaner Production (2012), doi:10.1016/j.jclepro.2011.12.032

In this paper, two optimisation problems have been performed and each problem had two objectives detailed below. For each optimisation there were nine variables that were optimised which are detailed in Table 2. In each case one objective is to maximise the CO₂ capture rate, which is the mass fraction of CO₂ separated from the flue gas. The second objective is to either maximise the net power generated by the power station, which consists of the power generated by the steam turbine minus the power loads of the auxiliaries, or to minimise the DCOE as calculated using a net present value analysis.

- Opt. 1: Maximise the CO₂ capture rate and maximise the net power generation.
- Opt. 2: Maximise the CO₂ capture rate and minimise the differential cost of electricity (DCOE).

For each of the two optimisation problems a population of 200 individuals were used in the optimisation. The NSGAI algorithm was used for 50 generations in which time the Pareto front was well established. The Pareto front for the first optimisation is provided in Fig. 5 whilst the Pareto front for the second optimisation is given in Fig. 6. The individual solutions that make up the Pareto front can then be used to calculate a range of other indicators that can be plotted as a function of the CO₂ capture rate, such as the cost of CCS (Fig. 7), the energy penalty (Fig. 8), the DCOE (Fig. 6) and the capital cost of the heat exchanger network (Fig. 9). The values of the optimisation variables can also be plotted as a function of the capture rate and thus enable the designer to determine the optimum value of those variables over a range of capture rates (See Figs. 10–12).

4. Discussion

4.1. Optimisation 1 – maximise net power

Fig. 5 shows the Pareto front for the first optimisation problem and represents, for the given capture technology and the given parameters, the maximum power that can be generated for the power station with the addition of CCS. As would be expected, Fig. 5 shows that an increase in the CO₂ capture rate will lead to reductions in the net power produced by the power station. This is due to the increase in the heat required for solvent regeneration and power for the CO₂ compression and auxiliaries with the increase in the amount of CO₂ captured. The individual optimised solutions that make up the Pareto front and are shown in Fig. 5 can be used to estimate the cost of CCS for a given capture rate when optimising for maximum power. These results are shown by the “x” marks in Fig. 7. The cost of CCS decreases as the capture rate increases, with

Table 2
List and range of variables used in both optimisation problems (Opt.1 and Opt. 2).

Variable	Unit	Range minimum	Range maximum
Solvent lean loading	mol HCO ⁺ /mol K ⁺	0.11	0.416
Solvent flowrate	kg/s	800	5910
Solvent temperature	°C	40	71.5
Absorber feed gas temperature	°C	40	71.5
Stripper pressure	bar	0.5	8.165
Stripper feed temperature	°C	70	133.5
Absorber packing height	m	10	47.5
Stripper packing height	m	10	47.5
Heat exchanger minimum approach temperature (ΔT_{min})	°C	6	36

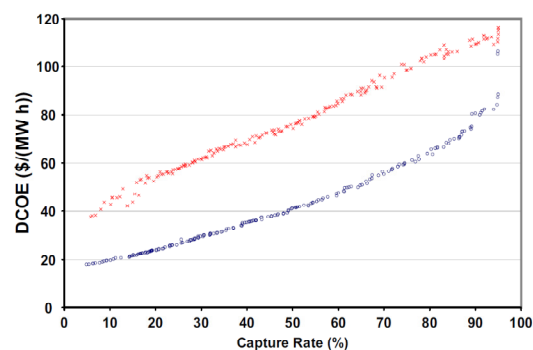


Fig. 6. Pareto optimal solutions for the minimisation of DCOE and maximisation of capture rate (Opt. 2) (○) and the DCOE for the optimal solutions in Opt. 1 (×).

a minimum cost per tonne of CO₂ avoided of close to \$100. Due to the economies of scale of the CCS infrastructure, the cost of CCS is more than halved by capturing 90% of the flue gas CO₂ compared to 10%.

A plot of the energy penalty, the ratio of the change in efficiency of the power station due to the addition of CCS relative to the efficiency of the original power station, for the optimised solutions is given in Fig. 8. Interestingly, when optimising for maximum net power, the energy penalty is negative for capture rates up to 40% of the CO₂ emissions. The energy penalty is negative because there is considerable waste heat in the power station studied and this can be used to provide the required heat for the new CCS infrastructure and/or increase the amount of steam generated, so that the power produced in the turbines can be increased. Of course, to utilise this waste heat is likely to require additional heat exchange area and modifications to the steam turbine. In reality, it is unlikely that the energy penalty in any CCS project would be negative as that would require an increase in the power generated by the electric generator and associated equipment which will usually not be rated for greater than the existing power station loads. However, it shows that there is the potential for much lower energy penalties than anticipated at low capture rates provided additional heat exchange area is supplied and the turbine can handle, or is modified to handle, the additional steam flow.

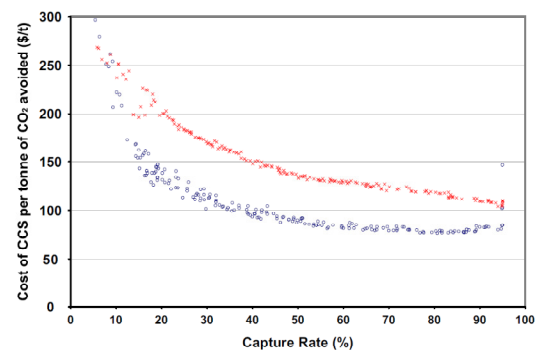


Fig. 7. The cost of CCS for the optimal solutions for Opt. 1 (×) & Opt. 2 (○).

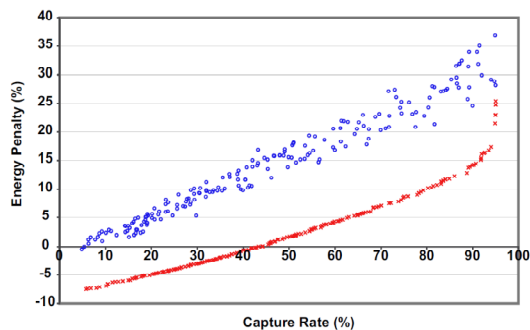


Fig. 8. Energy penalty for the optimised solutions for Opt. 1 (x) & Opt. 2 (o).

The increase in net power available at low capture rates with additional heat utilisation in this example is likely to be greater than that encountered in other regions as the low fuel costs relative to capital cost in the Victorian power sector currently favour operating at lower than the maximum efficiencies. Therefore, with additional capital the efficiencies can be increased. However, even with low or negative energy penalties at low capture rates in this case study, the cost of CCS still favours higher capture rates as shown by Fig. 7. At low capture rates, generating the maximum power still requires significant capital expenditure for the additional heat exchanger area (Fig. 9) and steam turbine modifications. At very low capture rates the capital costs for additional heat exchanger and steam turbine modifications are close to \$500M, which captures very little CO₂ and provides only 7% additional net power. Whereas, an additional \$500M in heat exchanger area will enable capture rates of up to 90%, albeit with an energy penalty of around 14%.

When optimising the CCS process conditions for maximum net power, there are two distinct stripper pressures (3.25/6 bar) that are favoured (refer to Fig. 10). The temperature of the reboiler for those two stripper pressures corresponds (including a ΔT_{\min} of 6 °C) to the condensation temperature of two of the steam turbine extraction points. Therefore, if the pressure of the steam extracted from the turbine change, then the corresponding optimal stripper pressures are likely to be different. The ΔT_{\min} of the heat exchanger network for all the optimised solutions that maximise the net

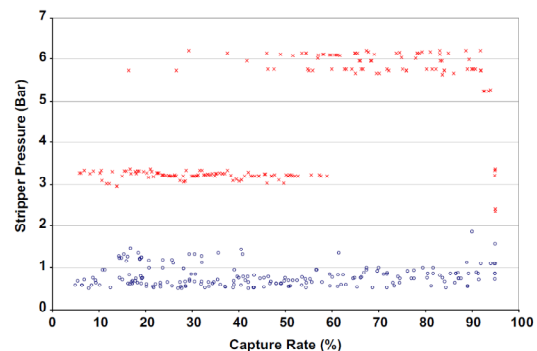


Fig. 10. Stripper pressure for the optimised solutions for Opt. 1 (x) & Opt. 2 (o).

power is (not surprisingly) at the lower bound of the variable (6 °C) as shown in Fig. 11; however, that means the heat exchanger network costs are likely to be high which is confirmed in Fig. 9. Also, to maximise the net power the majority of the solutions had the flue gas temperature at the lower end of the range (Fig. 12). By decreasing the flue gas temperature, the water content of the flue gas is reduced, which means the CO₂ partial pressure is increased and the amount of water that needs to be removed in the stripper reduces; both of which lead to reductions in the heat required for the stripper reboiler.

4.2. Optimisation 2 – minimise DCOE

The second optimisation problem aims to determine the minimum DCOE for a given CO₂ capture rate and the Pareto optimal solutions are represented by the “o” marks in Fig. 6; and obviously the DCOE increases as the capture rate increases. If a price paid for emitting the CO₂ is included in the cost estimate based on the results from the optimisation, it will be possible to determine what capture rate provides the minimum DCOE for the given price of CO₂.

The DCOE for the optimised solutions from Opt. 1 are also shown on Fig. 6 and for all capture rates the DCOE for the optimisation based on maximising the net power is greater than when it is optimised to minimise the DCOE. This suggests, that maximising the net power from the power station, in this case study, so in the

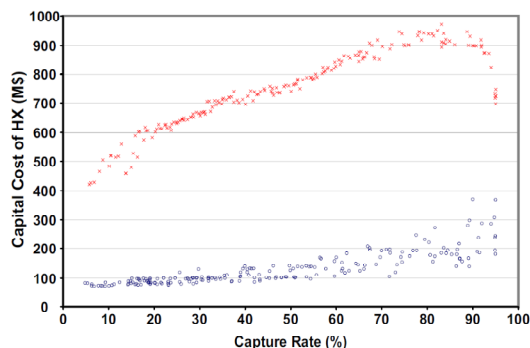


Fig. 9. The capital costs of the heat exchangers for the optimised solutions for Opt. 1 (x) & Opt. 2 (o).

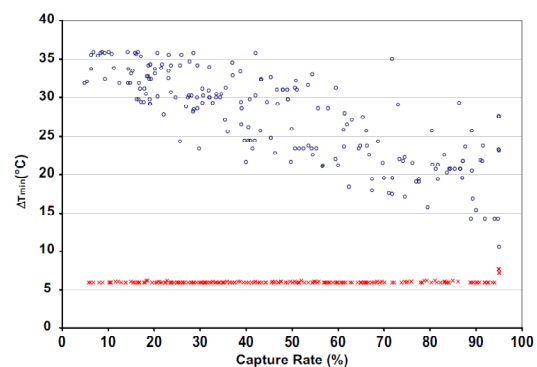


Fig. 11. The ΔT_{\min} for the optimised solutions for Opt. 1 (x) & Opt. 2 (o).

Please cite this article in press as: Harkin, T., et al., Optimisation of power stations with carbon capture plants – the trade-off between costs and net power, Journal of Cleaner Production (2012), doi:10.1016/j.jclepro.2011.12.032

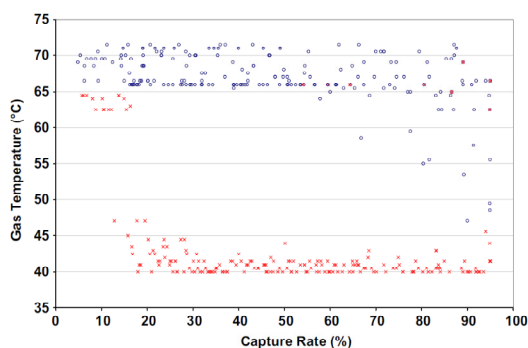


Fig. 12. The flue gas temperature for the optimised solutions for Opt. 1 (x) & Opt. 2 (o).

Victorian context, does not provide the most inexpensive power. This is confirmed by the energy penalty for the two optimised solutions (Fig. 8). The energy penalty when trying to minimise the DCOE is consistently more than ten percentage points greater than for the solutions when optimising for net power.

As a consequence of the second optimisation which minimises the DCOE, the cost of CCS is also less expensive than when compared to maximising the net power. As shown in Fig. 7 the Opt. 2 results, when optimising to minimise the DCOE, are generally around \$50 per tonne of CO₂ less than for Opt. 1 when optimising for net power. The cost of CCS curve for the Opt. 2 results is quite flat between capture rates of 50% and 90% with the cost per tonne of CO₂ avoided between \$76 and \$85 over that region, with the minimum cost at a CO₂ capture rate of 80%.

The main contributor for the higher DCOE when trying to maximise the net power is the increase in the capital costs for the infrastructure to maximise the power generation, in particular the heat exchanger network (Fig. 9). The increase in capital costs also have a flow on effect for the maintenance costs, which are estimated as a proportion of the capital costs of equipment.

4.3. Optimal ΔT_{\min}

The ΔT_{\min} for the heat exchanger network has a large impact on the capital costs of the network and therefore the ΔT_{\min} when optimised to minimise the DCOE tends to values greater than lower limit. As shown in Fig. 11, the ΔT_{\min} for the optimised solutions ranges from 10 °C to 36 °C. This is clearly in contrast to the results from the first optimisation study where the majority of solutions were close to the lower limit of 6 °C. Although the solutions from the second optimisation do not provide a clear optimum ΔT_{\min} there is a definite trend that as the capture rate is increased, the optimum ΔT_{\min} decreases. This study used a single ΔT_{\min} for all types of streams. As the addition of CCS to power stations requires integration of streams with low heat transfer coefficients, like the flue gas, and those with high heat transfer coefficients, like condensing steam, it may be possible to reduce the heat exchanger costs by using different ΔT_{\min} for different types of streams. The economic optimum for those streams with low heat transfer coefficients is usually greater than for those streams with higher heat transfer coefficients.

4.4. Optimal stripper pressure

To minimise the DCOE the majority of the optimised solutions have a stripper pressure between 0.5 bar and 1.5 bar (Fig. 10), which

is significantly lower than the 3 bar–6 bar pressures obtained when optimising the net power. The reason for this can be explained by the use of one of the optimal solutions, 80% capture with a stripper pressure of 0.86 bar, and comparing the results of this solution to the same solution with a stripper pressure of 3 bar. The DCOE increases from 63.5 to 74.5 \$/(MW h) due to the increase in stripper pressure. For potassium carbonate systems, lower stripper pressures reduce the regeneration energy requirements, but obviously increase the compressor power requirements. The trade-off in energy between the two often results in only marginal differences in net power as shown in Harkin et al. (2011). However, as the ΔT_{\min} increases, the steam extraction temperature for the same stripper pressure increases and therefore the power lost from the turbine increases while the power used in the CO₂ compressor stays the same. Therefore, lower pressures appear to be favourable with higher heat exchanger approach temperatures. As both the reboiler and steam condensation have relatively high heat transfer coefficients the area penalty for reducing the ΔT_{\min} on those services is likely to be small, once again this suggests that a single ΔT_{\min} may limit the optimal design. In addition to the increase in costs for increases in stripper pressure due to the additional energy penalty, as the stripper pressure is increased the lean and rich solvent heat exchanger duties also increase. Therefore the heat exchanger area and costs for the lean and rich heat exchangers will also be greater.

4.5. Optimal flue gas temperature

Another difference between the results of the two optimisation problems is the optimal flue gas temperature (Fig. 12). In the first optimisation, when maximising the net power, the flue gas tended to the lower limit, around 45 °C. Whereas, when trying to minimise the DCOE, the majority of the flue gas was cooled to only 65 °C–70 °C. The dew point of the flue gas is 65 °C and therefore there is a large increase in the cooling requirement, and therefore heat exchanger area, to lower the temperatures below 65 °C. This can be shown by comparing the results from a case that represents an optimum solution at 80% capture which will therefore have a relatively high flue gas temperature of 66 °C with the same case, but with a flue gas temperature of 45 °C. If the values of all other variables are kept constant then the case with 45 °C will have a higher capture rate (~90%) and therefore will suffer higher CO₂ compression power penalties. Therefore to compare the cases on a more even basis, the solvent flowrate is also lowered in the second case to maintain an 80% capture rate. The values of the variables used in the two cases are provided in Table 3 and the important results from the cases are shown in Table 4.

The DCOE for the case with 45 °C is higher than that for the case with 66 °C by close to 5 \$/(MW h). The main contributor to this difference is due to the additional area for the cooling of the flue

Table 3
Values for the decision variables to compare the impact of the flue gas temperature.

Variable	Unit	Case 66 °C	Case 45 °C
Solvent lean loading	mol HCO ⁺ /mol K ⁺	0.207	0.207
Flue gas temperature	°C	66	45
Solvent flowrate	kg/s	4530	3400
Solvent temperature	°C	60	60
Stripper pressure	bar	0.86	0.86
Stripper feed temperature	°C	73.5	73.5
Absorber packing height	m	20	20
Stripper packing height	m	37.5	37.5
Heat exchanger minimum approach temperature (ΔT_{\min})	°C	21.3	21.3

Table 4
Results comparing the impact of flue gas temperatures on cases at 66 °C and 45 °C.

Result	Unit	Case 66 °C	Case 45 °C	Case 45 °C with DCC
CO ₂ capture rate	%	80.5	80.9	80.9
Total flue gas heat	MW	1505	1750	1750
Reboiler duty	MW	641	493	493
Gross power	MW	460	487	487
Net power	MW	368	395	395
Total capital cost	MS	611	841	648
Total purchased cost	MS	341	469	362
HX purchased cost	MS	177	309	192
Total operating cost (incl. storage and Lost Power)	MS/y	118	124	112
Fixed operating and maintenance Costs	MS/y	37	50	39
Cost for lost power	MS/y	39	31	31
DCOE	\$(/MW h)	63.5	68.4	58.5

gas. Cooling to 45 °C requires an additional 250 MW of cooling, which is estimated to increase the total heat exchanger area from $2.7 \times 10^5 \text{ m}^2$ to $4.0 \times 10^5 \text{ m}^2$. Of the additional $1.3 \times 10^5 \text{ m}^2$ of area, $1.27 \times 10^5 \text{ m}^2$ can be attributed to the flue gas side of the heat exchanger due to the low heat transfer coefficients on the flue gas side. Therefore any mechanism to reduce this area may reduce the costs of the CCS project. As this cooling duty is invariably below the process pinch point (invariably located at the stripper reboiler temperature), there is unlikely to be a large energy penalty from direct contact cooling (DCC). DCC's have been suggested in most solvent studies to not only provide the final cooling, but to also remove dust and potentially sulphur upstream of the absorber. With a DCC the amount of cooling that needs to be performed will not change considerably, however the heat exchangers required for the cooling will be between the recirculating DCC cooling medium and utility cooling water (the benefits of air cooling are not assessed in this work). Therefore, the cooling duty will be the same, however the heat transfer coefficients for the DCC cooling medium will be higher than flue gas, but the approach temperatures in the heat exchangers will be lower. The result is likely to be an area requirement of approximately $2.85 \times 10^5 \text{ m}^2$ in total. However additional costs for the DCC will also need to be factored in. Assuming a purchased cost of 10 MS for the DCC, the increase in the net power produced by the low flue gas temperatures compensates for the additional expense of the DCC and leads to a reduction in the DCOE (refer to Table 4) by approximately 5 \$(/MW h).

4.6. Review of technique

The combination of simulation, automated heat integration, cost estimation and MOO has a number of advantages but also a number of drawbacks that need to be considered. MOO using genetic algorithms cannot ensure a global optimum is found, however given the non-linear relationship of many industrial applications the stochastic nature of the method enables a good search of optimisation space. Combining simulation with MOO enables the construction of rigorous models of the process using well known commercial process simulators. There are many benefits to having a rigorous model for optimisation but if the simulation is not well defined and does not converge rapidly then the computation time for optimisation can be lengthy. When MOO and simulation are combined with heat integration and cost estimation the optimisation includes details on the thermodynamics and economics of the process and allows trade-offs between the two to be evaluated. In this case study, being able to optimise the multiple variables with many impacts on both the power produced by the power station

and the costs of generating that power was seen by the authors to far outweigh the computational time for each optimisation (~24 h) problem. Moreover, the benefits of being able to determine what variables have the biggest influence on the objectives and their settings helps the designer to finalise a practical design with confidence. Additionally, it could enable competing technologies to be compared, taking into account both the thermodynamics and economics of the systems.

5. Conclusion

The addition of a CCS plant to a typical Victorian brown coal fired power station capturing 90% of the CO₂ in the flue gas without heat integration or optimisation had an energy penalty of 38%, whereas the minimum energy penalty can be as low as 14%–16%. However to minimise the DCOE and consequently the cost of CCS, the optimum energy penalty is likely to be between these values at approximately 25%–30%.

The combined heat integration and optimisation approach is a useful way of determining the estimated maximum net power generation possible from a power station with the addition of CCS and even more importantly the cost of CCS and the DCOE. The optimisation technique allows the designer to determine quickly the optimum setting for a range of variables. It also directs the designer to what variables are important and why they are important and provides insight to the designer that may enable cost reductions to occur. In the example provided, a significant proportion of the estimated cost is due to the flue gas heat exchanger. These costs may be reduced with the use of a DCC and therefore the net power can be kept as high as possible by keeping the flue gas temperature low, whilst minimising the costs for the heat exchanger to do so. The results also showed that larger minimum approach temperatures in the heat exchangers lead to a more cost effective solution, but an even more cost effective solution may be found using different approach temperatures for different services.

The combination of heat integration, cost estimation and optimisation will be useful at the early stages of process design to screen options and also further in the design to optimise the operating values of solvent plants for specific power stations. This methodology is widely applicable to any and all CCS applications and will provide directions for optimising operational strategies for low emission fossil fuelled industries. The techniques are equally applicable to new and retrofit solutions and may well lead to different outcomes based on a range of project specific combinations such as plant efficiencies, fuel cost, capital cost profile and CCS technologies employed.

Acknowledgement

The authors acknowledge the funding to support this research provided by the Australian Government through its CRC Program and the Victorian Government through its ETIS Brown Coal R&D program.

Appendix. Linear model to maximise the power generation

A linear programming model is used to determine the maximum amount of power that can be generated with a given steam cycle from the available heat represented by the GCC of a process. This method is useful for the design of new steam turbines and/or existing steam turbines, however it assumes that the efficiency of the steam turbines does not change with the amount of steam that is generated or extracted from each stage of the turbine and therefore for existing turbines modifications to the

turbine may be required for this to be accurate. A steam turbine model, with three steam mains and a single stage of reheat is provided in Fig. 13 for reference (the model in this paper actually has seven steam levels but only three levels are shown here for simplification). For this method to work, obviously there needs to be net heat available in the process, this can be seen by generating the GCC for the power station (excluding the steam cycle) and the CCS process. The next task in determining the energy targets of the process is to provide the details of the steam cycle; including the main steam pressure and temperature (P_1 and T_1), the reheat temperature for any reheat stages (T_{R2}), the pressure of all the steam headers including the last condensing stage (P_2 to P_n), any pressure drops in the heat exchangers and the efficiency of each stage of the turbine.

Once the details of the steam cycle are determined or assumed, the power generated by steam through each stage of the steam turbine can be calculated by multiplying the flowrate of steam for the given stage of the turbine by the specific amount of work that the steam will generate, as represented by Equation (1).

$$W_{i,i+1} = F_i \cdot \eta_{i,i+1} (H_i - H_{isen}(P_{i+1}, S_i)) \quad (1)$$

Therefore the total amount of power that is generated by steam at level i is calculated by the summation of the power produced through each steam turbine from level i to the condensing stage (stage n) as per equation (2).

$$W_{i,n} = F_i \sum_{i=1}^{i=n-1} \eta_{i,i+1} (H_i - H_{isen}(P_{i+1}, S_i)) = F_i \omega_i \quad (2)$$

If steam is extracted/used at any stage that steam will no longer produce power and therefore the contribution of that steam needs to be subtracted from the total power calculation, which is accounted for, by subtracting the flowrate of steam extracted (f_i) as per equation (3).

$$\begin{aligned} W &= \sum_{i=1}^{i=n-1} (F_i - f_i) \sum_{i=1}^{i=n-1} \eta_{i,i+1} (H_i - H_{isen}(P_{i+1}, S_i)) \\ &= \sum_{i=1}^{i=n-1} (F_i - f_i) \omega_i \end{aligned} \quad (3)$$

Equation (3) calculates the amount of power that will be generated for a given rate of steam generated and extracted at each steam level. Therefore this is the value that we are trying to maximise using linear programming. As can be seen from the equations (1)–(3), provided that the steam pressure levels are pre-

defined then equation (3) is linear. The next stage of determining the steam turbine energy targets is to add the thermodynamic constraint to the linear programming problem. The thermodynamic constraint is that steam can only be generated where there is a net surplus of heat in the process. This can be evaluated by generating steam composite curves (SCC) which must be less than or equal to the energy in the GCC at every temperature. The SCC is generated by determining the amount of energy (ΔH_i) required to generate the F_i kilograms of steam and the amount of energy (Δh_i) that can be used by the f_i kilograms of steam extracted from the steam turbine. Firstly a list of all the temperatures that make up the GCC is generated (referred to as t_0 to t_{\max}). Then for each steam level the energy difference between the steam in the steam header, and the steam/condensate at each temperature on the list, is calculated (Refer to equations (4) and (5)). When the steam header occurs upstream of a re-heater, the energy required by the re-heater is included in the energy of the steam. For steam generation, the enthalpy is calculated at a temperature $\frac{1}{2} \Delta T_{\min}$ above the actual temperature of the steam. The GCC temperatures already take into account a decrease of the hot streams by $\frac{1}{2} \Delta T_{\min}$, so when the two are combined, a total of ΔT_{\min} is taken into account. Likewise the enthalpy of the steam that is extracted from the turbine and used for heating is calculated at a temperature $\frac{1}{2} \Delta T_{\min}$ greater than the actual temperature.

$$\Delta H_{i,t} = H_i - H_{i,t} \quad (4)$$

$$\text{If } i \text{ includes reheat and } t > T_{R1} \text{ then: } \Delta H_{i,t} = H_i - H_{i,t} + H_{i,R2} - H_{i,t}$$

$$\Delta h_{i,t} = h_i - h_{i,t} \quad (5)$$

$$\text{If } i \text{ includes reheat and } t > T_{R1} \text{ then: } \Delta h_{i,t} = h_i - h_{i,t} + h_{i,R2} - h_{i,t}$$

The SCC is therefore the list of net heat required by the steam cycle at every temperature and is created by the summation of energy for the generation and extraction of each steam level at every temperature as defined by Equation (6).

$$\forall t = t_0 \text{ to } t_{\max} : \sum_{i=1}^{i=n} (F_i \Delta H_{i,t} - f_i \Delta h_{i,t}) \leq H_{GCC,t} \quad (6)$$

One further constraint is added that the steam extracted from the turbine must clearly be no larger than the net steam generated in the stages upstream, ie. the steam must have been generated before it is able to be used (Refer to equation (7)). Determining the turbine energy targets is therefore a constrained linear programming problem as defined by equations (3), (6) and (7).

$$\text{Maximise } W = \sum_{i=1}^{i=n-1} (F_i - f_i) \omega_i \quad (3)$$

$$\text{Subject to } \forall t = t_0 \text{ to } t_{\max} : \sum_{i=1}^{i=n} (F_i \Delta H_{i,t} - f_i \Delta h_{i,t}) \leq H_{GCC,t} \quad (6)$$

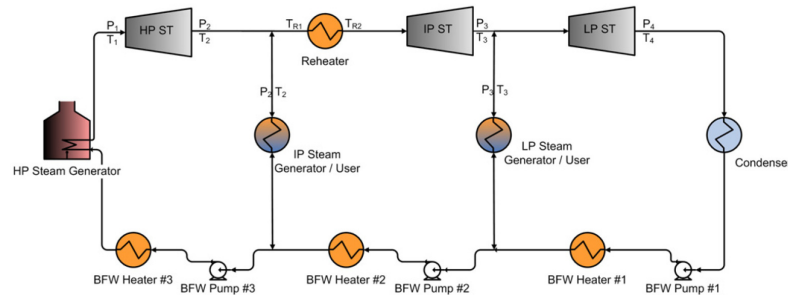


Fig. 13. Steam turbine with three pressure levels and a single stage of reheat.

Please cite this article in press as: Harkin, T., et al., Optimisation of power stations with carbon capture plants – the trade-off between costs and net power, Journal of Cleaner Production (2012), doi:10.1016/j.jclepro.2011.12.032

$$\forall i = 1 \text{ to } n : \sum_{i=1}^{i=i} (F_i - f_i) \geq 0 \quad (7)$$

The maximum steam turbine energy targets can then be solved using linear programming, producing the maximum amount of energy for a given turbine from the given GCC. An example of the SCC plotted with the GCC is shown in Fig. 4. The method described can also be used with other equality constraints to enable the method to be used for retrofit applications, for example the main steam flowrate (F_1) may be set to be equal to the existing main steam flow rate (as per the case study used in this paper) and the linear programming problem will still be able to be solved using linear programming algorithms.

References

- Allinson, G., Neal, P., Ho, M., Wiley, D., McKee, G., 2006. CCS Economics Methodology and Assumptions RPT06–0080; CO₂CRC, Canberra, Australia. Available at: www.co2crrc.com.au/publications/index.php (accessed 01.11.11.).
- Aspen Technology Inc., 2008. Rate-based Model of the CO₂ Capture Process by K₂CO₃ Using Aspen Plus. Aspen Technology Inc., Cambridge, USA.
- Ataei, A., Yoo, C., 2010. Combined pinch and exergy analysis for energy efficiency optimization in a steam power plant. *International Journal of the Physical Sciences* 5 (7), 1110–1123.
- Bernier, E., Marechal, F., Samson, R., 2010. Multi-objective optimization of a natural gas-combined cycle with carbon dioxide capture in a life cycle perspective. *Energy* 35, 1121–1128.
- Bhutani, N., Tarafder, A., Rangaiah, G.P., Ray, A.K., 2007. A Multi-platform, multi-language environment for process modelling, simulation and optimisation. *International Journal of Computer Applications in Technology* 30 (3), 197–214.
- Botros, B.B., Brisson II, J.G., 2010. Steam optimisation with increased flexibility in steam power island design. *Chemical Engineering Transactions* 21, 313–318.
- Bouillon, P.A., Lemaire, E., Mangiaracina, A., Tabasso, C., 2011. First Results of the 2.25t/h Post-combustion CO₂ Capture Pilot Plant of ENEL at the Brindisi Coal Power Plant with MEA from 20 to 40wt Session 7, 1st post-combustion capture conference, Abu Dhabi, United Arab Emirates, 17–19 May 2011.
- CO₂CRC Technologies Pty Ltd, 2011. A Process and Plant for Removing Acid Gases PCT/AU2011/000462. Australia.
- Cousins, A., Wardhaugh, L.T., Feron, P.H.M., 2011a. Preliminary analysis of process flow sheet modifications for energy efficient CO(2) capture from flue gases using chemical absorption. *Chemical Engineering Research & Design* 89 (8A), 1237–1251.
- Cousins, A., Wardhaugh, L.T., Feron, P.H.M., 2011b. A survey of process flow sheet modifications for energy efficient CO(2) capture from flue gases using chemical absorption. *International Journal of Greenhouse Gas Control* 5 (4), 605–619.
- Davidson, R.M., 2007. Post Combustion Carbon Capture from Coal Fired Plants - Solvent Scrubbing. CCC/125, IEA Clean Coal Centre, Cheltenham, UK.
- Deb, K., Pratap, A., Agarwal, S., Meyarivan, T.A.M.T., 2002. A fast and elitist multi-objective genetic algorithm: NSGA-II. *Evolutionary Computation, IEEE Transactions on* 6 (2), 182–197.
- Desideri, U., Paolucci, A., 1999. Performance modelling of a carbon dioxide removal system for power plants. *Energy Conversion and Management* 40 (18), 1899–1915.
- Dhole, V.R., Linnhoff, B., 1993. Total site targets for fuel, cogeneration, emissions, and cooling. *Computers and Chemical Engineering* 17, S101–S109.
- Dreher, T., Dugan, C., Harkin, T., Hooper, B., 2011. Towards large scale CCS. *Energy Procedia* 4, 5549–5556.
- Endo, K., Nguyen, Q.S., Kentish, S.E., Stevens, G.W., 2011. The effect of boric acid on the vapour liquid equilibrium of aqueous potassium carbonate. *Fluid Phase Equilibria* 309 (2), 109–113.
- Furukawa, S.K., Bartoo, R.K., 1997. Improved Benfield Process for Ammonia Plants. UOP, Des Plaines, Illinois. Accessed at: www.uop.com/objects/85Imprvdbenfieldamm.pdf (accessed 08.04.10.).
- Gas Processors Suppliers Association, 1998. Engineering Data Book, eleventh ed. Gas Processors Suppliers Association, Tulsa, USA.
- Ghosh, U., Kentish, S., Stevens, G., 2008. Absorption of carbon dioxide into potassium carbonate promoted by boric acid. *Energy Procedia* 1 (1), 1075–1081.
- Girardin, L., Bolliger, R., Marechal, F., 2009. On the use of process integration techniques to generate optimal steam cycle configurations for the power plant industry. *Chemical Engineering Transactions* 18, 171–176.
- Harkin, T., Hoadley, A., Hooper, B., 2010. Reducing the energy penalty of CO₂ capture and compression using pinch analysis. *Journal of Cleaner Production* 18 (9), 857–866.
- Harkin, T., Hoadley, A., Hooper, B., 2011. Using multi-objective optimisation in the design of CO₂ capture systems for retrofit to coal power stations. *Energy*. doi:10.1016/j.energy.2011.06.031.
- Hooper, B., Murray, L., Gibson-Poole, C., 2005. Latrobe Valley CO₂ Storage Assessment RPT05–0108; CO₂CRC, Melbourne, Australia.
- IEA-GHG, 2006. CO₂ Capture in Low Rank Coal Power Plants. 2006/1. IEA Greenhouse Gas R&D Programme, Cheltenham, UK.
- Jassim, M.S., Rochelle, G.T., 2006. Innovative absorber/stripper configurations for CO₂ capture by aqueous monoethanolamine. *Industrial & Engineering Chemistry Research* 45 (8), 2465–2472.
- Kapil, A., Bulatov, I., Kim, J., Smith, R., 2010. Exploitation of low-grade heat in site utility systems. *Chemical Engineering Transactions* 21, 367–372.
- Karimi, M., Hillestad, M., Svendsen, H.F., 2011. Capital costs and energy considerations of different alternative stripper configurations for post combustion CO(2) capture. *Chemical Engineering Research & Design* 89 (8A), 1229–1236.
- Khalilpour, R., Abbas, A., 2011. HEN optimization for efficient retrofitting of coal-fired power plants with post-combustion carbon capture. *International Journal of Greenhouse Gas Control* 5 (2), 189–199.
- Klemes, J., Dhole, V.R., Raissi, K., Perry, S.J., Puigjaner, L., 1997. Targeting and design methodology for reduction of fuel, power and CO₂ on total sites. *Applied Thermal Engineering* 17 (8–10), 993–1003.
- Le Moulec, Y., Kanniche, M., 2011. Optimisation of MEA Based Post-combustion CO₂ Capture Process: Flowsheeting and Energetic Integration Session 2b, 1st Post Combustion Capture Conference, Abu Dhabi, United Arab Emirates, 17–19 May 2011.
- Lee, E.S.Q., Ang, A.Y.W., Rangaiah, G.P., 2008. Optimize your process plant for more than one objective. *Chemical Engineering* 115 (9), 60–66.
- Linnhoff, B., Flower, J.R., 1978. Synthesis of heat-exchanger networks 1. Systematic generation of energy optimal networks. *Aiche Journal* 24 (4), 633–642.
- Linnhoff, B., Alanis, F.J., 1989. A systems approach based on pinch technology to commercial power station design. *Analysis & Design of Energy Systems: Fundamentals & Mathematical Techniques* 10 (2), 31–43.
- Mimura, T., Simayoshi, H., Suda, T., Iijima, M., Mituoka, S., 1997. Development of energy saving technology for flue gas carbon dioxide recovery in power plant by chemical absorption method and steam system. *Energy Conversion and Management* 38 (Suppl. 1).
- Oyenekan, B.A., Rochelle, G.T., 2009. Rate modeling of CO₂ stripping from potassium carbonate promoted by piperazine. *International Journal of Greenhouse Gas Control* 3 (2), 121–132.
- Peters, M.S., Timmerhaus, K., West, R.E., 2003. *Plant Design and Economics for Engineers*, fifth ed. McGraw-Hill, New York, USA.
- Pfaff, L., Oexmann, J., Kather, A., 2010. Optimised integration of post-combustion CO(2) capture process in greenfield power plants. *Energy* 35 (10), 4030–4041.
- Plaza, J.M., Van Wagener, D.H., Fraile, P., Chen, E., Rochelle, G.T., 2011. Modelling CO₂ Capture Using Concentrated PZ Session 5b, 1st Post-combustion Capture conference, Abu Dhabi, United Arab Emirates, 17–19 May 2011.
- Rangaiah, G.P., 2009. Multi-objective Optimization: Techniques and Applications in Chemical Engineering. World Scientific, Singapore.
- Reddy, S., Scherffus, J., Freguia, S., Roberts, C., 2003. Fluor's Econamine FG Plus technology. Session on capture and separation - Sorbents Second National Conference on carbon Sequestration, Alexandria, VA, 5–8 May 2003.
- Romeo, L.M., Bolea, I., Escosa, J.M., 2008. Integration of power plant and amine scrubbing to reduce CO₂ capture costs. *Applied Thermal Engineering* 28 (8–9), 1039–1046.
- Schneider, R., Schramm, H., 2011. Environmentally friendly and economic carbon capture from power plant flue gases: The SIEMENS PostCap process Session 3b, 1st Post Combustion Capture Conference, Abu Dhabi, United Arab Emirates, 17–19 May 2011.
- Schoon, L., Straelen, J., 2011. Development of a precipitating carbonate technology for post-combustion CO₂ capture Session A5, 6th Trondheim CCS conference, Trondheim, Norway, 16 June 2011.
- Sharma, S., Rangaiah, G.P., Cheah, K.S., 2011. Multi-objective optimization using MS Excel with an application to design of a falling-film evaporator system. *Food and Bioprocess Processing*. doi:10.1016/j.fbp.2011.02.005.
- Smith, R., 2005. *Chemical Process Design and Integration*. John Wiley & Sons Ltd, West Sussex, England.
- Standards Australia Limited, 2010. AS1210–2010 Pressure Vessels. SAI Global Limited, Sydney, Australia.
- Stoffregen, T., 2011. New Results from the PCC Pilot Plant Niederlausitz Session 7, 1st Post Combustion Capture Conference, Abu Dhabi, United Arab Emirates, 17–19 May 2011.
- Svendsen, H.F., Tobiesen, F.A., Mejdell, T., Hoff, K.A., 2008. Method for capturing CO₂ from exhaust gas. World Intellectual Property Organization. WO 2008/072979 A1.
- Zachary, J., 2008. Options for reducing a coal-fired power plant's carbon footprint: part I. *Power* 5 June 2008.

Chapter 9

Conclusions and Recommended Further Work

9.1 Conclusions

Carbon Capture and Storage is potentially a very useful technology to reduce CO₂ emissions from fossil fuel fired power stations, and from most reports on reducing anthropogenic CO₂ emissions to reduce human induced climate change, it is recommended as one of a range of technologies required to ensure the reductions are performed at the least cost. It is an inherent feature of the technology that the addition of CCS to a power station will lead to energy penalties due to the energy required to separate and compress the CO₂. It is possible to reduce the energy penalties associated with CCS by reusing heat in the solvent process back into the steam cycle of the power station. Many solvent plant designs include heat recovery from the flue gas, the stripper condenser, and the CO₂ compressor intercoolers into the boiler feed water heating. However, methods to determine the best use of the available heat and the minimum energy targets for a range of solvent process options has not been a well studied or articulated process.

It is clear that a systematic approach to determine the minimum energy targets for the addition of CCS is important to enable the range of options, be it solvent process options, or power station designs to be compared on an even basis. In this thesis two such methods have been proposed, the first is referred to as the 'extraction' method and the second is the 'superstructure' method. Both methods are based on the fundamental rules of pinch analysis but use linear programming to automate the optimisation.

The extraction method, based on determining the minimum amount of extraction steam from a steam turbine to satisfy the energy deficit that is created by the addition of the CCS equipment, is useful for retrofit applications where the minimum amount of changes may be desired. It provides the minimum energy penalty for a given process, assuming a minimum approach temperature in the heat exchanger network and that the turbine efficiency is not changed with changes to the extraction steam flowrates. The method however, also had deficiencies in that the extraction steam optimisation could only be for steam extracted downstream of any reheat stages of the steam cycle and would not allow for changes to the steam generation rates.

The superstructure method overcomes these difficulties by determining the optimum steam generation and extractions rates for a given steam cycle and given process. The method enables steam to be extracted upstream of a reheater, and steam to be generated and inducted into the turbines at every steam level. The superstructure method can also allow constraints on the amount of steam generated that means the method can mimic the extraction method. The superstructure method is very suitable for greenfield projects as the steam rates suggested can be used in the design of a new turbine, however it can also be used in the screening studies of a

retrofit application to determine the improvements that may be obtained by modifying the existing steam turbine to better utilise the new heat distribution of the power station with CCS.

The superstructure method was developed to overcome the above-mentioned deficiencies associated with using the extraction methods in complex stream cycles. It has similarities to a mixed integer linear programming (MILP) method developed by Marechal and Kalitventzeff (1991). The methods use similar constraints in the linear programming for heat to cascade between the process and the utilities, however the objective in the superstructure method is to maximise power from the steam turbine whilst the objective of the MILP model of Marechal and Kalitventzeff (1991) is to minimise a linearised cost function.

The use of pinch analysis, whether used in the extraction method or the superstructure method, has demonstrated that the energy penalty associated with the addition of CCS can be reduced with better heat integration. Various studies with different boundary conditions and objectives have shown the benefits of heat integration. In Chapter 3 where 90 % of the CO₂ was captured from two brown coal power stations using a generic solvent which required a 3 GJ/t CO₂ of thermal energy for solvent regeneration, the net energy penalty for two power stations were reduced from 39 % and 28 % to 24 % and 14 % respectively, just by improving the heat integration. Similar results were obtained in Chapters 5 and 6 where the energy penalty was reduced from 38 % for a rate promoted potassium carbonate solvent down to 14 % for an optimised solvent system with heat integration. A similar result was obtained for Chapter 8, however when the cost of the heat exchanger network was factored into the cost objective function and the process optimised to minimise the differential cost of electricity (DCOE) the optimal energy penalty was between 25 and 30 %, still significantly lower than the un-integrated case, but not as low as the minimum energy penalty that was found to be possible by previous studies.

For brown coal power stations, pilot plants have been constructed to demonstrate research to pre-dry the brown coal using low grade heat with the aim of improving the power station efficiency. From the results provided in Chapter 3 it can also be concluded that the overall energy penalty associated with the addition of CCS can be reduced with the inclusion of coal pre-drying technology. However, it is not clear from the early targeting work that combines coal pre-drying with CCS, whether the energy savings will justify the additional capital expenditure.

Another conclusion that can be made from the early targeting work provided in Chapter 3 and Appendix E is that the optimal combustion air-preheat is likely to change with the addition of CCS. In Appendix E the net power that is produced from the power station is not improved once the

air-preheat temperature is greater than 120 °C. This temperature corresponds to the pinch point of the power station with CCS and is lower than the existing pre-heat temperature of 150 °C. However, this conclusion was reached using the extraction method, whereas with the superstructure method, which allows additional high pressure steam generation above the predefined amount of the existing power station, the optimal air preheat temperature may be different again.

It is obvious from the results obtained in Chapter 3 that the amount of steam required to regenerate the solvent for CCS is significant and that modifications will need to be made to the steam turbine to enable the steam rates in the low pressure end of the turbine to be reduced, especially if the efficiency of the turbine is to not be significantly affected. The modifications to the steam turbine as well as additional modifications to the heat exchanger network that would be required to minimise the energy penalty and potentially the addition of coal pre-drying will lead to increases in the cost of the CCS retrofit. The economic optimum will likely be at an energy penalty that is higher than the minimum. The energy penalty is also likely to be higher than the minimum targets suggested in the early chapters of the thesis to ensure that the plant integration does not affect the operability of the power station, especially when turn-down effects are taken into consideration. Although this thesis has focused on developing targets for the minimum energy penalty, preliminary designs suggest that the designs that approach the minimum energy penalties could be achieved by mainly using waste heat for boiler feed water heating. Under design conditions, trim heaters and coolers could be provided to maintain steady performance of the process and a significant challenge to achieving low energy penalties whilst still maintaining operability would be to design a system that enables the same controllability at off-design, part-load conditions.

The first objective of the thesis is to determine minimum energy penalties for Australian coal fired power stations using solvent based CCS. These targets are provided for a typical solvent system in Chapter 3 of the thesis. One point that is clearly important is the minimum system approach temperatures that are assumed for the analysis. The energy penalty targets show some sensitivity to the minimum approach temperature (ΔT_{\min}) where the gross power that is produced from a power station with a ΔT_{\min} of 3 °C is 205 MW, compared to 190 MW for a ΔT_{\min} of 20 °C. However, even with a ΔT_{\min} of 20 °C the gross power produced from the steam turbine is still substantially higher than without heat integration which produces only 172 MW.

In Appendix F the use of a promising new compression technology, shockwave compression, is compared for CO₂ compression to the conventional in-line compression. Both the in-line and shockwave compression have similar power requirements, however the shockwave compressor

provides better quality heat in the intercoolers. By integrating the waste heat into the steam cycle the power station with the shockwave compressor is able to produce more power than that with the in-line compressor. Appendix F utilised simulation and automated heat integration to compare two technologies, the comparison of multiple technologies could be enhanced by addition of MOO , as it could reveal what conditions advantage one technology over another.

The combination of Multi-objective optimisation (MOO) using rigorous process simulation combined with pinch analysis also allows for the optimum value of a number of variables to be determined. It allows for the trade-offs between increased capital costs associated with reduced minimum approach temperatures and increased net power to be analysed more thoroughly. Chapter 4 describes a framework for the combination of MOO with process simulation and heat integration for power stations with CCS. The combination of heat integration and MOO has been used sparingly in process synthesis and shows promise for not only application of CCS and power stations, but for many energy intensive chemical processes. The framework developed in Chapter 4 is interestingly, very similar to that developed, at a similar time, independently by Bernier et al. (2010). Bernier et al. (2010) also use MOO and MILP based heat integration of a power station but for a natural gas combined cycle with MEA solvent capture system, and they focused on optimising the costs to reduce the life-cycle global warming potential of natural gas combined cycle power stations. Additionally, the steam network they used for the MILP based heat integration, that was developed by Marechal and Kalitventzeff (1999), includes water injection for direct contact desuperheating. Whereas, the framework developed in this thesis enables indirect heat exchange to desuperheat the steam. Indirect desuperheaters will have thermodynamic advantage by utilising the higher temperature of the superheated steam, but there is the potential that the capital cost of such heat exchangers will prohibit their use and if that is the case direct desuperheaters may be preferable.

The MOO using simulation and heat integration framework is used in Chapter 5 to illustrate the importance of designing the solvent plant for a given power station. Many solvent based CCS studies focus on minimising reboiler energy demands in the belief that this will lead to reductions in the energy penalty. However, Chapter 5 established particularly for potassium carbonate based processes, that reducing the reboiler energy may not always result in the minimum energy penalty overall when the entire system is considered. It is clear from the results in Chapter 5 that the trade-offs between the compressor power and the reboiler energy results in different optimal stripper pressures depending on the objective of the analysis.

In Chapter 5 comparative studies also illustrated the importance of not only the solvent plant process, but the power station design and environmental conditions of the power station in

determining the energy penalty of a process. Therefore when considering a technology to retrofit a power station, the operating conditions of the power station will impact the choice of technology and will also impact the energy penalty, which is likely to have a big impact on the DCOE of the project.

The Pareto curves of net power versus rate of CO₂ captured by the CCS equipment generated by the MOO framework also provide options for power stations to maximise profits by controlling the amount of CO₂ captured. The rate of CO₂ captured could be decreased, by adjusting operating conditions, at times when electricity prices are high to maximise the net power produced by the power station. This has been suggested in other studies, but generally by allowing the flue gas to bypass the CCS equipment, or by storing the rich solvent in a large tank for processing at a time when the value of electricity is low. However, this work suggests that there are alternatives to control the amount of CO₂ captured, namely by adjusting the solvent flowrate and lean loading.

If the CO₂ rate is reduced to take advantage of high electricity prices, turn-down of equipment will be an issue. However, the turn-down rate of absorbers are generally less effected by the solvent rate compared to the vapour rate, and therefore by controlling the solvent loading and flowrate rather than bypassing the absorbers should lead to larger turn-down ratios. The reduction in regeneration energy will impact the amount of steam extracted from the turbine and therefore the turn-down of the steam turbine is likely to be an issue which requires consideration. The turn-down rate of individual CO₂ compressors are also likely to be an issue, but with the multiple compressors that are expected to be used in large scale CCS projects, the operating range of the bank of compressors is anticipated to be wide. A combination of flue gas by-pass and solvent side CO₂ capture control may prove to provide a larger operating range than either alone.

Chapter 6 demonstrated that the optimisation framework developed provides results that approach the maximum net power or minimum energy penalty quite rapidly. The technique provides, within tens of generations, a curve that shows the maximum amount of power that can be generated for a given CO₂ capture rate. Whilst it may take longer to determine the exact values of the decision variables to achieve the very minimum energy penalty, the important design variables, those that have the biggest impact, converge quickly. The speed of the convergence to an optimal value by each variable also usually flags the level of importance each variable will have in minimising the energy penalty.

For rate-promoted potassium carbonate solvents the flue gas temperature entering the absorber is shown to greatly impact the energy penalty, where lower temperatures, less than 45 °C help to reduce the energy penalty. The solvent solution temperature is not as important for maximising

the net power, with no clear optimum value found between 40 and 72 °C. However, the solvent temperature will be important when considering the water balance of the CO₂ capture system. The solvent flowrate mainly impacts the amount of CO₂ captured whilst the optimum lean loading remains relatively constant for most capture rates. Surprisingly, in this case study the stripper pressure is not as important as other design variables and as a result the optimum stripper feed temperature varies depending on the pressure used in the stripper. The stripper pressure is set to produce a reboiler temperature that is able to be serviced by the available steam.

In Chapter 7 the superstructure and extraction methods were compared. The superstructure method allows steam to be generated at the most useful temperature for the available heat in the power station combined with CCS. Some opportunities to reduce the energy penalty associated with CCS are revealed by this method. Because there is more low grade heat available from the solvent process and the CO₂ compressors, it is possible to increase boiler feed water heating by utilising the waste heat, this opens up the opportunity to produce more high pressure and low pressure steam. By generating more steam it is possible to compensate partially for the loss of steam extracted to regenerate the solvent. However to achieve these benefits, boilers and turbines may need to be modified to enable the additional high pressure steam generation and to ensure the high pressure stage of the turbine can handle the additional flow. Likewise new steam networks and equipment may be required to generate the low pressure steam and enable it to be inducted into the turbine.

Utilising the superstructure method to determine the optimal steam flowrates could potentially lead to reductions in the energy penalty occurring with minimal cost implications. Provided there is existing design margins in the heat exchange area of the boiler and the maximum steam rate in the steam turbine. Chapter 7 showed that the largest reductions in temperature driving forces were found in the reheat, economiser and air-preheat sections of the boiler. Therefore, it is in these sections that excess area will be crucial to enable the full benefits presented by the superstructure method. Understanding the boiler and steam turbine maximum steam rate and adding these into the superstructure problem definition will produce results that are more likely to be able to be implemented with minimal changes to the existing equipment.

As noted previously, some modifications will need to be made to the steam turbine to accommodate the amount of steam that will be extracted for solvent regeneration even with the best current solvent system. Therefore, it will be prudent to review what other modifications need to be performed to help maintain or improve the existing turbine efficiency, allow for redistribution of the loads in the turbine and to enable sufficient turn-down of the power station and/or the solvent system.

The final objective of the thesis is to optimise the CCS process with a view not only to the energy penalty but the economics of a project, which is demonstrated in Chapter 8. This chapter compares for a given capture rate the optimisation to maximise the net power of the power station with CCS to the optimisation to minimise the DCOE of the addition of CCS. Interestingly, for the optimisation to maximise the net power, the energy penalty by a retrofit project can be negative (in other words, more power is produced) up to a capture rate of approximately 40 % for the typical brown coal fired power station operating in Australia. This opportunity can show how it may be possible to add CCS to a power station in stages. For example in the early stages of CCS implementation, where the amount of CO₂ captured is low, but the capital infrastructure is also much lower than what is required for full scale capture, and the energy penalty is small. Such an approach would minimise the project risk during this early stage. At a later stage, the capacity of the CCS infrastructure could be increased to enable higher capture rates, as the price of CO₂ increases. Whilst the price per unit of CO₂ avoided will be higher at lower capture rates, the DCOE is much lower. Although, the optimisation suggests that negative energy penalties may be possible, the cost to provide the required heat exchange area, the increased steam rate and generator capacity is likely to be prohibitive. However, it does illustrate that there is the potential for much lower energy penalties than anticipated at low capture rates provided additional heat exchange area is available or is supplied and the turbine can handle, or is modified to handle, the additional steam flow. The DCOE could be even further reduced in the situation where the Government funds the capital expenses rather than imposing a price on carbon being emitted.

The second optimisation case study provided in Chapter 8 enables the trade-off of increased net power production from the power station and the additional capital costs to provide that power. In particular, the impact of the minimum heat exchanger approach temperatures is investigated. The optimum ΔT_{\min} when optimising to minimise the DCOE for capture rates between 80 and 90 % is around 20 °C. However, what is not clear is whether capital costs will be lower and/or the net power is increased by allowing each stream to have a different ΔT_{\min} , rather than a single global ΔT_{\min} .

The optimal stripper pressure for rate-promoted potassium carbonate solvents, when costs are taken into account, is between 0.5 to 1.5 bar. When the costs are not taken into consideration the optimal pressure is different. The change in optimal pressure is mainly due to the larger optimal minimum approach temperatures that are desired when costs are taken into account. Larger approach temperatures lead to comparably larger losses in the power produced by the steam turbine compared to the reductions in the compressor power as the stripper pressure is increased. Therefore, it is possible that if different minimum approach temperatures are provided

for different streams, then the optimal stripper pressure may again be different. Another factor which increases the cost of the project as the stripper pressure is increased is the cost of the lean solvent cooler and rich solvent heater, as the pressure increases the duty and the heat exchanger area required for these exchangers increases and the costs for these heat exchangers can be significant.

The maximum net power produced by a power station is obtained by low flue gas temperatures entering the solvent system, but the economic optimisation suggested that higher flue gas temperatures will optimise the DCOE. By analysing the main cost difference between the two cases, the heat exchange area contribution of the flue gas turns out to be a large component of the capital costs. Therefore, the overall costs are likely to be reduced by the use of a direct contact cooler (DCC) rather than trying to utilise the heat in flue gas once the flue gas starts to condense. There is a significant amount of low grade heat available in the condensation of water in the flue gas, but the capital costs to utilise this heat are high, so unless a low capital cost solution can be found to utilise this heat it is likely that the most cost effective solution will be the use of a DCC.

In the case provided in Chapter 8 the optimal energy penalty to minimise the DCOE is between 25 and 30 %. This is lower than the case without heat integration (38 %) but higher than the minimum energy penalty suggested with high levels of heat integration and large heat exchanger areas (14 %).

9.2 More General Insights

The combination of simulation, heat integration, cost estimation and multi-objective optimisation has proven to be useful at the early stages of process design to screen options for the addition of CCS to power stations. It is also found to be useful to optimise and understand better the important operating values of solvent plants for specific power stations. The methodology described in the thesis is widely applicable to any and all CCS applications, as proven by it being used not only in post-combustion applications, but for use with an integrated gasification and combined cycle process as illustrated in Appendix G. The method will provide directions for optimising operational strategies for low emission fossil fuelled industries. The techniques are equally applicable to new and retrofit solutions and may well lead to different outcomes based on a range of project specific combinations such as plant efficiencies, fuel cost, capital cost profile and CCS technologies employed.

Although there have been similar approaches in combining both heat integration and multi-objective optimisation, this would appear to be the first study where it is employed in a retrofit

situation, where some components are fixed in their design, some new equipment is required and some equipment would be modified. This is a more complicated scenario than a greenfield development, where all equipment may be costed as new.

The combination of MOO, simulation and automated heat integration has only been reported recently and very sparingly, however the insights that can be obtained by this technique are great. Therefore, it is considered that this framework could, and should, be used to identify improvements in many other energy intensive industries. It is useful for creating a Pareto curve of the objectives and to determine the optimum value of the decision variables in the study, but it can also be used to determine the relative importance of the decision variables. The speed at which the various decision variables converge to their ultimate value is an indication of the importance of that variable to the objectives. In this thesis the speed of convergence was determined qualitatively by reviewing the optimum values of the decision variables after different generations. However, determining a quantifiable designation for the speed of convergence of the decision variables would be a valuable addition to multi-objective optimisation tools.

9.3 Recommended Future Investigations

The thesis provides the framework that will be able to be adopted for future technology or project specific research for the addition of CCS to power stations. However, there is still considerable uncertainty about some carbon capture equipment and in particular the cost of this equipment. As more detailed designs are completed for demonstration and full scale capture plants the cost functions will be improved to better reflect the actual costs of the equipment so that more accurate estimates of the capital versus operating trade-off can be explored. As the work moves from targeting to design the film heat transfer coefficients of different services could be revised to improve the area estimation tools and as a consequence the cost estimations for heat exchangers may also be improved.

The cost estimation could also be expanded to include greenfield power stations and therefore a full optimisation of a new power station could be developed. The full-scale optimisation would be able to include optimising the level of coal pre-drying, excess air and air-preheat on the boiler side as well as the optimisation of the steam cycle and the solvent capture plant.

A number of other optimisation studies could be completed to increase the knowledge of the process including;

- MOO including the minimum approach temperatures of each type of stream as a variable.

- MOO with the objectives of minimising capital and operating expenses at a given capture rate.
- MOO including adjusting the pressure of the flue gas into the absorber to look at the trade-off between reductions in the regeneration energy compared to increases in the fan power.
- MOO including a DCC, the cut-off temperature of where the flue gas heat enters the DCC can be used as a variable to determine the optimal temperature for the trade-off between recovering the heat in the flue gas and the capital cost to do so.
- Heat integration study comparing integrally geared compressors to shockwave compressors. Where the integrally geared compressors are likely to have lower compressor power requirements, but the shockwave compressor will have higher quality heat in the intercoolers, so the overall impact on the net power could favour either of these compressors.

The optimisation suggests that the net power of a power station could be maximised by increasing the steam rate through the high pressure turbine to compensate for the loss of power in the low pressure turbine. Whilst there have been several studies on how to overcome the reduction in steam in the low pressure turbine, there are none on how to shift the load to the high pressure turbine. A study of common turbines and what capacity they may have for an increase (and/or what modifications are required to allow an increase in capacity) would help to identify whether the minimum energy penalties suggested by transferring load to the high pressure turbine is likely to be possible and what kind of expense this may require. Also in the cost estimation tools it was assumed that the steam turbine would be replaced. However it could be expected that significant savings may occur by modifying rather than replacing the steam turbine, therefore estimation tools based on how much the steam turbine varies from the base case rather than complete replacement may be useful for optimising retrofit cases.

It would also be useful to look at the turn-down capabilities of CCS equipment based on flue gas bypass compared to solvent flowrate and lean loading adjustments or a combination of the two to determine how flexible the processes will be for maximising power station profits by controlling the amount of CO₂ captured.

References

Bernier, E., F. Marechal and R. Samson (2010). "Multi-objective optimization of a natural gas-combined cycle with carbon dioxide capture in a life cycle perspective." *Energy* 35: 1121-1128.

Marechal, F. and B. Kalitventzeff (1991). Heat and mechanical power integration, a MILP approach for optimal integration of utility systems. 22nd Symposium of the working party on use of computers in chemical engineering, COPE'91., Barcelona, Spain, Elsevier.

Marechal, F. and B. Kalitventzeff (1999). "Targeting the optimal integration of steam networks: Mathematical tools and methodology." Computers & Chemical Engineering 23: S133-S136.

Appendix A

Detailed description of heat integration program

Outline of Excel/VBA based program used for heat integration.

Contents

1. Introduction	140
2. Overview: MOO-Heat integration-Economics	140
3. Set up steps (Steps 1 – 4)	141
3.1 Step 1 - MOO Setup	141
3.2 Step 2 – Set up simulation	143
3.3 Step 3 – Set up problem specific analysis	144
3.4 Step 4 – Set up Pinch Analysis.....	146
4. Run MOO, simulation, heat integration and cost estimation (Steps 5 -11).....	147
4.1 Step 5 – Run MOO.....	147
4.2 Step 6 – Assign value to the decision variables	147
4.3 Step 7 – Run simulation	148
4.4 Step 8 – Pinch Analysis.....	149
4.4.1 GetStreamData	149
4.4.2 CleanStreamData	151
4.4.3 OrgStreamData	161
4.5 Step 9 – Post Pinch Analysis Processing.....	164
4.5.1 LPOptimisation2.....	164
4.5.2 Balanced_CC.....	173
4.5.3 Area Targeting.....	174
4.6 Step 10 – Calculate Objectives.....	176
4.7 Step 11 – Objective comparison	177
4.8 Step 12 – Results.....	178
5. Conclusion.....	178
References	179

1. Introduction

An automated heat integration program was required to complete this thesis in order to enable the multi-objective optimisation (MOO) program to be used for the optimisation without having to develop a superstructure that contains all the potential heat exchange options for the process. The program needs to get stream data information from a simulation package, in this case Aspen Plus®, needs to have data input about the steam cycle and needs to estimate the physical properties of water to model the steam cycle. MS Excel has been used as the platform for the program and therefore the program is written in VBA (Visual Basic for Applications). Aspen Plus® incorporates OLE automation and therefore information can be passed to and from Aspen Plus® using VBA. To estimate the physical properties of water the open source VBA code 'X-Steam' developed by Holmgren (2011) which is based on IAPWS IF-97 was used. It would also be possible to utilise superstructures developed in Aspen Plus® of the steam cycles to achieve the same outcome. The original MOO that was used at Monash by Shah et al. (2008) was a Multi-platform Multi-Language Environment (MPMLE) for MOO where VBA was used as the interface between a MOO algorithm (NSGA-II) coded in C++ and the process simulations which were developed in Aspen HYSYS®. The only drawback with this system was that the interface between the VBA and C++ program did not allow for binary variables to be incorporated or allow for the MOO to be re-started using the results from previous runs as the basis for the new MOO. An alternative which has been used for work in this thesis is a VBA based version of NSGA-II developed by Sharma et al. (2011). As the program is Excel based, it is easy to link the MOO program with the heat integration program as they are both based in MS Excel and VBA.

2. Overview: MOO-Heat integration-Economics

The flowsheet of the program incorporating the MOO, the heat integration and the economic estimation is provided in Figure 1. Whilst the aim of this appendix is to provide the detail for steps 8 and 9, some of the programming details required in the other steps to ensure steps 8 and 9 can be carried out are also provided.

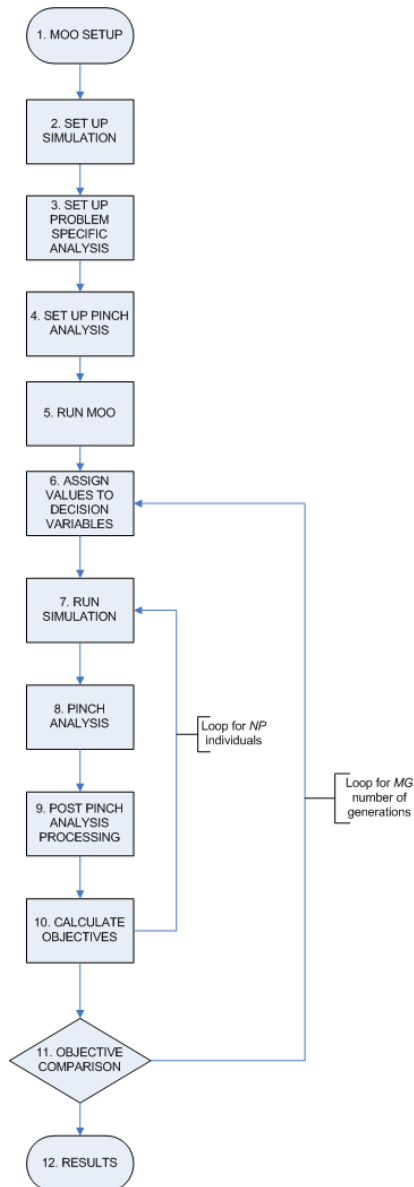


Figure 1: Overview of the MOO - Heat integration - Economics flowsheet

3. Set up steps (Steps 1 – 4)

3.1 Step 1 - MOO Setup

In this step the objectives, variables, constraints and NSGA-II specific constants including population size, maximum generations, random seed and mutation probability are selected and input onto the MOO Main Program interface (MPI) (see Figure 2). The objective functions, variables and constraints can be set up using the interface buttons. The MOO program determines the values for the design variables at each generation, and part of the programming requires the objectives and constraints to be calculated and imported into the appropriate cells on the MPI.

Main Program Interface (Scroll Down for Instructions)

Inputs										
Algorithm:		Non-Dominated Sorting Genetic Algorithm - II				Load DNA:		Yes ▼ 1		
Objective Functions:		DCOE		CAPTURE RATE						
Value	Cell	33	31.71							
Goal		Minimize	Maximize							
Design Variables: Value Cell Minimum Maximum Type Bits		<div style="display: flex; justify-content: space-between; border-bottom: 1px solid black; padding-bottom: 5px;"> Add Objective Functions </div>								
		<div style="display: flex; justify-content: space-between; border-bottom: 1px solid black; padding-bottom: 5px;"> Add Decision Variables </div>								
		DT	FG Temp	Solvent Temperatur	Solvent LL	Stripper Pres	Abs Height	Str Height	Str Feed Tem	Solvent Flowrate
		19.05882353	65	44.5	0.2168	0.74	12.5	30	80.5	1700
		6	40	40	0.11	0.5	10	10	70	800
		36	71.5	71.5	0.416	8.165	47.5	133.5	5910	
		Continuous	Continuous	Continuous	Continuous	Continuous	Continuous	Continuous	Continuous	
		8	6	6	8	9	4	4	7	9
Constraints:		Capture Rate		DCOE						
Set Cell		32	33							
Compare Type		Lesser	Greater							
Constraint		95	0							
Weight		1	1							
Algorithm Options:		Population Size		Maximum Generations		Random Seed		Selection Type		
		200		25		0.6		Tournament ▼		
Crossover Type		Two Point ▼		Crossover Probability		Mutation Type		Mutation Probability		
				0.9		Bit-Wise ▼		0.1		
NumF		2		Multiple of Generations for Saving Results		5 ▼				
NumX		9								
NumC		2								
		Run MOO								
		25 200								

Figure 2: MOO NSGA-II Main program interface

3.2 Step 2 – Set up simulation

In this thesis Aspen Plus® has been used for simulating the power station and the CO₂ capture technology. It is important when setting up the simulation that the variables which represent the decision variables are inputs to the simulation so that their values can be adjusted during the optimisation. I used a calculator block 'INPUT' for the values of all the decision variables to be exported to Aspen Plus®. In 'INPUT' the values are set up as variables of type 'Parameters' such as DV1, DV2 etc. In the calculator block a second variable will be defined such as exDV1, exDV2 etc which will be used to export the value of the decision variable to the appropriate variable in the simulation. This is done by making each exDV equal to the corresponding DV in the Fortran code within the calculator block. It would be possible to go directly from the VBA program to the simulation operating variable, however going via the calculator block is advantageous for the following reasons;

- The VBA programming of the decision variables becomes more simplified as only the object description of the calculator block (eg *myAspSim.Tree.Data.Elements("Flowsheeting Options").Calculator.Elements("INPUT").Input.Elements("FVN_INIT_VAL").Elements(i).Value*) is required and not the object description of every decision variable. Where 'i' in the above description is an integer value.
- If other variables are dependent on the decision variable, and the decision variable is added as a 'Parameter' type of variable, then the other variables can refer directly to the decision variable from another calculator blocks. For example if the regenerator pressure is the first decision variable, it will be called DV1 and be parameter 1. Therefore in a separate calculator block the compression ratios for the CO₂ compressor can be calculated with reference to parameter 1, which is the regenerator pressure.
- It makes the MOO and simulation link more obvious and enables decision variables to be added or removed easily.
- The sequence of the calculator block can be forced to be the first in the simulation calculation sequence, therefore ensuring all variables are updated before the simulation is run.

Results from the simulation that are required for the heat integration and economics estimation are handled in a similar manner. A calculator block called 'RESULTS' is created and the values of any results that are required for further analysis are imported into the calculator block. All the results can then easily be taken from the simulation and used back in the heat integration program.

It is important when setting up the simulation that the heat curves are generated for any of the streams that will be used in the heat integration program. This is done by adding a new 'Hcurve' on any heat exchanger, vessel or column that heat curves are desired for. The heat curves need to have the Heat Duty as the independent variable for the format to be exported correctly into the heat integration program.

3.3 Step 3 – Set up problem specific analysis

In this step both the utilities information and the cost estimation are set up. These are set-up in a different workbook (referred to as 'SHICE.xls') from the MOO program workbook ('MS_Excel_MOO_1.xls'). The utilities information is provided in the form of a MS Excel based superstructure of the steam cycle, an example of the superstructure is provided in Figure 3. Only three levels of the steam turbine are shown in this figure for clarity; however there are seven levels of steam with one level of condensate in total. For a given steam cycle there are a number of parameters that are required to be added (these are the blue cells shown in Figure 3); the temperature and pressure of each steam level including the condensate, the isentropic and mechanical efficiency of each stage of the turbine and the film heat transfer coefficient (HTC) for the superheated steam, steam generation/condensation and the condensate. The isentropic efficiency if not known can be estimated from Equation [1] (Girardin et al. (2009)) or any similar equation.

$$\eta_{i,i+1} = 0.919 - 0.549 \left(1 - \frac{P_i - P_{i+1}}{P_i} \right) \quad [1]$$

The superstructure uses these details and the 'X-Steam' functions to estimate the performance of the steam cycle based on given flow rates through each stage of the turbine.

The cost estimation is also achieved in MS Excel, the main equipment and operating costs have been estimated as per the equations provided in Appendix B and C respectively. The cost estimations require information from both the simulation and the heat integration program. As mentioned in section 3.2, the information that is required from the simulation is put into the 'RESULTS' calculator block and therefore can be exported to MS Excel where it can be used in the cost estimation equations. As the heat integration program is written in VBA / MS Excel the results that are required for cost estimation can easily be used in the cost estimation.

Steam Levels											HTC Data		W/m2K
Name	Tf	To	Pf	xi	hi	ho	Flowrates/	ΔT	ΔT	PC (MW/kg/s)	Turbine		
Main	538.0	44.7	164.0	1.000	3402	187	433.00	Global	19.0588	1.420	Condensin	0.095 bar	2353
HP1	351.4	44.7	45.7	1.000	3084	187	27.46	Global	19.0588	1.120	Condensin	44.7 °C	5000
IP1	428.7	44.7	19.5	1.000	3312	187	-24.59	Global	19.0588	0.908			2727.27
IP2	317.6	44.7	9.3	1.000	3093	187	-265.36	Global	19.0588	0.694			
LP1	247.0	44.7	4.5	1.000	2957	187	0.00	Global	19.0588	0.561			
LP2	179.3	44.7	2.3	1.000	2827	187	53.19	Global	19.0588	0.434			
LP3	79.4	44.7	0.5	0.977	2590	187	62.81	Global	19.0588	0.202			
LP4	44.8	44.7	0.005	0.917	2384	187	-286.51	Global	19.0588	0			

Calc. SteamFlow

Balance CC

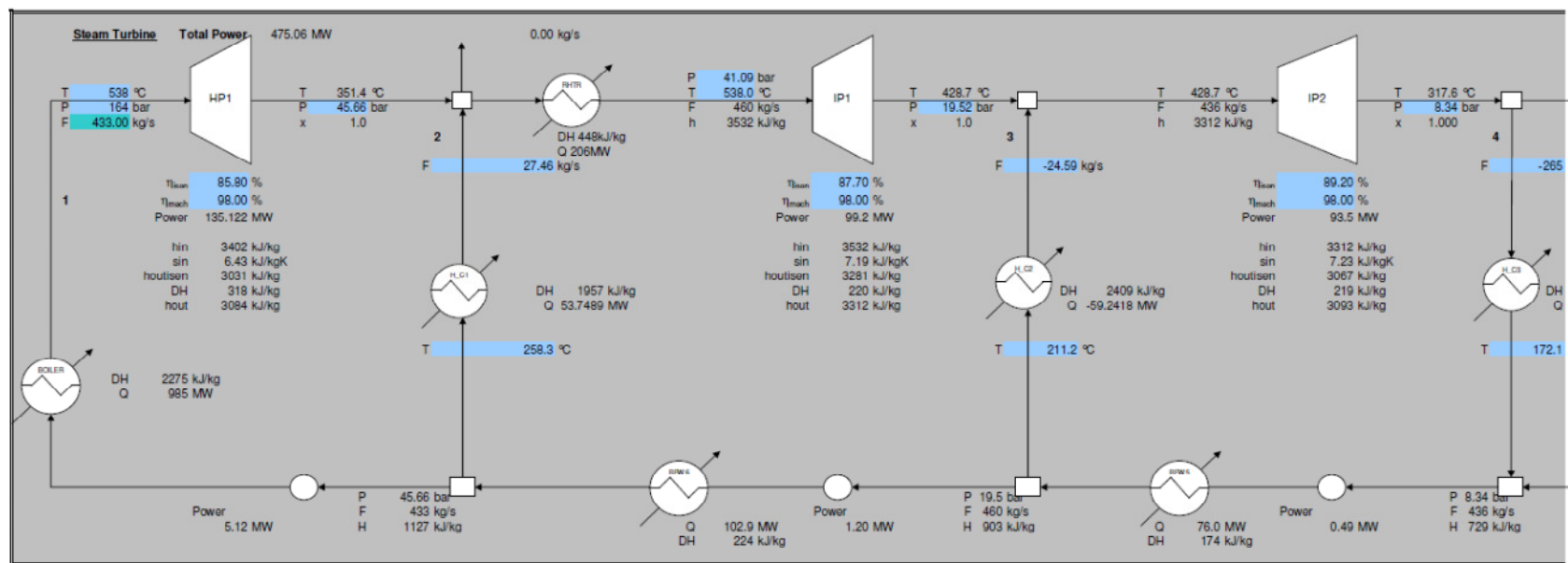


Figure 3: Example of steam cycle superstructure. Only three levels of the cycle are shown for clarity.

3.4 Step 4 – Set up Pinch Analysis

The aim of this step is determine which streams in the simulation will be included in the heat integration program. It is achieved using a MS Excel sheet called 'BlockSelection' within the heat integration program (Refer to Figure 4). The sheet and VBA code in the buttons enables the user to select the simulation file, add multiple simulations and select the blocks that represent the streams that will be used in the heat integration program. Additional information is required to be added to the streams including the stream ΔT_{min} and the film heat transfer coefficient. The ΔT_{min} can be the global ΔT_{min} or it can be different for each stream. In the latter case the ΔT_{min} that is input here is the total ΔT_{min} that would apply if two streams with the same ΔT_{min} are used in a single heat exchanger. Therefore, if two streams with different ΔT_{min} 's are located in a single exchanger, the contribution to the total ΔT_{min} is half of each streams ΔT_{min} . When the 'Add Blocks' button is clicked, the VBA code examines the simulation to compile a list of all the blocks in that simulation, it is then up to the user to select any of those blocks to be used in the analysis. However, unless the blocks have a heat curve that is both, named '1' and has been solved, then the program will not run completely. In future revisions of the program it may be useful to limit the list of blocks to those that have a solved heat curve so no errors are created later. Once the blocks have been selected it is up to the user to define a ΔT_{min} and a HTC for each block.

All Blocks	Selected Blocks	ΔT	HTC (W/m ² K)
ABSORBER	AIR-HEAT	Global	316.20
AIR-HEAT	FGHX	Global	69.22
AIRHEAT	RADIANT	Global	227.94
AIRLK	RICHX	Global	1907.02
AIRMIX	LEANHX	Global	1907.02
AIRSPLIT	STRIPPER	Global	642.91
ASH-SEP	STRIPCON	Global	4330.13
ATTEMP1	H1	Global	3429.49
BFWPUMPS	H2	Global	3429.49
BWSPLIT	H3	Global	3429.49
BOILER	H4	Global	3429.49
BURN			
C1			
C2			
C3			
C4			
C5			
CEP			
COAL-CAR			
COMBGAS			
COMP-SEP			
COMPWORK			
COND			
CONDMX			
DEAER			

Figure 4: Worksheet for selecting simulated streams used in the heat integration program.

4. Run MOO, simulation, heat integration and cost estimation (Steps 5 -11)

4.1 Step 5 – Run MOO

Once the problem has been defined the 'Run MOO' button on the MOO NSGA-II Main Program Interface (MPI) starts the program. The majority of the code in this part of the program was written by Sharma et al. (2011), however the interface between the MOO program and the simulation, heat integration and cost estimation (SHICE) program was developed during this thesis.

The SHICE program is called once for every set of decision values (*individual*) from within the optimisation program; an example of the required code is given in Figure 5. In this example the main SHICE procedure 'AutomateMOORun' is started, and then once this program has been completed the results of the objective for the given values of the decision variables are put back into the MPI of the optimisation program. In this particular example the constraints are also equal to the objectives so they directly input into the MPI by referring the constraint cells on the MPI to the appropriate objective cell on the MPI. Whereas in other optimisation problems where the constraints are different to the objectives, a mechanism to put the constraints back into the MPI is required.

```
Dim wbtarget As Workbook
Dim myresult As Variant
Dim Opt As Variant
Dim intOptNum As Integer
Set wbtarget = Workbooks("SHICE.xls")
myresult = Application.Run(wbtarget.Name & "!AutomateMOORun", 0, Counter3, 2)
Opt = myresult
For intOptNum = 1 To UBound(Opt)
    ThisWorkbook.Sheets("MOOSetup").Cells(6, 3 + intOptNum) = Opt(intOptNum)
Next intOptNum
```

Figure 5: Example calling procedure from within the optimisation program to run the SHICE program.

4.2 Step 6 – Assign value to the decision variables

The MOO program on the first generation randomly determines values for the decision variables and these get stored into the appropriate cells on the MPI. The MOO program uses a random number generator to determine these values within the minimum and maximum values defined on the MPI. In subsequent generations the values of the decision variables are determined by the MOO algorithm based on combinations of the best solutions from previous generations and

random mutations. More information on the algorithm can be found in the article by Deb et al. (2002).

4.3 Step 7 – Run simulation

For each individual the procedure *AutomateMOORun* is called from the MOO program. The purpose of this procedure is firstly to use another procedure, *AutomateSingleRun*, to run the Aspen simulation. The *AutomateSingleRun* procedure has a number of functions, including running the simulation, however if the simulation encounters errors the procedure is stopped and the *AutomateMooRun* takes control. So if the simulation completes with no errors, then *AutomateMooRun* collects the objective values so they can be transferred back to the MOO program, on the other hand if the simulation does not converge *AutomateMOORun* re-initialises then re-runs the Aspen Plus® simulation. If again the simulation does not converge, the simulation is reset to a known good starting point and then the simulation, with the desired values of the decision variables, is tried once more. If the simulation still does not converge the objective values are given bad values (high for minimisation problems and low for maximisation problems) and the program control is handed back to the MOO program.

The *AutomateSingleRun* procedure as well as running the simulation has a number of other procedures within it; *AutomateInput*, *GetStreamData*, *CleanStreamData*, *OrgStreamData*, *LPOptimisation2*, *Balance_CC*, *AreaTargeting* and *AutomateResults*. The purpose and details of all the procedures will be provided in the following sections.

The *AutomateInput* procedure gets all the values of the decision variables that are relevant to the simulation for the given individual and puts them into the calculation block 'INPUT' of the simulation. The decision variables are obtained from the *AspenTransfer* worksheet in the SHICE.xls workbook. These cells that contain the values of the decision variables are directly referenced to the corresponding cells of the decision variables on the MPI. After the decision variables are transferred into the simulation, the simulation is run. An example of the code required to run the simulation is provided in Figure 6. In this example the simulation is made visible, although it is also possible for Aspen Plus® to run in the background. It is necessary to suppress the dialogs (*myAspSim.SuppressDialogs = True*) or else every time the simulation is completed, the program would stop and wait for the user to make an action to clear the Aspen Plus® dialog box. The simulation engine is then started by the 'Run2' command; the 'Run2' has a Boolean option which is used to determine synchronicity; TRUE means the simulation is run asynchronously, whilst FALSE means it is run synchronously. Although the Aspen Plus (2003) documentation suggests that when the simulation is visible it should always be run

asynchronously and for the purposes of a sequential programming structure, that was used in the SHICE program, running asynchronously should work more consistently, however that has not been found to be the case. The simulation has been operated synchronously throughout the work completed in the thesis with fewer issues.

```
Dim FileName As String
Dim myAspSim As HappLS

'The simulation name is stored in Worksheet Blockselection
FileName = Worksheets("BlockSelection").Cells(6, 2)
Set myAspSim = GetObject(FileName)
myAspSim.Visible = True
myAspSim.SuppressDialogs = True
myAspSim.Run2 False
```

Figure 6: Example of code required to run the Aspen Plus® simulation.

In the example of code above only one simulation can be used for the pinch analysis, for more than one simulation to be included, both procedures *AutomateMOORun* and *AutomateSingleRun* would have to be changed to pass the decision variables to the appropriate simulation, and then to run and ensure all simulations are converged. The rest of the SHICE programming is designed to allow multiple simulations to be used.

4.4 Step 8 – Pinch Analysis

The pinch analysis steps are performed after the simulation has converged in three main procedures which are called from the *AutomateSingleRun* procedure; they are *GetStreamData*, *CleanStreamData* and *OrgStreamData*.

4.4.1 GetStreamData

1. A user defined TYPE called *Datta* is declared to store the stream data information from the simulation. An instance called *StreamData()* of the *Datta* TYPE is also declared. The *Datta* TYPE has a number of properties which are described in more detail in Table 1.
2. The total number of blocks that represent streams to be included in the pinch analysis is tallied. This is the total number of blocks from all simulations listed on the *BlockSelection* worksheet.
3. In determining the total number of streams each 'Radfrac' column is tested to see whether it includes a reboiler or condenser heat curve, if either of these are included then either/both of these are added to the list of streams. Each stream in the list, including the 'Radfrac' reboilers and condensers, will each have an instance of *StreamData* created to store the data for the stream. The streams are identified and stored in *StreamData* by a sequential number.

Table 1: Properties defined in the user defined type *Datta* which is used to store the stream data in the instance *StreamData* used in the *GetStreamData* and *GetHCData* procedures.

Property	Description	#	Element Description
.DataPoints()	For stream information	7	1 Name of Block. 2 Sequential Number (Not actually used in the final program – replaced by ‘.Count’). 3 If it is a Radfrac if it includes a condenser(1), reboiler(2), or both(3). 4 Full name: For radfrac including a condenser/reboiler it is Name of the block with ‘_Cond’ or ‘_Reb’. 5 The simulation location and name. 6 The stream ΔT_{min} . 7 The streams HTC.
.HData()	For heat curve data from Aspen	3 x <i>Num</i>	<i>Num</i> is the number of rows of data produced by Aspen for the heat curve 1 The StreamData Fullname with ‘-’ plus a sequential number for each row of data from Aspen. 2 The Heat Duty from the heat curve in Aspen 3 The Temperature from the heat curve in Aspen
.Count	For the sequential number	1	1 Sequential Number

4. A procedure *GetHCData* is called for each instance of *StreamData*. In this procedure the heat curve data for each stream is collected. It is stored in the *.HData()* property for each instance of *StreamData*.
5. The stream ID (sequential number), Fullname, heat duty, temperature, ΔT_{\min} and HTC are also copied into the 'StreamData' worksheet in SHICE.xls.

4.4.2 CleanStreamData

1. A user defined TYPE called *StreamInfo* is declared to store the stream data information. An instance called *StreamData()* of that TYPE is also declared. The *StreamInfo* TYPE has a number of properties which are described in more detail in Table 2.
2. The number of streams listed on the 'StreamData' worksheet is totalled.
3. Any 'Bad' data from this list is removed. Occasionally Aspen Plus® will provide data with errors, these will normally show up as an empty heat duty or temperature cell. If this is the case, the row with the missing data is deleted.
4. For each stream, all the data is collected and stored in the *StreamData* collection. The number of data points for the stream is determined and then for each stream the data points are ordered; this is necessary as the heat data can be distorted and out of order for fluids at or near the critical point, as the data for the dew and bubble point are added to the list of data. Once it has been ordered the stream information is added to the '*Data()*' property in the *StreamData* collection.
5. Then for each stream the amount of data is reduced by linearising the larger number of data points into smaller more manageable levels of data. The result will be a linearised temperature-enthalpy relationship such as those shown in Figure 7. In the two examples shown in Figure 7 the Aspen Plus® data is for hot streams and therefore the linearised data is always colder than the detailed data obtained from Aspen Plus® so that the heat integration is always linearised conservatively. For cold streams the linearisation is on the hot side. The linearisation requires a number of steps detailed below.

Table 2: Properties defined in the user defined type *StreamInfo* which is used to store the stream data in the instance *StreamData* – used in the *CleanStreamData* procedure.

Property	Description	#	Element Description
.Count	Total number of data points	1	1 Number of data points
.Data()	To store the initial stream data	5 x <i>Num</i>	<i>Num</i> is the number of data points for the stream 1 FullName 2 Heat Duty 3 Temperature 4 ΔT_{min} 5 HTC
.FinalCount	Number of data points	1	1 Number of data points required to define the simplified representation
.FinalData()	To store the simplified stream data as lines	4 x <i>FinalTot</i> -1	<i>FinalTot</i> is the number of lines used to represent the heat curve 1 Tin 2 Tout 3 ΔH 4 $(\Delta H)/(Tout-Tin)$
.PointData()	To store the simplified stream data as points	2 x <i>FinalTot</i>	1 Temperature 2 Enthalpy

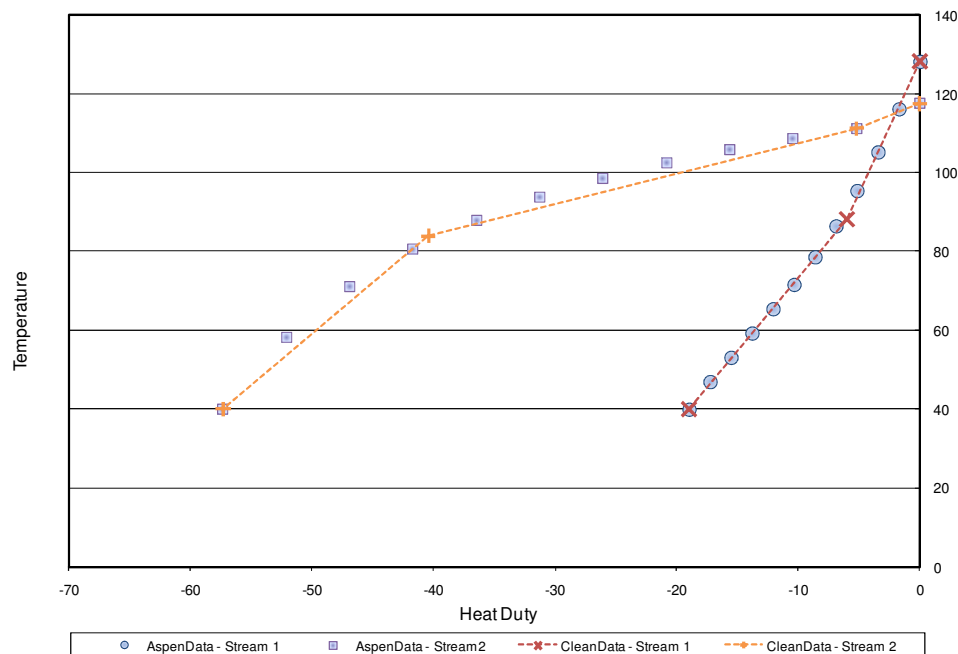


Figure 7: Example of linearising the heat data extracted from Aspen

6. The following steps occur for each stream one after the other. Data is re-arranged and stored in a $3 \times (N-1-M)$ matrix in the variable *TempStreamData()*. The data that comes from Aspen Plus® is in a $2 \times N$ matrix with the independent variable being the cumulative enthalpy change of the stream in question and the dependent variable as the corresponding temperature. This is converted into a matrix where the points are converted to line segments with the format; Temperature In, Temperature Out, and Enthalpy change. In this process, a temperature change of 0.02°C is provided for the boiling/condensing region for streams that are pure components; a non-zero temperature change is required for the data processing that occurs later. This step will also reduce the number of data points that occur if the boiling/condensing region is represented by more than two data-points. Hence the number of points will be reduced by M , where M represents the number of data-points greater than two in a condensing/boiling region.
7. The data is then converted back to a simple temperature-enthalpy relationship and stored in a $2 \times (N - M)$ matrix in *PointData()*. This *PointData()* is then used in the *BothMethods* procedure to simplify/linearise the stream. The *BothMethods* procedure is detailed in steps 8 to 12 and shown in Figure 8.

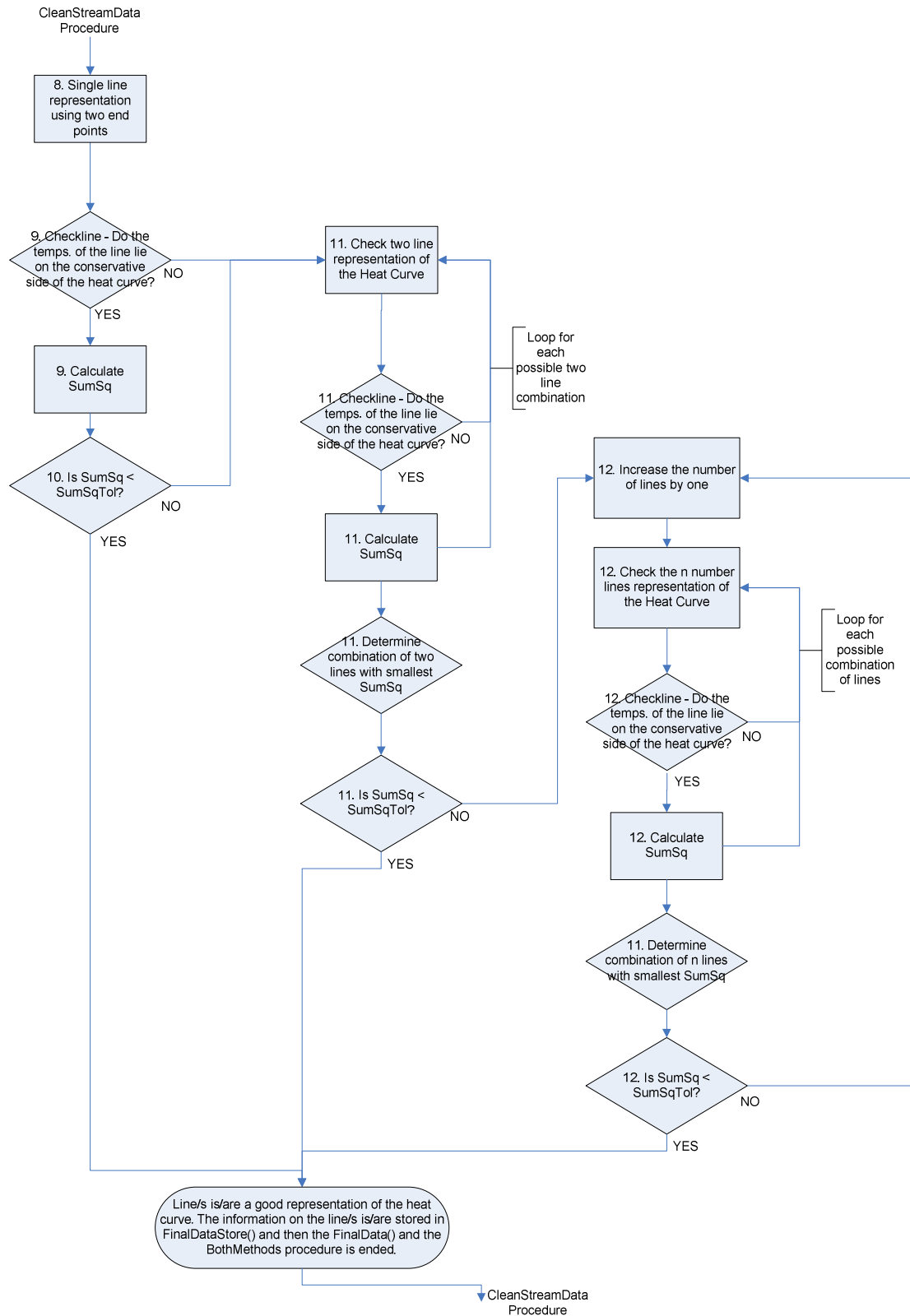


Figure 8: Representation of the algorithm used in the *BothMethods* procedure to determine a linearised representation of the heat curve data.

8. The first step of the *BothMethods* procedure is to see whether a single line can represent the stream. The line takes the form of $Temperature = Gradient \times Enthalpy + Intercept$. The gradient is the first element and the intercept is the second element in the array *MCarr()*. The line is constructed as a straight line through the two end points. The two end points are also stored in the array variable *PointArr()* as two sets of temperature-enthalpy data corresponding to the end-points of the straight line. The *MCarr()* and *PointArr()* are then sent to a function *Checkline* which tests to see whether the line meets a number of criteria. If the line meets those criteria it becomes the simplified linearised version of the stream heat curve. If the line does not meet that criteria; then a single line is not sufficient to represent the straight line and two or more lines are required to represent the stream heat curve.
9. The *Checkline* function goes through every point in the *PointData()* variable and checks to see that the temperature is less than the temperature (for cold streams) of the straight line plus a temperature tolerance. In this thesis a temperature tolerance of 0.5 °C has been used. For hot streams, the temperature must be greater than the temperature of the straight line minus the temperature tolerance. If all points are within the tolerance then the line is on the correct side of the heat curve, within the given temperature tolerance, and the check is said to be TRUE. Using a temperature tolerance means that the heat-curves may not always be conservative, and therefore it would not be advisable to make the temperature tolerance greater than 0.5 °C. The *Checkline* function also calculates the variable *SumSq*, which is the sum of the square of difference between the temperature of the *PointData()* and the temperature of the straight line at every point, $(SumSq = \sum (T_{PointData()} - T_{Straightline})^2)$.
10. If the *Checkline* function returns TRUE then the *PointArr()* information is stored in a new array called *FinalDataStore()*. Now that we know the straight line is on the correct side of the heat curve, within the temperature tolerance provided, another test is conducted to ensure that the line is a good enough fit to represent the heat curve. A line is said to be a good fit if the *SumSq* calculated by the *Checkline* function is less than a specified tolerance. The tolerance is calculated using the *SumSqTol* function. The *SumSqTol* function determines a tolerance based on the sum of the square of the difference between the average temperature of the heat curve and a given deviation of that temperature (refer to Equation [2]). The average temperature (T_{Ave}) is based on the two end point temperatures of the heat curve and the average deviation (Tolerance) used in the thesis is 5 %. If *SumSq* is less than *SumSqTol* then the straight line is used as the simplified representation of the heat curve and the data stored in *FDStore()* variable using the *FinalDataStore* procedure and the *BothMethods* procedure skips to the last step (*Final:*) where the data stored in *FDStore()* is transferred to the

FinalData() variable which is exported from the *BothMethods* procedure to the *StreamData()* variable in the main *CleanData* procedure. If *SumSq* is not less than *SumSqTol*, then more lines are required to represent the heat curve.

$$SumSqTol = \text{Total Number of points} \times (T_{Ave} \times \text{Tolerance})^2 \quad [2]$$

11. As a single line cannot represent the heat curve sufficiently, the next step is to test whether two lines are sufficient to represent the heat curve. To do this the *BothMethods* procedure develops a number of two line combinations (*NumOptions*) that might be able to represent the heat curves. The *NumOptions* is equal to the total number of two line combinations that can exist that will pass through the endpoints of the heat curve, which is calculated using Equation [3], see example in Figure 9.

$$NumOption = (PointTot-2) \times (PointTot-2+1) / 2 \quad [3]$$

Where *PointTot* is equal to the total number of points that makes up the heat curve.

The possible combinations of lines are stored in the variable *CombData().Data()* (*CombData()* is of the TYPE *CombArray()* which is a user defined type defined in the *FactorialsandCombinations* module of SHICE.xls). There are *NumOptions* instances of the *CombData()* variables each with two *Data()* points. The *CombData(i).Data(1)* point is equal to the heat curve data point that the line from the first data point passes through, and the *CombData(i).Data(2)* point is equal to the heat curve data point that the second line from the last data point passes through. This is illustrated using the example provided in Figure 9 in Table 3. Note that this method only gets the combination of lines that are on the ‘outside’ of the data points (ie. the combination of lines passing through points 1 and 4 and points 5 and 2 which intersect on the ‘inside’ of the data-points is not included). This is generally going to be acceptable as the cold streams will generally have a concave shape and hot streams will have a convex shape and so the ‘inside’ combinations will not be conservative. However, it would be also possible to modify the *BothMethods* procedure in the future to include these combinations, for those streams that do not follow this generalisation, as the lines are checked later for conservatism using the *Checkline* function. The next step is for each combination of two lines to determine the gradient and intercept for both lines and the point where the two lines intersect. After that, for each combination of two lines the *Checkline* function is called, for any pair of lines that pass the *Checkline* function test, the *SumSq* is computed. The combination of lines with the lowest *SumSq* is selected and the data stored in the *FDStore()* variable. If the *SumSq* of the combination selected is less than *SumSqTol* then the combination of two lines is used as the simplified representation of the heat curve and the *BothMethods*

procedure is ended after transferring the *FDStore()* data to the *FinalData()* variable; If *SumSq* is not less than *SumSqTol*, then more lines are required to represent the heat curve.

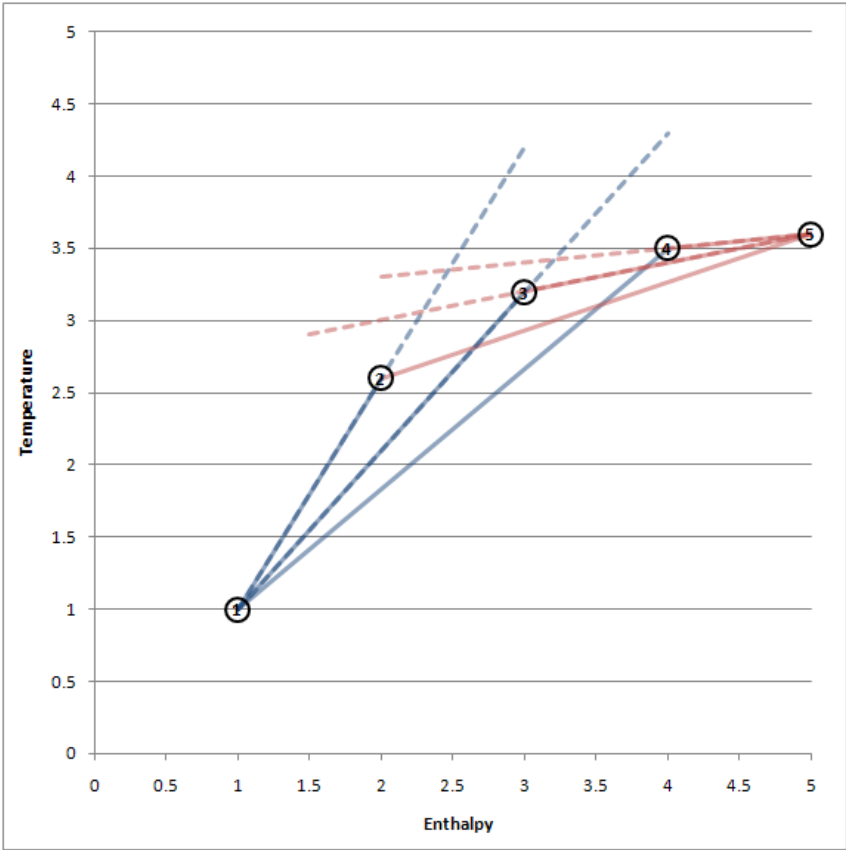


Figure 9: Example of options for two-line combination to represent heat curve

Table 3: Line Option for the example provided in Figure 9.

CombData	.Data(1) (Line from heat curve data Point 1 through Point X)	.Data(2) (Line from heat curve data Point 5 through Point X)
1	2	2
2	2	3
3	2	4
4	3	3
5	3	4
6	4	4

12. The next step involves using three or more lines to represent the heat curve. Starting with three lines, the general procedure involves; determining a number of three line combinations, determining the best of those combinations, if the *SumSq* of the best of those combinations is less than *SumSqTol* then the procedure is ended, otherwise the number of lines is increased by one and the procedure is repeated. The procedure assumes that in the representation of the heat curve the terminal or end points must be equal to the actual heat curve end points.

Therefore any combination of lines must pass through the end points. The combinations of lines are based on lines that are either tangential to the heat curve data points or a line created by two adjacent points. The tangential lines, in this case refers to the line where the angle (β) made by the tangent line and two lines made between the point in question and the two adjacent points are equal (refer to Figure 10). The tangential array is found for all the points except the two end points, the calculations required to get the tangent are provided in Equations [4] - [9] and the gradient and intercept that define the line are stored in the *TanArr()* variable. Where *n* in these equations refers to the sequential number of the heat curve data point.

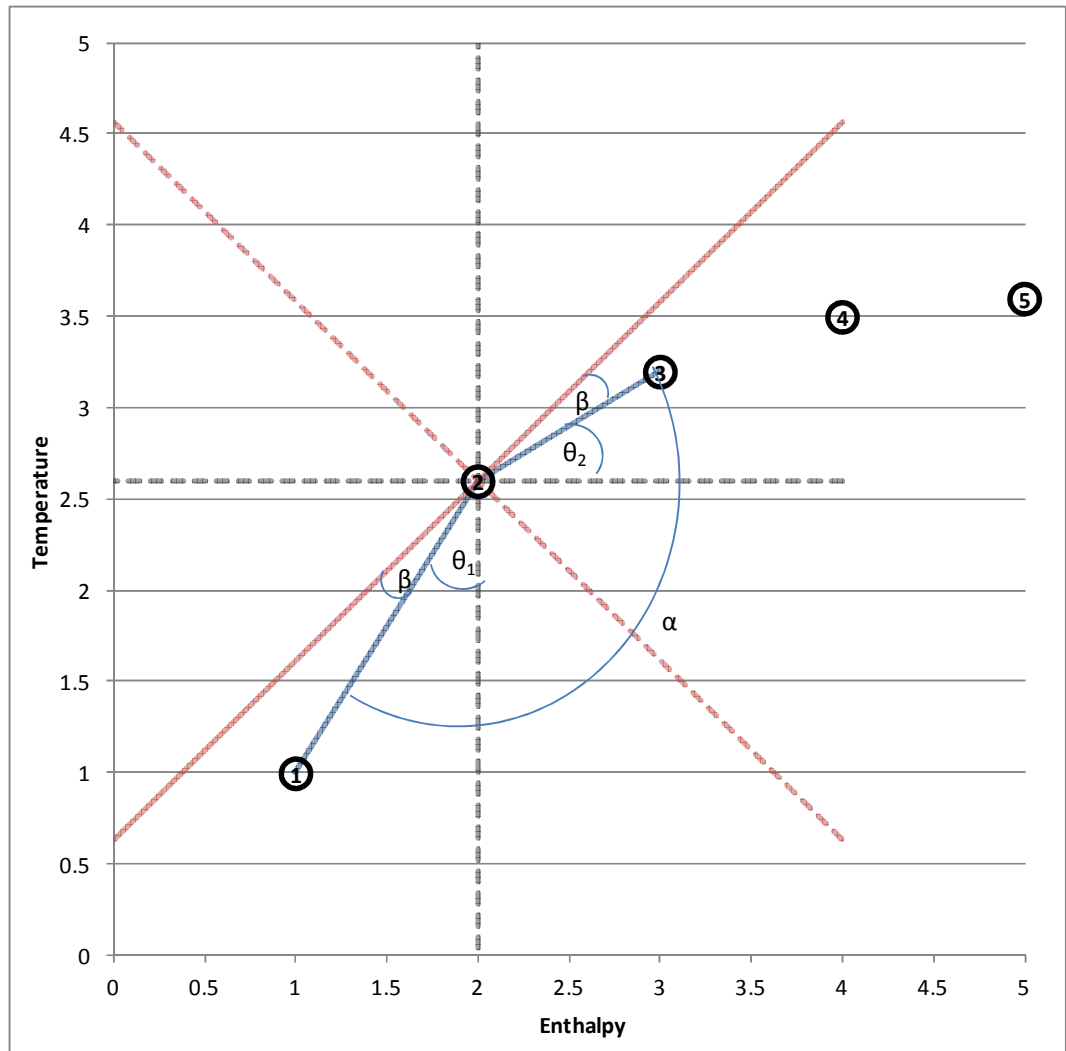


Figure 10: Representation of the method used to determine the tangent (solid red line) of the heat curve data points using the second point as an example.

$$\Theta_1 = \tan^{-1}(H_n - H_{n-1}) / (T_n - T_{n-1}) \quad [4]$$

$$\Theta_2 = \tan^{-1}(T_{n+1} - T_n) / (H_{n+1} - H_n) \quad [5]$$

$$\alpha = \Theta_1 + \Theta_2 + 90^\circ \quad [6]$$

$$\beta = 90^\circ - \alpha/2 \quad [7]$$

$$\tan Arr(1,n) = 1 / \tan(\Theta_1 + \beta) \quad [8]$$

$$\tan Arr(2,n) = T_n - \tan Arr(1,n) \cdot H_n \quad [9]$$

Another array called *GradArray()* is also established that represents the line between each data point and the proceeding data point. As well as assuming that the representation of the heat curve passes through the end points, the procedure also assumes that the lines from the end points pass through at least one other data point. Therefore, the next step is to determine the number combinations and the actual data points that the lines from the two end points will pass through. For example, if there are five data points then the two end lines, one originating from point 1 and one from point 5 can pass through three different combinations of other data points. Those points are (2 & 3), (2 & 4) and (3 & 4), each combination of two points is referred to as an 'option'. The next step is to test each option. For each option, the first task is to define the two lines between the end points and the internal points and this data is stored in the variable *PointArr()*. Obviously if we take the example of the first option, and assume that we are still trying out three lines to represent the heat curve, then with a straight line between points 1 and 2 and another straight line between points 3 and 5 defined then the third straight line must be between points 2 and 3 (Refer to Figure 11A). Therefore in these cases where the number of internal lines (ie the number of lines minus two) is equal to the difference between the sequential number of the data points used in the option, then the lines will be defined by straight lines between the internal data points. When this is not the case, say for the second option using points 2 and 4 (Refer to Figure 11B), then the internal lines are defined either by the tangent or gradient lines of the data points as defined by the *TanArr()* and *GradArr()*. The definition (gradient plus intercept) of the two outer lines are calculated and stored in the *MCarr()* and then the internal lines are calculated in the *JoinTwoLines* procedure.

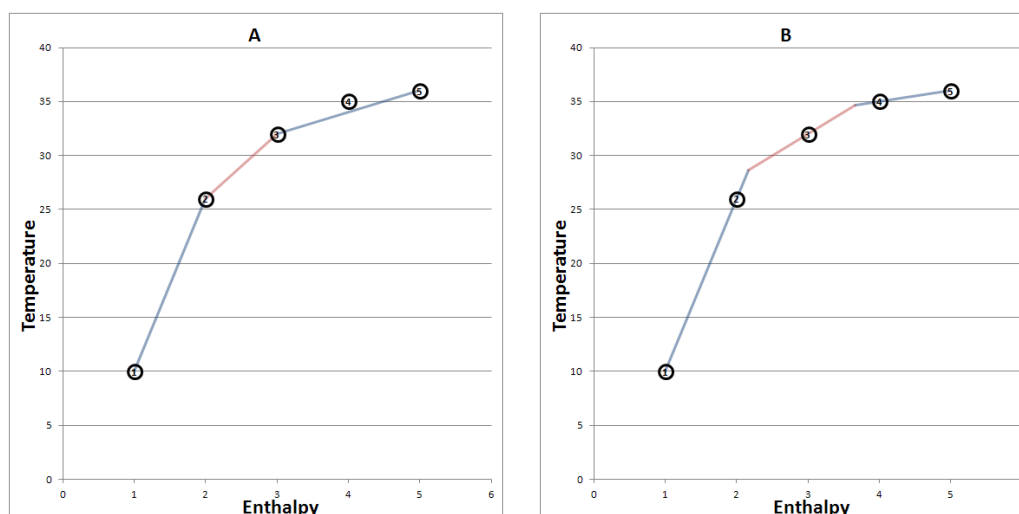


Figure 11: Example of 3 line representation used to simplify the heat curve data. (A) External lines intersect data points 2 and 3 and therefore the internal line is a straight line between the two points. (B) External lines intersect points 2 and 4 and the internal line in this case is drawn using the tangent of the third data point.

The first task of the *JoinTwoLines* procedure is to determine the number of combinations and the actual data points that can be used to define the internal lines. Following on from the example used, data points 2, 3 and 4 can be used to define the third line. Therefore for each possible data point/combination of data points, the line formed by the tangent of the data point is used join with the two external lines to form the definition of the lines. So for each possibility the lines and the points that define that possibility are generated, the lines are then checked to ensure they lie on the correct side of the heat curve, using the *Checkline* function, and the *SumSq* of the representation is calculated. The same procedure is then repeated using the gradient of all the data points rather than the tangent. Once this is complete, the data for the representation with the lowest *SumSq* is stored in the variable *FDStore2()* and we are returned to the *BothMethods* procedure. Here the best representation for the given option is tested against the previous options and the option with the lowest *SumSq* is stored in the *FDStore()* variable. Once all the options have been tested, then if the *SumSq* of the best option is lower than *SumSqTol*, then that option is used to represent the heat curve and the information for those lines is stored in *FinalData()*. If it is not, then the number of lines is increased by one and the procedure is repeated. Obviously once the number of lines is equal to the number of data points minus one, then the representation will be equal to the actual heat curve as exported from Aspen Plus® and no data consolidation/linearisation was possible.

13. The *FinalData()* obtained from the *BothMethods* procedure is stored for each stream in the *StreamData().FinalData()* and *StreamData().PointData()* variables. The data is then exported from the VBA program to Excel into the 'StreamData' and 'Streams' sheets.

4.4.3 OrgStreamData

The purpose of the *OrgStreamData* procedure is to organise the appropriate stream data and then perform the problem table algorithm (Smith (2005)). It can be used for balanced data (ie. including the utilities), and may be used with raw or shifted temperatures. The first use of this procedure does not include the utilities and uses the shifted temperatures. The steps involved are as follows;

1. The data is stored on sheets 'Processed Data' and 'Interval Data'. The procedure *Clear* is used to remove old data from these sheets.
2. The Global ΔT_{\min} is defined as the value provided in the cell 'B3' in 'Processed Data' worksheet.
3. The number of stream segments that are included is determined using the *NumItems* procedure. The number of stream segments depends on the number of streams and the linearisation of those streams. A heat curve that requires two lines to be represented has two stream segments and a heat curve that requires three lines has three stream segments and so forth. The stream segment data is taken from the data on the 'Streams' worksheet. The data is copied from this worksheet into the 'Processed Data' worksheet in a given format required for performing the problem table algorithm (Refer to Figure 12). If the utilities are included, the information from the 'UtilityStreams' worksheet is also included, and the data is stored in the 'Balanced Data' worksheet.

Energy Requirement Number	Energy requirement Name	Stream Cold	T_s (°C)	T_t (°C)	T_s (°C)	T_t (°C)	CP (MW/°C)	$\Delta H = CP\Delta T$ MW	HTC (W/m ² K)
1	RADIANT-1	Hot	1328	1023	1321	1016	1.48	453	228
2	FGHX-1	Hot	1023	72	1016	65	1.08	1031	69
3	AIR-HEAT-2	Cold	188	296	195	303	0.70	-76	316
4	STRIPPER_Reb-1	Cold	151	152	157	159	291.41	-527	643
5	LEANHX-1	Hot	152	70	145	63	9.28	764	1907
6	H3-1	Hot	132	65	125	58	0.10	7	3429
7	H1-1	Hot	130	65	123	58	0.08	5	3429
8	H4-1	Hot	128	88	121	81	0.15	6	3429
9	H2-1	Hot	127	45	120	38	0.09	7	3429
10	STRIPCON-1	Hot	117	111	110	104	0.84	5	4330
11	STRIPCON-2	Hot	111	84	104	77	1.29	35	4330
12	H4-2	Hot	88	40	81	33	0.27	13	3429
13	STRIPCON-3	Hot	84	40	77	33	0.39	17	4330
14	RICHX-1	Cold	68	109	75	115	9.85	-398	1907
15	H1-2	Hot	65	40	58	33	0.14	3	3429
16	H3-2	Hot	65	40	58	33	0.14	3	3429
17	H2-2	Hot	45	40	38	33	0.15	1	3429
18	AIR-HEAT-1	Cold	22	188	29	195	0.69	-114	316

Figure 12: Format used on 'Processed Data' worksheet for evaluating the problem table algorithm.

4. The *Elements* procedure is used to fill in the last information which is the sequential 'Energy Requirement Number' and the ΔH which is calculated by multiplying the mass heat capacity (CP) and the temperature change (ΔT).
5. The excel '*Sort*' function is then used to sort the data in descending order based on the supply temperature.

6. A list of temperatures included in the problem table algorithm is established using the *TemplIntervals* procedure. The *TemplIntervals* procedure stores all the temperatures in an array of variables *Templnts()*, all supply and target temperatures are stored in the *Templnts()* array. All the temperatures in the *Templnts()* array are ordered in descending order. Any duplicate temperatures are removed from the list and then the final temperatures are listed across the top of the 'Interval Data worksheet'. In this instance we are trying to perform a pinch analysis so the temperatures that are used are the shifted supply (T_s^*) and target (T_t^*) temperatures.
7. The next step is to prepare the 'Interval Data' worksheet, which is done using the *IntData* procedure. This procedure calculates and lists the ΔT of between each temperature and lists them on the 'Interval Data' worksheet. The headings for the 'Energy Requirement Number' and the other elements required to be calculated for the problem table algorithm are listed and can be seen in the first column of the example provided in Figure 13.

Interval Data	1321	1016	303	195	159	157	145	125	123
ΔT		306	713	108	35	2	12	20	2
1		-1	0	0	0	0	0	0	0
2		0	-1	-1	-1	-1	-1	-1	-1
3		0	0	1	0	0	0	0	0
4		0	0	0	0	291	0	0	0
5		0	0	0	0	0	0	-9	-9
6		0	0	0	0	0	0	0	0
7		0	0	0	0	0	0	0	0
8		0	0	0	0	0	0	0	0
9		0	0	0	0	0	0	0	0
10		0	0	0	0	0	0	0	0
11		0	0	0	0	0	0	0	0
12		0	0	0	0	0	0	0	0
13		0	0	0	0	0	0	0	0
14		0	0	0	0	0	0	0	0
15		0	0	0	0	0	0	0	0
16		0	0	0	0	0	0	0	0
17		0	0	0	0	0	0	0	0
18		0	0	0	1	1	1	1	1
$\Sigma CP_c - \Sigma CP_h$		-1	-1	0	0	291	0	-10	-10
ΔH		-453	-773	-41	-14	527	-5	-193	-20
Heat Flow	0	453	1226	1267	1281	754	759	952	972
Positive Heat Flow	0	453	1226	1267	1281	754	759	952	972
ΣCP_h		1	1	1	1	1	1	10	10
ΣCP_c		0	0	1	1	292	1	1	1
ΔH_h		453	773	118	38	2	13	206	21
ΔH_c		0	0	76	24	529	8	14	1
Thot	1321	1016	303	195	159	157	145	125	123
CCHot	2352	1899	1126	1009	970	968	955	749	728
Tcold	1321	1016	303	195	159	157	145	125	123
CCcold	2352	2352	2352	2275	2251	1722	1714	1701	1699

Figure 13: Example of the layout and details included on the 'Interval Data' worksheet.

8. The CP of the stream segments that exist in each temperature interval is now added to the 'Interval Data' worksheet using the *CPData* procedure. This procedure uses the *StreamData()* array to store all the information of the stream segments. The array is a $n \times 5$ array where the n represents the number of stream segments included in the analysis, the five elements stored in the *StreamData()* array for each stream segment are; 0 = Energy Requirement Number, 1 = Hot or Cold stream designation, 2 = Shifted supply temperature (T_s^*), 3 = Shifted target temperature (T_t^*) and 4 = The mass heat capacity (CP) of the stream. The procedure then goes through, for each temperature interval, and determines which streams exist in that interval. The CP's of hot streams are considered negative and cold streams are considered positive. The sum of all of the hot stream CP's is calculated and likewise the sum of the cold stream CP's is evaluated. The summation of the cold streams CP's minus the hot streams CP's is calculated and listed, followed by the ΔH , which is calculated by multiplying the previous result by the temperature interval ΔT . The 'Heat Cascade' or 'Heat Flow' is also calculated for each temperature interval, which is the summation of the negative ΔH of all the proceeding temperature intervals from the hottest temperature down to the coldest temperature. The sum of hot and cold CP's and ΔH 's are also listed on the 'Interval Data' worksheet.
9. This information allows the pinch point to be determined using the *PosHeatFlow* procedure. The pinch point is where the heat cascade is at the minimum point. If the heat cascade has a negative energy at the pinch point then sufficient hot utility is added to the heat cascade to make the heat available in every temperature interval at least greater than, or equal to, zero. The new positive heat cascade is provided on the 'Interval Data' worksheet. This also defines the grand composite curve; the temperatures are provided by the list of temperatures and the positive heat flow provides the available enthalpy in the system at those temperatures.
10. The hot and cold composite curves are also able to be calculated using the *CompCurves* procedure. The temperatures are the same as the temperatures used in the grand composite curve. The enthalpy values for both the hot and cold composite curves are determined from the lowest temperature to the highest temperature (in reverse order to how they are listed on the 'Interval Data' worksheet). The hot composite curve always starts with an enthalpy of zero at the lowest temperature and then the other enthalpy values are calculated by summing all of the ΔH of the hot streams. Whereas the cold composite curve will always start off with the enthalpy equal to the residual heat in the grand composite heat cascade, which represents the required cold utility, as the initial enthalpy at the lowest temperature. The other enthalpy values are then calculated by summing the cold stream ΔH values with the residual cold utility requirements for each temperature interval.

11. There are also procedures that can be used to plot either the grand composite curve (*PlotGCC*) or the hot and cold composite curves (*PlotCompCurves*), but these are not used explicitly in the SHICE program so they do not slow down the optimisation.

4.5 Step 9 – Post Pinch Analysis Processing

The post pinch analysis processing involves using the grand composite curve and determining the maximum amount of power that can be generated using the steam system described in Step 3. This requires the use of a set of linear equations explained in further detail in the following steps. The post pinch analysis is performed using the *LPOptimisation2* procedure. Subsequently the balanced composite curves can be generated, with the *Balanced_CC* procedure, which are then used to estimate the required heat exchanger area in the *AreaTargeting* procedure.

4.5.1 LPOptimisation2

A new user defined data Type *SteamCurve* is required for this procedure, the details of *SteamCurve* can be found in Table 4. Two instances, *Steamlevels()* and *SteamLevelsUse()*, of the *SteamCurve* are created and used in the *LPOptimisation2* procedure or sub procedures.

1. The first step is to calculate the amount of power that is generated by each unit of steam going through each section of the turbine which is determined in the *PowerLossCoeff* procedure. This procedure uses the 'SteamInfo' worksheet (See Step 3 and Figure 3) as the basis. The program cycles through each of the steam levels listed on this worksheet and sets the flow rate equal to 1 kg/s whilst all other flow rates are set to zero. The amount of power then generated in the turbine for each steam level is calculated by the worksheet and the result is added back to the worksheet under the heading 'PC' (Refer to Figure 3).
2. The next step involves determining how many temperatures are used to define the GCC of the process and storing those temperatures in the *GCCTIs()* array.
3. Then the *GenSteamData* procedure is used to generate the temperature-enthalpy relationships for each steam level. This procedure has multiple sub procedures to complete this task. The temperature-enthalpy relationship can be based on a unit of steam or on the actual flow rate of the steam level as defined on the 'SteamInfo' worksheet. In the sequence described here, the first use of the *GenSteamData*, called from the *LPOptimisation2* procedure, the temperature-enthalpy relationship is based on a single unit of steam for each steam level. Firstly, the data on the 'UtilityStreamData' worksheet is deleted and the heat transfer coefficients for subcooled water, steam generation/evaporation and superheated steam are obtained from the user defined values on the 'SteamInfo' worksheet. Then for each steam level the temperature-enthalpy relationship is calculated.

Table 4: Properties defined in the user defined type *StreamCurve* which is used to store the stream data in *Steamlevels* and *SteamlevelsUse* – used in the *LPOptimisation2* procedure.

Property	Description	#	Element Description
.StmNme	Name of the steam level	1	
.Ti	Temp. of the steam level	1	
.Tf	Temp. of the condensate level	1	
.Pi	Pressure of the steam level	1	
.Xi	Dryness fraction of steam level	1	
.Hi	Enthalpy of the steam level	1	
.Ho	Enthalpy of the condensate	1	
.Flow	Flow rate of the steam level	1	
.DT	ΔT_{\min} of the steam level	1	
.PLC	Power coeff. of the steam level.	1	
.Tsats	Saturation temperature of the steam level	1	
.HsatV	Enthalpy of saturated vapour	1	
.HsatL	Enthalpy of saturated liquid	1	
.THData()	Temperature-Enthalpy data	2 x n	n refers to the number of data points required to represent the T-H relationship 1 Temperature 2 Enthalpy
.TEMCPHTC()	To store the steam curve lines	5 x (n-1)	n refers to the number of data points required to represent the T-H relationship 1 Temperature Start 2 Temperature End 3 ΔH 4 $CP = \Delta H / (\text{Temperature End} - \text{Temperature Start})$ 5 Heat transfer coefficient
.IntervalCount	No. of points to define T-H after cleaning up the data.	1	
.Temp()	List of temps. including $\pm \frac{1}{2} \Delta T_{\min}$	1 x n	n refers to the number of data points as defined by the interval count
.Enth()	List of enthalpies	1 x n	n refers to the number of data points as defined by the interval count

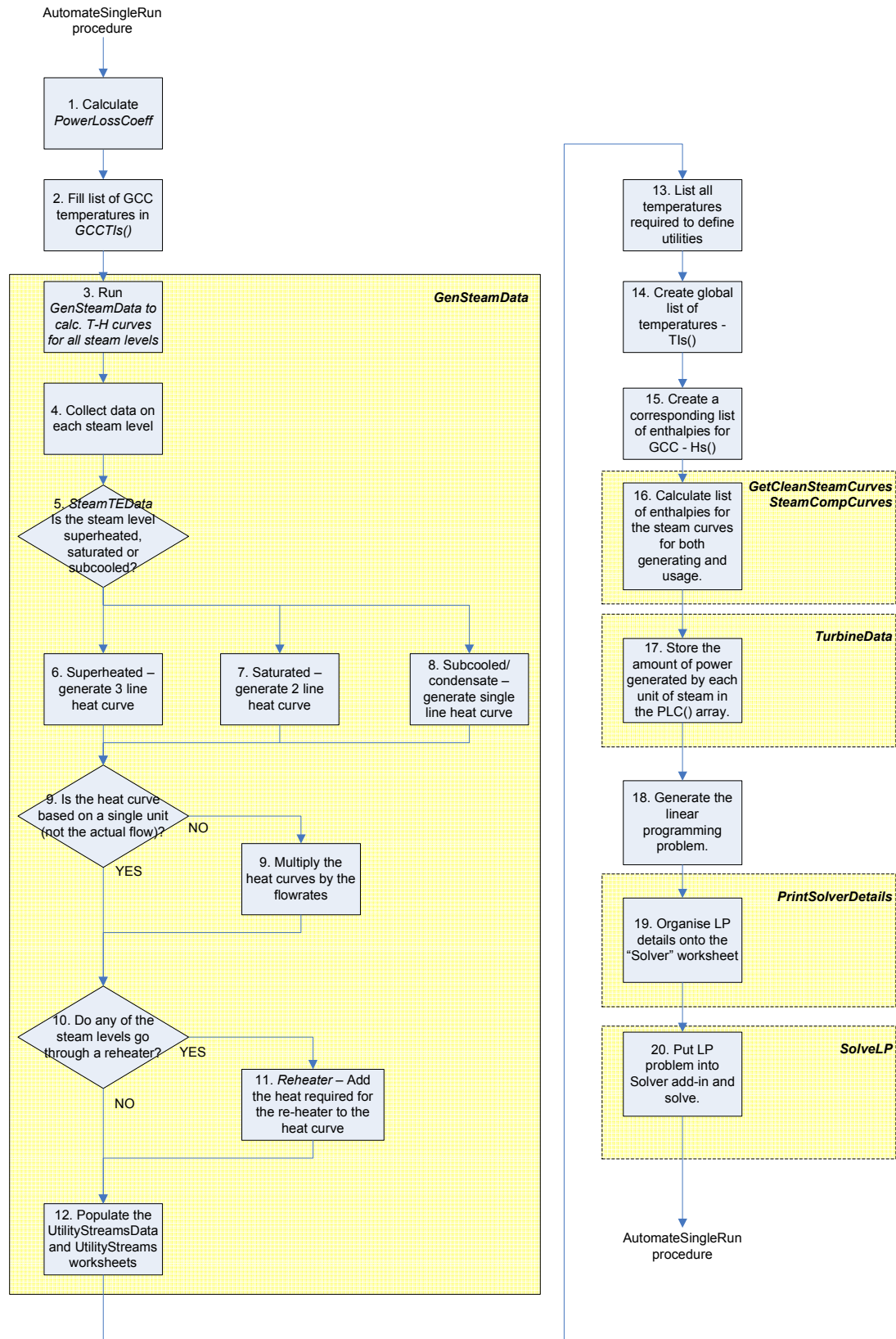


Figure 14: Representation of the algorithm used in the LPOptimisation2 procedure used to calculate the optimum steam rates for the given grand composite curve.

4. The data for the steam level is transferred from the 'SteamInfo' worksheet into the *SteamLevel()* variable including the Name, temperature and enthalpy of the steam level and the condensate, the pressure, dryness fraction, flow rate, ΔT_{\min} and power coefficient. This data is sufficient to generate the temperature, enthalpy and heat transfer coefficient data which is created using the *SteamTEData* procedure.
5. The saturation temperature and the enthalpy of the saturated water and steam are calculated for the steam level, using functions from the 'X-Steam' program, and stored in the *Steamlevel()* variable. Three options exist for the steam level, depending on the conditions of the steam; it may be superheated, saturated or a subcooled stream. Using the enthalpy (H_i) of the steam level as the basis, three different procedures will be called depending on the quality of the steam.
6. Superheated steam is represented by four temperature-enthalpy data points, so three straight lines. The four data points are the superheated steam inlet, the saturated steam, the saturated water and the final sub-cooled condensate point. The temperature-enthalpy data is stored in the *.THData()* variable. As the problem table algorithm requires boiling/evaporating streams to be represented with a non-zero gradient the saturated steam temperature is increased by 0.1 °C and the saturated water temperature is lowered by 0.1 °C. The enthalpy stored in *.THData()* is the difference between the enthalpy at the given temperature and the original steam level enthalpy. The *.TEMPHTC()* variable data also used to store the information required to represent the heat curve as three lines; temperature in, temperature out, ΔH , heat capacity and the heat transfer coefficient.
7. Saturated steam is represented by three temperature-enthalpy data points and therefore two straight lines. The data points include the initial steam condition, saturated liquid and the final condensate. The initial steam condition can include steam that is not completely dry, as the initial steam point enthalpy is taken as the actual steam level enthalpy not the saturated vapour enthalpy. The data for these streams is calculated and stored in *.THData()* and *.TEMPHTC()*.
8. Subcooled liquid is represented by a single straight line and therefore two temperature enthalpy data points which are defined from the initial steam level conditions and the final condensate conditions. The data for these are also stored in the variables *.THData()* and *.TEMPHTC()*.
9. Once the heat curves have been defined per unit of steam, then if the instance of *GenSteamData* is to represent the actual steam flow rates then the ΔH , CP and enthalpy are multiplied by the flow rate to get the heat curve based on the total flow rate.

10. Any steam levels that pass through a reheater as they travel through the steam cycle need to have the heat curves adjusted for the amount of energy added to the steam in the reheater. At the moment, this requires the user to explicitly add the streams that pass through a reheater to the code. In the example code below the first two streams pass through the reheater. The *Reheater* procedure is then used for each stream that passes through the reheater to add the heat required for the reheater to the heat curves.

```
For StmID = 1 To 2  
    Call Reheater(Steamlevel, StmID, IncFlow)  
Next StmID
```

11. The temperature, pressure and enthalpy of the stream on the outlet of the reheater is collected from the 'SteamInfo' worksheet. The inlet conditions to the reheater are, for the given structure, equal to the same conditions as the second steam level. If the reheater conditions are different then the code for the reheater will need to be modified. A list of temperatures is created combining the temperatures that represent the heat curve of the stream and the inlet and outlet temperatures of the reheater. The temperature list is sorted and duplicate temperatures are removed. The enthalpy of the steam at every temperature is calculated by interpolation, likewise the enthalpy of the reheat is also calculated. The list of temperatures then replace the temperatures in the *.THData()* variable of the steam level and the corresponding enthalpy is the sum of the enthalpy of the original steam heat curve plus the reheater heat curve. The *.TEMCPHTC()* variable is then also changed to include the new reheater data.
12. Now that the heat curves for all the steam levels have been calculated the data is populated into the 'UtilityStreamData' worksheet. The steam level or ID, name, enthalpy, temperature and ΔT_{\min} is added to the worksheet, as the heat curves are built with minimal number of lines and would benefit little by linearisation, the data is put in both the raw data columns and the clean data columns in the 'Utilitystreamdata' worksheet. The information is also populated in the 'UtilityStreams' worksheet which is analogous to the 'Streams' worksheet but contains the information for the steam cycle. The *GenSteamData* procedure is now finished and we return to the main *LPOptimisation2* procedure.
13. After the steam cycle heat curve data populates the worksheets, all the temperatures that define the steam cycle heat curve are added to the *UteTIs()* array. Two more arrays are created from this array; *UteTIsGen()* and *UteTIsUse()*. These arrays store the temperatures that define the steam cycle heat curves, but shifted to account for if the heat curves are used for steam generation or steam extracted from the turbine to be used for heating

requirements. The *UteTIsGen()* list increases the temperatures by half the streams ΔT_{\min} , whereas the *UteTIsUse()* list decreases the temperatures by half the streams ΔT_{\min} . This is so that ΔT_{\min} between the steam heat curves and the GCC for any two streams will be equal to the sum of half of each of ΔT_{\min} of each stream.

14. The next step is to make a list of all temperatures that are used to define the GCC and the steam heat curves. This is achieved by joining the *GCCTIs()*, the *UteTIsGen()* and the *UteTIsUse()* arrays into one array called *TIs()*. This array is then sorted and duplicate temperatures are deleted.
15. Once the list of temperatures has been created the enthalpies that correspond to the temperatures in the *TIs()* array need to be calculated. Obviously a lot of those enthalpies are already defined for all the temperatures in the *GCCTIs()* array, these enthalpies are located on the 'Interval Data' worksheet and are in this step copied into the *GCCH()* array. A new array of enthalpies, *Hs()*, is created to accommodate the enthalpies that correspond to all the temperatures in the *TIs()* array. The values in the new *Hs()* array is calculated using the enthalpies in the *GCCH()* array where corresponding temperatures exist in the *GCCTIs()* array and by interpolation when the temperatures do not exist.
16. Now that the values for the GCC for all the temperatures has been determined, the enthalpy for each of the steam curves needs to be calculated for all the temperatures in the *TIs()* array. This is achieved by the procedure *GetCleanSteamCurves* and *SteamCompCurve*.
GetCleanSteamCurves gets the temperature-enthalpy data for each steam level from the 'UtilityStreamData' worksheet, in particular the temperature and enthalpy values. The temperatures are shifted temperatures that are increased by half the streams ΔT_{\min} for the *Steamlevels()* variable representing the generation curves and decreased by the same amount for the *SteamlevelsUse()* variable representing the steam extracted from the turbines. The *SteamCompCurve* procedure converts the *.Temp()* and *.Enth()* data in the *Steamlevels()* and *SteamlevelsUse()* variables into a full list for temperatures and enthalpies corresponding to all temperatures in the *TIs()* array into the variables *SCCGen()* and *SCCUse()*. The actual enthalpy is calculated using the *SteamH* procedure, and equals the difference in energy between steam at the temperature provided by *TIs()* array and the final state of the steam, ie that of condensate, taking into account that the temperature is the shifted temperature as defined by the *.Temp()* and *.Enth()* data. *SCCGen()* and *SCCUse()* will be slightly different due to the use of shifted temperatures.
17. The next step is to store the amount of power that can be generated by each unit of steam calculated in the *PowerLossCoeff* procedure for each steam level into the *PLC()* array.

18. Now all the required data has been calculated, we need to arrange the linear programming problem to be solved. The linear problem is arranged in the 'Solver' worksheet using the *PrintSolverDetails* procedure, then added to the MS Excel Solver add-in using the *SolveLP* procedure. The following details are for setting up the linear problem for the superstructure method. The equations and matrix form of the problem can be found in detail in Chapter 4.
19. The *PrintSolverDetails* procedure starts by clearing all previous contents on the 'Solver' worksheet. Headings are then added as per the cells coloured grey in Figure 15, which shows a steam network with three steam levels. The power coefficients for the steam levels are also added, they are positive for steam that is generated and negative for steam that is extracted from the turbine. The temperatures are added from *TIs()* array to the second column and the corresponding enthalpies that define the grand composite curves are added from the *Hs()* array into the column under the heading 'GCC H'. The data in the columns titled 'StmGen' and 'StmUse' is extracted from the *SCCGen()* and *SCCUse()* arrays. The 'StmUse' data added to the sheet is the negative value of the *SCCUse()* value. The values in the columns under the titles 'LHS', 'SCC' and 'PinchPoint' are calculated by formulas that are entered into the 'Solver' worksheet by the *PrintSolveDetails* procedure. The three formulas are provided below;
- LHS: '=SUMPRODUCT(RC[-9]:RC[-4],R2C3:R2C8)', This calculates the sum of the product of the steam flow rate and the energy in the steam at each temperature. Obviously the row and columns will vary depending on the number of steam levels, but this is taken into account automatically.
 - SCC: '=R4C[-1] - RC[-1]', This represents the steam composite curves.
 - PinchPoint: '=IF(ABS(RC[-1] - RC[-4])<0.001,1,0)' This identifies the location of the points where the steam composite curves pinches with the grand composite curve. Pinch points are designated by the number '1'.

Variables	T	StmGen1	StmGen2	StmGen3	StmUse1	StmUse2	StmUse3	GCC H	Sign	LHS	SCC	PinchPoints
Solution		433	27.4642	0	0	0	460.4642					
Objectives		1.420464	1.120238	0.907506	-1.42046	-1.12024	-0.90751	Maximise	=	227.9534		
Constraint 1	1321.429	3.663115	3.344687	3.124945	-3.66311	-3.34469	-3.12495		>=	239.0624	0	1
Constraint 2	1015.629	3.663115	3.344687	3.124945	-3.66311	-3.34469	-3.12495	453.0476	>=	239.0624	0	0
Constraint 3	544.9412	3.663115	3.344687	3.124945	-3.66311	-3.34469	-3.12495	963	>=	239	0	0
Constraint 4	531.0588	3.568352	3.311343	3.124945	-3.66311	-3.34469	-3.12495	978	>=	197	42	0
Constraint 5	435.627	2.916924	3.082126	3.124945	-3.01169	-3.11547	-3.12495	1081.888	>=	-91.2492	330.3115	0
Constraint 6	421.7447	2.822162	3.048782	3.092121	-2.91692	-3.08213	-3.12495	1096.939	>=	-133.197	372.2595	0
Constraint 7	358.379	2.38962	2.896584	2.942298	-2.48438	-2.92993	-2.97512	1165.641	>=	-255.679	494.7417	0
Constraint 8	356.4025	2.380876	2.890505	2.937625	-2.47089	-2.92518	-2.97045	1167.784	>=	-257.481	496.5432	0
Constraint 9	356.2025	1.478655	2.88989	2.937152	-2.46953	-2.9247	-2.96998	1168	>=	-647.941	887.0036	0
Constraint 10	344.4966	1.421831	2.853889	2.909475	-2.38962	-2.89658	-2.9423	1180.692	>=	-660.79	899.8528	0
Constraint 11	342.5201	1.412236	2.847811	2.904801	-2.38088	-2.89051	-2.93763	1182.835	>=	-662.96	902.0224	0
Constraint 12	342.3201	1.411265	2.847196	2.904328	-1.47866	-2.88989	-2.93715	1183.052	>=	-663.18	902.2419	0
Constraint 13	324.5102	1.32481	2.792422	2.862218	-1.3922	-2.83512	-2.89504	1202.361	>=	-682.729	921.7914	0
Constraint 14	310.6279	1.25742	2.749728	2.829395	-1.32481	-2.79242	-2.86222	1217.413	>=	-697.967	937.0297	0
Constraint 15	303.0412	1.220591	2.726395	2.811457	-1.28798	-2.76909	-2.84428	1225.638	>=	-706.295	945.3574	0
Constraint 16	51.74905	0.000728	0.00066	0.000645	-0.06812	-0.06173	-0.06038	1232.615	>=	-27.4695	266.5319	0
Constraint 17	51.64905	0.000243	0.00022	0.000215	-0.06763	-0.06129	-0.05995	1232.649	>=	-27.4937	266.556	0
Constraint 18	51.59905	0	0	0	-0.06739	-0.06107	-0.05973	1232.665	>=	-27.5057	266.5681	0
Constraint 19	37.8667	0	0	0	-0.00073	-0.00066	-0.00065	1237.22	>=	-0.2972	239.3596	0
Constraint 20	37.7984	0	0	0	-0.0004	-0.00036	-0.00035	1237.243	>=	-0.16188	239.2243	0
Constraint 21	37.7667	0	0	0	-0.00024	-0.00022	-0.00022	1237.256	>=	-0.09907	239.1615	0
Constraint 22	37.7167	0	0	0	0	0	0	1237.275	>=	0	239.0624	0
Constraint 23	33.06882	0	0	0	0	0	0	1239.104	>=	0	239.0624	0
Constraint 24	33.05882	0	0	0	0	0	0	1239.104	>=	0	239.0624	0
Constraint 25	29.09118	0	0	0	0	0	0	1236.379	>=	0	239.0624	0
		433	433	460.4642	460.4642	460.4642	0					

Figure 15: Example of the setup for the linear program.

20. The *SolveLP* procedure uses the MS Excel Solver Add-in to solve the LP problem set up in the 'Solver' worksheet. Obviously the Solver add-in needs to be installed on the version of Excel used, and the 'SOLVER' reference must also be selected in the VBAProject reference list. The Solver add-in only accepts references in the 'A1' Excel format; however it is much easier to set-up the problem using the 'RC' format as the relative references can include coding to allow for changes to the references depending on how many steam levels are used. Therefore, the formulas are created using the 'RC' format and the in-built VBA *ConvertFormula* function converts the formula to the 'A1' format. The Solver add-in is reset and then the following formulas are created and added to the Solver add-in. Where absolute values for the row or column number are given below, they may actually be coded to change depending on the number of steam levels or constraints exist. More details on how to operate the Solver add-in from VBA can be found in VirginiaTech (2010).

- strObjFunc: '=R3C12', This is the objective function which is the total amount of power generated by the steam turbine, it is calculated on the 'Solver' worksheet as the sum of the steam flowrates multiplied by the corresponding power coefficient. This is added to the Solver add-in as the 'Target' cell using the 'SolverOk' function and set to be maximised by changing the range of cells 'strVarsA1' which is the 'A1' representation of the 'strVars' formula.
- strVars: '=R2C3:R2C8', These are the steam flowrates. They are the cells that are adjusted to maximise the steam turbine power generation.

The two proceeding points are used to set up the linear problem objective. Now the constraints need to be added. The first set of constraints is that the steam composite curve must be less than or equal to the grand composite curve at all temperatures. Therefore, the number of constraints is equal to the number of temperatures in the *Tls()* array. Each constraint is added to the Solver add-in using a loop in VBA, with 'i' in the following points being used as a counter for each row that represents each temperature;

- strLHS: '=R(i+4)C13', This refers to the enthalpy of the SCC.
- strRHS: '=R(i+4)C10', This refers to the enthalpy of the GCC.

Using the 'SolverAdd' function (see below), 'strLHSA1' which the 'A1' representation of 'strLHS', is added as the cell reference. The relation is equal to 1, which is the 'less than or equal to relation' and the constraint 'strRHSA1' is added which is the 'A1' representation of 'strRHS'.

```
SolverAdd cellref:=strLHSA1, Relation:=1, Formulatext:=strRHSA1
```

The next set of constraints is that steam can only be extracted from the turbine if there has been sufficient steam generated. Firstly the cumulative steam flow is calculated on the 'Solver' worksheet as shown as the last row in Figure 15. Formulas are exported from VBA to the cells. The formulas are in the following form; StmGen1, StmGen1 – StmUse1, StmGen1 – StmUse1 + StmGen2, StmGen1 – StmUse1 + StmGen2 – StmGen2, this pattern continues till the final steam level. These cells are then added to the Solver add-in as a constraint that they must all be greater than or equal to zero.

Further constraints can be added directly to the solver add-in if certain steam flow rates are constrained. For example, if the main steam rate should be equal to a given value, for example 433 kg/s, then the following code would ensure this is the case.

```
SolverAdd cellref:="$C$2", Relation:=2, Formulatext:=433
```

The solver options shown below are also included; It is important to assume that the solver is linear to speed up the solver completion time as the problem is a linear problem by definition. Assuming that the cell values are non-negative is also important to ensure that the steam flow rates are real non-negative values.

```
SolverOptions MaxTime:=100, Iterations:=100, Precision:=0.000001, AssumeLinear _
:=True, StepThru:=False, Estimates:=1, Derivatives:=1, SearchOption:=1, _
IntTolerance:=5, Scaling:=False, Convergence:=0.0001, AssumeNonNeg:=True
```

The Solver add-in is then run using the code '*mySolverResult = SolverSolve(True)*', which ensures that the solver add-in is run without returning a dialog box, which is important to maintain the uninterrupted repetition of the SHICE program. A diagnostic value is returned to the *mySolverResult* variable. If the diagnostic value is zero, then a solution could not be found for the problem. This could occur for a number of reasons; one of those may be if the reboiler duty is greater than the amount of heat generated by the combustion of the coal. If a solution cannot be found, then all steam flowrates are set to zero and therefore no power is generated for this solution. If a solution has been found, then the Solver add-in is finished and the optimal steam rates are saved - '*SolverFinish(1)*'. Both the *SolveLP* and *LPOptimisation2* procedures are now complete and we are returned to the *AutomateSingleRun* procedure to create the balanced composite curves.

4.5.2 Balanced_CC

The *Balanced_CC* procedure calculates the balanced hot and cold composite curves which includes all the streams, including the steam cycle and the turbine condenser.

1. Now that the optimum steam flowrates have been determined, the steam cycle is fully defined. The optimum steam flowrates are transferred from the 'Solver' worksheet to the 'SteamInfo' worksheet. Obviously, in the 'SteamInfo' worksheet there is only room for one flow rate per steam level. Therefore, both the 'StmGen' value and the 'StmUse' value from the 'Solver' worksheet is obtained and if the 'StmGen' doesn't equal zero then this is used as the value, if 'StmUse' doesn't equal zero then the negative of this value is used as the flow rate.
2. The utility stream data is calculated using the *GenSteamData* procedure which is explained in section 4.5.1 step 3. However, this time the flow rate is included so the temperature-enthalpy relationship is dependent on the flow rate of the steam.
3. The steam data is now stored on the 'UtilityStreamData' and the 'UtilityStreams' worksheets. However, streams that represent steam generation are arranged with an inlet temperature greater than the outlet temperature and a negative enthalpy. Therefore, the inlet and outlet temperatures are swapped and the enthalpy, which is calculated by the CP multiplied by the difference between the outlet and inlet temperature, will become positive. The CP of the streams representing steam extracted from the turbine are initially stored as negative values,

these are changed to positive values and therefore the enthalpy of these streams will become negative as the change in temperature is negative.

4. The *OrgStreamData* procedure is now called (See section 4.4.3); this time both the utility and stream data is used. In overview, this procedure gets the data from both the 'Streams' and 'UtilityStreams' worksheets, adds them to the 'Balanced Data' worksheet, and performs the problem table algorithm in the 'Balanced Interval Data' worksheet.
5. At this point the curves will be balanced except for the total cooling duty. This can be calculated as it is simply the cooling duty that is left between the hot and cold composite curve and can therefore be found as the starting enthalpy of the cold composite curve. The starting enthalpy is the value stored in the last cell on the 'Balanced Interval Data' worksheet on the row that defines the cold composite curve (CCcold). The cooling water flow (kg/s) is calculated assuming a $CP\Delta T$ of 0.0418 MJ/kg and returned to the worksheet 'CoolingUtilities' where the cooling water data is stored. This infers a cooling water temperature rise of 10 °C. If both air and cooling water cooling was to be included, this is where in the program the split could be calculated. The cooling water data is then copied from the 'CoolingUtilities' worksheet to the 'UtilityStreams' worksheet. Then the *OrgStreamData* procedure is run a last time using un-shifted temperatures to create the balanced composite curves, including the water with the actual ΔT between the hot and cold curves shown.

4.5.3 Area Targeting

The area targeting methodology that is provided in Appendix D has been programmed in the *AreaTargeting* procedure. It uses the data from the un-shifted balanced composite curves as the basis for the heat exchange ΔT and the film heat transfer coefficients specified for each stream.

1. Using the *CompCurveDetails* procedure the hot and cold composite curves are collected from the 'Balanced Interval Data' worksheet and stored in the arrays *HotCC()* and *ColdCC()*. The arrays store the enthalpy and temperature in a $2 \times n$ array where the n refers to the number of elements required to define the composite curve. Any duplicate entries in the composite curves on the 'Balanced Interval Data' worksheet are deleted from the list stored in the arrays.
2. The area targeting method divides the composite curves into discreet enthalpy intervals. The enthalpy intervals are defined by wherever the hot or cold composite curves change. Therefore, the composite curves need to be arranged so that the temperature of the composite curve is defined at each and every enthalpy that is defined. This is completed in the *AddTemps* procedure. New arrays, *HotData()* and *ColdData()*, are used to store the

expanded composite curve data. These arrays are $3 \times 2n$ arrays, the first element is the enthalpy, the second the temperature, and the third is an indicator. Where n is the number of elements in the *HotCC()* and *ColdCC()* arrays and is twice as big as it needs to be, in order to contain all the enthalpy data from both composite curves. The *HotData()* array is constructed first. All the enthalpy and temperature data from the *HotCC()* array is copied into the first half of the *HotData()* array and all the third element in the first half of the array is changed to '1'. Then the enthalpies from the *ColdCC()* are added to the second half of the *HotData()* array and the third element for the second half of the array is set to '0'. Now we have a list of all the enthalpies used to define the hot and cold curves, but only the temperatures used to define the hot curve. The array is then sorted, based on the enthalpy, in descending order. Where the enthalpies have no corresponding temperature, as the indicated by the third element containing a '0', the temperatures are interpolated from the temperatures that do exist. The same process is used to get the *ColdData()* array.

3. The next step is to set up the 'AreaTargeting' worksheet using the *EnthIntervals* procedure with the list of enthalpies, the hot and cold temperatures that correspond to those enthalpies, the enthalpy difference between two adjacent enthalpies, the stream segment numbers and other headings as shown in Figure 16.

Enthalpy	3767.465	3767.465	3438.681	3314.417	3206.342	3202.424	2811.75	2789.045	2743.025	2696.469
ΔH		4.55E-13	328.784	124.2637	108.0752	3.917943	390.6747	22.70502	46.01996	46.55586
Hot T(°C)	1328.37	1328.37	1106.446	1022.57	922.8884	919.2747	558.9416	538	495.5542	452.614
Cold T(°C)	538	538	428.6859	387.3707	351.4378	349.4613	349.2613	338.791	317.5691	296.1
1		0	6499.504	6499.504	0	0	0	0	0	0
2		0	0	0	15664.11	15664.11	15664.11	15664.11	15664.11	15664.11
3		0	0	0	0	0	0	0	0	0
4		1256.144	1256.144	1256.144	1256.144	0	0	0	0	0
5		22.09596	22.09596	22.09596	22.09596	0	0	0	0	0
6		0	0	0	0	814.1461	0	0	0	0
7		0	0	0	0	0	390661.3	0	0	0
8		0	0	0	0	0	0	0	0	0
9		0	0	0	0	28.2922	28.2922	28.2922	28.2922	28.2922
10		0	0	0	0	0	0	0	0	0
11		0	0	0	0	0	0	0	0	0
12		0	0	0	0	0	0	0	0	0
13		0	0	0	0	0	0	0	0	0
14		0	0	0	0	0	0	0	0	0
$\Delta T(\text{Hot})$		0	221.924	83.87601	99.6816	3.613658	360.3331	20.94164	42.44585	42.94012
$\Delta T(\text{Cold})$		1.14E-13	109.3141	41.3152	35.93286	1.976506	0.2	10.47033	21.22192	21.46905
$\Sigma Q_{\text{onH}}(\text{Hot})$		0	1442396	545152.5	1561424	56604.74	5644298	328032.2	664876.5	672618.9
$\Sigma Q_{\text{onH}}(\text{Cold})$		1.45E-10	139729.7	52810.73	45930.81	1665.084	78137.93	8365.833	16956.4	17153.86
ΔT_{LM}		1024	732.6232	656.2497	602.7632	570.6316	360.2322	204.4	188.3979	167.0196
Area(m ²)		1.42E-13	2159.535	911.1824	2666.643	102.1146	15885.41	1645.783	3619.112	4129.891
Area Total (m ²)		31119.67								

Figure 16: Example of the layout of the Area Targeting worksheet

4. The final step is performed in the *CPonHData* procedure. Here the stream segment data is copied from the 'Balanced Data' worksheet into the *StreamData()* array. The information

stored in the *StreamData()* array includes, for all stream segments, the segment number, whether it is a hot or cold stream, the supply and target temperatures, the CP and the film HTC. Then for each enthalpy interval in turn, all the streams are tested to see whether they fall in that region. If they fall in that region then the streams CP divided by HTC is copied into the cell on the row that defines the stream and the column that defines the enthalpy interval. Also, the value of CP / HTC is added to the variable *QonHh* or *QonHc*, depending on whether the stream is hot or cold; this enables the sum of the hot and the sum of the cold streams CP / HTC to be calculated. After all streams in the enthalpy interval are completed the ΔT of the hot and cold streams in the enthalpy interval is calculated and stored on the 'AreaTargeting' worksheet, followed by the hot and cold sums of the enthalpy on the heat transfer coefficient - which is the *QonHh* or *QonHc* multiplied by the corresponding ΔT , then the log mean temperature difference in the enthalpy interval. All of this is then used to estimate the area of the enthalpy interval according to Equation [10](Smith (2005)). The total estimated area is then just the sum of all the areas for each enthalpy interval.

$$A_{INTERVAL} = \frac{1}{\Delta T_{LMk}} \left[\sum_i^{HOT\ STREAMS\ I} \frac{q_{i,k}}{h_i} + \sum_j^{COLD\ STREAMS\ J} \frac{q_{j,k}}{h_j} \right] \quad [10]$$

ΔT_{LMk}	= log mean temperature difference for the interval <i>k</i>
$q_{i,k}$	= stream duty on hot stream <i>i</i> in enthalpy interval <i>k</i>
$q_{j,k}$	= stream duty on hot stream <i>j</i> in enthalpy interval <i>k</i>
h_i, h_j	= film transfer coefficients for hot stream <i>i</i> and cold stream <i>j</i> (including wall and fouling resistances)
<i>I</i>	= total number of hot streams in enthalpy interval <i>k</i>
<i>J</i>	= total number of cold streams in enthalpy interval <i>k</i>

4.6 Step 10 – Calculate Objectives

This step is used to calculate the objectives of the optimisation program and any constraints that are set in the MOO program. In the example that follows to illustrate the procedure, the objectives are the DCOE and the CO₂ capture rate. The *AutomateResults* procedure is used to extract the variables that are in the Aspen Plus® 'RESULTS' calculator block and transfer them to the Excel worksheet named 'AspenTransfer'. Now any results that are required from the Aspen model have been imported into the SHICE program and can be used for the economic and energy analysis.

The capital costs of the equipment is calculated in the 'Economics' worksheet using the equations that are defined in Appendix B. Likewise the operating costs as described in Appendix C are calculated on the same 'Economics' worksheet. The operating cost data requires a number of

parameters on the net power generated by the power station, which are provided by the summary page 'EnergyResults'. On this worksheet the net power and the CO₂ avoided is calculated by importing the gross power from the steam turbines as determined by the linear programming and the auxiliary power requirements and CO₂ rates as imported from the Aspen model. The 'EconomicParameters' worksheet is then used to perform an NPV analysis of the capital and operating costs.

Now that the objective values have been calculated, the *AutomateMOORun* procedure calls the *GetOptimisationVariables* procedure to get the two objectives, the DCOE and the Capture rate from the 'EconomicParameters' worksheet and the 'EnergyResults' worksheet and store them in the *Opt()* variable. The *GetDecisionVariables* procedure is then used to store the decision variables listed on the 'AspenTransfer' worksheet into the *DVs()* array. Another procedure *WriteResults* is called from *AutomateMooRun* and is used to print the generation and population number, the simulation status (Success, warnings, errors etc), the objective values and the decision values and the number of attempts the simulation had to converge. These details are printed to a text file called 'Results.txt' which can be found in the same directory as the SHICE.xls program.

This completes the *AutomateMOORun* procedure and the control returns to the MOO program. As detailed in Section 4.1, the optimisation objectives are then transferred from the *Opt()* variable back onto the MOO MPI. Now under the control of the MOO program, the SHICE program will be called for every individual in the generation and runs through steps 7-10 for every individual (therefore NP times). The results of every individual are stored for comparison in step 11.

4.7 Step 11 – Objective comparison

All the objectives for the NP individuals in the generation have been calculated and stored along with the values of the decision variables that formed those results. After each generation has been evaluated the individuals from that generation are added to the NP best individuals from previous generations. The list is then ranked according to rules of the NSGA-II algorithm and the NP top ranking individuals are retained. The values of the decision variables for the next generation are determined by the NSGA-II genetic algorithm based on that NP group of individuals. The MOO and the SHICE programs continue to loop until the maximum number of generations (MG) is run.

4.8 Step 12 – Results

At the completion of the MG iteration the final NP top ranked individuals form the Pareto optimal solution and the results are presented in the 'Final Results' worksheet in the MOO Excel workbook. It is possible if the Pareto front does not look like it has reached a near optimal result to continue for more generations. This is completed by changing the 'LoadDNA' checkbox on the MOO MPI to 'Yes' and then running the MOO program again. This will continue the optimisation for a further MG generations using the results of the previous run as a starting point.

5. Conclusion

This appendix has detailed the main steps required for the combined multi-objective optimisation, simulation, heat integration and cost estimation used throughout the thesis. Clearly each problem that is detailed in the thesis requires modifications to be made to sections of this program; however the steps involved will remain similar to those outlined in this appendix.

References

- Aspen Plus (2003). Aspen Plus 12.1 User Guide, Aspen Technology Inc.
- Deb, K., A. Pratap, S. Agarwal and T. A. M. T. Meyarivan (2002). "A fast and elitist multiobjective genetic algorithm: NSGA-II." Evolutionary Computation, IEEE Transactions on 6(2): 182-197.
- Girardin, L., R. Bolliger and F. Marechal (2009). On the use of process integration techniques to generate optimal steam cycle configurations for the power plant industry. 12th international conference on Process Integration, Modelling and Optimisation for Energy Saving and Pollution Reduction (PRES'09), Rome, Italy.
- Holmgren, M. (2011). "X-Steam Tables for MS Excel version 2.6." Retrieved 16/9/2011, from http://www.x-eng.com/XSteam_Excel.htm.
- Shah, N., A. F. A. Hoadley and G. P. Rangaiah (2008). Multi-objective optimisation of multi-stage gas phase refrigeration systems. Multi-objective optimisation: Techniques and Applications in Chemical Engineering. G. P. Rangaiah, World Scientific Publishing Company Pty Ltd, Singapore.
- Sharma, S., G. P. Rangaiah and K. S. Cheah (2011). "Multi-objective optimization using MS Excel with an application to design of a falling-film evaporator system." Food and Bioprocess Processing doi: 10.1016/j.fbp.2011.02.005.
- Smith, R. (2005). Chemical Process Design and Integration. West Sussex, England, John Wiley & Sons Ltd.
- VirginiaTech. (2010). "Programming with Solver." Retrieved 1st Feb 2010, from http://www.nvc.vt.edu/rmajor/bit5474/Solver_Programming.doc.

Appendix B

Capital Cost Estimation Methodology for Process Design of Carbon Capture.

Cost functions and source data for the estimation of capital costs for use with process design studies of carbon capture at coal fired power stations in Australia

Contents

1. Introduction	182
2. Equipment Items.....	184
2.1 Feed Gas Fan	184
2.2 Solvent Pumps.....	185
2.3 CO ₂ compressor	186
2.4 Absorber.....	188
2.5 Stripper	189
2.6 Separation Vessels	189
2.7 Heat Exchangers.....	191
2.8 Steam Turbine	192
References	193
Appendix 1 - Feed Fan Capital Cost Function	194
Appendix 2 - Centrifugal Pumps Cost Curves.....	195
Appendix 3 - CO ₂ Compressor Cost Curves	196
Appendix 4 - Absorber Cost Curves	197
Appendix 5 - K-Factor Derating	199
Appendix 6 - Separator Vessel Sizing	200
Appendix 7 - Pressure Vessel Pressure Factor	201

1. Introduction

Capital costs for equipment are built up from cost curves/functions from literature or scaled from known equipment costs. Where only cost curves exist these have been converted to cost functions so that the cost can be generated automatically and the details of the cost function derivation are provided in the appendices. The cost functions will be generated at a specific currency and date; these are converted to Australian dollars using the average currency conversion of the year of the data generation (Refer to Table 1) and then adjusted to the required year (in the example the year 2008 is used) costs using the chemical plant cost indices (Refer to Table 2).

Table 1: Average yearly exchange rate for the Australian dollar versus other currencies (<http://www.rba.gov.au/statistics/hist-exchange-rates/index.html>).

Year	USD	GBP	EUR
1990	0.78	0.44	
1991	0.78	0.44	
1992	0.73	0.42	
1993	0.68	0.45	
1994	0.73	0.48	
1995	0.74	0.47	
1996	0.78	0.50	
1997	0.74	0.45	
1998	0.63	0.38	
1999	0.64	0.40	0.61
2000	0.58	0.38	0.63
2001	0.51	0.36	0.58
2002	0.55	0.36	0.58
2003	0.66	0.40	0.58
2004	0.74	0.40	0.59
2005	0.76	0.42	0.61
2006	0.76	0.41	0.60
2007	0.84	0.42	0.61
2008	0.85	0.46	0.57
2009	0.80	0.51	0.57

Table 2: Annual Chemical Engineering Chemical Plant Index (CEPCI) (Source Chemical Engineering Nov 2009, Nov 2000, Nov 1995)

Year	Index	Year	Index	Year	Index
1957-59	100	1995	381	2002	396
1989	355	1996	382	2003	402
1990	358	1997	387	2004	444
1991	361	1998	390	2005	468
1992	358	1999	391	2006	500
1993	359	2000	394	2007	525
1994	368	2001	394	2008	575

Table 3: Nomenclature

SYMBOL	DESCRIPTION	UNITS
a,b,c,d,e,f,g,h,i	Constants for equations when curve fitting the cost curves	
A	Area	m ²
C	Cost of the equipment in Australian dollars unless otherwise stated.	\$
D	Diameter	m
f	Metal Design Tensile Strength	kPa
F _p	Pressure factor	
H	Height of vessel	m
K	K-Factor for sizing separators	m/s
L _{RT}	Liquid residence time	s
m	Mass Flow	kg/s
mCO ₂	Mass of CO ₂	kgCO ₂ /s
N	Number of trains / units	
p	Power	kW
P	Pressure	kPa
P _d	Design pressure	kPa
ΔP	Pressure increase/decrease	kPa
Q	Volumetric Flowrate	m ³ /s
t	Vessel metal thickness	mm
V	Velocity	m/s
W	Weight	kg
Φ	Pump capacity factor (Q×ΔP)	m ³ .kPa/s
η	Welded joint efficiency	
ρ	Density	kg/m ³
Subscripts		
1, 2	Identifier, when comparing two pieces of equipment	
Absorber	CO ₂ Absorber	
Compressor	CO ₂ Compressor	
Fan	Feed gas blower	
I	Inlet	
ko	Knockout Drum	
L	Liquid	
O	Outlet	
Pump	Solvent pump	
ref	Reference factor (parameter for equipment item with known capital cost).	
ST	Steam Turbine	
v	Vessel	
V	Vapour	
hx	Heat exchanger	

2. Equipment Items

Each type of equipment item is detailed in the following sections with the reasons for the selection of the type of the equipment detailed. For each item the method of sizing the equipment to sufficient detail for the capital cost estimation to occur is detailed and the cost functions are provided. In some cases there are more than one cost functions, each is detailed and an example calculation is provided for each equipment item to help identify the most appropriate cost function for the service.

2.1 Feed Gas Fan

The flue gas that is fed to a solvent plant for post combustion will usually require a fan to provide driving force to enable the flue gas to proceed through the absorber. The pressure increase is small but the flowrate will be large. These fans will be similar to power station forced draft and induction fans and may replace the existing induction fans that are supplied upstream of the power station stack. Power stations forced draft and induced fans may be axial or centrifugal. Axial fans typically have higher capital costs but better efficiencies over a range of flowrates using variable pitch blades. Centrifugal fans dominate in induced draft applications as they handle particulates better than axial and can also generate more head with a single stage.

The isentropic efficiency of centrifugal fans with backward curved (or airfoil) blades will generally be greater than 80% (Drbal et al. (1996)). Maximum size of fans is shown in Sinnott (1998) as approximately 140 m³/s for centrifugal fans and 280 m³/s for axial fans. Although GPSA (2004) and Peters et al. (2003) have maximum sizes lower than Sinnott. Campbell (1992) recommends centrifugal for flowrates between 0.1 and 60 m³/s and axial for those greater than 30m³/s but has no upper size limit. There are four centrifugal induction fans at Hazelwood for each boiler with flowrates of 180 m³/s. There are two centrifugal forced draft fans with approximately 160 m³/s.

Feed Gas Fan Capital Cost Functions

The capital cost of the feed gas fan can be approached by two methods; the first is applied by Ho (2007) (Equation [1]) and Sinnott (1998) (Equation [2]) and is based on the cost of compressors correlated by the power requirements. The second method is from Peters et al. (2003) (Equation [3])(Appendix 1) which uses the volumetric flowrate.

$$C_{\text{Fan}} = 800p \quad \text{Cost Basis: \$A} \quad \text{Year Basis: 2005} \quad \text{Power Basis: kW} \quad [1]$$

$$C_{\text{Fan}} = 500p^{0.8} \quad \text{Cost Basis: £} \quad \text{Year Basis: 1992} \quad \text{Power Basis: kW} \quad [2]$$

$$C_{\text{Fan}} = 341Q + 1696 \quad \text{Cost Basis: \$US} \quad \text{Year Basis: 2002} \quad \text{Flowrate Basis: m}^3/\text{s} \quad [3]$$

Example

A single unit at Hazelwood, fan for carbon capture:

$$Q = 730\text{m}^3/\text{s}$$

$$\Delta P = 5\text{kPa}$$

$$p = 4470\text{ kW}$$

Assume maximum size of induction fan means four fans are required (only affects Equation [2]).

Table 4: Example of feed gas fan capital cost estimation

Equation	Raw Cost	Australian Cost	2008 Australian Cost (\$Million)
[1]	3576000	3576000	4.4
[2]	$4 \times 137268 = 549070$	1307310	2.1
[3]	250626	455684	0.7

2.2 Solvent Pumps

The solvent circulation requires between one and two sets of pumps depending on the relative pressure difference between the absorber and the stripper and the column heights. The solvent flowrate will range between approximately 15 and 40 kilograms of solution per kilogram of carbon dioxide for a potassium carbonate solvent system. Therefore, for Hazelwood between 500 to 3000 kg/s (1500 to 9000 m³/h) of solution for each unit. The head required will usually be less than 5 bar (50 m) but may be higher if high pressure regeneration is used. Due to the high flowrates and low pressure requirements single stage centrifugal pumps will generally be used (Sinnott (1998) Pg 185, Peters et al. (2003) Pg 509). The isentropic efficiency of centrifugal pumps at flowrates above of 1000 m³/hr should be greater than 80% (nominally 85%)(Peters et al. (2003) Pg 516).

Maximum size of pumps shown in Sinnott (1998) as 1x10⁵ m³/hr, GPSA (2004) and Peters et al. (2003) are less at 4000 and 2000 m³/hr, however the boiler feedwater pumps at Hazelwood can each handle flowrates greater than 4x10⁵ m³/hr. Therefore the maximum size has is considered to be 5x10⁵ m³/hr.

Solvent Pump Capital Cost Functions

The capital cost of the solvent pump will be estimated using the cost curves provided by Peters et al. (2003) (Pg 518) (Appendix 2). Ho (2007) and Sinnott (1998) do not provide a cost estimation method for pumps. The Peters et al. (2003) (Equation [4]) method uses the capacity factor (volumetric flowrate multiplied by pressure head) to estimate the cost of the pump, however the capacity factor is only relevant up to around 200 m³.kPa/s. Where typical solvent pumps will have

a capacity factor of around 1000 m³.kPa/s. Another method proposed is to scale the costs from a similar pump installed in a Benfield plant Furukawa and Bartoo (1997). The pump was for 5900 usgpm (1340 m³/hr) and cost \$1.037million installed. Therefore the purchase cost can be estimated by assuming Lang factor of four for pumps the purchase cost would be \$259k (Equation [5]).

$$C_{\text{pump}} = 10^{2.5+3.26 \log(\Phi) - 2.37 \log(\Phi)^2 + 0.62 \log(\Phi)^3} \quad \text{Cost Basis: \$US; Year Basis: 2002;} \quad [4]$$

$$\Phi: \text{m}^3/\text{s} \times \text{kPa}; \quad \text{Range: } \Phi < 200 \text{m}^3 \cdot \text{kPa}/\text{s}$$

$$C_{\text{pump}} = 259250(Q/Q_{\text{ref}}) \quad \text{Cost Basis: \$US; Year Basis: 1997;} \quad [5]$$

$$Q_{\text{ref}} = 0.372 \text{m}^3/\text{s}$$

Example:

Hazelwood lean solvent pump for carbon capture:

$$Q = 9000 \text{m}^3/\text{hr} = 2.5 \text{m}^3/\text{s}$$

$$\Delta P = 5 \text{bar} = 500 \text{kPa}$$

$$p = 1.15 \text{ MW}$$

$$\Phi = 1250 \text{m}^3 \cdot \text{kPa}/\text{s}$$

Table 5: Example of lean solvent pump capital cost estimation

Equation	Raw Cost	Australian Cost	2008 Australian Cost (\$Million)
[4]	187970000	3417648000	496 ^{Note 1}
[5]	1741000	2353000	3.5

Note 1: The capacity factor for this pump is five times greater than the recommended range of the equation.

2.3 CO₂ compressor

The CO₂ will be compressed to supercritical conditions (>72 bar) for transport to a storage site. The level of compression will depend on the distance to, and the quality of, the storage site or the distance and pressure level of the CO₂ network that the project is tying into. The basis for heat integration studies will be that 100 bar is required.

For this duty reciprocating compressors are not suitable due to the capacity of most CO₂ recovery projects Habel and Wacker (2009). Therefore there are three options considered for CO₂ compression in Australian conditions (Australian temperatures preclude the use of refrigeration of CO₂ into the liquid state); Single shaft compressor train, integrally geared compressor and shockwave compression. A single shaft compression train will generally have around four to five stages (with around 3 impellers for each stage) the polytropic efficiency starts at around 82% for

the first stage and decreases to 70% for the last stage Winter (2009). Integrally geared compressors enable the speed of each impeller to be set independently and therefore the efficiency will generally be higher and the CO₂ can be cooled between each impeller. Integrally geared compressors will generally have around 7-10 stages (Winter (2009), Habel and Wacker (2009)) and therefore will generally be more compact (less total number of impellers) and be more efficient. Shockwave compression enables compression ratios of approximately 10 and therefore will generally require only two stages of compression. The capital cost is expected to be approximately 50 to 60 % of a conventional integrally geared compressor Baldwin (2009).

Maximum compressor size for MAN Turbo is around 110 kg/s at 1.1 bar or 245000 Am³/h Habel and Wacker (2009).

CO₂ Compressor Capital Cost Functions

The capital cost of the CO₂ compressors can be approached by three similar methods; the first is applied by Peters et al. (2003) (Equation [6])(Appendix 3), the second by Sinnott (1998) (Equation [7]) and the third by Ho (2007)(Equation [8]). All equations are based on the compressors power requirements.

$$C_{\text{compressor}} = 873p^{0.9438} \quad \text{Cost Basis: \$US;} \quad \text{Year Basis: 2002;} \quad \text{Power Basis: kW} \quad [6]$$

Range: p = 80-6000 kW

$$C_{\text{compressor}} = 500p^{0.8} \quad \text{Cost Basis: £} \quad \text{Year Basis: 1992;} \quad \text{Power Basis: kW} \quad [7]$$

$$C_{\text{compressor}} = 800p \quad \text{Cost Basis: \$A;} \quad \text{Year Basis: 2005;} \quad \text{Power Basis: kW} \quad [8]$$

Example

CO₂ compressor for 90 % capture of a single unit from Hazelwood with a stripper at 1.5 bara, 4 stages of a single shaft compressor to 75 bar followed by a CO₂ pump (not included in the price).

$$m = 75 \text{ kgCO}_2/\text{s}$$

$$p = 21400 \text{ kW}$$

Table 6: Example CO₂ compressor capital cost estimation

Equation	Raw Cost	Australian Cost	2008 Australian Cost (\$Million)
[6]	10667404	19395280	28.2 ^{Note 2}
[7]	1456468	3467781	5.6 ^{Note 3}
[8]	17120000	17120000	21

Note 2: The power for this compressor is nearly four times greater than the maximum power of the cost curve the equation is derived from.

Note 3: The power for this compressor is more than forty times greater than the maximum power of the recommended for the equation.

2.4 Absorber

In a standard solvent plant the CO₂ absorber will be a metal absorption column. Plants of significant scale are likely to be built with unconventional designs and materials (such as concrete columns), however at this stage the costing is based on conventional metal columns with maximum diameter of 12.8m (Chapel and Mariz (1999)). The absorber columns of conventional equipment will invariably need to be made out of stainless steel to minimise corrosion.

Absorber Capital Cost Functions

The capital cost of the Absorber determined using the cost curves from Peters et al. (2003) (Equation [9]) (Appendix 4) for columns based on the column height, diameter, material (multiplier of 3 for stainless steel) and pressure factors (1 for atmospheric absorption). Another method is that used by Ho (2007) (Equation [10]), these costs are based on the number of absorber trains, absorber sizes are limited to 12.8 m and the costs are not affected by the height of the absorber. Absorber costs are around A\$12M per train in 2005. An alternative method for the absorber could be to base the costs on the metal weight as per the separation vessels described in section 2.6 which also allows for a pressure factor to be included.

$$C_{\text{absorber}} = 3 \times (-2244 + 2956D_v + 1241H + 1205D_v^2 + 913D_vH + 20.93H^2 - 42D_v^2H + 2.4D_vH^2 - 0.5H^3) \quad [9]$$

Basis: \$US; Year Basis: 2002;

Range: $D_v = 0.5 - 4\text{m}$, $H = 0.5 - 50\text{m}$

$$C_{\text{absorber}} = 12N \quad \text{Basis: \$A; Year Basis: 2005;} \quad [10]$$

Example

CO₂ absorber of a single unit from Hazelwood, which is 75 kg-CO₂/s at a 90 % capture rate. The height of the column is a variable in the simulation and a base height of 25 m was selected (20 m packing plus 3 m for sump and 2 m for liquid distribution and demister pad) the diameter of the column is provided by Aspen Plus and is 15 m. Given the maximum size is suggested as 12.8 m then two columns would be required with diameters approximately of 10.6 m ($D_{v2} = D_{v1} \sqrt{(A_2/A_1)}$).

Table 7: Example of Absorber capital cost estimation

Equation	Raw Cost	Australian Cost	2008 Australian Cost (\$Million)
[9]	$2 \times 3 \times 340482 = 2042893$	3714351	5.4
[10]	24000000	24000000	29.5

2.5 Stripper

In a standard solvent plant the CO₂ stripper/regenerator will be a metal desorption column. Plants of significant scale are likely to be built with unconventional designs and materials, however at this stage the costing is based on conventional metal columns with maximum diameter of 12.8 m Chapel and Mariz (1999). The stripper columns of conventional equipment will invariably need to be made out of stainless steel to minimise corrosion.

Stripper Capital Cost Functions

The capital cost of the stripper can be estimated using the same cost curves as for the absorber from Peters et al. (2003) (Equation [9])(Appendix 4) for columns based on the column height, diameter, material and pressure factors. Another method is that used by Ho (2007) (Equation [11]), her costs are based on the amount of CO₂ that is released from the stripper and is not affected by the height, diameter or number of strippers required. Stripper costs are around 160 A\$/kgCO₂/hr in 2005. Another method for the strippers could be based on metal weight as per the separator vessels as per section 2.6 which also allows for a pressure factor.

$$C_{\text{stripper}} = 3 \times (-2244 + 2956D_v + 1241H + 1205D_v^2 + 913D_vH + 20.93H^2 - 42D_v^2H + 2.4D_vH^2 - 0.5H^3) \quad [9]$$

Basis: \$US; Year Basis: 2002;

Range: $D_v = 0.5 - 4\text{m}$, $H = 0.5 - 50\text{m}$

$$C_{\text{stripper}} = 160 \times m_{\text{CO}_2} \times 3600 \quad \text{Basis: \$A; Year Basis: 2005} \quad [11]$$

Example:

CO₂ stripper of a single unit from Hazelwood, which at a 90 % capture rate is 75 kg-CO₂/s. The height of the column is a variable in the simulation and a base height of 20 m was selected (15 m packing plus 3 m for sump and 2 m for liquid distribution and demister pad) the diameter of the column is provided by Aspen Plus and is 10.6 m.

Table 8: Example of Stripper capital cost estimation

Equation	Raw Cost	Australian Cost	2008 Australian Cost (\$Million)
[9]	302893	550714	0.8
[11]	43200000	43200000	53.1

2.6 Separation Vessels

Separation vessel will be required for the compressor knock-out drums after each intercooler and the stripper separator. The knock out drums will be vertical knock-out drums with demister pads, (the stripper separator will also be designed vertically even though in the final design it is likely to be horizontal). The diameter will be sized using the K-Factor method (Equation [12]) with K

estimated from the values given in GPSA (1998) (Appendix 5) based on the pressure and the service of the separator vessel (Equation [13]). The vessel height is then calculated using Figure 1 and the vessel thickness is calculated using guidelines from AS1210 to calculate the minimum thickness of the vessel based on the longitudinal weld calculated by (Equation [14]) plus the corrosion allowance assumed to be 3 mm. The vessel thickness will be based on stainless steel 304 which has a design tensile strength of 80 MPa at 300 °C, a class 2 vessel construction with a welded joint efficiency of 0.85 (Appendix 6).

$$D_v(m) = \sqrt{\frac{4Q}{\pi \cdot K \sqrt{(\rho_L - \rho_v) / \rho_v}}} \quad [12]$$

$$K (m/s) = 0.11 \times 0.7 \times 135 \times P^{-0.0626} / 100 \quad [13]$$

$$t = \frac{P_d D}{2f\eta - P_d} + 3 \quad [14]$$

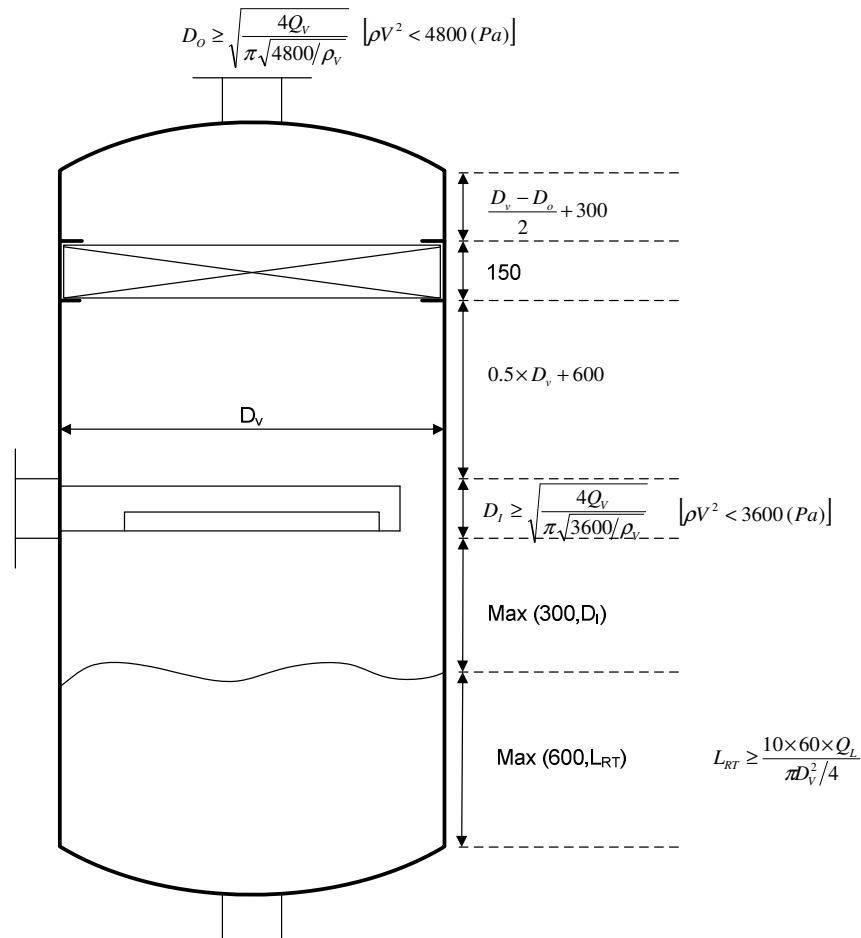


Figure 1: Separation vessels dimensions

Separation Vessels Capital Cost Functions

The capital cost of the separation vessels can be estimated based on the metal weight of the vessel, a material factor and a factor based on the vessel pressure (Peters et al. (2003)). For 304 stainless steel the material factor suggested by Peters et al. (2003) is between 2 – 3.5 and so will be taken as 2.8 in this study. The impact on the cost due to the design pressure of the vessel is calculated by [16] which is determined from data supplied by Peters et al. (2003) in Appendix 7.

$$C_{ko} = 73F_p W^{0.66} \quad \text{Cost Basis: \$US; Year Basis: 2002; W = Weight (kg);} \quad [15]$$

$$F_p = 0.091P^{0.849} + 0.83 \quad P = \text{Pressure (bar)} \quad [16]$$

Example

This example is based on the first knock-out drum of the CO₂ compressors for a single unit from Hazelwood at a 90 % capture rate with the stripper operating at 1 bara. The first knock-out drum is at 2.95 bara, the diameter of the knock-out drum is 4.5 m with a height of 7.4 m (Note - low aspect ratio of 1.7 may lead in reality to opt for a horizontal vessel). The vessel weight is 16411 kg.

Table 9: Example of knock-out drum capital cost estimation

Equation	Raw Cost	Australian Cost	2008 Australian Cost (\$Million)
[15]	48831	88785	0.13

2.7 Heat Exchangers

Size and price of heat exchangers may be calculated in two ways for this research; the first is for screening studies which uses the composite curves to determine an area and then uses that area to estimate the cost of the heat exchangers. The second method is a more rigorous method which calculates the area for each heat exchanger once the PFD has been completed and then uses this to estimate the costs of each exchanger.

Method 1 - Area Targeting: The first method uses balanced composite curves to estimate the required heat exchanger area. The method is detailed in Smith (2005) Pg388. It requires estimating film transfer coefficients (including wall and fouling resistances) for the hot and cold streams and may include a cost-weighting parameter where the stream may require heat exchangers that will be more/less expensive than the average.

Heat Exchanger Cost Functions

Method 1 - Area Targeting: A general cost function that can be applied to all the heat exchangers is used in this method. One is used by Girardin et al. (2009) based on the number of units anticipated and the total area.

$$C_{hx} = 7038N(A/N)^{0.7948}$$

Cost Basis:\$US;

Year Basis: 2006

[17]

2.8 Steam Turbine

The steam turbine will require modifications with the addition of CCS as a significant amount of steam will need to be extracted from the low pressure end of the turbine to provide the heat for solvent regeneration. It is difficult to estimate the costs for these modifications. When heat integration is applied, to maximise the recovery of heat into the steam to produce the maximum amount of energy may require shifting some of the load that is taken from the low pressure turbine and replaced by increasing the load on the high pressure turbine. This will invariably require modifications to all parts of the steam turbine and the costs for the modifications may approach replacement costs. Therefore, under these circumstances the cost estimation is for a replacement steam turbine.

Steam Turbine Capital Cost Function

Capital cost functions for steam turbines have been provided by Girardin et al. (2009).

(Equation [18]) and are based on the gross power produced by the steam turbine.

$$C_{ST} = 10^{(1.93778 + 1.45483\log(p) - 0.08838\log(p)^2)}$$

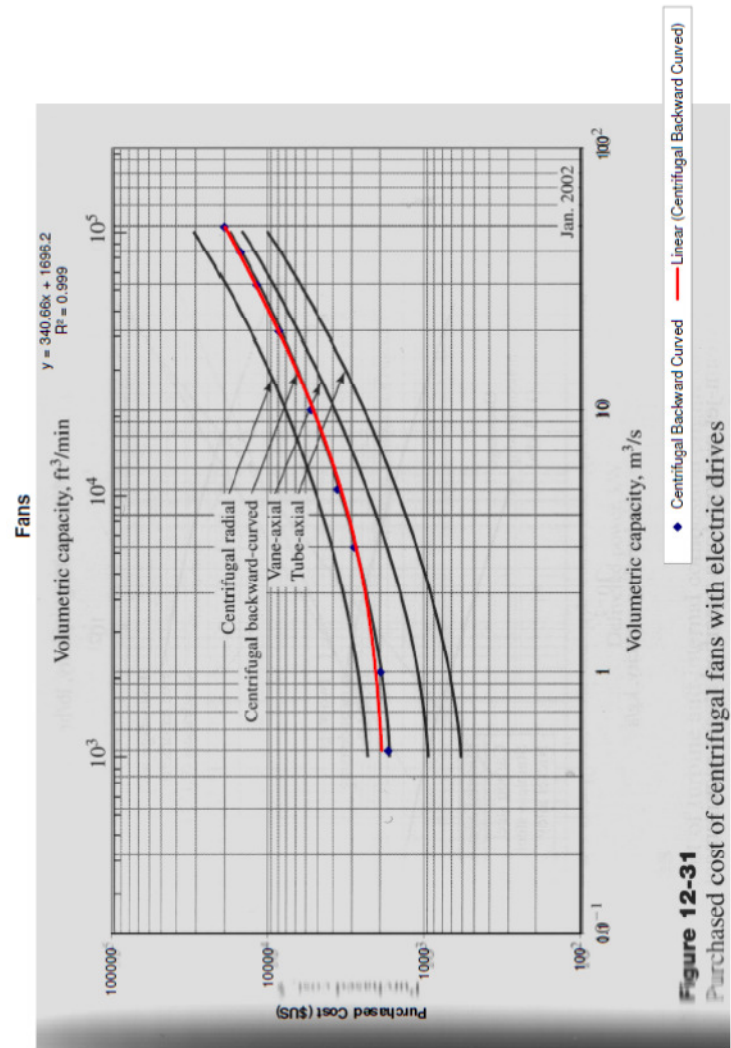
Cost Basis: \$US; Year Basis: 2002

[18]

References

- Baldwin, P. (2009). "Low-cost, high-efficiency CO₂ compressors." Carbon Capture Journal(11).
- Campbell, J. M. (1992). Gas Conditioning and Processing. Norman, Oklahoma, Campbell Petroleum Series.
- Chapel, D. G. and C. L. Mariz (1999). Recovery of CO₂ from flue gases: Comercial trends. Canadian society of chemical engineers annual meeting, Saskatoon, Saskatchewan, Canada.
- Drbal, L. F., P. G. Boston, K. L. Westra and B. Veatch (1996). Power plant engineering, Springer.
- Furukawa, S. K. and R. K. Bartoo (1997). Improved Benfield Process for Ammonia Plants. UOP. Des Plaines, Illinois.
- Girardin, L., R. Bolliger and F. Marechal (2009). On the use of process integration techniques to generate optimal steam cycle configurations for the power plant industry. 12th international conference on Process Integration, Modelling and Optimisation for Energy Saving and Pollution Reduction (PRES'09), Rome, Italy.
- GPSA (1998). Engineering Data Book. Tulsa, Oklahoma.
- GPSA (2004). Engineering Data Book. Tulsa, Oklahoma.
- Habel, R. and C. Wacker (2009). "Innovative and proven CO₂ compression technology for CCS and EOR." Carbon Capture Journal(11).
- Ho, M. (2007). Techno-economic modelling of CO₂ capture systems for Australian industrial sources. School of Chemical Sciences and Engineering. Doctor of Philosophy Thesis, UNSW.
- Peters, M. S., K. Timmerhaus and R. E. West (2003). Plant design and economics for engineers. New York, McGraw-Hill.
- Sinnott, R. K. (1998). Coulson & Richardson's Chemical Engineering Volume 6. Oxford, Butterworth-Heinemann.
- Smith, R. (2005). Chemical Process Design and Integration. West Sussex, England, John Wiley & Sons Ltd.
- Winter, T. (2009). "The right solution for CO₂ compression - integrally geared compressors from Siemens." Carbon Capture Journal(11).

Appendix 1 - Feed Fan Capital Cost Function



Equipment Reference	Centrifugal Backward-curved
Cost Date	Peters & Timmerhaus Fig 12-31 Pg 533
Currency Basis	Jan-02 \$US
Purchased Cost (\$US)	Volumetric Capacity (m³/s)
1700	0.5
1900	1
2800	3
3600	5
5300	10
8500	20
11800	30
15000	40
19000	50
Calculate	730
	250378

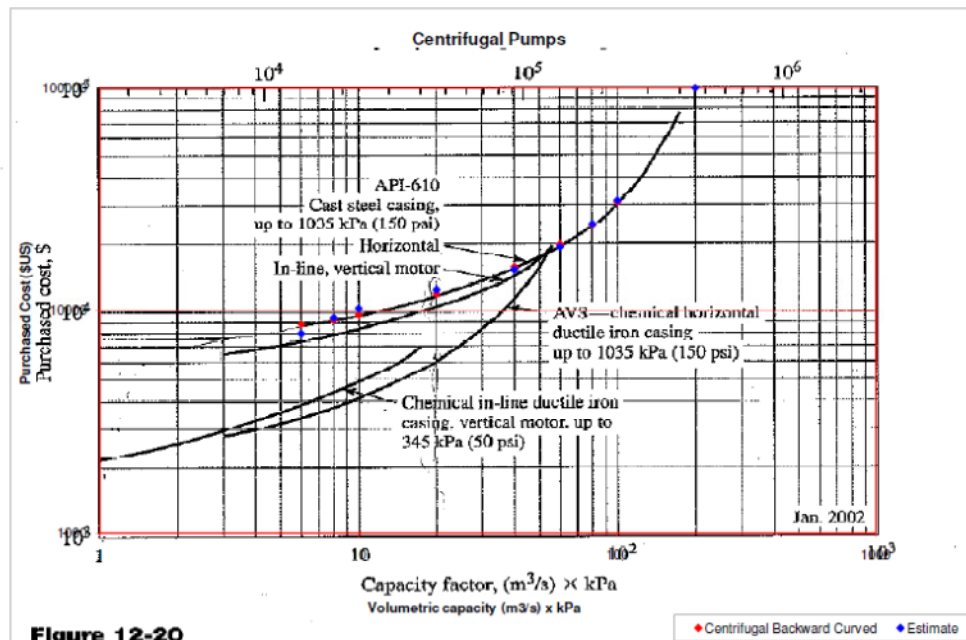
Appendix 2 - Centrifugal Pumps Cost Curves

Equipment Centrifugal Pumps
Reference Peters & Timmerhaus Fig 12-31 Pg 533
Cost Date Jan-02
Currency Basis \$US

a 2.5028263
b 3.2578349
c -2.3724523
d 0.62069483

Purchased Cost (\$US)	Volumetric Capacity x kPa (m ³ .kPa/s)	Estimate
8650	6	7830.892507
9100	8	9272.630504
9600	10	10207.13121
11900	20	12373.06493
15800	40	15315.97281
19800	60	19237.41662
24200	80	24462.30577
30750	100	31206.5238
100000	200	99960.98978
Calculate		
47398625310	1250	2122660
31207	100	

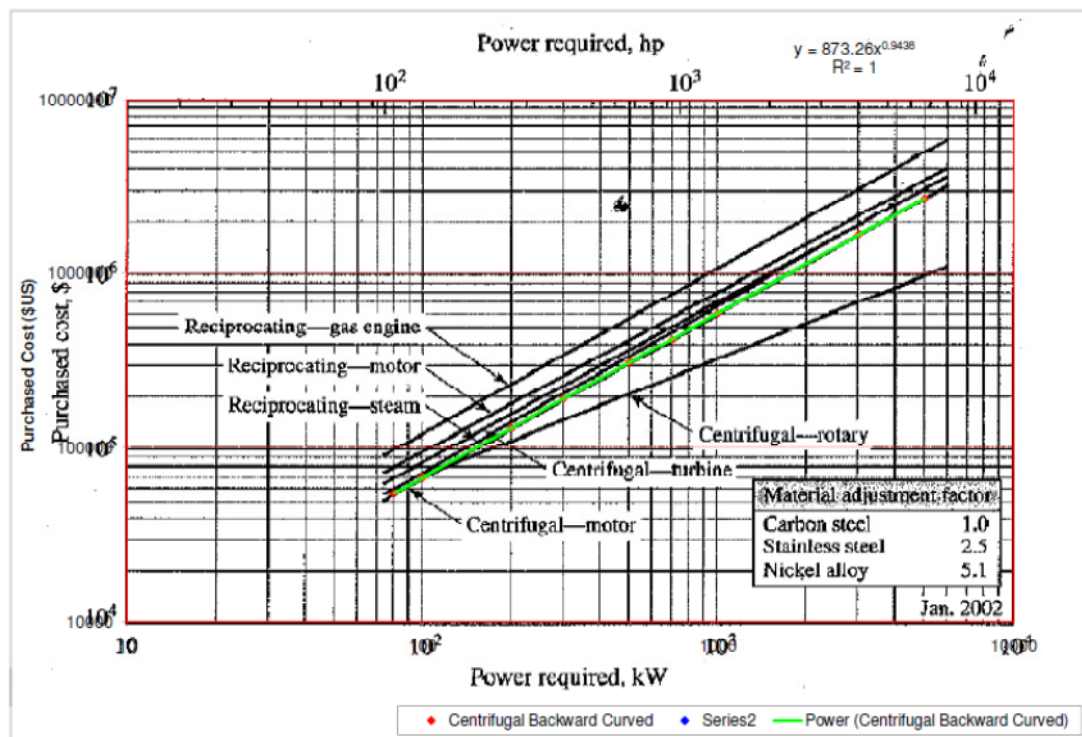
$$C_{\text{pump}} = 10^{a+b \log(\Phi) - c \log(\Phi)^2 + d \log(\Phi)^3}$$



Appendix 3 - CO₂ Compressor Cost Curves

Equipment Centrifugal Compressor
Reference Peters & Timmerhaus Fig 12-28 Pg 531
Cost Date Jan-02
Currency Basis \$US

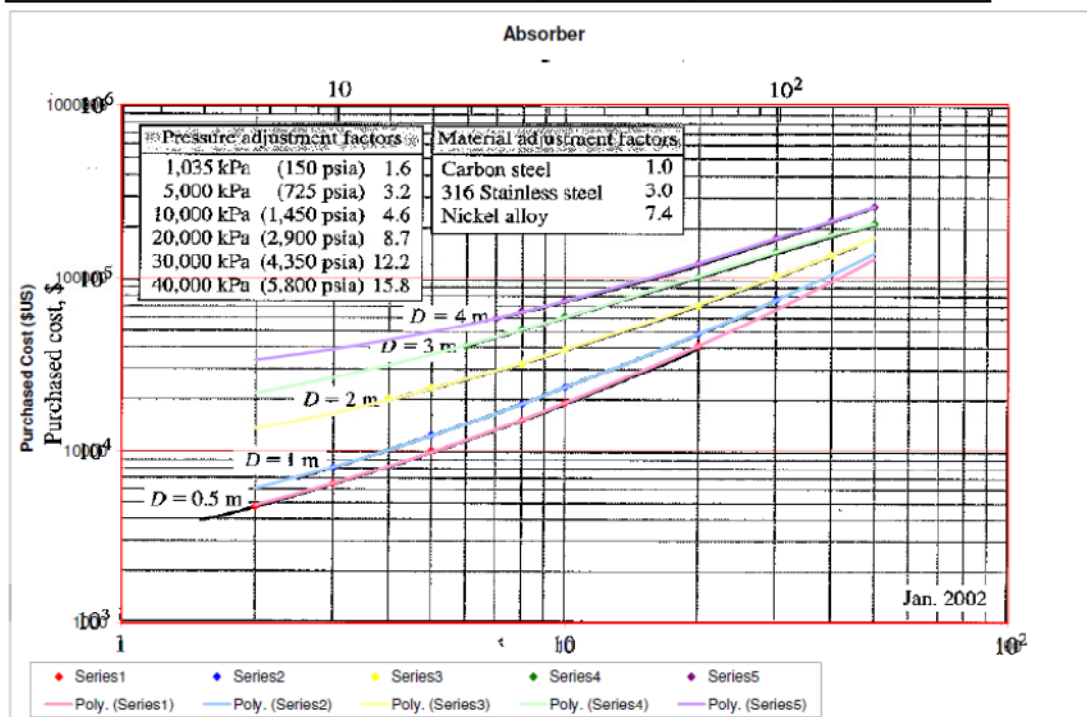
	Purchased Cost (\$US)	Power Required kW
	54500	80
	67500	100
	130000	200
	190000	300
	310000	500
	420000	700
	590000	1000
	1680000	3000
	2700000	5000
Calculate	1670516	3000



Appendix 4 - Absorber Cost Curves

Equipment Absorber
Reference Peters & Timmerhaus Fig 15-11 Pg 793
Cost Date Jan-02
Currency Basis \$US

D	0.5	1	2	3	4
Vertical Height	Purchased Cost	Purchased Cost	Purchased Cost	Purchased Cost	Purchased Cost
m	(\$US)	(\$US)	(\$US)	(\$US)	(\$US)
2	4750				
3	6450	8000			
4			20000		
5	10000	12300	23000		
6				40000	
7					58000
8	15000	18500	31500	50500	64000
10	18800	23000	38000	59800	73500
20	40000	47000	69000	101000	120000
30		74000	103000	141000	168000
40			134000	175000	213000
50				204000	255000



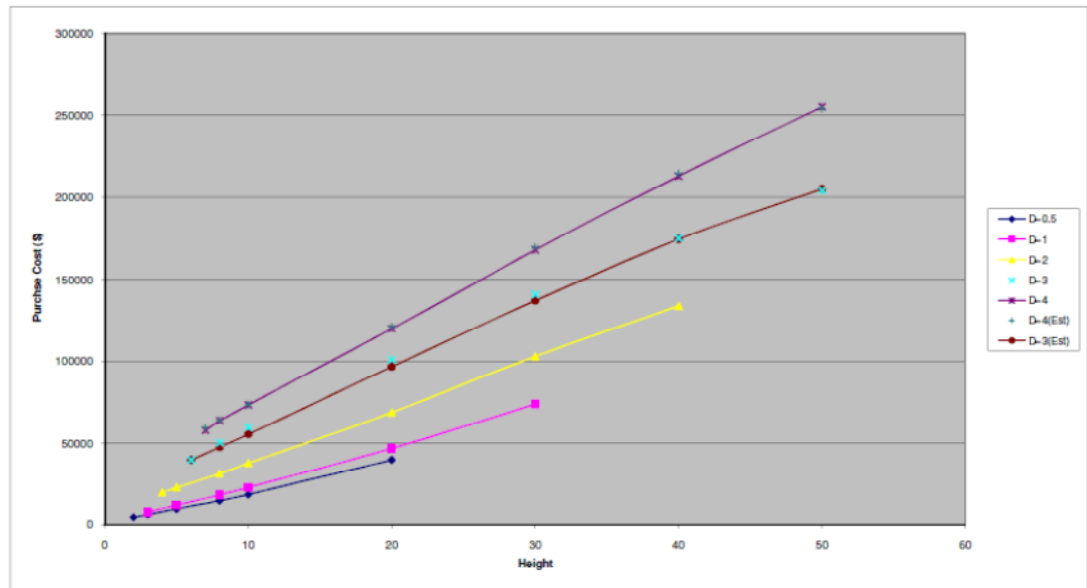
Curve Fitting

		Actual Values		Poly2 estimate	
D	H	C	SStot		
0.5	2	4750	4699933446	2993	
0.5	3	6450	4469732840	4780	
0.5	5	10000	4007657309	8459	
0.5	8	15000	3399596703	14189	
0.5	10	18800	2970910643	18115	
0.5	20	40000	1109293673	38116	
1	3	8000	4264881552	8448	
1	5	12300	3721739431	12996	
1	8	18500	3003704279	20047	
1	10	23000	2530699734	24866	
1	20	47000	692008824.6	49478	
1	30	74000	481551.8825	72746	
2	4	20000	2841536097	20461	
2	5	23000	2530699734	23561	
2	8	31500	1747746703	33067	
2	10	38000	1246517916	39546	
2	20	69000	18542157.94	72748	
2	30	103000	881730036.7	105089	
2	40	134000	3683754279	133561	
3	6	40000	1109293673	39981	
3	8	50500	520116400.4	47823	
3	10	59800	182413673.1	55795	
3	20	101000	766954279.2	96746	
3	30	141000	4582469431	137317	
3	40	175000	10341657309	174502	
3	50	204000	17080905794	205294	
4	7	58000	234275491.3	59724	
4	8	64000	86602764	64317	
4	10	73500	37612.48852	73612	
4	20	120000	2180323976	121471	
4	30	168000	8966942158	169432	
4	40	213000	19514396703	214488	
4	50	255000	33012687612	253634	
			1.464E+11	119	
				0.999184767	

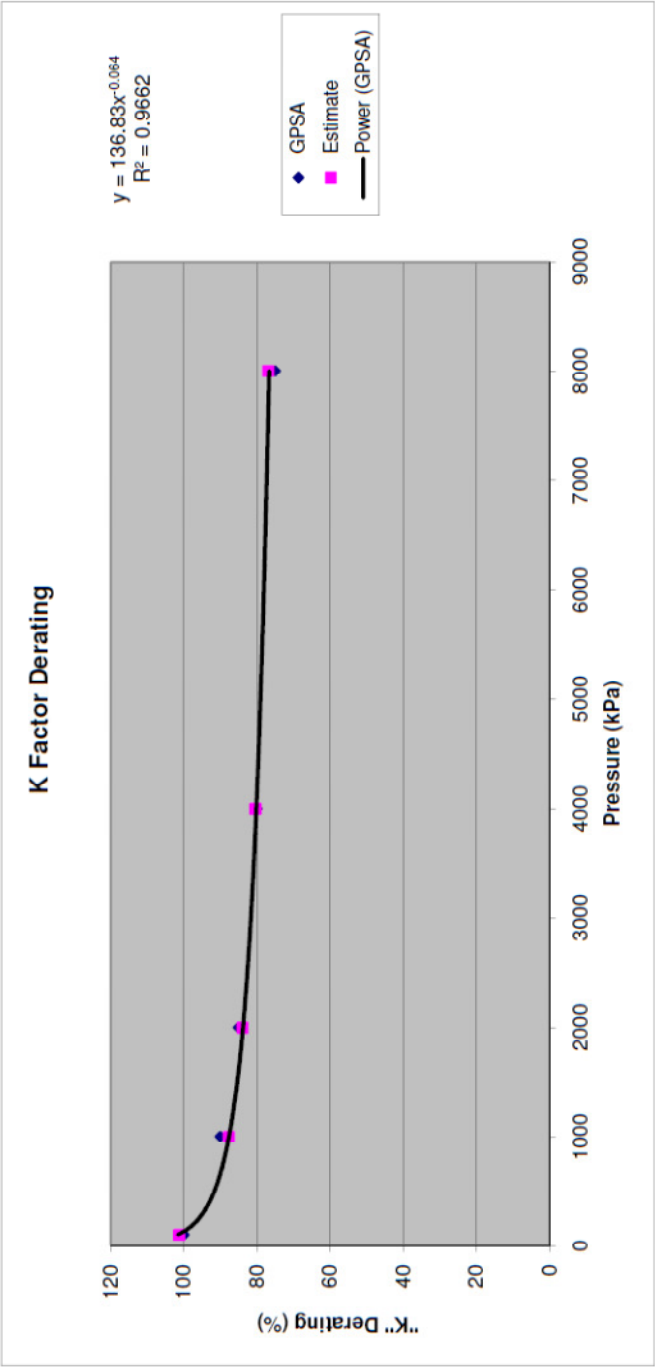
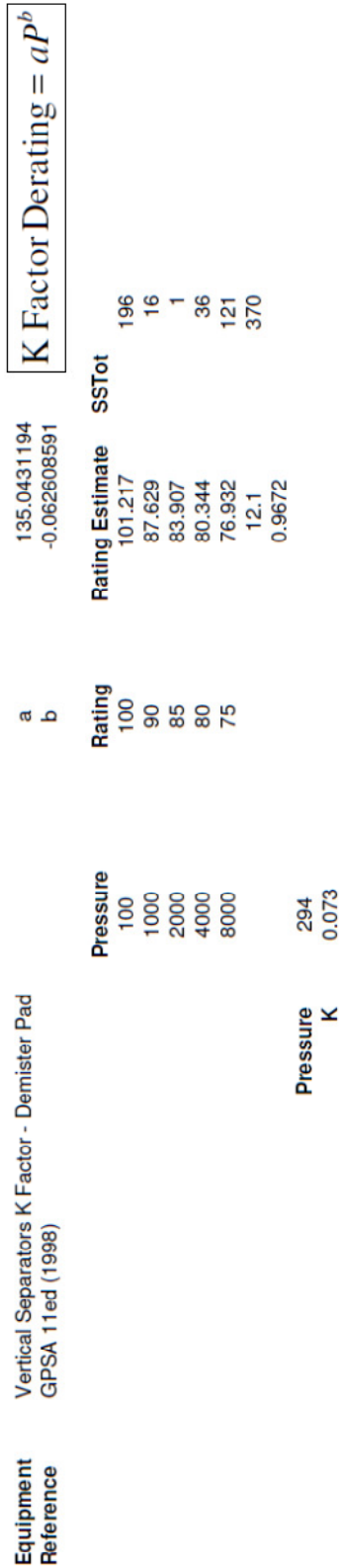
a	-2244.698
b	2955.858 31332.09
c	1240.76 31019.01
d	1205.221 135418.7
e	912.9555 241933.2
f	20.93412 13083.82
g	-42.08014 -118203
h	2.411019 15973
i	-0.501111 -7829.87

$$C = a + bD + cH + dD^2 + eDH + fH^2 + gD^2H + hDH^2 + iH^3$$

D	H	
10.6	25	340482
		1021446



Appendix 5 - K-Factor Derating



Appendix 6 - Separator Vessel Sizing

Knock Out Drum Sizing

Pressure	294	kPaa
Vapour Massflow	76.03694	kg/s
Liquid Massflow	2.105167	kg/s
Vapour Density	5.18	kg/m ³
Liquid Density	845	kg/m ³
Feed Flowrate	78.14	kg/s
Feed Density	5.32	kg/m ³

K	0.073	m/s
a	135.0431	
b	-0.06261	

$$K (m / s) = 0.11 \times 0.7 \times aP^b / 100$$

K Factor derating based on pressure and service
(0.7 = compressor suction drum) (GPSA 11Ed.)

D _v	4.489	m
D _o	0.784	m
D _i	0.848	m
L _{RT}	0.094458	m
H	7.443	m
H/D	1.658	

$$D_v = \sqrt{\frac{4Q}{\pi \cdot K \sqrt{(\rho_L - \rho_v) / \rho_v}}}$$

Vessel Thickness Calculations AS1210 - 1997

Design Pressure	P _d	368	kPaa		
Tensile strength (@ Design Temp.)	f	80.0	MPa	304 @300 °C	AS1210
Welded Joint eff.	η	0.85		Assume Class 2, spot Welding Checks	
Inside Diameter	D _i	4489	mm		

Thickness (3.7.3) of a cylindrical shell:

Longitudinal Weld	t	12.162	mm	$t = \frac{PD_i}{2f\eta - P}$
Circumferential Joint	t	6.073	mm	$t = \frac{PD_i}{4f\eta - P}$
Corrosion Allowance	Ca	3	mm	
Total Thickness	T	15.2	mm	
Metal Volume of Cylinder		1.786	m ³	

Thickness (3.12.5.1) of semi-elliptical end (2:1)

h	1122	mm	
Fk	1.000		
t	12.162		$t = \frac{PD_i Fk}{2f\eta - P}$
Metal Volume of Heads	0.266	m ³	V = 0.345 x π x D ² x t
Total Metal Volume of Vessel	2.051	m ³	
Total Weight of Vessel	16411	kg	(Assume 8000kg/m ³)

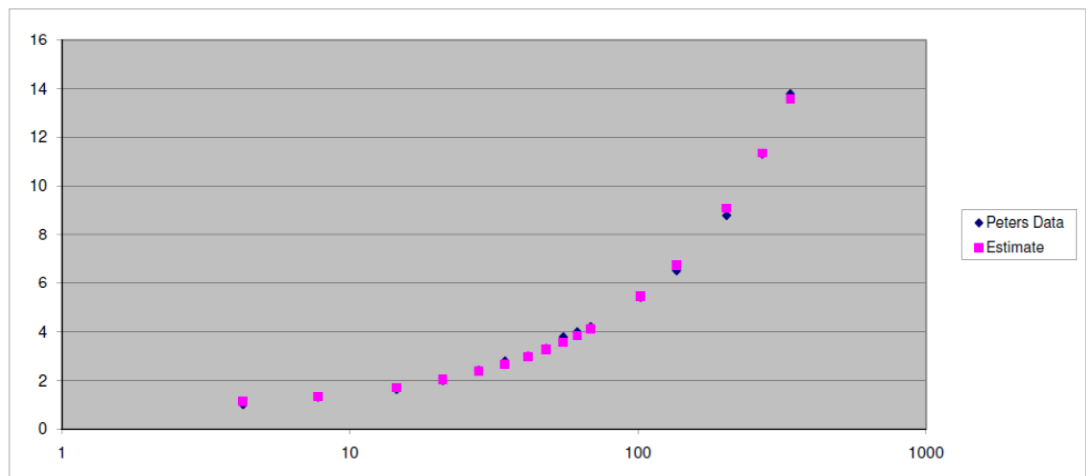
Appendix 7 - Pressure Vessel Pressure Factor

Equipment Pressure Vessels
Reference Peters & Timmerhaus Eqn 12-50 Pg 553
Cost Date Jan-02
Currency Basis \$US

a 0.090775
 b 0.849106
 c 0.83

$$\text{Pressure factor} = aP^b + c$$

Pressure (Bar)	Cost Factor	Estimate	SSTot
4.25	1	1.141369	13.69
7.75	1.3	1.347755	11.56
14.5	1.6	1.710454	9.61
21	2	2.035372	7.29
28	2.4	2.368545	5.29
34.5	2.8	2.666682	3.61
41.5	3	2.978395	2.89
48	3.3	3.260763	1.96
55	3.8	3.558468	0.81
61.5	4	3.829805	0.49
68.5	4.2	4.117219	0.25
102	5.4	5.43893	0.49
136	6.5	6.713841	3.24
203	8.8	9.096896	16.81
270	11.3	11.36186	43.56
338	13.8	13.57469	82.81
		0.340627	204.36
		0.998333	



Appendix C

Operating Cost Estimation Methodology for Process Design of Carbon Capture.

Cost functions and source data for the estimation of operating costs for use with process design studies of carbon capture at coal fired power stations in Australia

Contents

1. Introduction	204
2. Fixed operating and maintenance costs	204
3. Variable operating costs	204
3.1 Cooling water costs	205
3.1.1 Annual charge for capital cost (C_c)	205
3.1.2 Annual charge for FOM for cooling water system (C_{FOM})	205
3.1.3 Charge for electricity usage (C_p)	206
3.1.4 Charge for make-up water (C_w)	206
3.1.5 Charge for chemicals and demineralisation (C_d)	206
3.2 Process water make-up costs	207
3.3 Chemical replacement costs	207
3.4 Lost power costs	207
3.5 CO ₂ storage costs	207
3.5.1 Latrobe Valley CO ₂ storage assessment	208
3.6 Feedstock costs	209
3.7 Catalyst costs	209
References	210

1. Introduction

The addition of post-combustion capture (PCC) to a power station, results in the reduction in net power from the power station due to the additional heat and power required by the PCC capture plant. There are additional costs involved in the addition of CCS including the capital cost for the equipment and operating costs for the new equipment and additional utilities. This report deals with the estimation of operating costs.

The operating costs include fixed operating and maintenance costs and variable operating costs. The variable operating costs will vary for each scenario but is likely to include cost of cooling, make-up water and chemicals, electricity, labour costs and a cost for CO₂ storage.

2. Fixed operating and maintenance costs

The fixed operating and maintenance (FOM) charges are calculated from the total installed capital cost as per the methodology used in Allinson et al. (2006). The insurance is based on 2 % of the total installed costs (TIC) as per Ho (2007) and the rest of the fixed operating and maintenance charges are 4 % of the TIC as per Allinson et al. (2006).

Labour costs are also considered to be fixed costs. The labour costs are estimated using a combination of Allinson et al. (2006) and IEA-GHG (2006), the costs for maintenance are included in the FOM cost given above, the direct operating labour is estimated using a five shift pattern and if not estimated in detail the supervision is included by increasing the operating labour cost by 20%, the administration and general overheads labour is included by a further 30% increase in costs (ie. Total labour = Direct labour x1.2x1.3). The cost for each individual is taken from IEA-GHG (2006) as \$82,000 (50k€/yr). For an IGCC plant the number of operating personnel is estimated as 90 people IEA-GHG (2006), therefore to include supervision and administration staff this is increased to 140 people in total. For a CCS retrofit to a power station it is assumed that there are two operators plus a single maintenance person on shift on a five shift pattern. This equates to a total additional labour force of 24.

3. Variable operating costs

Variable operating costs will depend on the process being studied, however generally will include cooling water costs, make-up water and chemicals, electricity, labour costs and costs for storage.

3.1 Cooling water costs

In large CCS projects the amount of cooling required will be significant and where cooling water is used will require a significant increase in the cooling water capacity of the power station.

Therefore, there is likely to be a capital cost involved in the construction of new cooling water systems. The capital cost could be added to the overall capital cost for the project or can be included as an annual charge included with the operating cost. The later approach has been selected for this work.

The components to determine the cost of the cooling water include;

- Charge for capital cost
- Charge for maintenance on cooling water system
- Charge for electricity use for cooling water pumps
- Charge for make-up water
- Charge for chemicals and demineralisation

The total cost is related back to the cooling water duty required (Q in MW) and is provided by summing the individual components found in the following sections.

3.1.1 Annual charge for capital cost (C_c)

Capital cost data for the cooling water tower is calculated using Equation [1] which is from Bekdash and Moe (2003) for concrete columns in 2003 \$US based on the flowrate of cooling water (in GPM). The capital cost given by this relation is the total installed cost. The flowrate of cooling water can be estimated from the cooling duty required assuming that the cooling water temperature rise is limited to 10 °C using Equation [2]. These can be converted into an annualised capital charge using Equation [3].

$$C (\$M \text{ US } 2003) = 10^{-6} \times (-10^{-10}f^3 - 10^{-5}f^2 + 70.552f + 61609) \quad f = \text{Flowrate(GPM)} \quad [1]$$

$$f (\text{GPM}) = 15850.3 \times Q / 41.2 \quad Q = \text{Cooling duty (MW)} \quad [2]$$

$$C_c (\$M \text{ US } 2003) = Cr(1+r)^n / [(1+r)^n - 1] \quad r = \text{the discount rate} \quad [3]$$

n = project life

3.1.2 Annual charge for FOM for cooling water system (C_{FOM})

As per section 2 the annual total FOM is 6 % of the total installed capital cost which can be estimated from Equations [1] and [2] as per Equation [4].

$$(\$M \text{ US } 2003) = 0.06 \times 10^{-6} \times (-10^{-10}f^3 - 10^{-5}f^2 + 70.552f + 61609) \quad [4]$$

3.1.3 Charge for electricity usage (C_p)

The majority of the electricity for the cooling water system is used in the cooling water pumps (assuming that natural draft cooling towers are used). The power can be estimated using Equation [5]; we assume for this work that the total head (h) required for the pumps is 30 m, comprising 20 m of vertical lift and 10 m (~ 100 kPa) of piping and heat exchanger pressure loss, and a pump efficiency (η) of 0.8. The cost is then calculated by multiplying the power by the cost of electricity (C_e) and the capacity factor (Φ) (yearly running time of the plant).

$$P \text{ (MW)} = f \times h \times 9810 / (\eta \times 15840.3 \times 10^6) = Q \times h \times 9810 / (\eta \times 41.2 \times 10^6) \quad [5]$$

$$C_p (\$/\text{M}/\text{yr}) = P \times C_e \times \Phi / 10^6 \quad [6]$$

3.1.4 Charge for make-up water (C_w)

The amount of make-up water (W_m) required is a combination of evaporation losses (W_e), drift losses (W_d) and blowdown losses (W_b). The losses can be estimated using data provided by Perry (1999) [Pg 12-17]. The range of the cooling water (ΔT) is assumed to be 10°C as previously discussed and the blowdown losses are estimated using five concentration cycles.

$$W_e = 0.00153 \times W_c \times \Delta T = 0.0153 W_c \quad [7]$$

$$W_d = 0.002 \times W_c \quad [8]$$

$$W_b = W_e / 4 \quad [9]$$

$$W_m = W_e + W_d + W_b = 0.021125 W_c \quad [10]$$

The cost of the make-up water is therefore the amount of make-up water multiplied by the cost of the make-up water, the value for this is $\$20/\text{megalitre}$ as per Allinson et al. (2006) as given in Equation [11].

$$C_w (\$/\text{M AU}/\text{yr 2006}) = 0.02 \times 0.021125 W_c \times 3600 \times \Phi / 10^6 \quad W_c \text{ (m}^3/\text{s)} \quad [11]$$

$$W_c \text{ (m}^3/\text{s)} = Q / C_p \Delta T = Q / 41.2 \quad [12]$$

3.1.5 Charge for chemicals and demineralisation (C_d)

Details for typical costs for the chemical and demineralisation have not been sourced and are assumed to be minor compared to other costs of the cooling water system in Australian systems where the fresh water is clean.

3.2 Process water make-up costs

The process make-up water costs uses the same cost for make-up water as provided in section 3.1 for cooling water make-up. The process water costs will depend on the process but will include the water balance where water is lost in the exhaust gases.

In post combustion capture plants the make-up water is required when the amount of water lost in the absorber is greater than the amount dropped out upstream of the absorber, and in the stripper separator and CO₂ compressors. If water is produced in the process no credit is provided. For the Foster Wheeler IGCC process the make-up water consists of; steam for the gasifier (9kg/s) and WGSR (63kg/s), the water balance over the wet scrubber and the CO₂ absorber.

3.3 Chemical replacement costs

The main chemical replacement costs for solvent capture plants will be for the make-up solvent. In the case of potassium carbonate the solvent losses are mainly contributed to the absorption of sulphur to form potassium sulphate (K₂SO₄). Therefore, the make-up rate of solvent, either as potassium hydroxide (KOH) or Potassium carbonate (K₂CO₃) can be estimated by the total sulphur in the fuel. The sulphate removal process is likely to include some loss of potassium carbonate therefore the solvent losses based on sulphur loads may include a factor, nominally 2 until better data is obtained.

$$\text{Mass Potassium carbonate} = \text{Mass Sulphur} \times 138.206 / 32.06 \quad [13]$$

$$\text{Mass Potassium hydroxide} = 2 \times \text{Mass Sulphur} \times 56.106 / 32.06 \quad [14]$$

The cost of potassium hydroxide can be estimated as approximately \$0.35/kg (\$15/100lb) from ICIS market reports.

3.4 Lost power costs

When the analysis is on a retrofit, power used in the CO₂ capture and compression needs to be accounted for. This can be taken into account using the market price of electricity which is nominally 40 \$/MWh in Victoria.

3.5 CO₂ storage costs

If the CO₂ storage costs are not explicitly calculated and included in the analysis a nominal CO₂ storage cost is required to account for the capital and operating costs associated with storing the CO₂. For Victorian analysis the CO₂ storage cost is obtained from a study conducted by CO₂CRC for the Latrobe Valley (Hooper et al. (2005)) at \$5.79 in 2008 dollars per tonne of CO₂ stored. The

report determines a cost of \$10.90 (2005) per tonne of CO₂ avoided for a 15 Mtpa storage scenario. However, this includes CO₂ compression costs which in the heat integration studies are included in the capture side of the equation. Therefore when these costs are removed and the cost is escalated to 2008 the value of 5.79 \$/tonne CO₂ (refer to Section 3.5.1 below).

3.5.1 Latrobe Valley CO₂ storage assessment

In the Latrobe Valley CO₂ storage assessment the CO₂ compression operating costs are a combination of the energy cost (23 \$/MWh) for the 189 MW required for compression and the fixed operating costs which are 3 %, 4 % and 5 % of the capital cost for the first ten years, the next fifteen years and the last fifteen years respectively. The cost break down is shown in Table 3 and Table 4, the capital costs are escalated from 2005 using the CPI and the operating costs are escalated assuming 3.5% inflation.

Table 1: Capital and operating costs of CO₂ storage at Latrobe Valley. Case B1 Hooper et al. (2005).

Item	Total real capital cost	Annual real operating cost
	\$A Million	\$A Million
Compression	408	50-58
Pipeline	242	2.4
Injection	516	10.3
Oil Well Remediation	34	0
Total	1199	62-71

Table 2: Cost of storage including and excluding CO₂ compression

Item	2005 Cost Including Compression	2008 Cost excluding compression
PV Capex (\$m)	1295	1038
PV Opex (\$m)	934	201
PV CO ₂ Stored (Mt)	214	214
PV CO ₂ avoided (Mt)	205	205
\$/t CO ₂ Stored	10.4	5.79
\$/t CO ₂ avoided	10.9	6.06

Table 3: Cash Flow from Latrobe Valley Storage Assessment including compression

		Yr					
	Totals	-2	-1	0-9	10-18	19-24	25-39
Real Capex	1199	583	583	0	0	1.619	1.619
Real Opex	2705	0	0	63	67.1	67.1	71.2
Real CO ₂ Stored	600	0	0	15	15	15	15
Real CO ₂ Avoided	573	0	0	14.34	14.34	14.34	14.34

Table 4: Cash Flow from Latrobe Valley Storage Assessment excluding compression in 2008 dollars.

		Yr					
	Totals	-2	-1	0-9	10-18	19-24	25-39
Real Capex	973	466	466	0	0	1.989	1.989
Real Opex	2705	0	0	14.08	14.08	14.08	14.08
Real CO ₂ Stored	600	0	0	15	15	15	15
Real CO ₂ Avoided	573	0	0	14.34	14.34	14.34	14.34

3.6 Feedstock costs

Where the analysis is done for a full scale plant and not a retrofit the cost of the fuel needs to be included. The nominal cost of Victorian brown coal will be 1 \$/GJ (LHV).

3.7 Catalyst costs

Catalyst costs will only be required for pre-combustion capture with water-gas shift reactors and the consumption of catalyst will need to be estimated on a case by case basis. The cost of the catalyst can be estimated from IEA-GHG (2006) as 33000 \$/t (20000€/t). For the FW IGCC process the consumption is estimated as 128t/y.

References

- Allinson, G., P. Neal, M. Ho, D. Wiley and G. McKee (2006). CCS economics methodology and assumptions. CO2CRC. RPT06-0080.
- Bekdash, F. and M. Moe (2003). A tool for budgetary estimation of cooling towers unit costs based on flow. Symposium on cooling water intake technologies to protect aquatic organisms, Arlington, VA.
- Ho, M. (2007). Techno-economic modelling of CO₂ capture systems for Australian industrial sources. School of Chemical Sciences and Engineering. Doctor of Philosophy Thesis, UNSW.
- Hooper, B., L. Murray and C. Gibson-Poole (2005). Latrobe Valley CO₂ Storage Assessment CO2CRC.
- IEA-GHG (2006). CO₂ Capture in Low Rank Coal Power Plants. IEA Greenhouse Gas R&D Programme. Report Number: 2006/1.
- Perry, R. (1999). Perry's Chemical Engineers' Handbook, McGraw-Hill, New York.

Appendix D

Heat Exchanger Area Estimation

Outline of the method and constants used to estimate the required heat exchanger area of the new CCS equipment.

Contents

1. Introduction	213
2. Theory	213
3. Film heat transfer coefficients	214
3.1 Detailed tube-side heat transfer coefficient estimation	216
3.2 Detailed heat transfer coefficient estimation using HTFS	216
4. Programming – Area estimation	219
References	219

1. Introduction

It is necessary to estimate the costs of the heat exchangers as part of the capital cost estimation of new CCS equipment. In the optimisation process used in the thesis, the maximum net power can be determined for the power station with a given CO₂ capture technology and a given minimum temperature driving force using linear programming. The heat exchanger network required to provide the maximum net power from the power station is not configured at this stage of the design. However using the heat exchanger area targeting method described by Smith (2005), it is possible to estimate the heat exchanger area required to provide the heat exchanger network capable of producing the maximum net power from the power station.

2. Theory

The heat exchanger area targets are based on the balanced composite curves. The balanced composite curves are the hot and cold composite curves of the entire process including the utilities. In the case of the power station with CCS it includes all streams from the power station, the CCS equipment and the steam cycle. The balanced composite curves are divided into vertical enthalpy intervals and for each vertical interval the area can be estimated using Equation [1] assuming that there is a single overall heat transfer coefficient for every heat exchanger required and there is true counter-current heat transfer in that vertical enthalpy interval. However, this Equation [1] is only effective when the individual heat transfer coefficients for all the streams in the network are similar. For power stations there can be very large differences between the heat transfer coefficients of various streams, the flue gas heat transfer coefficient will be much smaller than the condensing steam coefficients. Therefore the individual heat transfer coefficients can be incorporated into Equation [1] and the area of each interval summed to get the total network area as provided by Equation [2].

$$A_{NETWORKk} = \frac{\Delta H_k}{U \Delta T_{LMk}} \quad [1]$$

$$A_{NETWORK} = \sum_k^{INTERVALS K} \frac{1}{\Delta T_{LMk}} \left[\sum_i^{HOT STREAMS I} \frac{q_{i,k}}{h_i} + \sum_j^{COLD STREAMS J} \frac{q_{j,k}}{h_j} \right] \quad [2]$$

$A_{NETWORKk}$ = heat exchange area for vertical heat transfer required by interval k

$A_{NETWORK}$ = heat exchanger area for vertical heat transfer for the whole network

ΔT_{LMk} = log mean temperature difference for the interval k

U	= overall heat transfer coefficient
$q_{i,k}$	= stream duty on hot stream i in enthalpy interval k
$q_{j,k}$	= stream duty on hot stream j in enthalpy interval k
h_i, h_j	= film transfer coefficients for hot stream i and cold stream j (including wall and fouling resistances)
I	= total number of hot streams in enthalpy interval k
J	= total number of cold streams in enthalpy interval k
K	= total number of enthalpy intervals

3. Film heat transfer coefficients

Film heat transfer coefficients for the various streams are detailed in Table 1. The film heat transfer coefficients (h_i) include the fluid heat transfer coefficient (h) and the fouling factor (h_F) as per Equation [3]. The influence of the wall resistance has been ignored, because this is generally small compared to the fluid resistance, especially when compared to the film coefficients of the flue gas. The values in Table 1 are provided from a range of sources as detailed. Where a range of values is provided in the literature sources, the geometric mean of the range is used for conservatism. In some cases, detailed in Table 1, a particular value rather than the geometric mean has been selected; in these cases the reasoning is provided.

$$\frac{1}{h_i} = \frac{1}{h} + \frac{1}{h_F} \quad [3]$$

Table 1: Film heat transfer coefficients (h_i = Total film heat transfer coefficient, h = fluid film heat transfer coefficient, h_f =Fouling heat transfer coefficient)

Duty	h_i W/m ² K	h W/m ² K	Reference (Smith (2005))	h_f W/m ² K	Reference ([1]Smith (2005),[2]Sinnott (1998), [3] TEMA (1999))
Flue Gas	69.2	71	Gases (10-500)	3162	[2] Flue Gas (2000-5000)
Flue Gas - Condensing Region ¹	4330	8660	Condensing steam (5000-15000)	8660	[1] Steam Contaminated (5000-11000)
Regenerator Condenser ¹	4330	8660	Condensing steam (5000-15000)	8660	[1] Steam Contaminated (5000-11000)
Regenerator Reboiler	4330	4472	Water Evaporation (2000-10000)	8124	[1] BFW (6000-11000)
Compressor Intercoolers ¹	3429	8660	Condensing steam (5000-15000)	5678	[3] CO ₂ Vapour and Liquid
Lean Solvent	1907	3464	Water (2000-6000)	4243	[1] Aqueous Salt Solutions (3000-6000)
Rich Solvent	1907	3464	Water (2000-6000)	4243	[1] Aqueous Salt Solutions (3000-6000)
Boiler Feed Water	2429	3464	Water (2000-6000)	8124	[1] BFW (6000-11000)
Steam Generation	2884	4472	Water Evaporation (2000-10000)	8124	[1] BFW (6000-11000)
Steam Superheating / Desuperheating	1905	2353 ²	Gases (10-500)	10000 ³	[1] Good Quality (20000), Contaminated (5000-11000) [2] (4000-10000)
Steam Condensing	5000	10000 ⁴	Condensing steam (5000-15000)	10000 ³	[1] Good Quality (20000), Contaminated (5000-11000) [2] (4000-10000)
Condensate Cooling	2727	6000 ⁵	Water (2000-6000)	5000 ⁵	[1] Distilled 11000; [2] Steam Condensate (1500-5000)
Cooling Water	1907	3464	Water (2000-6000)	4243	[1] Good Quality CW (3000-6000) Poor Quality CW (1000-2000) [2] 3000-6000
Radiant section	227	245 ⁶	Gases (10-500)	3162	[2] Flue Gas (2000-5000)
Air heater	317	353 ²	Gases (10-500)	3162	[2] Flue Gas (2000-5000)

¹The film transfer coefficient and fouling factor are selected as condensing steam as the primary fluid that is condensing is water.

²The film transfer coefficient was estimated using the detailed estimates as provided in Section 3.1 and 3.2.

³Estimated at the higher end of the range as the steam would be good quality steam.

⁴ Arithmetic average of the range provided.

⁵Top of the range as it would be good quality water.

⁶Arithmetic mean rather than geometric mean. The geometric mean appeared to be too conservative for due to the impact of the radiant heat transfer .

3.1 Detailed tube-side heat transfer coefficient estimation

In the case of the steam superheating/desuperheating more detailed estimates have been created using the method in Sinnott (1998) (Pg606) and provided as Equations [4] to [7]. The method is for estimating tubeside heat transfer coefficients and therefore should provide a good estimation for the superheating/desuperheating film coefficients when they are performed on the tubeside of an exchanger.

$$h_i = \frac{Nu k_f}{d_e} \quad [4]$$

$$Nu = C \cdot Re^{0.8} \cdot Pr^{0.33} \cdot \left(\frac{\mu}{\mu_w} \right)^{0.14} \quad [5]$$

$$Re = \rho u_t d_e / \mu \quad [6]$$

$$Pr = Cp \mu / k_f \quad [7]$$

Table 2: Steam superheating /desuperheating film transfer coefficient estimation

			Steam Superheating / Desuperheating
Fluid Factor	C	-	0.021
Density	ρ	kg/m ³	46
Fluid Velocity	u_t	m/s	10
Equivalent Diameter	d_e	m	0.05
Viscosity	μ	Ns/m ²	2.48E-05
Viscosity at Wall	μ_w	Ns/m ²	0.00002482
Heat Capacity	Cp	J/kgK	2677
Thermal Conductivity	k_f	W/mK	0.1122
Reynolds Number	Re	-	926672
Prandtl Number	Pr	-	0.5925
Nusselt Number	Nu	-	1049
Heat Transfer Coeff.	h	W/m ² K	2353

3.2 Detailed heat transfer coefficient estimation using HTFS

To improve the accuracy of the air pre-heater air side heat transfer coefficient an estimation of the potential film coefficient has been conducted assuming that the air is located on the outside of a tube in a finned heat exchanger. The summary of the HTFS program is provided in Figure 1. It is also possible that the air preheat could be on the tube side in that case the heat transfer coefficient is likely to be lower (refer to Figure 2). Many power stations use rotary air-preheaters and therefore the film coefficients may be different again. In the work for the thesis the results from the air being on the outside (Figure 1) have been used.

File: AirHeater-AirCooler.EDR

Date: 2/09/2011

Time: 4:02:25 PM

1	Unit Length/Width/Height							6.1549 / 9.7343 / 0.3633		m		Tube inclination		Horizontal				
2	Baysperunit	2	Bundles per bay		2	Tube Rows	8	Passes	1	X-side flow direction		0	Degrees					
3	Staggered-even rows to right											Tube flow orientation		Counter Current				
4	Total surface	5394.6	Ext surface/bundle		1348.7	Bare/Bundle	113.4	m²		Ratio (Total/Bare)		11.89						
5	Design with fixed outside flow																	
6	Performance of the Unit																	
7	Process Data		Tube Side		X-Side		Heat Transfer Parameters											
8	Total flow	kg/s	In	Out	In	Out	Total heat load				kW		23300.7					
9	Gas						Effective MTD				°C		299.88					
10	Vapor		100	100	100	100	Actual/required area ratio(dirty/clean)				2.06 /		2.06					
11	Liquid		0	0			Coef/Resist (Bare)				W/(m² K)		m² K/W		%			
12	Cond./Evap.						Tube side film				963.2		0.00104		36.71			
13	Temperature	°C	500	396.92	20	248.9	Tube side fouling						0		0			
14	Quality/Humidity ratio		1	1			Tube wall				28378.2		0.00004		1.25			
15	Pressure	bar	40	39.77474			Outside fouling						0		0			
16		Pa			101326	101326	Outside film				570		0.00175		62.04			
17	DP		0.22526		85		Overall fouled				353.6		0.00283					
18	Velocity	m/s	22.25	18.88	3.64	6.48	Overall clean				353.6		0.00283					
19																		
20	Liquid Properties						Tube Side Pressure Drop						bar		%			
21	Density	kg/m³				Inlet nozzle			0.02962			13.1						
22	Viscosity	mPa s				Inlet header			0.00143			0.63						
23	Specific heat	kJ/(kg K)				Inside tubes			0.18013			79.65						
24	Th Cond	W/(m K)				Across pass connections			0			0						
25	Surface tension	N/m				Other header			0.00138			0.61						
26	Vapor Properties						Outlet nozzle			0.01359			6.01					
27	Density	kg/m³	11.64	13.72	1.2	0.68	Outside Pressure Drop			Pa			%					
28	Viscosity	mPa s	0.0288	0.0247	0.0181	0.0275	Ground clearance			0			0					
29	Specific heat	kJ/(kg K)	2.271	2.262	1.007	1.035	Fan inlet			3			3.17					
30	Th Cond	W/(m K)	0.071	0.0586	0.0257	0.0419	Bundle			84			94.39					
31	Two-Phase Properties						Louvers			0			0					
32	Latent heat	kJ/kg				Steam Coil			0			0						
33	Molecular weight		18.71		28.96		Plenum			0			0					
34																		
35	Heat Transfer Parameters						Heat Load						kW					
36	Reynolds No. vapor		169948.8	198309.9	5359.36	3536.54	Vapor			23300.7								
37	Reynolds No. liquid					Cond./Evap.			0									
38	Prandtl No. vapor		0.92	0.95	0.71	0.68	Liquid			0								
39	Prandtl No. liquid					Input/Actual duty ratio			1									
40																		
41	Tubes / Fin		Last row number			8												
42	Tubes per bundle		344	Tube OD / ID		mm	22.2 / 18.9	/	/	/								
43	Tube material	Carbon Steel	Fin type		G-finned													
44	Length effective	m	4.726	Fin material		Aluminum 1060												
45	Length actual	m	5	Fin tip diameter		mm	40											
46	Transverse pitch	mm	52.44	Fin thickness		mm	0.28											
47	Longitudinal pitch	mm	45.42	Fin frequency		#/m	433											
48	Pitch angle		30	Root diameter		mm	22.2											
49	Th Cond	W/(m K)	50.5835	Th Cond		W/(m K)	218.3292											
50	Surface effectiveness		0.95	Surface effectiveness		0.95												
51																		
52	X-side and Fan				Headers and Nozzles				Weights				kg					
53	Type draft		Forced		Inlet				Other		Inlet header		2874.5					
54	Fans/bay		1		Box				Box		Other header		2843.1					
55	Vol./fan (Act/Std)	m³/s	41.51	41.677	Header type				585.79		569.12		Inlet nozzle		125.2			
56	Face vel. (Act/Std)	m/s	1.92	1.93	Header depth				mm		In		Out		Outlet nozzle		118.2	
57	Fan diam./% cov.	m	3.6576	46.06	No. of nozzles				1		1		Tubes and fins		1911.2			
58	Sum./Win. des. Temp	°C	20	0	Nozzle ID				mm		352.42		341.31		Side frms/supports		956.7	
59	Abs pwr/fan-Winter	kW	6.154		Hom. Velocity				m/s		22.01		19.92		Bundle - dry		8829	
60	Abs pwr/fan-Summer	kW	5.734		Rho*V2				kg/(m s²)		5641		5442		Bundle - wet		10257.7	
61	Drive efficiency		95												Unit bundles - dry		35315.9	
62	Fan efficiency		65												Unit bundles - wet		41030.8	

Figure 1: HTFS output for the air-side heat transfer coefficient of the air-preheater with the air on the shell side.

Heat Exchanger Thermal Design

Shell&Tube V7.1

Page 1

File: AirHeater-S&T-AirTubeside.EDR

Date: 5/09/2011

Time: 3:49:05 PM

1	Size	1250	x	5100	mm	Type	BES	Hor	Connected in	7 parallel	1 series	
2	Surf/Unit (gross/eff/finned)	1675.1	/	1331.5	/			m ²	Shells/unit	7		
3	Surf/Shell (gross/eff/finned)	239.3	/	190.2	/			m ²				
4												
5	PERFORMANCE OF ONE UNIT											
6			Shell Side		Tube Side		Heat Transfer Parameters					
7	Process Data		In	Out	In	Out	Total heat load		kW	23305		
8	Total flow	kg/s	100		100		Eff. MTD/ 1 pass MTD		°C	308.34/ 308.34		
9	Vapor	kg/s	100	100	100	100	Actual/Reqd area ratio - fouled/clean					1.01 / 1.01
10	Liquid	kg/s	0	0	0	0						
11	Noncondensable	kg/s	0		0		Coef./Resist.	W/(m ² K)	m ² K/W	%		
12	Cond./Evap.		0		0		Overall fouled	57.2	0.01747			
13	Temperature	°C	500	396.94	20	250	Overall clean	57.2	0.01747			
14	Dew / Bubble point	°C					Tube side film	64.8	0.01544	88.35		
15	Quality		1	1	1	1	Tube side fouling		0	0		
16	Pressure	bar	40	39.82893	1.05	1.01188	Tube wall	25933.8	0.00004	0.22		
17	Delta P allow/calc	bar	1	0.17107	0.04	0.03812	Outside fouling		0	0		
18							Outside film	500.9	0.002	11.43		
19												
20	Liquid Properties						Shell Side Pressure Drop					bar %
21	Density	kg/m ³					Inlet nozzle	0.01608	9.4			
22	Viscosity	mPa s					Inlet space Xflow	0.02151	12.57			
23	Specific heat	kJ/(kg K)					Baffle Xflow	0.05663	33.1			
24	Therm. cond.	W/(m K)					Baffle window	0.02447	14.3			
25	Surface tension	N/m					Outlet space Xflow	0.01908	11.15			
26	Molecular weight						Outlet nozzle	0.0333	19.47			
27	Vapor Properties						Intermediate nozzle					
28	Density	kg/m ³	11.64	13.74	1.25	0.67	Tube Side Pressure Drop				bar %	
29	Viscosity	mPa s	0.0288	0.0247	0.0186	0.0283	Inlet nozzle	0.0073	19.16			
30	Specific heat	kJ/(kg K)	2.271	2.262	0.992	1.036	Entering tubes	0.00207	5.44			
31	Therm. cond.	W/(m K)	0.071	0.0586	0.0244	0.0387	Inside tubes	0.01576	41.34			
32	Molecular weight		18.71	18.71	28.94	28.94	Exiting tubes	0.00522	13.69			
33	Two-Phase Properties						Outlet nozzle					0.00777 20.37
34	Latent heat	kJ/kg					Intermediate nozzle					
35												
36	Heat Transfer Parameters						Velocity / Rho*V2					m/s kg/(m s ²)
37	Reynolds No. vapor	197325.4	230241.9	71373.27	46961.86		Shell nozzle inlet	13.79	2215			
38	Reynolds No. liquid						Shell bundle Xflow	10.99	9.3			
39	Prandtl No. vapor	0.92	0.95	0.76	0.76		Shell baffle window	7.84	6.63			
40	Prandtl No. liquid						Shell nozzle outlet	20.88	5863			
41	Heat Load		kW		kW		Shell nozzle interm					
42	Vapor only	23305.5		23304.5								m/s kg/(m s ²)
43	2-Phase vapor	0		0			Tube nozzle inlet	35.43	1567			
44	Latent heat	0		0			Tubes	26.07	48.32			
45	2-Phase liquid	0		0			Tube nozzle outlet	66.45	2939			
46	Liquid only	0		0			Tube nozzle interm					
47												
48	Tubes		Baffles		Nozzles: (No./OD)							
49	Type	Plain	Type	Single segmental	Shell Side Tube Side							
50	ID/OD	mm 40.79 / 44.45	Number	6	Inlet	mm 1 / 355.6 1 / 660.4						
51	Length act/eff	mm 5100 / 4054	Cut(%d)	25.55	Outlet	1 / 273.05 1 / 660.4						
52	Tube passes	1	Cut orientation	H	Intermediate	/ /						
53	Tube No.	336	Spacing: c/c	mm 430	Impingement protection		None					
54	Tube pattern	90	Spacing at inlet	mm 964.45								
55	Tube pitch	mm 55.56	Spacing at outlet	mm 939.58								
56	Insert	None										
57	Vibration problem: Tasc/TEMA Possible / No				RhoV2 violation				No			

Figure 2: HTFS output for the air-side heat transfer coefficient of the air-preheater with the air on the tubeside.

4. Programming – Area estimation

The heat exchanger area targeting methodology that is detailed here has been added to the SHICE program, which is detailed in Appendix A. The programming algorithm required to use this method is explained in detail in that appendix.

References

- Sinnott, R. K. (1998). Coulson & Richardson's Chemical Engineering Volume 6. Oxford, Butterworth-Heinemann.
- Smith, R. (2005). Chemical Process Design and Integration. West Sussex, England, John Wiley & Sons Ltd.
- TEMA (1999). Standards of the tubular exchanger manufacturers association. New York, Tubular Exchanger Manufacturers Association Inc.

Appendix E

Redesigning the cold end of a lignite power station for CO₂ capture.

Conference Proceedings – 4th International conference on clean coal technologies (CCT2009), Dresden, Germany, 2009.

Redesigning the cold end of a lignite power station for CO₂ capture

Trent Harkin^{1,2} Andrew Hoadley² Barry Hooper¹

¹Cooperative Research Centre for Greenhouse Gas Technologies (CO2CRC)

²Department of Chemical Engineering, Monash University, Clayton, VIC 3800, Australia
Campus

Abstract

The efficiency of lignite power stations is reduced by the addition of carbon capture and storage (CCS). With CCS added to power plants the flue gas temperature needs to be reduced, the heat currently released in the flue gas stack may be useful in offsetting the impact of CCS on the power plant efficiency. A 200MWe (nominal) train of an existing pulverised brown coal fired power plant currently burning undried coal is used as a basis for comparison. Using pinch analysis heat integration targeting and design is used to provide reductions in the overall energy penalty and therefore the costs of implementing CCS. The work shows that proper integration of the CCS plant can reduce the energy penalty from 39% to 24%, with further reductions possible if the coal is pre-dried. The majority of the changes required to a power plant are found to be at the cold end of the flue gas and the impact of pre-heating the air is useful only to a limited temperature.

1. Introduction

A traditional lignite fired power station involves the recovery of heat from the flue gas down to the acid dew point of the flue gas. When a safety margin is also included, the flue gas often leaves the chimney at temperatures in excess of 150°C. However with carbon capture, there is a need to cool the flue gas to close to ambient temperature to remove moisture and maximise the efficacy of the carbon capture technology. If part of the energy in the flue gas below the dew point is recovered, then this can be used to offset the large energy burden required for carbon capture and storage (CCS).

When CCS is added to a power plant, the efficiency of the power plant will invariably be reduced due to the added heat and/or power requirements of the capture technology employed as well as the work required to compress the CO₂ for transport and storage. The reduction in the efficiency of the power plant is often referred to as the energy penalty which is the ratio of the drop in efficiency caused by CCS to the original efficiency (Equation 1). The energy penalty attributed to the addition of CCS can be approximately 30-40% (IPCC 2005).

$$\text{Energy Penalty} = \frac{\Delta E}{E_{\text{ref}}} = 100 \times (\eta_{\text{ref}} - \eta_{\text{CCS}}) / \eta_{\text{ref}} \quad (1)$$

Pinch analysis has been used in the process industries since the 1970's to improve the efficiency of process plants and the process was applied by Linnhoff and Alanis(1989) to show how a power plants performance could be improved by adjusting the flowrates of extraction steam. With the inclusion of CCS to power plants, the heat and power requirements change and pinch analysis may assist in developing flowsheets that reduce the energy penalty. Pinch analysis looks at the entire heating and cooling requirements of the plant and tries to maximise the process to process heat exchange to minimise the amount of

utilities required. In the case of a power plant, the pinch analysis aims to maximise the use of the energy in the flue gas and other hot streams to supply the required heating demands of the steam generation and now the CCS plant. Minimising the amount of extraction steam required to provide that heat maximises the amount of work extracted from the steam. Pinch analysis relies on ensuring there is a minimum driving force or temperature difference between the hot stream and the cold stream, as the minimum driving force, ΔT_{\min} , increases, the amount of additional energy required to meet the process heating demands also increases.

In this work pinch analysis is applied to a brown coal fired power plant fitted with CCS. It provides targets for the energy penalty associated with the addition of CCS for non-integrated plants compared to integrated power plants, as well as identifying the impact pre-drying the coal and altering the air-preheat temperature has on the energy penalty.

2. Background

The basis of this work is a 200MWe(nominal) subcritical brown coal fired power plant. The power plant has no steam reheat and only uses 2 low pressure feedwater heaters resulting in a relatively low efficiency plant. Refer to Figure 1 for a representation of the plant.

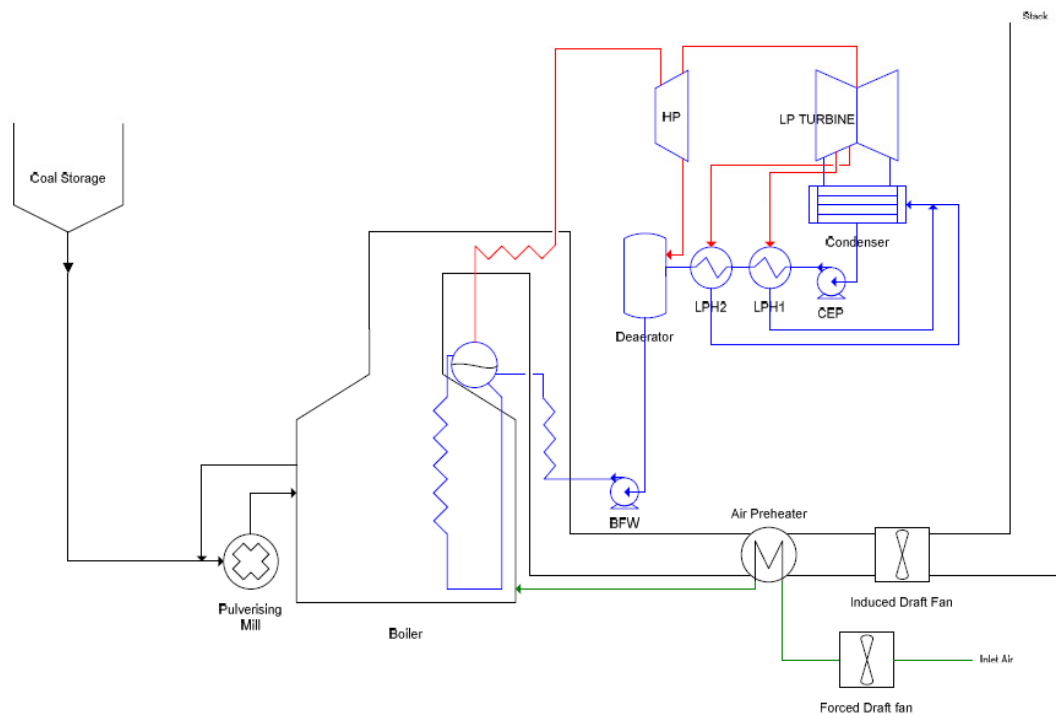


Figure 1 Basic diagram of power plant used as a basis

A model of the base power plant has been developed in Aspen Plus® and validated against a Gatecycle™ model of the same plant. The Aspen model includes the coal drying in the pulverising mill, coal combustion, flue gas heat recovery and simulation of the steam cycle. As the conventional and most advanced form of CO₂ capture for flue gas is solvent absorption, this has been used for this study. The pressure increase across the induced draft fan has been increased to account for the additional pressure drop across the solvent plant.

The CCS plant and associated equipment would nominally be located downstream of the electrostatic precipitator and the induced draft fan. In this case the flue gas has more than 200ppmv of SO_x so for this study it is assumed that flue gas desulphurisation (FGD) will be required upstream of the solvent plant. Due to the low level of NO₂ (<10ppm) in the flue gas, no additional equipment is considered for NO_x removal. Wet FGD using lime or limestone will be considered as the basis for this work and the flue gas entering the desulphurisation unit will be cooled down to 40°C. There are no heating/cooling requirements for the FGD, unit but a nominal electrical requirement for the fans and pumps of 3MW is included.

After the FGD unit the flue gas enters the solvent absorption column where 90% of the CO₂ is captured producing a high purity (>99% after dehydration) CO₂ stream. The solvent capture plant is based on an MEA plant modelled using Aspen Plus® with all heating/cooling curves prorated to a reboiler duty of 3GJ/tCO₂ to provide results comparable to leading solvent technologies. The CO₂ is compressed to 100bar in a four stage compressor with intercooling and water removal. The water removal energy requirements are 1.5MWe (5.5kWe/tCO₂).

The high water content of lignite makes electricity production from lignite inherently less efficient in comparison to drier coals. In conventional pulverised coal fired power plants the coal is dried in the pulverising mills using hot flue gas at temperatures around 1000°C. By pre-drying the coal using low temperature heat to extractor evaporate the moisture, the efficiency of a power plant can be improved (Li 2004). Lignite drying technology has been the focus of much work and commercial processes are being demonstrated. The drying needs to be performed at low temperatures (<180°C) to avoid the loss of volatile components that are required for good coal combustion.

For this study when the effect of coal drying is reviewed it will be assumed that the coal will be heated from ambient temperature, assumed to be 25°C up to at least 100°C. The net steam generated by the dewatering process will also be assumed to be available for heating requirements if required. A general diagram of the plant including CCS is shown in Figure 2.

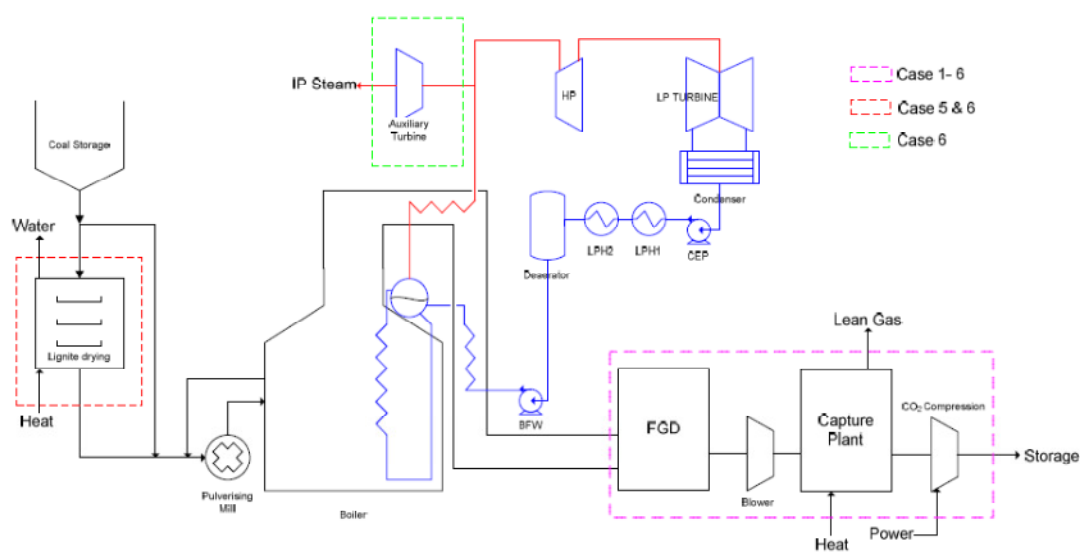


Figure 2 Power plant with CCS and Drying

A number of cases have been considered, using the model, which are detailed below. In this study it has been assumed that all heat and power for the CCS plant will be supplied using the heat and power available from the power plant and that the minimum temperature driving force is 3°C. The effect of adjusting the ΔT_{\min} has previously been reported by Harkin et al (2008).

1. Base Case: Existing power plant with no CCS.
2. Non-integrated CCS: Power plant with CCS added, heat for solvent reboiler supplied by steam from next available steam extraction point.
3. Integrated CCS: Power plant with CCS and best heat integration possible.
4. Basic retrofit: Integrate the CCS plant only with the power plant downstream of the economiser, ie. make no changes to the power plant upstream of the economiser.
5. Drying case: Integrate coal pre-drying and CCS to the existing power plant.
6. Drying and Additional steam case: Generate extra steam with the additional heat available in the flue gas at higher temperatures due to the coal pre-drying. Use the additional steam to generate the required power for the CO₂ compression through an auxiliary turbine, letting the steam down to the required level to supply the solvent reboiler.

In addition to the six cases discussed, the effect of air preheat on the design was investigated using Case 3 as a basis and adjusting the level of air preheat from no air preheat to a preheat temperature of 250°C.

3. Results

Table 1: Plant performance for the six cases.

Case		1	2	3	4	5	6
Raw Coal Rate	kg/s	86.6	86.6	86.6	86.6	86.6	86.6
Moisture Content (Inlet to mill)	wt%	60.8	60.8	60.8	60.8	45	45
Steam Production	kg/s	208	208	208	208	208	248
Steam Extraction							
HP Exhaust (177°C)	kg/s	10.9	111.6	54	58.4	42.1	53
LP Bleed 1 (110°C)	kg/s	11.4	11.4	0	3.7	7.1	6.8
LP Bleed 2 (84°C)	kg/s	8.7	8.7	0	0.2	0	0
Electricity Produced	MW	220	172	205	201	208	203
Plant Auxiliary Power	MW	14	22.1	22.1	22.1	22.1	22.8
CO ₂ Compression Power	MW	-	24.8	24.8	24.8	25.2	1.7*
Net Electrical Power	MW	206	125	158	154	161	178
Net Cycle HHV Efficiency	%	23	14.0	17.6	17.2	17.9	20
Energy Penalty	%	-	39	23.5	25.2	22.1	13.5
CO ₂ Emissions	t/MWh	1.46	0.24	0.19	0.19	0.15	0.14

*The CO₂ compression power in this case is offset by the addition of an auxiliary stream turbine.

Table 2: *Effect of Air preheat on Case 3*

Air Preheat Temperature	°C	18	75	100	120	200	250
Boiler Theoretical Temperature	°C	1195	1221	1233	1243	1280	1303
Process Pinch point (Hot composite curve temperature)	°C	121	121	121	117	117	117
Heating requirements	MW	161	140	130	125	125	125
HP Steam flowrate	kg/s	70	61	57	54	54	54

The heating requirement listed in Table 2: is the amount of heat that is required by the process to ensure the CCS and power plant heating requirements are met; where the HP steam flowrate is that required to meet this heating requirement.

4. Discussion

4.1 Base case (Case 1)

A neutral ΔT_{\min} , has been used by others (Farhad et al. 2008) to define the global ΔT_{\min} at which a power plant could be redesigned with a new heat exchanger network to get the same efficiency as the existing power plant. The base case has a neutral ΔT_{\min} of 30°C, this indicates that the existing power plant efficiency could be improved if the ΔT_{\min} was decreased and the plant redesigned to achieve the targets alluded to by the pinch analysis. With a ΔT_{\min} of 3°C the HP steam flow could be reduced to 3.2kg/s which would provide approximately 3MWe of additional power an increase of only 1.5%.

The power plant used in this study has a high flue gas stack temperature of around 260°C and a relatively high flue gas flowrate due to its low efficiency. Therefore in this case there is potential for up to 250MW of energy in the flue gas from the chimney exhaust temperature down to ambient temperature, which is 28% of the total thermal energy of the boiler and more than the required energy for the solvent reboiler for this plant. However, much of the heat available is due to the condensation of the water in the flue gas which does not occur until lower temperatures. Only 40% of the 250MW is available at temperatures greater than 65°C, and less than 30% is available above 120°C (the solvent reboiler temperature) and therefore a lot of the energy available in the flue gas will be difficult to utilise.

The advantage of using pinch analysis to determine the minimum energy penalty associated with the addition of CCS is that the available energy in all the hot streams are considered and they are applied so that they are used in the most efficient manor possible for a given steam flowrate.

4.2 Non-integrated (Case 2) compared to the integrated case (Case 3)

The non-integrated case (Case 2) requires 226MW of heating for the solvent regeneration at temperatures greater than 120°C; this increases the steam flow from the HP bleed by 100kg/s. Whereas the integrated case (Case 3) requires only 54kg/s of HP steam, reducing the HP steam energy utilised by 130MW. This is more than that available in the flue gas above 120°C (<80MW) and therefore comes from making more appropriate use of the heat across the entire plant. However, it is not just the impact of improvements in the base plant, as from section 4.1 this only lead to 3MWe improvement. The integrated case including CCS has a 33MWe improvement over the non-integrated case. The energy penalty reduces from 39% for the non-integrated case to 24% for the integrated case, which is a significant improvement.

4.3 Basic Retrofit Model (Case 4)

The basic retrofit model shows that the changes to the power plant do not require wholesale changes to the boiler itself to achieve significant reductions in the energy penalty. The basic retrofit option involves only changes made to the boiler feedwater before it enters the economiser and to the flue gas after the economiser. However, even restricting the process changes to this region, the energy penalty reduces from a non-integrated case of 39% down to 25%. Given the energy penalty for this case is only marginally worse than the totally integrated case (24%), it appears that the majority of the redesigning of the heat exchanger network will be at the cold end of the power plant.

The heat exchanger design for this case includes both novel heat exchanger arrangements and those that are currently employed to achieve these targets, including;

- Air preheat using a combination of flue gas, CO₂ compressor intercoolers and steam.
- Low pressure boiler feedwater heating with both flue gas and steam.
- The solvent stripper reboiler with both flue gas and steam.

4.4 Impact of drying and extra steam generation (Cases 5 and 6)

For this power plant adding on pre-drying of the brown coal has aided in reducing the energy penalty. Adding pre-drying resulted in a 2% improvement in the energy penalty in comparison to the integrated CCS case without pre-drying. With coal pre-drying included, the air preheat is removed entirely to reduce the maximum combustion temperature. However in this case the theoretical flue gas temperature still increases by just over 110°C. This increase may limit the level of pre-drying that is able to be achieved due to constraints of the existing boiler.

For case 6, it is assumed additional steam is produced and is utilised in a new auxiliary turbine. There is sufficient heat in the boiler flue gas to provide at least 20% additional steam, which can be used to provide enough energy in the auxiliary turbine to offset the CO₂ compression power and provide a significant amount of steam at the desired level for the solvent stripper. The energy penalty for this case reduces to 14%; however it is likely to have high capital costs due to increasing the amount of steam produced in the boiler and the introduction of a new turbine.

4.5 The impact of changing the degree of air preheating

As can be seen from Table 2: the amount of air-preheat for this power plant is only useful up to the pinch point of the process (~120°C). The energy penalty improves / reduces up until the air preheat reaches the pinch point, then any additional air preheat does not lead to improved energy penalties.

A pre-heater leads to an additional amount of heat added to the flue gas that is equal to the amount of energy added to the air in the pre-heater. This increases the maximum temperature of the flue gas, but increases the amount of heat that is required to be extracted from the cold end of the flue gas. In a conventional power plant, air preheat is beneficial as it is used to increase the percentage of energy utilised from the flue gas. Ignoring the boiler casing and ash losses the boiler efficiency can be represented by equation 2;

$$\eta = \frac{(T_{fg} - T_s)}{(T_{fg} - T_o)} \quad (\text{Eq. 2})$$

η = Boiler Efficiency; T_{fg} = Theoretical flame temperature, T_s = Flue Gas Stack temperature, T_o = Ambient Temperature.

Therefore if T_{fg} increases both the denominator and the numerator of equation 2 increase by the same amount and the efficiency increases, as the air preheating increases the efficiency approaches unity.

However, for power plants with CCS where the flue gas needs to be cooled down to near ambient temperatures for the capture technology, the effect of air preheat appears to change. As the stack temperature approaches the ambient temperature, increasing the flue gas temperature does not lead to increases in the boiler efficiency. Nevertheless, the air preheat for a conventional power plant increases the boiler efficiency where the air preheat for a power plant with CCS just changes the distribution of heat, which may or may not be of benefit. Air preheating may still be valuable as it still increases the temperature of the flue gas. Refer to Figure 3 and Figure 4 which shows the high end of the hot composite curve showing the increase in the flue gas high end temperature and energy as the air preheat temperature is increased.

For this power plant, the air preheat that is below the pinch point uses energy in the flue gas that is currently in excess, that would otherwise require additional air / water cooling (Refer to Figure 3 and Figure 5). Therefore, the energy available at the high end of the flue gas is increased and the amount of additional cooling required is reduced, which provides a double benefit. Whereas, the air-preheat occurring above the pinch point is competing against other cold streams that require heating, and therefore has no benefit. So for this case and likely for other cases the air-preheat can be limited to the power plant pinch temperature. Furthermore, for retrofit cases where the boiler will often be constrained by a maximum temperature, removing the air preheat enables higher calorific fuels (drier) fuels to be burnt, which was shown in this study to reduce the energy penalty.

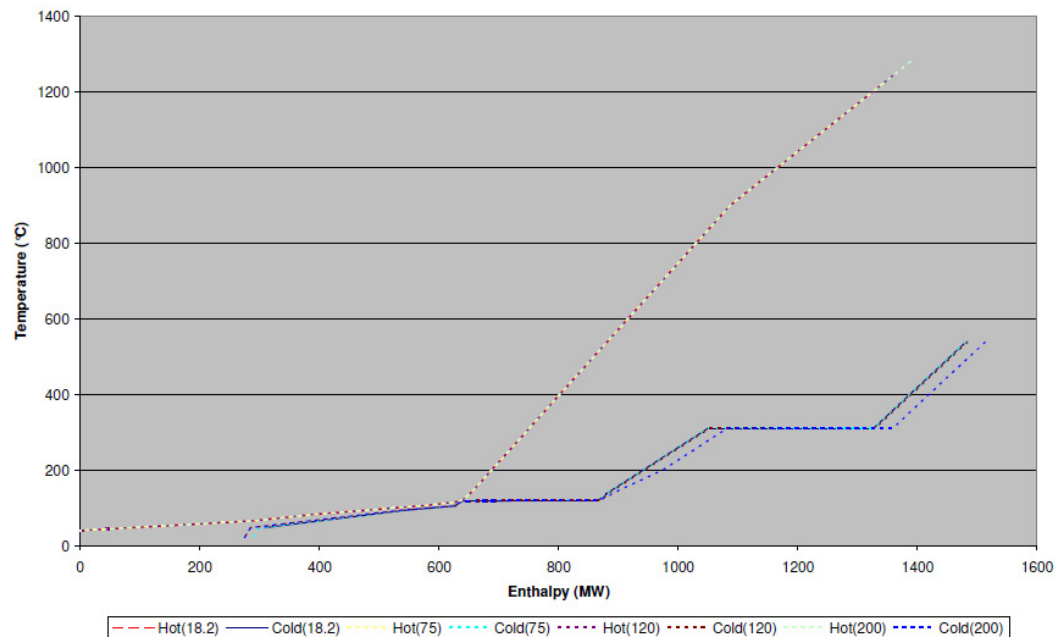


Figure 3 Unbalanced composite curves for varying amounts of air preheat

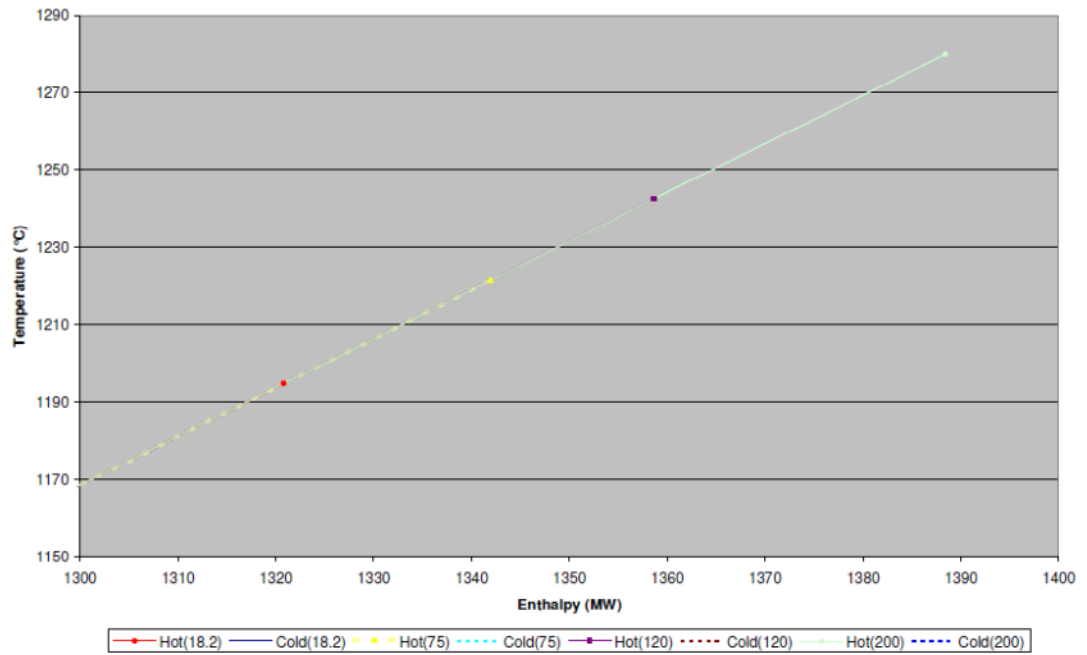


Figure 4 Hot end of unbalanced hot composite curve for varying amounts of air preheat

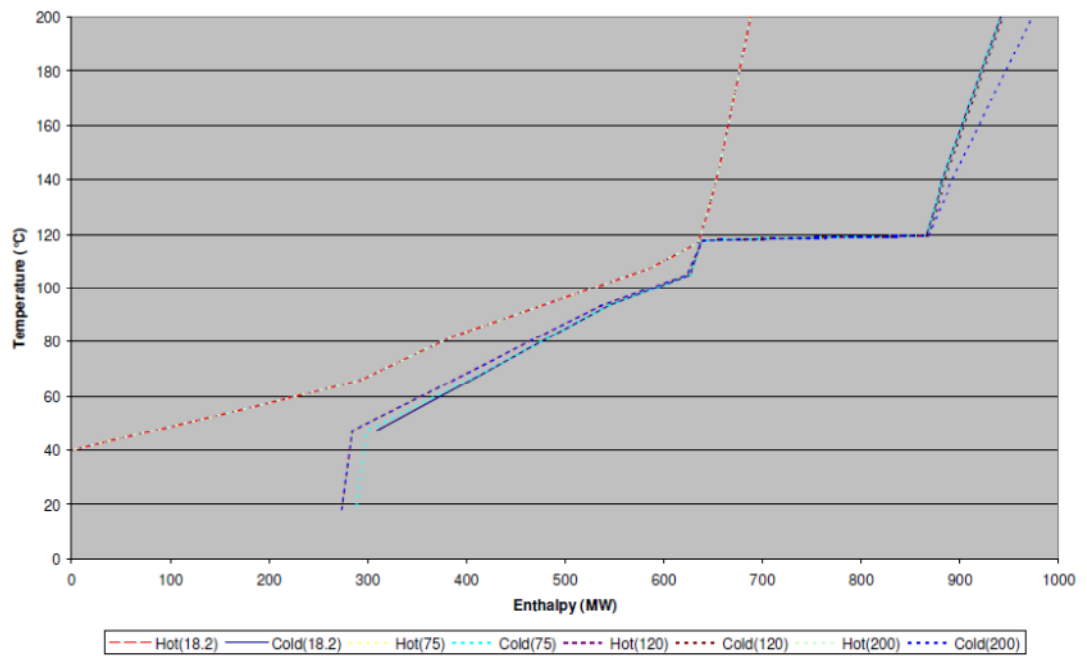


Figure 5 Cold end of unbalanced composite curves for varying amounts of air preheat

5. Conclusion

The design of pulverised power plants has evolved over the years leading to operation and efficiency improvements. When CCS is added to a power plant many of the standard design rules that currently exist may no longer be the most appropriate way of designing a power plant. Whilst the addition of a CCS plant will reduce the efficiency of a power plant, making changes to the cold end of the power plant will help to minimise the energy penalty associated with the addition of CCS.

Ensuring appropriate use of the flue gas energy will be important in reducing the energy penalty. Drying brown coal will enable further efficiency improvements that may help to offset the impact of adding CCS. The air preheat temperature may only be beneficial up to limited temperatures. The use of pinch analysis to help design power plants incorporating CCS is a valuable tool to help reduce the energy penalty. Novel heat exchanger arrangements and materials will be important to ensure the benefits suggested by this work will be able to be implemented.

6. References

- Farhad, S., M. Saffar-Avval and M. Younessi-Sinaki (2008). "Efficient design of feedwater heaters network in steam power plants using pinch technology and exergy analysis." *International Journal of Energy Research* **32**(1): 1-11.
- Harkin, T., A. F. A. Hoadley and B. Hooper (2008). Process integration analysis of a brown coal-fired power station with CO₂ capture and storage and lignite drying. *Ninth international conference on greenhouse gas technologies (GHGT-9)* Washington DC, USA, Elsevier.
- IPCC (2005). IPCC Special Report on Carbon Dioxide Capture and Storage. Prepared by Working Group III of the Intergovernmental Panel on Climate Change [Metz, B., O. Davidson, H. C. de Coninck, M. Loos, and L. A. Meyer (eds.)]: 442.
- Li, C.-Z. (2004). *Advances in the science of Victorian brown coal*, Oxford; Elsevier Ltd: Ch7. p361.
- Linnhoff, B. and F. J. Alanis (1989). *A systems approach based on pinch technology to commercial power station design*. The Winter Annual Meeting of ASME, San Francisco, California.

Appendix F

A comparison of the Process Integration of Shockwave CO₂ compression with conventional turbo machinery into PCC power station design.

Energy Procedia 4 (2011) 1339 – 1346

doi:10.1016/j.egypro.2011.01.192

GHGT-10

A comparison of the Process Integration of Shockwave CO₂ compression with conventional turbo machinery into PCC power station design.

Trent Harkin^{a,b,*}, Andrew Hoadley^b, Barry Hooper^a^aCooperative Research Centre for Greenhouse Gas Technologies (CO2CRC), The University of Melbourne, Vic. 3010, Australia^bDepartment of Chemical Engineering, Monash University, Clayton, Vic. 3800, Australia

Abstract

This paper discusses the energy penalty of solvent based post combustion capture for three different power stations and includes a comparison of shockwave CO₂ compression versus conventional turbo machinery on the energy penalty associated with carbon capture and storage. This study uses pinch analysis to determine targets for the energy penalty of three different power stations that include a brown coal power plant with no reheat stage, a more efficient brown coal power station and a black coal power station. Heat integration can be used to reduce the energy penalty of all power stations combined with CCS. It is also found that when heat integration is considered, the heat that can be recovered in shockwave compressor inter/after-coolers reduces the amount of steam that needs to be extracted from the steam turbine. Hence, the net power output from the power station will be higher when shockwave compressors are used for CO₂ compression compared to conventional turbo-machinery.

© 2011 Published by Elsevier Ltd.


Keywords: CCS, Post Combustion, Heat Integration, Compression

1. Introduction

Post Combustion Capture (PCC) of CO₂ from existing pulverised coal fired power stations will be an important tool in a carbon constrained environment in order to avoid stranding existing assets. A significant proportion of the estimated cost of carbon capture and storage (CCS) for PCC from coal-fired power stations is due to the additional energy expended to capture the CO₂ and to compress it for transport and storage. The two largest requirements for energy for a solvent based PCC plant are the heat to regenerate the solvent and the energy to compress the CO₂.

CO₂ compression using conventional turbo-machinery will typically require eight stages of compression and represent approximately one third of the capital and operating costs of a post combustion, amine based CCS system.

* Corresponding author. Tel.: +61-3-8344-5048; fax: +61-3-9347-7438

E-mail address: 

Conventional compression is typically limited by ensuring the Mach number of the inlet flow is less than 0.9 to avoid shockwaves in the blade passages, however this limits the stage speed and/or diameter and results in pressure ratios per stage of less than 2:1 for CO₂. As a consequence a typical CO₂ compression system for CCS requires between 8-10 stages to produce an overall ratio of 100:1. CO₂ compression can be simplified with shockwave compression. The design of these compressors is based on principles used in supersonic aircrafts and uses Mach numbers of greater than one and can obtain compression ratios of greater than ten per stage, thereby reducing the number of compression stages to just two for CCS [1].

With two stages of compression, shockwave compressors utilise fewer stages of inter-cooling and the compressor discharge temperatures are significantly greater than conventional turbo-machinery. This higher temperature heat can be utilised in the power station and carbon capture plant design to reduce the energy penalty impact associated with CCS. While not a feature of this paper the reduced number of stages and smaller physical footprint of the shockwave compression technology is also expected to reduce capital costs for compression [1].

The impact of a PCC plant will not only be dependent on the type of capture plant and compression employed, but will also depend on the original power plant to which it is applied. Power plants with lower efficiencies will require larger CCS units, but will generally have more low-grade waste heat which could be utilised to offset the impact of the addition of CCS. Brown coal power plants may be able to be retrofitted with pre-drying technology to improve the efficiencies, however this will reduce the amount of useful low-grade heat that is available and the overall energy penalty may or may not be improved by the addition of drying. Therefore, it is important to compare not only different capture and compression technologies, but to also compare them on a range of power station types.

This paper reviews the impact of adding a solvent based carbon capture plant with compression to three power stations and compares the net electrical power produced from the power station with varying levels of heat integration and with both conventional and shockwave compressors. This work expands on work that has been published previously [2, 3] and more details on the simulation basis and the methodology to perform the heat integration can be found in these papers. In this paper the additional heat and power required by the CCS plant is provided by the power station. Where there is a deficit of heat, steam is extracted from the turbine to provide the heat, which reduces the amount of power produced by the steam turbine. However the use of pinch analysis can reduce the amount of extraction steam required by using the available waste heat in other sources such as the compressor intercoolers, the solvent regenerator condenser and the flue gas.

2. Background to Case Studies

Two brown coal and one black coal power station will be used as examples with a generic amine based solvent capture plant. The first brown coal power station (Plant A) has a simple steam cycle with no reheat which is less efficient than the second brown coal power station (Plant B) which has a single reheat steam cycle, the same cycle that is used in the black coal power station (Plant C). The power stations are represented in Figure 1. For each power station there will be up to four cases studied, each with both conventional and shockwave compression.

1. Base Case: The existing plant with no CCS.
2. CCS: This case includes CCS, but with no heat integration. The regenerator is supplied steam from the best turbine extraction point. No heat is recovered in the CCS plant.
3. Integrated CCS: This case includes CCS and allows maximum heat integration between the power station and the carbon capture plant and compressor intercoolers using pinch analysis and a ΔT_{\min} of 3 °C.
5. CCS & Drying: Includes CCS and coal pre-drying from 60 wt% water to 45 wt% water. Air preheat is removed to minimise the increase in combustion temperature to around 100 °C.

Note that as the focus of this paper is on the comparison of conventional and shockwave compression there are fewer cases reported than covered in the previous work[2], however the case numbering of the previous work is applied in this paper. It should also be noted that the values in this paper cannot be compared directly to the previous

work [2] as the CO₂ compressor models used in this paper have been updated and are more detailed. The conventional compressors modelled in this paper are based on in-line single shaft compressor technology using the Dresser-Rand DATUM compressor estimating tool [4], the detail of the shockwave compressors were supplied by Ramgen Power Systems (Baldwin, P. 2010 pers. comm., 27 July).

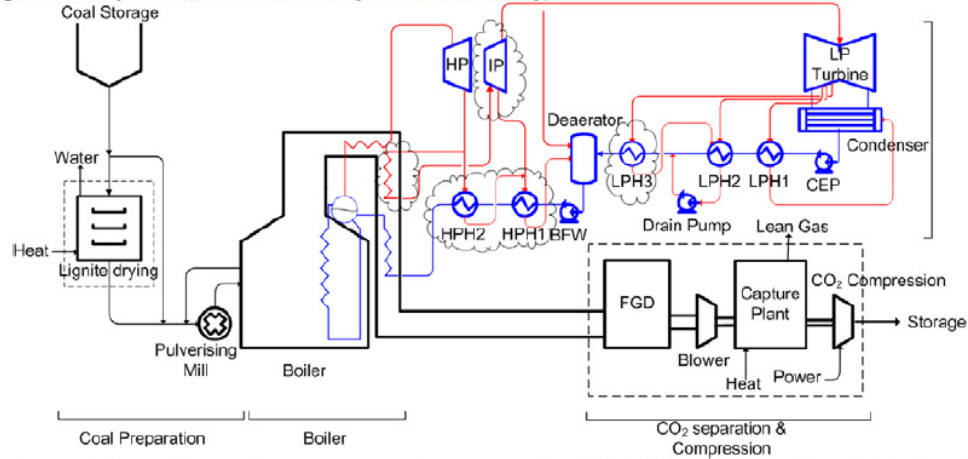


Figure 1 Power Station model. Dotted lines represent new equipment that may be added for CCS. Equipment in Plant B & C that is not in Plant A has been clouded.

3. Results

The results are presented in 6 parts; 3.1-3.3 contains the results of the individual power stations, 3.4 at the impact of the CO₂ pressure, 3.5 at the impact of ΔT_{min} and 3.6 compares the use of shockwave to conventional compression.

3.1. Plant A - Brown Coal Power Station

Table 1: Plant A – Brown Coal Power Station Results

		1	2	3	5
Conventional Turbo Machinery					
Steam Extraction Rates:					
HP Exhaust / LP 1 / LP 2	kg/s	10.9 / 11.4 / 8.7	111.6 / 11.4 / 8.7	52.8 / 0.2 / 0	41.05 / 7.1 / 0
Gross Electricity	MW	220	172	205	208
Auxiliary Power	MW	14	24	24	24
CO ₂ compression Power	MW	-	27	27	27
Net Electrical Power	MW	206	122	155	158
Efficiency (HHV)	%	23.0	13.6	17.3	17.7
Energy Penalty	%	-	40.9	24.9	23.3
Shockwave Compression					
Steam Extraction Rates					
HP Exhaust / LP 1 / LP 2	kg/s	10.9 / 11.4 / 8.7	111.6 / 11.4 / 8.7	47.3 / 0.5 / 0	35.6 / 8.5 / 0
Gross Electricity	MW	220	172	208	211
Auxiliary Power	MW	14	24	24	24
CO ₂ compression Power	MW	-	26	26	26
Net Electrical Power	MW	206	122	158	161
Efficiency (HHV)	%	23.0	13.6	17.6	17.9
Energy Penalty	%	-	40.7	23.2	22.0

This power station has a relatively low base efficiency of 23 % (HHV) without CCS, due to the very high moisture brown coal and the simple steam cycle. Therefore, with the addition of CCS the energy penalty is relatively high at 41 % due to the large amount of energy that is required for CO₂ capture compared with the amount of energy that the power station produces. However as this power station has low base plant efficiency there is a significant amount of waste heat available. The flue gas leaves the air-heater at 260 °C and therefore heat integration can enable significantly reduced energy penalties of 25 and 23 %. When heat integration is taken into account, coal pre-drying provides a small improvement in the energy penalty which is reduced by 1-2 % depending on the type of compressor installed.

For this power station the net electrical power production for the power station without heat integration does not favour either conventional compressors or the shockwave compressors as the net output is comparable. However, when heat integration is taken into consideration, the net electrical power production of the power station is greater with shockwave compression; the heat recovered from the compressor inter/after-coolers enables a reduction in the amount of extraction steam required.

The pinch point for the power station and the CCS plant is invariably located at the CCS solvent regenerator reboiler temperature, and therefore heat that is available above this temperature will be useful to reduce the energy penalty. Therefore it is clear that conventional compressors with exhaust temperatures around 130 °C cannot provide significant amounts of useful heat, whereas shockwave compressor intercoolers with temperatures greater than 220 °C will provide more useful heat (see section 3.6 for more detail).

3.2. Plant B – Higher Efficiency Brown Coal Power Station

Table 2: Plant B – Brown Coal Power Station with Reheat Results

		1	2	3	5
Conventional Turbo Machinery					
Steam Extraction Rates					
HP Exhaust / IP 1 / IP 2	kg/s	45.8 / 20.1 / 15.4	45.8 / 20.1 / 15.4	2.0 / 21.1 / 8.8	2.0 / 4.4 / 1.3
LP Bleed 1 / LP 2 / LP3	kg/s	13.9 / 25.8 / 15.1	13.9 / 206.7 / 15.1	5.2 / 189.7 / 0	0.5 / 208.1 / 0
Gross Electricity	MW	520	441	510	525
Auxiliary Power	MW	30	46	46	46
CO ₂ compression Power	MW	-	50	50	50
Net Electrical Power	MW	490	346	414	429
Efficiency (HHV)	%	28.0	19.8	23.7	24.5
Energy Penalty	%	-	29.5	15.6	12.5
Shockwave Compression					
Steam Extraction Rates					
HP Exhaust / IP 1 / IP 2	kg/s	45.8 / 20.1 / 15.4	45.8 / 20.1 / 15.4	2.0 / 14.6 / 5.0	2.0 / 0 / 0
LP Bleed 1 / LP 2 / LP3	kg/s	13.9 / 25.8 / 15.1	13.9 / 206.7 / 15.1	6.4 / 190.7 / 0	0 / 207.7 / 0
Gross Electricity	MW	520	441	517	530
Auxiliary Power	MW	30	46	46	46
CO ₂ compression Power	MW	-	48	48	48
Net Electrical Power	MW	490	347	423	436
Efficiency (HHV)	%	28.0	19.9	24.2	24.9
Energy Penalty	%	-	29.2	13.7	11.1

The second brown coal power station, Plant B, is more efficient than Plant A due to the higher complexity of the steam cycle which has high pressure feedwater heaters and steam reheat where Plant A does not. The energy penalty associated with the addition of CCS to the power station is therefore lower for the Plant B compared to Plant A when no heat integration is taken into account. The amount of CO₂ required to be captured and compressed per MW

of power produced will be less for Plant B compared to Plant A, and therefore the capture plant will have lower heat and power requirements and therefore lower energy penalty.

Heat integration can halve the energy penalty for this power station, reducing it from 29 % down to 14 %. There would be significant changes required to the power station to enable these energy savings to be made; the HP steam exhaust which is currently used for the high pressure feedwater heaters is reduced from 45.8 kg/s to 2 kg/s. Not only will another source of heat be required for the HP heaters, but the steam flowrate through the steam re-heater and IP turbine will increase by 44 kg/s so there is potential that both of these will need to be modified. Changes are also likely to be needed to the source of heat for the air-preheat or reductions in the temperature driving forces in the heat exchanger. Under all cases it appears as though the LP turbine would require modifications as the steam flow from the bleed point is increased by over 100 kg/s in each case. As with Plant A the addition of drying has a minor improvement in the energy penalty of the power station reducing it to 11 %.

The comparison of shockwave compression to conventional compression is the same for Plant B as it is for Plant A. When no heat integration is considered the net power from the power station is comparable for conventional and shockwave compression. When heat integration is included, the net electrical output of the power station with shockwave compression is higher for all cases, for Case 3 it is close to 10 MWe better than for conventional compression.

3.3. Plant C – Black Coal Power Station

Table 3: Plant C – Black Coal Power Station Results (Note that Case 5 is not applied to Plant C as no drying is required for black coal)

		1	2	3
Conventional Turbo Machinery				
Steam Extraction Rates				
HP Exhaust / IP 1 / IP 2	kg/s	25.0 / 16.0 / 18.5	25.0 / 16.0 / 18.5	5.4 / 20.0 / 14.4
LP Bleed 1 / LP 2 / LP 3	kg/s	6.8 / 11.0 / 14.5	100.8 / 11.0 / 14.5	106.5 / 0.1 / 0
Gross Electricity	MW	358	306	335
Auxiliary Power	MW	24	31	31
CO ₂ compression Power	MW	-	27	27
Net Electrical Power	MW	334	249	277
Efficiency (HHV)	%	36.0	26.9	29.9
Energy Penalty	%	-	25.4	16.9
Shockwave Compression				
Steam Extraction Rates				
HP Exhaust / IP 1 / IP 2	kg/s	25.0 / 16.0 / 18.5	25.0 / 16.0 / 18.5	5.8 / 17.0 / 11.8
LP Bleed 1 / LP 2 / LP 3	kg/s	6.8 / 11.0 / 14.5	100.8 / 11.0 / 14.5	107.7 / 0.2 / 0
Gross Electricity	MW	358	306	339
Auxiliary Power	MW	24	31	31
CO ₂ compression Power	MW	-	26	26
Net Electrical Power	MW	334	250	282
Efficiency (HHV)	%	36.0	27.0	30.4
Energy Penalty	%	-	25.1	15.5

The energy penalty associated with the black coal power station Plant C is less than both Plant A and B for the case with no heat integration, due to the higher base efficiency, which means less heat and power is required for the CCS plant per MW of electricity produced. However, when heat integration is included, the energy penalty of Plant B is lower than Plant C. This is due to Plant B having more waste heat available in the flue gas compared to Plant C, the flue gas temperatures of Plant B is 190 °C compared to 140 °C for Plant C.

When heat integration is not taken into account the power station sent out power for shockwave compressors and the conventional compression are comparable; with the power station with shockwave compression producing about 1 MWe more of sent out power than the conventional compression. When the heat available in the compressor inter/after-coolers is returned to the power station cycle and carbon capture plant, the net power generated by the power station is 5 MWe greater for shockwave compression compared to the conventional compression, which is an efficiency improvement of 0.5 % points.

3.4. Impact of CO₂ pressure

A CO₂ pressure of 100 bar will generally be close to the minimum discharge pressure required to meet transport and storage requirements. The suction pressure for many solvent plants could also be lower than 1.8 bar. If the compression ratio is increased, the compression power and the inter/after-cooler duties will also be increased. Using Plant C as an example, the impact of increasing the compression ratio to 150 has been reviewed in Table 4, including heat integration. With the compression ratio increase to 150 the configurations of the conventional compressor will change;

- 8 stage in-line compressors increase to 10 stages.
- A decrease in the in-line compression aero efficiency of the last two stages to ~62 and 56 % (polytropic).
- In-line compression prices will increase.
- Shockwave compressors will remain with 2 stages - shockwave compression can handle a compression ratio of 150, and therefore price increase will be marginal at most.

Increasing the compression ratio from 55.5 to 150 reduced the net electrical power output by 3.6 MWe for the shockwave compression and 7.3 MWe for conventional compression, therefore the performance of the shockwave compression relative to the conventional compression is improving as the compression ratio increases.

Table 4: Impact of increasing the CO₂ pressure to 150 bar on the black coal power station

		Conventional Compression	Shockwave Compression
Gross Electricity	MW	336	343
Auxiliary Power	MW	31	31
CO ₂ compression Power	MW	35	34
Net Electrical Power	MW	270	279
Efficiency (HHV)	%	29.1	30.1
Energy Penalty	%	19.1	16.6

3.5. Impact of ΔT_{min}

The ΔT_{min} used throughout this work is an optimistic 3 °C, which is based on the ΔT_{min} that can often be found in the feedwater heaters of power stations. However, a ΔT_{min} of 3 °C is unlikely to be a realistic minimum for a gas-gas exchanger like the air-preheater. Therefore the impact of varying the ΔT_{min} on the net electrical power is shown in Table 5 for Plant B. A ΔT_{min} of 3, 10 and 20 °C was used as well as a variable ΔT_{min} . The variable ΔT_{min} allows the different streams to have different ΔT_{min} , the overall ΔT_{min} for a heat exchanger will be the combination of half the two streams ΔT_{min} . The variable ΔT_{min} uses 5 °C for liquid streams, the regenerator reboiler and the extraction steam, 10 °C for steam generation, the CO₂ compressor intercoolers and the regenerator condenser, and 20 °C for the flue gas and air preheater.

The ΔT_{min} has a large impact on the energy penalty with the energy penalty increasing from 14 % to 26 % when increasing from 3 °C to 20 °C. However, when a variable ΔT_{min} is used that is likely to reflect more closely the economic ΔT_{min} , the energy penalty is not far from when a ΔT_{min} of 3 °C is used. This is due to only small regions actually having driving forces that are near the minimum. The impact of changing the ΔT_{min} is similar for both the conventional turbo machinery and the shockwave compression. In all cases the shockwave compression has a lower energy penalty when comparing the same ΔT_{min} .

Table 5: Impact of ΔT_{\min} on the Net Electrical Power Production for Plant B

			Conventional Turbo Machinery				Shockwave Compression			
ΔT_{\min}			3	10	20	Variable	3	10	20	Variable
Steam Extraction Rates										
	HP Exhaust	kg/s	2.0	2.0	2.0	2.0	2.0	2.0	2.0	2.0
	IP Bleed 1	kg/s	21.1	16.2	71.6	27.5	14.6	9.1	58.6	61.7
	IP Bleed 2	kg/s	8.8	10.4	0	9.6	5.0	7.2	0	5.2
	LP Bleed 1	kg/s	5.2	196.6	152.9	5.4	6.4	197.5	156.6	6.0
	LP Bleed 2	kg/s	189.7	1.4	47.3	189.8	190.7	4.5	50.9	190.6
	LP Bleed 3	kg/s	0	0	0	0	0	0	0	0
Net Electrical Power		MW	414	391	353	407	423	400	362	416
Energy Penalty		%	15.6	20.1	28.0	16.9	13.7	18.4	26.1	15.1

3.6. Shockwave Versus Conventional Compression

As seen in the cases above, the net work of the conventional in-line compressors and the shockwave compressors are similar with the shockwave compressors expected to be slightly lower. The in-line compressors are characterised by many stages of compression and therefore inter-cooling which lowers the average temperature of the gas to keep the net work as low as possible, but due to the unique CO_2 properties at higher pressures and the reduced component sizes, the efficiency of in-line compression in the later stages drops off considerably and this increases the net work. Whereas shockwave compressors are advantaged by maintaining high stage efficiencies but the net shaft work is increased by the relatively high average gas temperature. However, as shown in this study, the higher temperatures in the shockwave compressors exhausts may be utilised in the power station and/or carbon capture plant.

The temperature of exhaust gas from the Shockwave compressors is 220/230 °C whilst the conventional compressor is between 129–167 °C. For Plant B, the heat removed to cool the CO_2 in the shockwave compression is 28/49 MW for the first and second stage respectively, whereas the conventional compression has 13/14/16/36 MW for the four stages of cooling. Therefore, the total amount of cooling is comparable for the two cases; 77 MW compared to 79 MW, however the temperature at which the heat is available is very different.

The pinch point temperature divides the process into a process requiring heat (above the pinch) and a process releasing heat (below the pinch). This temperature is invariably located at the solvent plant reboiler temperature; approximately 118 °C for this solvent plant. Therefore, below 118 °C there is a surplus of heat in the process, in the example shown in Figure 2(A), close to 600 MW of cooling is required below the pinch point. Therefore, heat that is available above the pinch point is useful heat, and heat that is available below the pinch is not necessarily useful, as there is surplus of heat available from other sources at these temperature levels. Hence, a significant proportion of heat from the Ramgen intercoolers is useful heat, whilst almost all of the heat available in the conventional compressors will need to be removed using cooling utilities. This can be seen in Figure 2(B), which shows the available energy in the CO_2 in the Shockwave compressor inter/after-coolers and the conventional compressors inter inter/after-coolers. There is around 37 MW of heat available in the shockwave compressor inter/after-coolers above 118 °C compared to less than 12 MW for conventional compression. When actually incorporating the heat from the compressor inter/after-coolers it is more likely that the heat from shockwave compressors would be recovered as there is three times the amount of heat compared to the conventional compressors.

The heat available in the shockwave compression can be used in a number of locations; to offset close to 10 % of the heat required by the solvent regeneration, to provide heat to a portion of the boiler feed water or the air preheat and is able to provide close to 50 % of the heat for drying the coal (in this case where the coal is dried from 60–45 wt%). The best use of the heat in the shockwave compression inter/after-coolers is that which will utilise the high temperature of the exhaust CO_2 , and therefore thermodynamically the most favoured use of the energy is in boiler feed water heating or air pre-heat. It is possible in Plant B to heat up to 93 kg/s of boiler feed water to greater than 200 °C, this reduces the feedwater heating demand by close to 25 %.

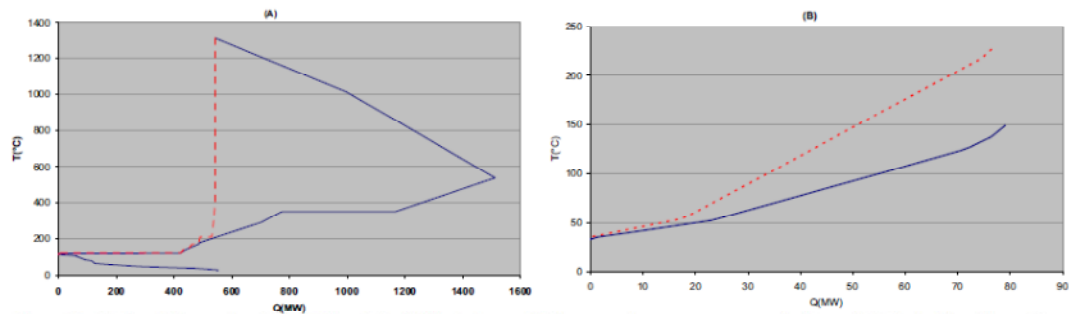


Figure 2 (A) Grand Composite Curve of Plant B (solid line) shown with the extraction steam curve required to satisfy the deficit of heat. (B) Amount of heat available in the conventional compressor inter/after-coolers (Solid line) compared to the shockwave compressor (dotted line).

As there is a surplus of heat in the process below 118 °C the fact that the shockwave compressors have less than 40 MW of heat below these temperatures compared to close to 70 MW for the conventional compressors, the cooling utility will be lower for the plant with properly integrated shockwave compressors. Additional cooling utilities lead to increases in auxiliary power requirements. Therefore, having lower cooling utilities benefits the shockwave compression system compared to conventional compressors.

4. Conclusion

The importance of heat integration is highlighted by the large reductions in energy penalty from the unintegrated cases (Case 2) to the integrated case (Case 3). The improvement in the energy penalty due to heat integration is between 36 and 52 % for the three cases. The actual improvement will be a trade-off between the capital cost of the heat exchanger network and the operability of the power station with the energy savings generated by the heat exchanger network.

For all cases in this paper the net electrical power from a power station with CCS using shockwave compression is greater than the power station using conventional inline turbo-machinery, especially when the heat in the inter/after-coolers is utilised in the power station or carbon capture process. There is also likely to be a reduction in cooling requirements using shockwave compression. Shockwave compression for CO₂ is a promising technology as it is expected to have a lower capital costs and smaller footprint than conventional turbo-machinery and from the results in this paper appears to fare more favourably from an energy perspective.

5. Acknowledgement

This work is prepared as part of the Latrobe Valley PCC project with support of the Victorian Government ETIS Brown coal R&D Program; International Power, Stanwell Corporation, Ramgen Power Systems and the Cooperative Research Centre for Greenhouse Gas Technologies (CO2CRC), which is funded through the Australian Government's Cooperative Research Centre program, other federal and state Government programs, CO2CRC participants and wider industry.

6. References

- [1] Baldwin, P., Low-cost, high-efficiency CO₂ compressors. *Carbon Capture Journal*, 2009(11).
- [2] Harkin, T., A. Hoadley, B. Hooper, Reducing the energy penalty of CO₂ capture and compression using pinch analysis. *Journal of Cleaner Production*, 2010. 18(9): p. 857-866.
- [3] Harkin, T., A.F.A. Hoadley, B. Hooper, Process integration analysis of a brown coal-fired power station with CO₂ capture and storage and lignite drying, in Ninth international conference on greenhouse gas technologies (GHGT-9) 2008, Elsevier: Washington DC, USA.
- [4] Dresser-Rand DATUM Estimation Tool. 2010 <http://turbocalc.dresser-rand.com/>. [visited 2010 Aug]

Appendix G

Optimisation of pre-combustion capture for IGCC with a focus on the water balance.

Energy Procedia 4 (2011) 1176 – 1183

doi:10.1016/j.egypro.2011.01.171

GHGT-10

Optimisation of pre-combustion capture for IGCC with a focus on the water balance

Trent Harkin^{a,b,*}, Andrew Hoadley^b, Barry Hooper^a^a*Cooperative Research Centre for Greenhouse Gas Technologies (CO2CRC), The University of Melbourne, Vic. 3010, Australia*^b*Department of Chemical Engineering, Monash University, Clayton, Vic.3800, Australia*

Abstract

Multi-objective optimisation is applied to the simulation of an IGCC power station with solvent based CCS technology. An Aspen Plus® model of the IGCC power station including CCS is interfaced with an Excel based genetic algorithm to optimise the process. The process is optimised with respect to capital cost and energy efficiency for a range of operating conditions of the solvent plant. This work is based on an air-blown gasification process consuming pre-dried lignite, it uses pinch analysis to design a HRSG for the IGCC power station with CCS to determine the power produced by the power station as well as estimating the additional capital costs due to the CCS equipment. The genetic algorithm then determines a range of non-dominated solutions by systematically adjusting the range of variables studied. Multiple-Objective Optimisation enables the decision makers to see a range of non-dominated options for multiple objectives. This can help to identify an appropriate technology or an operating regime for an individual technology that best suits the projects multiple objectives. In this example the gas temperature into the solvent absorber should be around 130 °C, the regenerator pressure should be around 2 bara and the lean solvent loading between 0.37 and 0.42 to maximise the net power output.

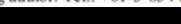
© 2011 Published by Elsevier Ltd.

Keywords: CCS, IGCC, Precombustion, Heat Integration, Optimisation

1. Introduction

Pre-combustion capture of CO₂ from the syngas of integrated gasification and combined cycle (IGCC) power generation has the advantage of separating CO₂ at higher partial pressures when compared to post-combustion capture from pulverised coal-fired power generation. The higher partial pressure of CO₂ will invariably make the separation of CO₂ from syngas easier, but pre-combustion capture will still reduce the power production from the power station significantly. The reduction in efficiency of an IGCC power station with carbon capture and storage (CCS) is due to additional energy requirements associated with the capture process. These include the need to compress the CO₂ for transport and storage, the energy to regenerate the solvent and potentially the need to remove water from the gas stream prior to the acid gas / CO₂ separation. There are a range of variables that can be adjusted that change the amount of CO₂ captured, the capital cost of the equipment or the efficiency of the power station by

* Corresponding author. Tel.: +61-3-8344-5048; fax: +61-3-9347-7438

E-mail address: 

adjusting the amount of energy required to regenerate the solvent, the amount of power produced by the gas and steam turbines and the amount of power to compress the CO₂.

In addition to the capture variables there are many variables that can be altered with respect to the IGCC power station, also the gasifier may be either an entrained flow, fixed or fluidised bed. It may be air or oxygen blown and may be operated at a range of pressures. The coal may be fed dry or as a slurry, and the syngas can be cooled by quench or using a heat recovery boiler. With pre-combustion capture of CO₂ the syngas will invariably need to undergo water-gas shift reaction (WGSR) to convert the CO to CO₂. This can be performed with a sour shift reactor or the sulphur removed prior to a clean shift reactor. The pre-combustion capture of CO₂ can occur with a variety of solvents including physical solvents such as Selexol™, Rectisol®, and Purisol® or Chemical solvents including carbonates and a variety of amines. The physical solvents generally have lower regeneration requirements but are water/heavy hydrocarbon soluble, whereas the chemical solvents generally have higher regeneration requirements, but enable the water to be balanced across the absorption column.

Water plays an important role in many stages of the IGCC process; such as in the gasification process, the WGSR, the CO₂ capture plant and the gas turbine (GT). The gasifier may require certain levels of water to be present in the coal and may also require a certain amount of steam to maintain the reaction. The water levels in the syngas will vary greatly depending on whether quench cooling or heat recovery is used. If clean WGSR is used, water may need to be reduced for the sulphur removal process. The WGSR itself will also require steam to minimise the amount of CO in the outlet of the reactor. The water may then need to be removed for, or as part of, the CO₂ absorption process, especially if a physical solvent is used. The amount of water in the clean gas that is sent to the GT will influence the amount of power generated in the turbine, as water content is increased the power output from the GT will increase, however the level of water in the GT will be limited by the turbine metallurgy.

A difficulty in the front-end stages of a project is to compare the wide range of options that will exist for each project especially when improvements in one objective, for example an increase in the power station efficiency may lead to a weakening of another objective, for example an increase in the capital costs. For IGCC with CCS this effect is compounded as changes that improve the power generated by the GT may increase the amount of energy required to regenerate the solvent which may reduce the power generated by the steam turbine (ST). Therefore each variable in the process may have many opposing impacts on both the amount of power generated from the power station and the cost to build and run the power station.

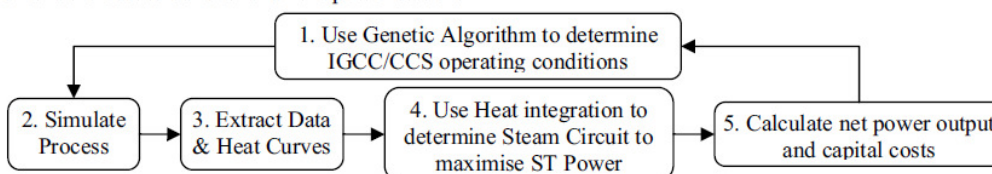


Figure 1 Flowchart to optimise the IGCC combined with CCS with respect to maximising power generation and minimising capital costs

In this paper the impact of some of the important CCS operating and design variables on the power produced by the IGCC plant and the capital cost to purchase the equipment for the IGCC will be reviewed for a specific IGCC plant. In particular, variables that impact the water balance in the process will be used so that the importance of water content on net power output can be assessed. The impact of cooling utilities on the water balance of the process is not included in the paper. The IGCC plant has been simulated with pre-combustion capture of CO₂. The power generated by the GT is calculated and heat integration (pinch analysis) combined with linear programming is used to determine the maximum amount of power that can be generated in the ST. Multiple-Objective Optimisation (MOO) is then used to find non-dominated solutions that maximise the amount of power generated from the power station at the minimum capital costs. Dominated solutions are the solutions that have higher capital costs for the same or lower net power production as another solution; the non-dominated solutions are the solutions that are not dominated by any other solution. By looking at the values of the variables in the non-dominated solution set, the

values that maximise the power at minimal capital costs can be determined. The flowchart for the optimisation is shown in Figure 1.

2. Background to Case Study

This paper uses the IEA report 2006/1 [1] on CO₂ capture in low rank coal power plants as a basis for the optimisation in particular Case 7 which uses a Foster Wheeler gasifier that is a fluidised bed type of gasifier operating at low pressure (36.5bar) using air as the partial oxidising agent. The syngas cooling is the heat recovery type with double stage sour shift. Where the IEA report [1] used Amine Guard FS process for CO₂ removal this paper uses potassium carbonate. A diagram of the process is included in Figure 2.

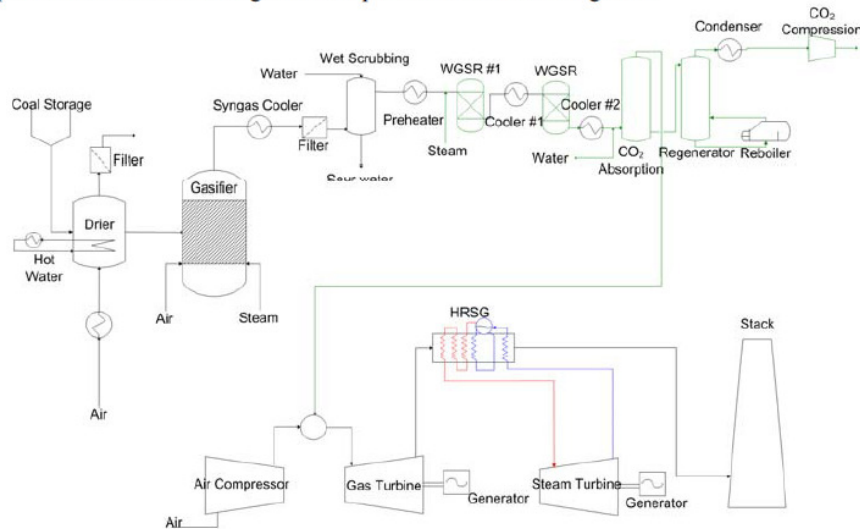


Figure 2 Simplified diagram of the Foster Wheeler IGCC process combined with capture of CO₂ using potassium carbonate

A simulation has been developed in Aspen Plus® including the coal pre-drying, the gas from the outlet of the gasifier through the wet scrubber, WGSR, solvent absorption, GT and HRSG. The solvent regeneration and CO₂ compression is modelled in the same simulation. The steam cycle is modelled in an Excel based program. The steam cycle consists of four possible steam levels that includes the ST condenser level and one level of reheat (Figure 3). The steam pressures for the steam levels are the same as that in the IEA report [1], except that the report uses a further four steam levels.

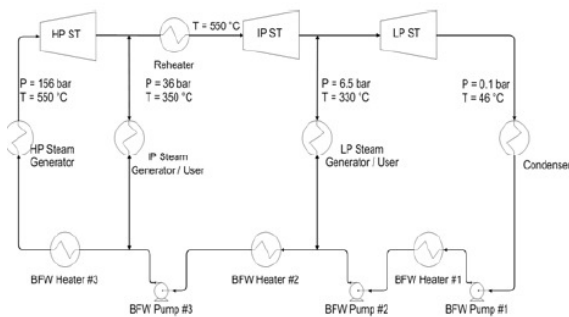


Figure 3 Steam cycle used in this paper

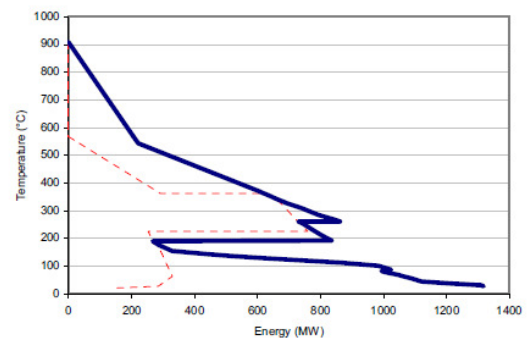


Figure 4 Grand Composite Curve (solid) and Steam Curve (dotted)

The steam generated/used at each steam level is calculated using linear programming to maximise the power in the ST. This approach has been used in [2, 3] for retrofit of post-combustion capture. Pinch analysis is used to generate a grand composite curve (Figure 4) which shows the amount of available heat in the process taking into account the heat that is required for the air and water heating in the pre-drier, generating steam for the gasifier and WGSR using condensate from the water removed upstream of the CO₂ absorption, the regenerator reboiler, the WGSR pre-heater, the turbine pre-heater and the air heater, and the heat that is available in the syngas cooler, the turbine exhaust gas, the air compressor intercooler, regenerator condenser, solvent cooler, the compressor intercoolers and the WGSR coolers.

The capital costs are estimated for the major equipment items using cost functions provided in Table 1 so the impact of the variables on the costs can be estimated. The heat exchanger area is estimated from the composite curves by summing the area required in each enthalpy interval [4] of the composite curves.

Table 1 Direct Cost / Cost Functions

Equipment Item	Base Year	Base Currency	Purchase Costs / Equations (in base year /currency) [in SA]
Coal Handling, Storage and Milling ¹	2006	€	53 [101]
Coal Drying ²	2006	€	9 [16]
Gasification ²	2006	€	131 [251]
Syngas Treatment & Conditioning ²	2006	€	24 [45]
Offsites & Utilities ²	2006	€	110 [210]
Heat Exchangers [5]	2006	\$US	$4223N(A/N)^{0.7948}$
Gas Turbine [5]	2006	\$US	$0.6 \times 10^4 (4.78 + 0.325 \log P + 0.0385 \log P^2)$
Steam Turbine [5]	2006	\$US	$0.6 \times 10^4 (1.94 + 1.455 \log P - 0.0884 \log P^2)$
CO ₂ Compressor [6]	2002	\$US	$873P^{0.938}$
Air Compressor ³	2006	€	$16.6 \times (P/106320)^{0.7}$
Pumps [6]			If $\Phi > 200$: $713Q$ If $\Phi < 200$: $10^{2.5+3.26 \log(\Phi) - 2.37 \log(\Phi)^2 + 0.62 \log(\Phi)^3}$
Separation Vessels / Absorber / Regenerator [6]	2002	\$US	$73(0.091 + p^{0.849} + 0.83)W^{0.66}$

Note 1 Values taken from IEA Report. Note 2 Values taken as 90% of the values given in the IEA report; the cost of heat exchangers was assumed to be 10% of the purchased costs of the equipment in the area. Note 3 Cost of air compressor prorated from IEA report using power with an index of 0.7. A = Heat Exchanger Area (m²), N = Number of streams, P = Power (kW), Φ = Capacity Factor (m³.kPa/s), p = Pressure (Bar), W = Vessel Weight (kg).

The IGCC power station with CCS is optimised with respect to maximising the net power produced from the power station whilst minimising the direct capital costs. The optimisation allowed the following variables to be adjusted within the bounds provided;

- Solvent lean loading: 0.1 - 0.415
- Stripper Pressure: 0.5 bar - 8.25 bar
- Solvent Temperature: 40 - 134.5 °C
- Absorber Feed Gas Temperature: 40 - 134.5 °C
- Absorber Packing Height: 10 - 47.5 m
- Stripper Packing Height: 10 - 47.5 m
- ΔT_{\min} : 6 - 36 °C

3. Results

3.1. Optimisation Results

ΔT_{\min} is the minimum temperature difference at the ends of any heat exchanger device. It is an important variable as it controls the amount of heat that can be recovered between two process streams. As ΔT_{\min} decreases the amount of heat that can be recovered increases, but the heat exchanger area required to transfer this heat also increases, which results in increases to the heat exchanger network costs. There is generally an economic trade-off between the amount of heat recovered and the capital costs of a project. Two optimisation cases were completed; one case with the ΔT_{\min} between heat exchangers was set at 20°C and one case where the ΔT_{\min} was not fixed.

The Pareto chart, which shows non-dominated solutions to the optimisation problem, is given in Figure 5, from which the following observations can be made;

- The ΔT_{\min} for the heat integration studies is very important. The solutions for the variable ΔT_{\min} are always lower than that for a fixed ΔT_{\min} , meaning that for the same amount of power the solutions where the ΔT_{\min} could vary, the solutions had a lower capital cost than those with ΔT_{\min} equal to 20°C.
- For low power/low capital cost solutions the ΔT_{\min} tends to be as high as possible, with virtually all solutions at or near the upper bound of the variable (36°C). However, for the solutions that generate more power (>760 MWe) the optimum ΔT_{\min} is gradually reduced.
- There is a large difference in the net power generated for the power station ranging from around 420 MWe to 840 MWe and the difference in capital costs for these cases varies by much less. The capital cost increases by only 26 % to double the net power output.
- The net power produced by the process, appears at the screening stage to allow more power to be generated than that suggested by the IEA report [1] of 686 MW.
- The purchased costs for the equipment is lower than the A\$1221M provided in the IEA report (€637M (2006)). This paper is not intended to compare process designs and cost estimates with the IEA report as the cost estimation methodology in this report is used as a screening tool rather than a rigorous evaluation. There are also no direct costs included for items such as piping and instrumentation.

As the case where ΔT_{\min} was allowed to vary obtained significantly better results, this will be the case that is carried forward in this paper.

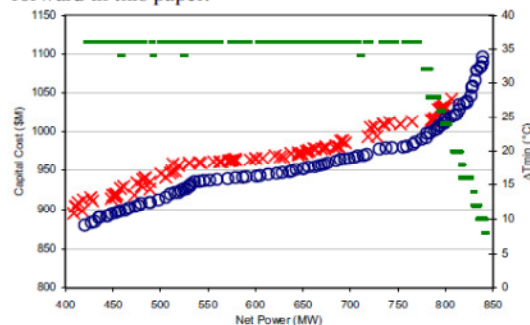


Figure 5 Comparison of the Pareto chart showing the non-dominated solutions for maximising the power generation and minimising the capital costs with a fixed ΔT_{\min} of 20 °C (x) compared to a variable ΔT_{\min} (o). Includes ΔT_{\min} for the non-dominated solutions (—).

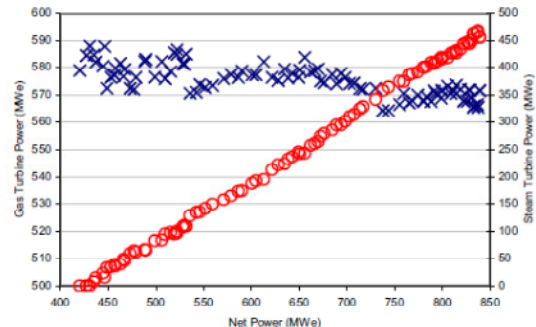


Figure 6 Variation in the Power produced by the Gas Turbine (x) and the Steam Turbine (o) for the optimised solutions

3.2. Variables Impacting the Net Power Generation

The power is produced by both the ST and the GT. Figure 6 shows the variation of these two parameters for the optimised solutions. The figure shows that for the optimised solutions, there is a much greater impact on the amount of power generated by the ST compared to the GT. The GT varies by only 25 MWe whereas the ST can produce between 0 and 460 MWe. The ST for the IEA report [1] produces 320 MWe.

There is a strong correlation between the reboiler energy and the net power as shown in Figure 7(A). As the net power increases, the reboiler energy drops constantly until the net power is 700 MWe where the reboiler energy plateaus. Therefore getting the operating conditions for the CO₂ capture plant optimised is paramount to maximise the net power produced. The regenerator pressure and solvent loading will have a large impact on the reboiler energy as shown in Figure 7(B). For potassium carbonate, lower pressures generally lead to lower heats of regeneration. For this IGCC arrangement, given the trade off between the compressor power and the power generated from the ST, it is apparent that in order to maximise the net power, the regenerator pressure should be around 2 bara. When the net power is low, optimised solution tend to have higher regenerator pressure of between 7–8 bara. As this region is characterised by low power from the steam turbine, the solutions tend to minimise costs by minimising the cost of both the CO₂ compressor and the steam turbine.

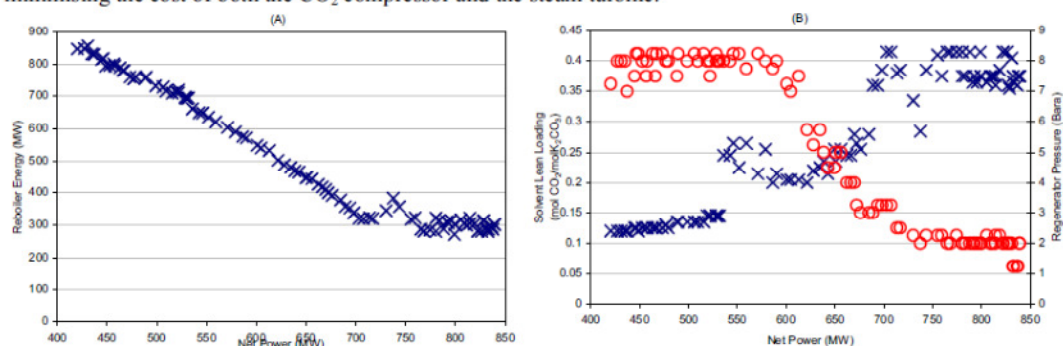


Figure 7 (A) The reboiler energy (x) and (B) The regenerator pressure (o) and solvent lean loading (x) for the optimised solutions.

The temperature of the regenerator reboiler is around 120 °C and 175 °C for regenerator pressures of 2 bara and 7.5 bara respectively. Despite the steam from the available extraction points condensing at 244 °C and 162 °C, the regenerator pressure has not been optimised to pressures that lead to reboiler temperatures that are operating at ΔT_{\min} below steam temperatures. It is possible to either adjust the steam cycle and re-perform the optimisation or add the steam cycle conditions to the list of variables to be optimised. This has not been performed for this paper but could lead to further improvements in the amount of power generated from the power station.

3.3. Variables Impacting the Capital Costs

The capital cost of much of the power station is fixed, and therefore it does not change appreciably for this optimisation due to the choice of variables (GT, air compressor) or the capital cost for the equipment item is minor (<\$20M) in the overall context (absorber, regenerator, separation vessels, pumps). The main equipment items that influence the capital cost are the ST, the CO₂ compressor and the heat exchanger network; these costs for the optimised solutions are shown in Figure 8. The ST cost is parabolic due to the linear increase in power generated by the ST (Figure 6) and the cost function used to estimate the capital cost. The CO₂ compressor costs around \$37M for the cases with high regenerator pressure and increases to around \$60M for the cases with lower regenerator pressure. The heat exchanger network shows the largest impact on the capital costs varying from around \$90M to \$240M. Between 550 MWe and 760 MWe the total costs increase by about \$45M; this is made up of a modest increase in the heat exchanger network of \$8M, whilst the ST and CO₂ compressor increase by \$12M and \$25M respectively. As the net power produced increases above 760 MWe the biggest impact in the costs is clearly the heat exchanger network, as the area increases due to the reduction in the ΔT_{\min} .

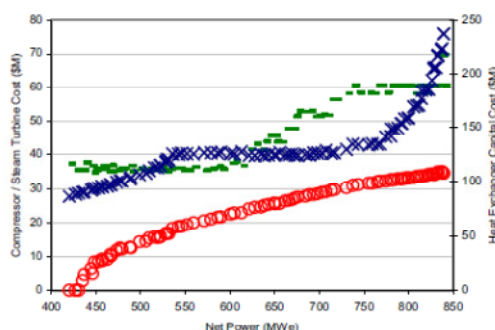


Figure 8 Capital cost variation for the CO₂ compressor (–), the Steam turbine (○) and the Heat Exchangers(×)

3.4. Impact on Water Balance on the Net Power Output

The impact of the water content on the overall power is shown in Figure 9. Although there is a clear correlation between the water content and the power produced by the GT, the impact of water is minor on the net power as shown by the lack of correlation between the two. However, the impact of operating variables on the water balance of the process is significant. The potassium carbonate process can be operated so that water is balanced, lost or gained over the absorber. A loss of water from the solvent into the gas stream will increase the GT power, but increase the make-up water demands, while a gain of water into the solvent will require higher reboiler energy to maintain solvent strength and a higher condenser duty.

The optimised gas and solvent temperatures are shown in Figure 10. The gas temperatures are tending to the upper bounds of the variable (134.5 °C), whilst the solvent temperature appears to have little impact on the overall results as shown by the lack of a correlation. Increasing the gas temperatures reduces the heat exchange required upstream and downstream of the absorber (and therefore costs) and increases the temperature of the rich solvent which has the positive effect of increasing the temperature of the solvent fed to the regenerator but also reduces the solubility of CO₂ in the solvent. The optimised solutions suggest that the benefits of higher gas temperatures outweigh the negatives. In all cases the gas temperature is greater than the solvent temperature, which means that water will be drawn from the gas stream into the solvent. To maintain solvent strength this water will need to be removed in the solvent condenser.

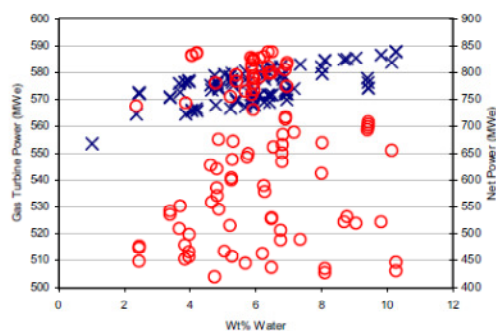


Figure 9 GT Power (×) and Net Power (○) versus water content in the gas stream leaving the absorber.

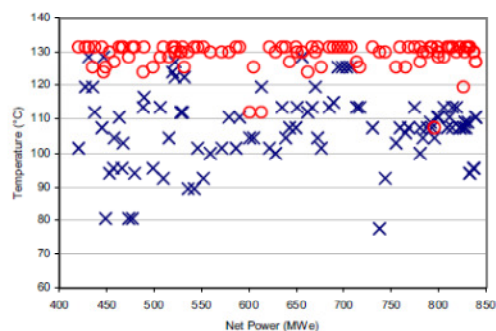


Figure 10 Gas (×) and Solvent (○) temperature for the optimised cases over the range of net power.

Water is required in the gasifier (9 kg/s), the WGS (63 kg/s) and as make-up for the wet scrubber (35 kg/s), this water can come from the water that drops out of the CO₂ compressors (~5 kg/s) and the water that drops out upstream of the absorber (44-80 kg/s) and the excess water in the regenerator condenser (0-30 kg/s). The maximum amount of the latter two sources of water combined will be approximately 80 kg/s. Therefore, it is clear that the

process requires around 107 kg/s of water and only produces around 85 kg/s. Water could be sourced from the vented fluidised air from the pre-drier (66 kg/s) or from the exhaust of the HRSG by cooling these gas streams below their dew point. The pinch analysis suggests that all hot streams need to be cooled to around 100 °C to maximise the power output from the ST, however streams that require cooling below 100 °C would require cooling utilities. Less cooling is required to recover water from pre-drier air compared to the HRSG exhaust, however the amount of water recovered for this gas stream would be approximately equal to the amount of water required as cooling water make-up if cooling water is used as the cooling utility. Therefore, recovering water from the exhaust gas streams would only be worthwhile if dry cooling is used.

4. Conclusion

MOO can be useful as a screening tool to determine parameters that will maximise power production at the minimum additional capital cost. A range of options are available to the designer that maximise the net power production at a given capital cost. The designer can then select which of these parameters to fix and which may be varied as part of a more detailed study.

The net power output of the IGCC process with CCS is affected by the operating variables of the carbon capture plant. Increasing the water into the GT is not the most important parameter to maximise the power output; ensuring that the CO₂ capture plant operating variables are optimised to minimise the reboiler energy is more important. A regenerator pressure of around 2 bar, a lean solvent loading of between 0.37 and 0.42 and a heat exchanger network with small ΔT_{\min} will maximise the simulated IGCC power station. To maintain a neutral water balance for the process either the air from the coal pre-drier or the HRSG exhaust would need to be cooled below the dew point.

5. Acknowledgement

This work is prepared as part of the CO2CRC/HRL Mulgrave Capture Project with support of the Victorian Government ETIS Brown coal R&D Program and the Cooperative Research Centre for Greenhouse Gas Technologies (CO2CRC), which is funded through the Australian Government's Cooperative Research Centre program, other federal and state Government programs, CO2CRC participants and wider industry.

6. References

- [1] IEA-GHG, CO₂ Capture in Low Rank Coal Power Plants, in IEA Greenhouse Gas R&D Programme. Report Number: 2006/1. 2006.
- [2] Harkin, T., A. Hoadley, B. Hooper, Reducing the energy penalty of CO₂ capture and compression using pinch analysis. *Journal of Cleaner Production*, 2010. 18(9): p. 857-866.
- [3] Harkin, T., A.F.A. Hoadley, B. Hooper, Process integration analysis of a brown coal-fired power station with CO₂ capture and storage and lignite drying, in Ninth international conference on greenhouse gas technologies (GHGT-9) 2008, Elsevier: Washington DC, USA.
- [4] Smith, R., *Chemical Process Design and Integration*. 2005, West Sussex, England: John Wiley & Sons Ltd.
- [5] Girardin, L., R. Bolliger, F. Marechal. On the use of process integration techniques to generate optimal steam cycle configurations for the power plant industry. in 12th international conference on Process Integration, Modelling and Optimisation for Energy Saving and Pollution Reduction (PRES'09). 2009. Rome, Italy.
- [6] Peters, M.S., K. Timmerhaus, R.E. West, *Plant design and economics for engineers*. 5th ed. 2003, New York: McGraw-Hill.